Probing Dynamic Regulation of Photosynthesis Using Harmonically Oscillating Light

Inaugural dissertation

for the attainment of the title of doctor
in the Faculty of Mathematics and Natural Sciences
at the Heinrich Heine University Düsseldorf

presented by

Yuxi Niu
from Xinjiang

Jülich, January 2024

from the institute

IBG-2: Pflanzenwissenschaften-Forschungszentrum Jülich

Published by permission of the
Faculty of Mathematics and Natural Sciences at
Heinrich Heine University Düsseldorf

Supervisor: PD Dr. Shizue Matsubara

Mentor: Prof. Dr. Oliver Ebenhöh

Date of the oral examination: 20/06/2024

EIDESSTATTLICHE ERKLÄRUNG

Ich, Frau Yuxi Niu, versichere an Eides statt, dass die vorliegende Dissertation von mir selbstständig und ohne unzulässige fremde Hilfe unter Beachtung der „Grundsätze zur Sicherung guter wissenschaftlicher Praxis an der Heinrich-Heine-Universität Düsseldorf“ erstellt worden ist. Die Dissertation habe ich in der vorgelegten oder in ähnlicher Form noch bei keiner anderen Institution eingereicht. Ich habe bisher keine erfolglosen Promotionsversuche unternommen.

Jülich, der 17. Januar 2024

dedicated to

Qingrong Kong (孔庆荣)

1938-2023

grandmother, benefactor,

inspirer

Summary

The sunlight that plants are confronted with in nature and that is used by plant photosynthesis is often highly dynamic. Multiple regulatory mechanisms have evolved to cope with natural light fluctuations, presumably leading to the resilience and robustness of photosynthesis. Recent studies have demonstrated that manipulating the kinetics and capacities of photoprotective mechanisms via genetic engineering holds promise for improving photosynthetic efficiency and crop productivity. However, an in-depth understanding of these fine-tuning mechanisms is still lacking due to the complexity of photosynthetic regulatory networks, the variability of light environments, and the limitations of sensing techniques.

This study investigated the dynamic regulatory processes of plant photosynthesis by a frequency-domain method using harmonically oscillating light to unveil distinct operational frequencies or frequency limits for the key molecular mechanisms contributing to the dynamic regulation of photosynthesis under fluctuating light. The frequency limits were characterized by changes in dynamic responses of plant photosynthesis to light oscillations of different frequencies, which were monitored here by measurements of chlorophyll fluorescence (ChlF) as well as the redox changes of plastocyanin (PC), primary donor of photosystem I (P700), and ferredoxin (Fd) proxies. Three response domains (α, α/β, β) occurring in the frequencies typical of plant canopies were determined, and two frequency limits separating these domains were identified (**Chapter 2**). Qualitative differences in the dynamic responses of photosynthesis between wild-type *Arabidopsis thaliana* and mutants that are deficient in rapidly reversible non-photochemical quenching (NPQ) components pointed to the existence of two frequency limits associated with PsbS protein- and violaxanthin de-epoxidase (VDE)-dependent NPQ. The PsbS-dependent mechanism operated at a frequency of about 1/10 Hz - 1/30 Hz, while the frequency limit of the VDE-dependent process was about 1/60 Hz - 1/120 Hz. The contrasting responses of two mutants lacking specific pathways of cyclic electron transport (CET), namely the PGR5/PGRL1-dependent pathway and the NDH-like complex-dependent pathway, also indicated that regulatory mechanisms with apparently similar functions may have distinct frequency limits in oscillating light. The PGR5/PGRL1-dependent CET seems to operate rapidly, as manifested by the contrasting responses of the *pgrl1ab* mutant and its wild-type plant at all

frequencies. The frequency limit of this CET pathway may lie beyond the frequencies tested in this study. The NDH-like complex-dependent CET, on the other hand, may operate at a frequency around 1/30 Hz - 1/60 Hz, as deduced from the changes in the dynamics of Fd redox states in the *crr2-2* mutant compared to its wild-type.

The results suggest that each of the dynamic regulatory mechanisms has its own operational frequency range within which the contributing molecular processes can function. If the frequency of light oscillation matched the specific frequency limit of a regulatory process, the signal was significantly amplified, resulting in a resonance. In contrast, when the light oscillation exceeded this specific frequency limit, this regulatory process was not able to keep pace with light changes and could respond only to the average light intensity. By exploiting such resonance properties, harmonically oscillating light can be used to characterize the inherent frequency limits of the different regulatory mechanisms and identify their contributions during light fluctuations.

The frequency 1/60 Hz induced abundant characteristic features of photosynthetic dynamics in the experiments shown in Chapter 2 and was thus used to investigate the effect of different amplitudes of light oscillations on dynamic regulation of photosynthesis (**Chapter 3**). The quantum yields related to PSI and PSII function and the redox changes of PC and Fd were examined in *Arabidopsis* wild-types and mutants by superimposing saturation pulses on harmonically oscillating light. The results suggest that the PGR5/PGRL1-dependent CET can contribute to the protection of photosystems even under light fluctuations with small amplitudes, while the NDH-like complex-dependent CET may act as a safety valve in light fluctuations with large amplitudes.

The dynamic relationships between irradiance and photosynthetic responses in changing light conditions were characterized by the fingerprint of ChlF under oscillating light (**Chapter 4**). The relationships observed in the oscillating light conditions were more complex than those found by traditional steady-state measurements. Responses in the fast oscillation frequencies (1 Hz - 1/10 Hz) can be explained solely by constitutive non-linearity due to saturation of photosynthetic pathways or to filling and emptying of the photosynthetic redox pools. Regulatory non-linearity emerged in slower oscillation frequencies (about 1/30 Hz), in which dynamic regulation of rapidly reversible NPQ (qE) contributed to the distortion of the relationships between irradiance and ChlF responses, with ChlF yield decreasing in the light-increasing phase. When the frequency was slow enough (< 1/120

Hz), photosynthesis appeared to reach a stationary state through the operation of regulatory processes, which effectively counteracted changes in light intensity and maintained the dynamic equilibrium of the photosynthesis systems.

Dynamics of photosynthesis in oscillating light are largely non-linear and information-rich due to the high variability of the amplitude and frequency of light changes. Sensing and analyzing the resonance features of regulatory processes and non-linear characteristics of photosynthetic responses using harmonically oscillating light can help us gain insights into different regulatory mechanisms and their functions in dynamically changing light environments.

Zusammenfassung

Das Sonnenlicht, mit dem Pflanzen in der Natur konfrontiert sind und das von der pflanzlichen Photosynthese genutzt wird, ist oft sehr dynamisch. Es haben sich zahlreiche Regulierungsmechanismen entwickelt, um mit den natürlichen Lichtschwankungen fertig zu werden, was vermutlich zur Widerstandsfähigkeit und Robustheit der Photosynthese beiträgt. Jüngste Studien haben gezeigt, dass gentechnische Modifikationen der Kinetik und der Kapazitäten von Lichtschutzmechanismen vielversprechende Möglichkeiten zur Verbesserung der photosynthetischen Effizienz und der Produktivität von Pflanzen aufzeigen. Aufgrund der Komplexität der photosynthetischen Regulationsnetzwerke, der Variabilität der Lichtverhältnisse und der begrenzten Möglichkeiten der Sensortechnik fehlt es jedoch noch an einem tiefergehenden Verständnis dieser fein abgestimmten Mechanismen.

In der vorliegenden Arbeit wurden die dynamischen Regulierungsprozesse der pflanzlichen Photosynthese mit Hilfe einer Frequenzdomänen-Methode unter Verwendung von harmonisch oszillierendem Licht untersucht, um unterschiedliche Betriebsfrequenzen oder Frequenzgrenzen für die wichtigsten molekularen Mechanismen aufzudecken, die zur dynamischen Regulierung der Photosynthese unter fluktuierendem Licht beitragen. Die Frequenzgrenzen wurden durch Veränderungen in den dynamischen Reaktionen der Photosynthese auf Lichtschwankungen charakterisiert und durch Messungen der Chlorophyllfluoreszenz (ChlF) sowie der Redoxveränderungen von Plastocyanin (PC), dem primären Donor des Photosystems I (P700) und Ferredoxin (Fd) eingeordnet. Es wurden drei Reaktionsbereiche (α, α/β, β) bestimmt, die in den für den Kronenbereich von Pflanzen typischen Frequenzen auftreten und es wurden zwei Frequenzgrenzen ermittelt, die diese Bereiche voneinander trennen (**Kapitel 2**). Qualitative Unterschiede in den dynamischen Reaktionen der Photosynthese zwischen dem Wildtyp von *Arabidopsis thaliana* und Mutanten mit Mutationen in den schnell reversiblen Komponenten des nicht-photochemischen Quenching (NPQ), weisen auf die Existenz von zwei Frequenzgrenzen hin, die mit dem PsbS-Protein und dem Violaxanthin-Depoxidase (VDE) abhängigen NPQ verbunden sind. Der PsbS-abhängige Mechanismus arbeitete bei einer Frequenz von etwa 1/10 Hz - 1/30 Hz, während die Frequenzgrenze des VDE-abhängigen Prozesses bei etwa 1/60 Hz - 1/120 Hz lag. Die gegensätzlichen Reaktionen von zwei Mutanten, denen spezifische Wege des zyklischen Elektronentransports (CET) fehlen, nämlich der

PGR5/PGRL1-abhängige Weg und der NDH-ähnliche Komplex-abhängige Weg, weisen ebenfalls darauf hin, dass Regulierungsmechanismen mit scheinbar ähnlichen Funktionen unterschiedliche Frequenzgrenzen bei oszillierendem Licht haben können. Der PGR5/PGRL1-abhängige CET scheint schnell zu funktionieren, wie die unterschiedlichen Reaktionen der pgrl1ab-Mutante und des Wildtyps bei allen Frequenzen zeigen. Die Frequenzgrenzen dieses CET-Wegs liegen möglicherweise jenseits der in dieser Studie getesteten Frequenzen. Die vom NDH-ähnlichen Komplex-abhängige CET könnte dagegen bei Frequenzen um 1/30 Hz - 1/60 Hz arbeiten, was aus den Veränderungen in der Dynamik der Fd-Redoxzustände in der crr2-2-Mutante im Vergleich zum Wildtyp abgeleitet werden kann.

Die Ergebnisse deuten darauf hin, dass jeder der dynamischen Regulationsmechanismen einen eigenen Frequenzbereich hat, innerhalb dessen die beteiligten molekularen Prozesse funktionieren können. Wenn die Frequenz der Lichtschwingung mit der spezifischen Frequenzgrenze eines regulatorischen Prozesses übereinstimmte, wurde das Signal deutlich verstärkt, was zu einer Resonanz führte. Überschreitet die Lichtschwingung hingegen diese spezifische Frequenzgrenze, kann dieser Regelungsprozess nicht mit den Lichtänderungen Schritt halten und nur auf die durchschnittliche Lichtintensität reagieren. Durch Ausnutzung solcher Resonanzeigenschaften kann harmonisch oszillierendes Licht genutzt werden, um die inhärenten Frequenzgrenzen der verschiedenen Regelungsmechanismen zu charakterisieren und ihre Beiträge bei Lichtschwankungen zu ermitteln.

Eine Frequenz (1/60 Hz), die in den Experimenten in Kapitel 2 zahlreiche charakteristische Merkmale der photosynthetischen Dynamik hervorgerufen hatte, wurde verwendet, um die Auswirkungen verschiedener Amplituden von Lichtschwingungen auf die dynamische Regulation der Photosynthese zu untersuchen (**Kapitel 3**). Die Quantenerträge, die mit der PSI- und PSII-Funktion und den Redoxveränderungen von PC und Fd zusammenhängen, wurden in *Arabidopsis*-Wildtypen und den Mutanten durch Überlagerung von Sättigungspulsen mit harmonisch oszillierendem Licht untersucht. Die Ergebnisse deuten darauf hin, dass die PGR5/PGRL1-abhängige CET zum Schutz der Photosysteme auch bei Lichtschwankungen mit kleinen Amplituden beitragen könnte, während die NDH-ähnliche Komplex-abhängige CET als Sicherheitsventil bei Lichtschwankungen mit großen Amplituden fungieren könnte.

Zusammenfassung

Die dynamischen Beziehungen zwischen Bestrahlungsstärke und photosynthetischen Reaktionen unter wechselnden Lichtbedingungen wurden durch detaillierte Untersuchungen von ChlF unter oszillierendem Licht charakterisiert (**Kapitel 4**). Die unter den oszillierenden Lichtbedingungen beobachteten Beziehungen waren komplexer als die, die bei herkömmlichen steady-state Messungen festgestellt wurden. Die Reaktionen bei den schnellen Oszillationsfrequenzen (1 Hz - 1/10 Hz) lassen sich ausschließlich durch konstitutive Nichtlinearität erklären, die auf die Sättigung der photosynthetischen Stoffwechselwege oder das Füllen und Entleeren der photosynthetischen Redox-Pools zurückzuführen ist. Bei langsameren Oszillationsfrequenzen (etwa 1/30 Hz) zeigte sich eine regulatorische Nichtlinearität, bei der die dynamische Regulierung der schnell reversiblen NPQ (qE) zur Verzerrung der Beziehungen zwischen Bestrahlungsstärke und ChlF-Antworten beitrug, wobei die ChlF-Ausbeute in der Phase der Lichterhöhung abnahm. Wenn die Frequenz langsam genug war (< 1/120 Hz), schien die Photosynthese einen stationären Zustand durch den Betrieb von Regulierungsprozessen zu erreichen, die Änderungen der Lichtintensität wirksam entgegenwirkten und das dynamische Gleichgewicht der Photosynthesesysteme aufrechterhielten.

Die Dynamik der Photosynthese bei oszillierendem Licht ist aufgrund der hohen Variabilität von Amplitude und Frequenz der Lichtänderungen weitgehend nichtlinear und informationsreich. Die Erfassung und Analyse der Resonanzmerkmale von Regelungsprozessen und der nichtlinearen Eigenschaften photosynthetischer Reaktionen unter Verwendung von harmonisch oszillierendem Licht kann uns helfen, Einblicke in verschiedene Regelungsmechanismen und ihre Funktionen in sich dynamisch verändernden Lichtumgebungen zu gewinnen.

Contents

Contents

Chapter 1

General introduction

1.1 Sunlight around plants

Sunlight, a vital energy source for life on Earth, exhibits dynamic characteristics. Before it traverses the Earth's upper atmosphere, the photon distribution of sunlight closely resembles that of an ideal blackbody radiator with a temperature of about 5250 °C. However, upon reaching sea level, sunlight undergoes attenuation in intensity and adjustment in spectral composition due to absorption and scattering by atmospheric constituents. Ozone, for example, absorbs photons at short wavelengths, while water vapor and oxygen absorb photons at long wavelengths (Waters, 1976; Smith, 1982; Solomon *et al.*, 1998).

Sunlight at the Earth surface exhibits remarkable variations in terms of its spectrum, intensity, and duration, influenced by the relative position of the Sun that is determined by time of day, season, latitude, and altitude (Herman & Goldberg, 1978; Smith, 1982; Chiang *et al.*, 2019), weather (Smith, 1982; Dengel *et al.*, 2015), atmospheric conditions (Smith, 1982; Kotilainen *et al.*, 2020), and air properties (Yang *et al.*, 2022). Variations in sunlight span multiple orders of magnitude, ranging from fractions of a second to diurnal or seasonal changes (Smith, 1982).

Sunlight around plants is more complex than in open areas. Plants typically grow within canopies, where light availability is spatially heterogeneous, influenced not only by changes in incident sunlight but also by canopy structures (Pearcy, 1990; Chazdon & Pearcy, 1991; Vierling & Wessman, 2000; Way & Pearcy, 2012). Absorption, scattering, and reflections of sunlight within the canopy weaken the intensity and change the spectrum of sunlight (Turnbull & Yates, 1993; de Castro, 2000). The canopy structure is not static and can be affected by external forces, such as wind-induced canopy movement and leaf flutter, thus exacerbating the fluctuations of sunlight (Roden & Pearcy, 1993; Pearcy *et al.*, 1996; Peressotti *et al.*, 2001; de Langre, 2008; Burgess *et al.*, 2021). Furthermore, plants are highly adaptable to changes in light conditions. They respond to variations in sunlight by adjusting their growth, developmental stage transitions, leaf orientation and structure (Fiorucci & Fankhauser, 2017; Küpers *et al.*, 2018; Poorter *et al.*, 2019). These adjustments by plants feed back into the fluctuations of sunlight within the canopy.

In such complex light environments, plants or leaves positioned within the canopy always experience intermittent exposure to brief episodes of sunlight, known as sunflecks (Pearcy, 1990; Lawson *et al.*, 2012; Way & Pearcy, 2012). Sunflecks play a significant role in canopy

photosynthesis, contributing significantly to the photosynthetically active radiation (PAR) of understory plants/leaves (Chazdon, 1988; Pfitsch & Pearcy, 1989; Naumburg *et al.*, 2001; Leakey *et al.*, 2005). To efficiently utilize this short-duration PAR from sunflecks, studies have found that plants improve post-illumination CO_2 assimilation by retaining the proton gradient across the thylakoid membrane and metabolites of the Calvin-Bension cycle (Pearcy, 1990; Kirschbaum *et al.*, 1998; Kono & Terashima, 2014). Furthermore, to protect photosynthesis from photodamage caused by sudden excess sunlight, plants have evolved a variety of photoprotective processes. The dynamic photoprotective regulation of photosynthesis in response to light fluctuations will be detailed in **Section 1.2**. According to the Smith and Berry classification (2013), sunflecks encompass light fluctuations with periods of less than 8 minutes. **Table 1.1** summarizes the factors contributing to sunflecks at distinct canopy depths (de Castro, 2000) based on different time intervals or frequency ranges. In this study, I focus on the dynamic regulation of photosynthesis in response to light fluctuations on a time scale ranging from 1 second (1 Hz) to 8 minutes (1/480 Hz) (marked bold in **Table 1.1**).

Table 1.1 The phenomena that result in fluctuations in photosynthetically active radiation (PAR) with different characteristic periods T and frequencies f=1/T in vegetation canopies.
Fluctuations in a low light environment: PAR can be very low for leaves that grow close to the ground in forest understories or crop fields under a dense canopy. Yet, wind and leaf flutter or plant swaying result in sunflecks of high light that can transiently reach the understory. Under larger canopy gaps, sun patches reach saturating light intensities even in understories.
Fluctuations in a medium light environment are observed within canopies. Wind-induced canopy/plant movement and the random changes that occur as a result of cloud movements and light incidence angle drift relative to canopy gaps can create sun and shade flecks and sun patches of various durations. Depending on the leaf position in the canopy, the fluctuations can reach direct sunlight values and above by adding scattered light.
Fluctuations in a high light environment with potentially photoinhibiting PAR-values occur in forest or crop canopies. Fluctuations that are caused by intermittent cloudiness are usually random and differ from wind-induced flecks and patches, as they are longer and against a high light background. Light fluctuates, and the PAR to which leaves are acclimated suddenly increases, potentially resulting in overexcitation and damage.

Period, T	1 s > T ≥ 10 ms	8 min > T ≥ 1 s	T ≥ 8 min
Frequency, f	100 Hz > f ≥ 1 Hz	1 Hz > f ≥ 2.1·10-3 Hz	$2.1 \cdot 10^{-3}$ Hz > f
Fluctuations against a low light background in vegetation understory	Leaf flutter (Roden & Pearcy, 1993) results in very brief sun flecks (Smith & Berry, 2013).	Plant swaying (Pearcy *et al.*, 1996) and transient gaps in the canopy (Chazdon & Pearcy, 1991) causes sun flecks (Pearcy *et al.*, 1996).	Earth rotation (Pearcy *et al.*, 1996) and canopy gaps (Smith & Berry, 2013) results in long duration sun patches (Smith & Berry, 2013).
Fluctuations against a medium range background occurring within-canopies	Leaf flutter (Roden & Pearcy, 1993) or plant swaying (de Langre, 2008) result in brief sun flecks (Pearcy, 1990).	Transient gaps in the upper canopy (Chazdon & Pearcy, 1991), wind induced canopy movement (Peressotti *et al.*, 2001) and intermittent cloudiness (Knapp & Smith, 1987) give rise to complex light pattern within canopies (Way & Pearcy, 2012; Kaiser *et al.*, 2018)	Earth rotation, canopy gaps and cloud movement result in sun (Smith & Berry, 2013) and cloud patches. Diurnal changes create regular irradiance changes (Chazdon & Pearcy, 1991)
Fluctuations against a high light background in outer canopies	Leaf flutter in canopies create high intensity sun flecks and shade flecks (Pearcy *et al.*, 1996).	Effects of plant swaying (de Langre, 2008) and intermittent cloudiness (Knapp & Smith, 1987) create sun and cloud flecks (Morales & Kaiser, 2020).	Slowly variable irradiance under overcast skies (Navrátil *et al.*, 2007), cloud movement, diurnal changes (Morales & Kaiser, 2020).

1.2 Dynamics of plant photosynthesis

Photosynthetic organisms, such as plants, algae, and cyanobacteria, undergo photosynthesis to use light energy to create organic matter and release oxygen as a by-product, serving as the primary energy source and oxygen supplier for most of life on earth.

Plant photosynthesis involves two major processes: light reactions and the Calvin-Benson cycle. Light reactions convert light into chemical energy via the processes of light harvesting, excitation of reaction centers, electron transport, and photophosphorylation. These are done in a complex system of mutually proton-coupled linear and cyclic electron transports (Ort & Yocum, 1996). The dynamics of light reactions span a wide range of timescales. Photon absorptions by photosynthetic pigments take only femtoseconds (10^{-15} s), while charge separations in reaction centers occur in picoseconds (10^{-12} s) (Nedbal & Koblížek, 2006; Rascher & Nedbal, 2006). The time scales of redox reactions within the electron transport chain span from nanoseconds to seconds (Kalaji *et al.*, 2012). The chemical energy generated in the forms of adenosine triphosphate (ATP) and reduced nicotinamide adenine dinucleotide phosphate (NADPH) is subsequently utilized in the Calvin-Benson cycle to fix CO_2 and synthesize carbohydrates. Processes in the Calvin-Benson cycle involve multiple energy-consuming enzymatic biochemical reactions, and its dynamics can vary across several orders of magnitude, ranging from sub-seconds to minutes.

Photosynthesis systems form a complex network of processes, from light absorption to CO_2 assimilation, with timescales that span many orders of magnitude. These processes are dynamically interconnected through redox potentials, electron chemical potentials, and energy supply and demand, possessing feedforward and feedback mechanisms that enable the system to maintain a dynamic equilibrium (Scheibe *et al.*, 2005; Horton, 2012). However, the external environments encountered by the photosynthesis systems, particularly light environments, are highly disordered and complex (**Section 1.1**). To respond effectively and adapt to these environmental disturbances, photosynthesis systems have evolved and rely on additional mechanisms designed to selectively regulate the dynamics of their constitutive regimes. These mechanisms are essential to achieve dynamic equilibrium, ensure high photosynthetic efficiency, enhance photoprotection, and gain overall robustness of photosynthesis (Kramer & Evans, 2011; Murchie & Niyogi, 2011; Lawson *et al.*, 2012; Murchie & Ruban, 2020).

These regulatory mechanisms can be classified based on the timescales over which they operate as evolutionary adaptation, developmental acclimation, and dynamic regulation (Walters, 2005; Athanasiou *et al.*, 2010; Lawson *et al.*, 2012; Kono & Terashima, 2014). Evolutionary adaptation takes place over many generations, spanning years or even longer periods, leading to lasting genetic adjustments in response to specific light environments (Kono & Terashima, 2014). Developmental acclimation operates over intermediate timescales, ranging from several hours or days to weeks (Walters, 2005; Athanasiou *et al.*, 2010; Schöttler & Tóth, 2014; Dyson *et al.*, 2015; Morales & Kaiser, 2020; Gjindali *et al.*, 2021). It involves adjustments in gene expression and protein abundance (Miller *et al.*, 2017; Schneider *et al.*, 2019; Niedermaier *et al.*, 2020), modifications in the stoichiometry of constitutive and associated photosynthetic apparatus (Chow *et al.*, 1990; Walters & Horton, 1995; Dietzel *et al.*, 2008; Schöttler & Tóth, 2014; Schöttler *et al.*, 2015), as well as changes in leaf anatomy (Oguchi *et al.*, 2005; Stewart *et al.*, 2015; Wei *et al.*, 2021), and plant morphology and structure (Peri *et al.*, 2007; Ballaré & Pierik, 2017) (**Figure 1.1**). Dynamic regulation occurs within a day, ranging from milliseconds to tens of minutes in response to short-term light fluctuations (Kono & Terashima, 2014). Changes based on developmental acclimation are generally irreversible, while dynamic regulation normally can be easily reversed when the light environment changes. Details of the short-term dynamic regulation are presented below.

Dynamic regulation in response to transient light fluctuations primarily consists of adjustments in the absorption and dissipation of light energy, modulations of electron transport rates and flows, and activations of enzymes in the Calvin-Benson cycle (summarized in **Figure 1.1**, see reviews in Eberhard *et al.* (2008); Kono and Terashima (2014) and Kaiser *et al.* (2019)).

Adjustments in the absorption and dissipation of light energy

When the absorbed light energy exceeds the load that photosynthesis systems can sustain, dissipation pathways become necessary to prevent the production of reactive oxygen species (ROS) and subsequent photodamage. Aside from absorbing energy and transferring excitation energy to reaction centers, the Light-Harvesting Complex of Photosystem II (LHCII) also functions as a site for converting excess photo-excitation into thermal energy (energy dissipation) (Horton *et al.*, 1996; Demmig-Adams *et al.*, 2014a; Nicol *et al.*, 2019), a process also known as non-photochemical quenching (NPQ) (Horton *et al.*, 1996; Li *et al.*,

2004; Murchie & Niyogi, 2011; Ruban, 2018; Ruban & Wilson, 2021). The transition from a light-harvesting state to an energy-quenching state may involve reversible conformational changes within the PSII–LHCII super-complexes (Johnson *et al.*, 2011; Ruan *et al.*, 2023). The molecular mechanisms that induce conformational changes and trigger the quenching of excess photo-excitation remain a subject of intense debate.

NPQ comprises interrelated processes that operate at various spatial and temporal scales. One rapidly modulated component, triggered by low luminal pH, is the rapidly reversible NPQ, often referred to as qE in the literature (Külheim *et al.*, 2002; Horton & Ruban, 2005; Ruban *et al.*, 2007). It involves two main processes: protonation of PSII subunit S (PsbS) (Li *et al.*, 2000; Niyogi, 2000; Li *et al.*, 2002a; Holt *et al.*, 2004; Li *et al.*, 2004; Roach & Krieger-Liszkay, 2012; Ruban, 2016) and activation of the xanthophyll cycle enzyme violaxanthin de-epoxidase (VDE) (Pfundel & Dilley, 1993; Gilmore, 1997; Niyogi *et al.*, 1998; Ruban *et al.*, 2007; Jahns & Holzwarth, 2012). PsbS is an integral membrane protein that does not appear to bind pigments (Bonente *et al.*, 2008), suggesting that PsbS itself is not a quencher (Croce, 2015; Fan *et al.*, 2015) and may function as a luminal pH sensor. The exact biochemical mechanism in vivo by which protonated PsbS activates NPQ has not been fully elucidated, but upon protonation, it appears to promote a conformational change of PSII-associated antennae (Kereïche *et al.*, 2010; Correa-Galvis *et al.*, 2016; Sacharz *et al.*, 2017). PsbS-dependent NPQ is the most rapidly responsive quenching process in plants, activated within seconds upon light exposure (Holzwarth *et al.*, 2009; Sylak-Glassman *et al.*, 2014). Another process is the activation of a thylakoid lumen-localized enzyme VDE by low luminal pH (Pfundel & Dilley, 1993; Niyogi *et al.*, 1998; Fufezan *et al.*, 2012), which converts violaxanthin to zeaxanthin via the intermediate antheraxanthin (Demmig *et al.*, 1987; Demmig-Adams, 1990). The role of accumulated zeaxanthin in rapidly reversible NPQ is debated (van Oort *et al.*, 2018; Tutkus *et al.*, 2019), with different models postulating potential direct quenching of chlorophyll's excited state (Holt *et al.*, 2005; Ahn *et al.*, 2008; Holzwarth *et al.*, 2009; Sylak-Glassman *et al.*, 2014) or facilitation of PSII-associated antenna aggregation (Sacharz *et al.*, 2017; Tutkus *et al.*, 2019). The rate of violaxanthin de-epoxidation depends on the rate of release from its binding sites, located primarily at PSII major and minor antenna proteins (Bassi *et al.*, 1999; Croce *et al.*, 1999; Caffarri *et al.*, 2001), which in turn affects zeaxanthin accumulation and ultimately energy dissipation (Jahns *et al.*, 2009; Kress & Jahns, 2017). Loosely bound violaxanthin can be rapidly released from PSII antenna complexes and converted to zeaxanthin to enhance

rapidly reversible NPQ within tens of seconds to minutes (Nilkens *et al.*, 2010). The zeaxanthin-dependent sustained quenching component, known as qZ (Nilkens *et al.*, 2010), is activated over tens of minutes during exposure to prolonged excess light, potentially involving the replacement of tightly bound violaxanthin with zeaxanthin in PSII-associated antenna complexes (Jahns *et al.*, 2009; Nilkens *et al.*, 2010; Dall'Osto *et al.*, 2012; Jahns & Holzwarth, 2012; Kress & Jahns, 2017).

Both PsbS- and VDE-dependent rapidly reversible NPQ mechanisms are crucial for plant fitness in fluctuating light conditions (Külheim *et al.*, 2002). Studies have shown that *Arabidopsis thaliana* mutants lacking PsbS or VDE exhibit normal growth under constant light but experience significant constraints in growth and development when exposed to changing light conditions, either in the field or in controlled conditions (Külheim *et al.*, 2002). These two mechanisms jointly induce thylakoid lumen pH-dependent down-regulation of PSII photo-excitation and regulate the photoprotective capacity of rapidly reversible NPQ (Müller *et al.*, 2001; Ruban *et al.*, 2012).

The light-harvesting capacity can be directly modulated by state transitions (qT), representing the movement of LHCII between PSII and PSI (Haldrup *et al.*, 2001; Allen, 2003; Dietzel *et al.*, 2008). This process adjusts the relative size of the antennae associated with the PSII and PSI reaction centers. Although qT is commonly considered to be one of the important components of NPQ, it does not quench energy per se, but rather influences the quenching of PSII fluorescence by redistributing energy absorption between PSII and PSI (Ihnken *et al.*, 2011). When PSII is overexcited, LHCII is phosphorylated and relocated to PSI (State 2), whereas when PSI is overexcited, phosphorylated LHCII is dephosphorylated and returned to PSII (State 1) (Wollman, 2001; Bonardi *et al.*, 2005; Dietzel *et al.*, 2008; Kargul & Barber, 2008). The phosphorylation/dephosphorylation of LHCII is influenced by light intensity and spectrum, responding to light conditions that lead to preferential excitation of one or the other photosystem, balancing the excitation of two photosystems, and optimizing electron transport (Bellafiore *et al.*, 2005; Mikko *et al.*, 2006; Pesaresi *et al.*, 2009; Pesaresi *et al.*, 2010). Thus, variations in factors in plant canopies, such as the relative position of leaves/plants in the canopy and the duration and intensity of exposure to sunflecks, may jointly influence qT. The exact contribution of qT to the dynamic regulation of photosynthesis to light fluctuations is still poorly understood. In vascular plants, the effect of qT on light harvesting is limited, with an estimated 15-20% of LHCII shifting. In unicellular organisms like green algae, in contrast, this proportion is

much larger, with around 80% of LHCII moving (Allen, 1992; Kono & Terashima, 2014). The qT is generally a slightly slower process compared to PsbS-dependent rapidly reversible NPQ (Eberhard *et al.*, 2008; Kono & Terashima, 2014).

When the aforementioned protective mechanisms are insufficient to cope with light-induced over-excitation, PSII initiates its "last resort" option: targeted destruction of PSII D1 proteins (Ruban, 2015; Kaiser *et al.*, 2019), leading to PSII photoinactivation. It is usually induced by ROS generated by over-excited chlorophylls or over-reduced redox components in the electron transport chain (Järvi *et al.*, 2015; Davis *et al.*, 2016; Foyer, 2018). Such photoinactivated PSII can be an effective quencher to dissipate excess light energy (Lee *et al.*, 1999; Matsubara & Chow, 2004). In contrast to rapidly reversible NPQ, relaxation of photoinhibition-related quenching, qI, involves slowly-developing and energy-consuming processes that encompass degradation, de novo synthesis and replacement (turnover) of PSII D1 protein (Kok, 1956; Murata *et al.*, 2007; Nawrocki *et al.*, 2021). Thus, it is a relatively slow reversible process that takes tens of minutes to hours or even days (Murchie & Niyogi, 2011; Kaiser *et al.*, 2019). The qI can also indirectly protect PSI from photodamage by diminishing electron flow from PSII to PSI (Murata *et al.*, 2007; Nawrocki *et al.*, 2021).

Modulations of electron transfer rates and flows

The dynamic regulation of plant photosynthesis in response to fluctuating light also involves direct modulation of electron transports by adjusting the rates of electron transfer and altering electron transfer pathways to divert electrons toward alternative sinks (See reviews in Eberhard *et al.* (2008); Kono and Terashima (2014) and Kaiser *et al.* (2019)).

Photosynthesis control is a luminal-pH dependent process that governs the rate of proton-coupled electron transport at the cytochrome b_6/f (Cyt b_6/f) complex (Rumberg & Siggel, 1969; Tikhonov *et al.*, 1981; Colombo *et al.*, 2016). The oxidation of plastoquinol (PQH2) at the Q0 site of Cyt b_6/f is the rate-limiting step of electron transport, the rate of which is influenced by the concentration of protons in the thylakoid lumen (Nishio & Whitmarsh, 1993; Hope *et al.*, 1994). When the luminal pH is low, the oxidation of PQH2 slows down by three to fourfold (Eberhard *et al.*, 2008), leading to a more reduced PQ pool and QA, but reducing the electron pressure in PSI (Kenji *et al.*, 2007; Tikhonov, 2013; Tikhonov, 2014). The activation of this process via luminal pH depends on the rates of ATP synthesis that exports protons from lumen to stroma (Kenji *et al.*, 2007; Tikhonov, 2013) and on the rates

of alternative electron transports that import protons and thereby accelerate lumen acidification, in addition to that by linear electron transport (Suorsa *et al.*, 2013). Under fluctuating light, photosynthesis control acts as a photoprotective mechanism that balances the excitation of two photosystems and avoids PSI photodamage (Suorsa *et al.*, 2013; Colombo *et al.*, 2016). It requires a lower luminal pH compared to the rapidly reversible NPQ (Schansker, 2022). Accordingly, photosynthesis control may not play a major role in coping with extremely rapid changes in light intensity due to hysteresis in lumen acidification, whereas it may be more effective under slow changes in light intensity (Kono & Terashima, 2014).

Redirecting electrons to alternative electron sinks is a highly dynamic form of regulation that balances the redox states of the electron transport chain components and thus protects photosynthesis. These alternative electron transports (AETs) involve a variety of mechanisms.

Among them, cyclic electron transports (CETs) (Tagawa *et al.*, 1963) play a crucial role in safeguarding PSI from excessive electron loading by transferring electrons from the PSI acceptor side back to the donor side of the Cyt b_6/f complex. Angiosperms are thought to have two CET pathways (Shikanai, 2014). The first one enables electron transfer from ferredoxin (Fd) to PQ pool via NADH dehydrogenase-like complex (NDH-like) (Yamamoto *et al.*, 2011; Peltier *et al.*, 2016). This complex is homologous to mitochondrial respiratory NAD(P)H:UQ oxidoreductase (Peltier *et al.*, 2016). However, the chloroplast NDH-like complex lacks NADH binding sites and is therefore proposed to react with Fd (Yamamoto *et al.*, 2011). The electron transport by the NDH-like complex is coupled to proton transport from the stroma to the lumen (Kouřil *et al.*, 2014; Strand *et al.*, 2017; Laughlin *et al.*, 2020). Although the molecular features of the NDH-like complex have been characterized, its physiological role in mediating CETs remains questionable (Peltier *et al.*, 2016; Nawrocki *et al.*, 2019; Ma *et al.*, 2021b). This doubt arises from its low stoichiometric ratio (1:100) to PSI (Burrows *et al.*, 1998) and the failure of its turnover rate to compensate for the quantitative deficit (Joliot *et al.*, 2004; Joliot & Johnson, 2011; Trouillard *et al.*, 2012; Nawrocki *et al.*, 2019). Another pathway of CETs in higher plants relies on the Proton Gradient Regulation 5 (PGR5) and Proton Gradient Regulation-like 1 (PGRL1) proteins (Munekage *et al.*, 2004; DalCorso *et al.*, 2008; Hertle *et al.*, 2013; Sugimoto *et al.*, 2013). Plants lacking this PGR5/PGRL1-dependent pathway exhibit low trans-thylakoid ΔpH, leading to compromised rapidly reversible NPQ (Munekage *et al.*, 2004; DalCorso *et al.*,

2008) and limited photosynthesis control (Yamamoto & Shikanai, 2019). Despite the evidence showing that this pathway contributes significantly to CETs (Munekage *et al.*, 2002; Munekage *et al.*, 2004; Nandha *et al.*, 2007; Johnson *et al.*, 2014; Yamori & Shikanai, 2016), there is still a lack of molecular understanding regarding its roles in electron transport (Nawrocki *et al.*, 2019). Some recent studies have explored the responses of CETs to fluctuating light and their roles in regulating linear electron transfer and supporting other photoprotective mechanisms (Suorsa *et al.*, 2012; Kono *et al.*, 2014; Yamori *et al.*, 2016). They showed that without CETs, exposure to fluctuating light leads to more reduced PSI (Suorsa *et al.*, 2012; Suorsa *et al.*, 2013; Kono & Terashima, 2016; Yamori *et al.*, 2016; Shimakawa & Miyake, 2018; Yamamoto & Shikanai, 2019; Zhou *et al.*, 2022).

In addition to CETs, other AET mechanisms also contribute to the dynamic regulation of photosynthesis. These pathways include the water-water cycle (WWC) (Asada, 1999), also known as the Mehler-ascorbate-peroxidase reactions, in which reduced electron carriers at the PSI acceptor side, like Fd, can directly be oxidized by O_2, producing superoxide radicals ($O^{\bullet-}_2$) that can rapidly be converted to H_2O_2. The H_2O_2 produced is then reduced to water by ascorbate peroxidase. Another pathway, plastid terminal oxidase (PTOX)-mediated chlororespiration (Peltier *et al.*, 2010), can also use O_2 as an alternative electron sink, which transfers electrons directly from PQ to O_2. While the content of PTOX under normal environments (only around 1% of the content of the PSII D1 protein) is considered of little relevance for photoprotection (Lennon *et al.*, 2003), in certain species that live in high light and low temperature (e.g., alpine plants), the amount of PTOX can increase reversibly, thus counteracting photodamage (Streb *et al.*, 2003). A further pathway is the malate shuttle, which mediates metabolic interactions between chloroplasts and mitochondria (Laisk *et al.*, 2007; Thormählen *et al.*, 2017). In this process, the reducing power NADPH generated in chloroplasts can undergo re-oxidation by the mitochondrial respiratory chain via the malate-oxaloacetate shuttle (Scheibe, 1987).

Most of these AETs, including CETs, have the potential to increase ATP production by transferring additional protons into the thylakoid lumen without producing the reducing equivalent NADPH (Kramer & Evans, 2011). These compensatory mechanisms address the ATP/NADPH deficit generated from the linear electron transfer for the Calvin-Benson cycle (Allen, 2002; Kramer *et al.*, 2004; Amthor, 2010). In light fluctuations, these AETs could effectively protect the linear electron transport and balance the energy supply and demand between the light reactions and the Calvin-Benson cycle. The rates of dynamic regulation

of AETs may exceed those of rapidly reversible NPQs (**Figure 1.1**). Despite extensive studies, information on the precise mechanisms of AETs in response to light or other environmental disturbances is still lacking.

Activations of enzymes in the Calvin-Benson cycle

Enzyme activation is important for the dynamic regulation of photosynthesis, primarily during the transition from dark or low light to high light. When the Calvin-Benson cycle is inactive, excess reductants on the acceptor side of PSI prompt the flow of electrons from ferredoxin to thioredoxin (Buchanan, 1980). Reduced thioredoxin activates the enzymes in the Calvin-Benson cycle, thereby consuming NADPH and accelerating linear electron flow (Buchanan, 1980). Initiating photosynthesis from an inactive state involves a cascade of events spanning from approximately a few minutes to tens of minutes (Buchanan, 1980; Edwards & Walker, 1983; Woodrow & Berry, 1988; Andersson, 2008). The ribulose 1,5-bisphosphate (RuBP) regeneration is typically activated in about 2-3 minutes, which is related to the activations of fructose-1,5-bisphosphatase (FBPase) and sedoheptulose-1,7-bisphosphatase (SBPase) (Kirschbaum & Pearcy, 1988; Sassenrath-Cole *et al.*, 1994; Kaiser *et al.*, 2015). The activation of the enzyme responsible for CO_2 carboxylation, ribulose-1,5-bisphosphate carboxylase/oxygenase (RuBisCO), takes more time, about 10 minutes or even longer (Mott & Woodrow, 2000; Kaiser *et al.*, 2015). In addition, the Calvin-Benson cycle may experience a transient limitation of inorganic phosphate during photosynthesis induction under some specific conditions (Stitt & Schreiber, 1988; Walker, 1992), which arises from the relatively slower activation of enzymes in sucrose synthesis (Huber & Huber, 1992) compared to those in the Calvin-Benson cycle (Stitt & Schreiber, 1988; Walker, 1992). Slow activations of enzymes in the Calvin-Benson cycle or downstream pathways can restrict the photosynthetic efficiency during induction.

Dynamics beyond the protein scale

In addition to the dynamic regulation of protein-protein interactions at the microscopic level introduced above, the dynamics on larger spatial scales, e.g., thylakoid macrostructure, also play significant roles in coping with light fluctuations. These dynamics involve thylakoid structure re-arrangement, chloroplast movement, and changes in stomatal conductance.

Under different light conditions, the thylakoid structure exhibits a high degree of variability (Johnson & Wientjes, 2020). Compared to conditions in dark-adapted, shaded, or PSI light, the grana diameter decreases (less stacking) with an increasing number of grana per chloroplast under low-intensity white light or PSII light conditions (Rozak *et al.*, 2002; Fristedt *et al.*, 2009a; Pietrzykowska *et al.*, 2014; Schumann *et al.*, 2017; Iwai *et al.*, 2018; Wood *et al.*, 2018; Wood *et al.*, 2019). Conversely, under high-intensity white light, these changes are reversed (Wood *et al.*, 2019), with the grana diameter becoming larger and more stacked than in the dark-adapted condition (Rozak *et al.*, 2002; Fristedt *et al.*, 2009b; Schumann *et al.*, 2017; Wood *et al.*, 2019). In photoinhibitory light conditions, grana diameter becomes smaller (less stacking), probably facilitating PSII repairment (Khatoon *et al.*, 2009; Herbstová *et al.*, 2012; Puthiyaveetil *et al.*, 2014).

On a somewhat larger scale, chloroplasts move toward areas receiving low light to enhance light absorption, while moving away to avoid over-excitation when exposed to strong direct light (Wada, 2013). In angiosperms, the effective wavelength for inducing chloroplast movement is blue light, mediated by specific blue-light photoreceptors: phototropins (Kagawa *et al.*, 2001; Sakai *et al.*, 2001; Banaś *et al.*, 2012).

In contrast to rapid changes in photosynthesis, stomatal responses are slower and often require tens of minutes to match the CO_2 demand for photosynthetic assimilation (Lawson & Blatt, 2014). Delayed opening of stomata upon light intensity increase restricts CO_2 uptake, while delayed closure of stomata in declining light intensity leads to unnecessary water loss (Lawson *et al.*, 2012). This temporal mismatch between stomatal conductance and photosynthetic carbon assimilation (Lawson & Blatt, 2014) limits photosynthetic efficiency under light fluctuations (Lawson *et al.*, 2010). Eliminating this stomatal limitation could significantly increase photosynthetic efficiency in C3 plants (Farquhar & Sharkey, 1982).

There are other regulatory mechanisms that also contribute to the dynamic regulation of photosynthesis, such as the slowly reacting form of NPQ qH (Malnoë, 2018; Malnoë *et al.*, 2018), cyclic electron flow around PSII (Miyake *et al.*, 2002), phosphorylation of PSII core proteins (Martinsuo *et al.*, 2003; Zhang & Xu, 2003; Bonardi *et al.*, 2005), and other related metabolic pathways (Edwards & Walker, 1983). This study focuses on the dynamics and roles of rapidly reversible NPQ and CETs in plant responses to changing light conditions.

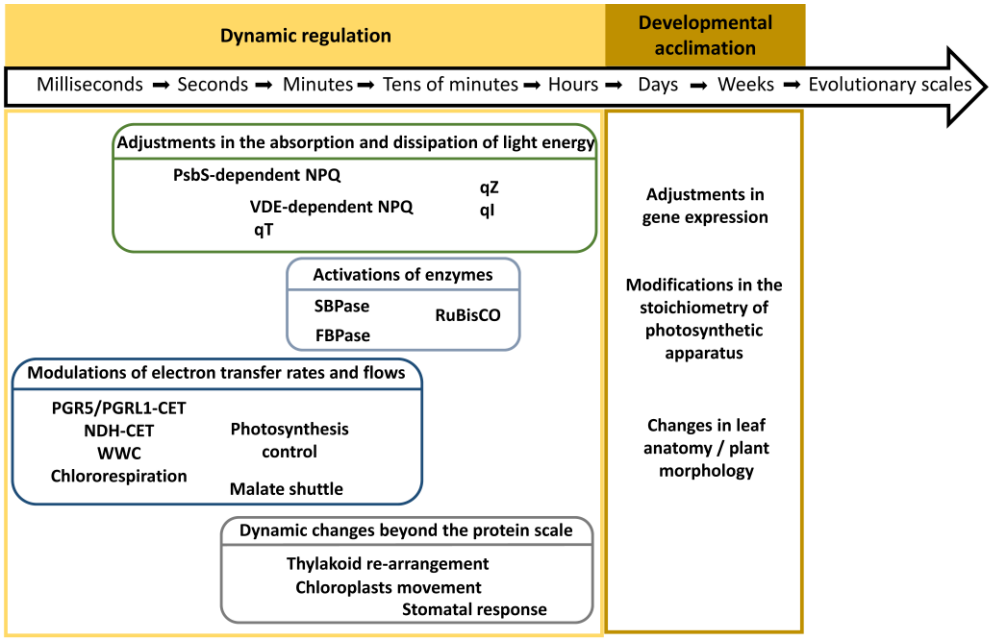

Figure 1.1 This schematic representation illustrates the time scales of dynamic regulation and developmental acclimation of photosynthesis to light environments in higher plants. The dynamic regulation scale spans milliseconds to hours. It encompasses processes such as adjustments in the absorption and dissipation of light energy (PsbS-dependent NPQ, VDE-dependent NPQ, qT- state transition, qI - photoinhibition, qZ - zeaxanthin-dependent sustained quenching), regulation of electron transfer rates (photosynthesis control) and flows (PGR5/PGRL1-dependent CET, NDH-like complex-dependent CET, WWC - water-water cycle, chlororespiration, malate shuttle), activation of the Calvin-Benson cycle enzymes (SBPase, FBPase, RuBisCO), and dynamic changes beyond the protein scales (thylakoid rearrangement, chloroplast movement, stomatal response). At the developmental acclimation scale, regulatory processes include changes in gene expression and protein synthesis, as well as alterations in leaf anatomy and plant morphology. This scheme is modified based on graphs presented by Eberhard *et al.* (2008); Lawson *et al.* (2012); Kono and Terashima (2014). The time scales provided here are derived from various data sources cited in the text, but should not be considered as precise values, as the time scales and the degrees of contribution of these regulatory mechanisms vary depending on experimental conditions and species.

1.3 What determines photosynthetic efficiency?

The inherent design of photosynthesis limits its energy conversion efficiency. In an idealized scenario of Z-scheme and carbon assimilation, eight photons are required to assimilate CO_2 into carbohydrates (Zhu *et al.*, 2008), setting the maximum energy conversion efficiency of carbon assimilation at 0.125. However, achieving this value is essentially impossible in reality due to inevitable energy losses. The theoretical values of maximum photosynthetic energy conversion efficiency were calculated to be 4.6% for C3 plants and 6% for C4 plants, considering energy loss factors such as photosynthetically active spectrum, leaf reflection and transmission, photochemical inefficiency, photorespiration, and so on (Zhu *et al.*, 2010). Despite these theoretical values, the actual maximum photosynthetic efficiency of plants observed in nature is normally much lower and varies considerably among species (Wullschleger, 1993; Hikosaka, 2010; Flood *et al.*, 2011). Genetic backgrounds, i.e., the evolutionary-scale adaptations, determine the ceiling of photosynthetic efficiency of each species (Lawson *et al.*, 2012). Additionally, developmental acclimations that modify plant morphology, leaf anatomy, and biochemistry can also largely influence the actual maximum photosynthetic efficiency (Gilbert *et al.*, 2011; Retkute *et al.*, 2015; Vialet-Chabrand *et al.*, 2017; van Bezouw *et al.*, 2019; Wei *et al.*, 2021). The developmental acclimations, especially to different light conditions, can also shape the capacities of short-term dynamic regulation of photosynthesis (Sassenrath-Cole & Pearcy, 1994; Sassenrath-Cole *et al.*, 1994) and photoprotection (Barker *et al.*, 1997; Alter *et al.*, 2012; Caliandro *et al.*, 2013; Schneider *et al.*, 2019).

The maximum photosynthetic efficiency is typically determined by measurements of O_2 evolution or CO_2 assimilation at different PAR levels. The constraints in photosynthesis described above lead to a bi-phasic response of photosynthesis to incident irradiance, commonly named P-I curves (**Figure 1.2**, blue curve, source: Tracy Lawson *et al*., 2012). In the light limited phase, photosynthetic efficiency is at its maximum and defined by the light-harvesting efficiency, which in turn is modulated by photoprotective mechanisms including NPQ (Kiss *et al.*, 2008; Krah & Logan, 2010; Murchie & Niyogi, 2011; Hasan & Cramer, 2012). Under high light intensity, the trans-membrane electrochemical potential and phosphorylation potential limit the transport of electrons, thus limiting the efficiency of photosynthesis (Murchie & Niyogi, 2011; Hasan & Cramer, 2012; Hoh *et al.*, 2023). This decline in photosynthetic efficiency continues with increasing light, leading to light

saturation of carbon assimilation, accompanied by an elevated risk of photodamage (Hasan & Cramer, 2012). The rate of CO_2 assimilation can become the limiting factor of photosynthetic efficiency in saturating light (Sukenik *et al.*, 1990), which depends on the turnover of RuBP and the balance between carbon assimilation and photorespiration (Zhu *et al.*, 2010; Hasan & Cramer, 2012). Even in the same plant, the maximum photosynthetic efficiency and its applicable irradiance are not universal values but are largely influenced by the leaf growth environments, developmental acclimations, pre-measurement conditions, and the conditions in which the measurements are taken (Zhu *et al.*, 2010; Murchie & Niyogi, 2011; Hasan & Cramer, 2012).

The maximum photosynthetic efficiency obtained from P-I curves is challenging to realize in natural light environments. The real-time rates of carbon assimilation under naturally fluctuating light are in constant flux and do not correspond directly to the steady-state rate of carbon assimilation at the same light intensity in P-I curves (see **Figure 1.2** red dots; source: Tracy Lawson *et al*., 2012). In dynamically changing environments, there is often an imbalance between the amount of energy absorbed and the amount of energy that can be utilized for carbon assimilation, thus necessitating continuous dynamic regulation to protect photosynthesis systems against excess light and electrons (Kramer & Evans, 2011). The actual photosynthetic efficiency in dynamically changing conditions is ultimately determined by a combination of genetic background (Wullschleger, 1993; Hikosaka, 2010; Flood *et al.*, 2011), developmental acclimation to pre-existing environmental conditions (Pearcy & Sims, 1994; Sassenrath-Cole & Pearcy, 1994; Rothstein & Zak, 2001; Oguchi *et al.*, 2005; Alter *et al.*, 2012; Schöttler & Tóth, 2014) and dynamic regulation in response to transient disturbances (Sassenrath-Cole *et al.*, 1994; Külheim *et al.*, 2002; Kramer *et al.*, 2004; Cheng & Fleming, 2009; Kaiser *et al.*, 2019; Murchie & Ruban, 2020). Individual factors limiting photosynthetic efficiency become challenging to discern in fluctuating light conditions.

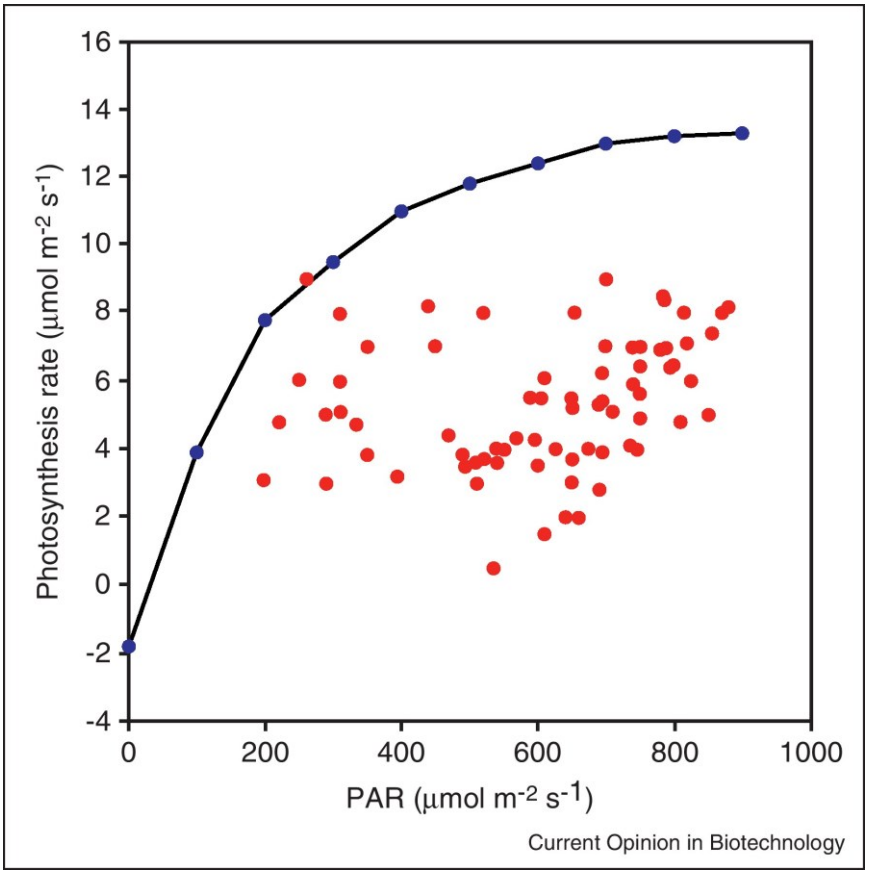

Figure 1.2 depicts the photosynthetic light response curve of *Phaseolus vulgaris*. The solid line illustrates the assimilation rate determined under different steady-state light intensities. These values were acquired at stomatal conductance greater than 400 mmol m^{-2} s^{-1}, carbon dioxide concentration of 360 mmol mol^{-1}, humidity at 1.6 kPa, and 24 °C temperature. The circles represent the observed variations in instantaneous photosynthesis rates recorded at different times for *Phaseolus vulglaris* grown in naturally fluctuating environments. All measurements were conducted on the youngest fully expanded leaves (source: Lawson *et al.*, 2012).

1.4 Difficulties in studying dynamic regulation of photosynthesis

Failure to promptly initiate photoprotective processes can result in photodamage upon rapid increases in light intensity (Kramer *et al.*, 2004; Davis *et al.*, 2017; Hoh *et al.*, 2023), while their slow relaxation may lead to losses in photosynthetic efficiency following sudden decreases in light intensity (Kramer *et al.*, 2004; Zhu *et al.*, 2010; Kromdijk *et al.*, 2016; Davis *et al.*, 2017; Hoh *et al.*, 2023). The dynamic regulatory processes, introduced in **Section 1.2**, are crucial in maintaining energy balance and protecting photosynthesis when the entire system is subjected to changing light environments (Kramer *et al.*, 2004; Eberhard *et al.*, 2008; Zhu *et al.*, 2010; Kromdijk *et al.*, 2016; Davis *et al.*, 2017; Hoh *et al.*, 2023). An in-depth understanding of these fine-tuning mechanisms is necessary to achieve robust and resilient photosynthesis, thereby improving photosynthetic efficiency in natural light, and ultimately enhancing crop productivity (Murchie *et al.*, 2009; Lawson *et al.*, 2012; Hoh *et al.*, 2023).

Much of the current knowledge of photoprotective mechanisms comes from studies of mutants of *Arabidopsis thaliana* or other species (Niyogi *et al.*, 1998; Li *et al.*, 2000; Hashimoto *et al.*, 2003; DalCorso *et al.*, 2008; Murchie & Niyogi, 2011). In mutants, changes in expression levels of key genes associated with specific photoprotective mechanisms lead to changes in their protein abundance that affect the capacities and kinetics of the respective photoprotective regulatory processes (Murchie & Niyogi, 2011). While these efforts have yielded significant advances in our understanding of the molecular mechanisms and physiology related to photoprotection, it is important to note that most of these studies have been conducted on plants grown under controlled conditions. The absence of certain photoprotective mechanisms may have a cascade of effects on plant growth and development in fluctuating light conditions, posing challenges to their survival (Suorsa *et al.*, 2012). As described above, growth environments and developmental acclimations strongly affect plants' capacities of photosynthesis and photoprotection. Thus, plants grown under controlled conditions will not have the equivalent regulatory capacity and dynamics of photosynthesis as seen in the same plants but grown in fluctuating environments.

Constraints in measurement techniques have limited the elucidation of regulatory mechanisms of photosynthesis under natural conditions, as measurements have always been

based on exposing plants to light variations in a single pattern and then tracking its effect on photosynthesis over time (Lawson *et al.*, 2012). Taking the most widely used close-proximity measurement method, pulse-modulated measuring light (PAM) with saturation pulses (SPs) as an example, plants are exposed to actinic light (AL) of constant intensity or an alternating pattern of dark or low light to high light (Kono *et al.*, 2014; Kono & Terashima, 2016; Yamori *et al.*, 2016; Yamamoto & Shikanai, 2019; Zhou *et al.*, 2022), with intermittent applications of multiple-turnover SPs (Schreiber, 2004). On the one hand, as stated above, it subjects plants to light variations in a single pattern to track the response of photosynthesis. On the other hand, some parameters determined with the SP method (e.g., NPQ) need to be measured in dark-adapted plants, which imposes additional constraints on the environmental conditions prior to measurements. This creates a major barrier to the use of these parameters in the greenhouse, field, and natural canopy. Importantly, dark adaptation may dramatically alter the dynamic regulation of photosynthesis compared to what occurs with naturally changing light. This discrepancy arises because thylakoid membranes are not rigid, but energized and rearranged during the dark-to-light transition (Ünnep *et al.*, 2017; Johnson & Wientjes, 2020; Li *et al.*, 2020; Hepworth *et al.*, 2021). Also, conformations of photosynthesis-related proteins undergo changes during the dark-to-light transition (Allen *et al.*, 1981; Horton *et al.*, 1991; Gilmore, 1997; Li *et al.*, 2000; Pascal *et al.*, 2005; Schansker *et al.*, 2011; Magyar *et al.*, 2018; Laisk & Oja, 2020; Sipka *et al.*, 2021). On a more macrostructural scale, re-allocation of chloroplasts (Wada, 2013) may occur during the transition from dark to light. These factors contribute to distinct non-linearities in the photosynthesis systems between darkness and light.

One exciting possibility is the manipulation of photoprotective mechanisms through genetic engineering as a means of improving photosynthetic efficiency and crop productivity. In recent years, this has been demonstrated in a variety of plants. For example, up-regulation of rapidly reversible NPQ-related enzymes and proteins, VDE, PsbS and zeaxanthin epoxidase (ZEP) in tobacco and soybean significantly accelerated the induction and relaxation of NPQ (Kromdijk *et al.*, 2016; De Souza *et al.*, 2022). This led to an improved photosynthetic efficiency under fluctuating light and ultimately increased the yield by 14% to 33% (Kromdijk *et al.*, 2016; De Souza *et al.*, 2022). However, following the same manipulation in *Arabidopsis thaliana*, there was no increase in biomass accumulation (Garcia-Molina & Leister, 2020). Another extensively studied enzyme is SBPase, which determines the rate of RuBP regeneration in the Calvin-Benson cycle (Poolman *et al.*, 2000;

Zhu *et al.*, 2007; Kaiser *et al.*, 2015). Studies on plants genetically manipulated for SBPase activity have shown that decreasing SBPase activity limited photosynthesis and growth in tobacco, rice, and Arabidopsis (Harrison *et al.*, 1997; Harrison *et al.*, 2001; Lawson *et al.*, 2006; Feng *et al.*, 2009; Rojas-González *et al.*, 2015), while increasing its activity enhanced photosynthesis and growth in tobacco, tomato, and wheat (Lefebvre *et al.*, 2005; Rosenthal *et al.*, 2011; Ding *et al.*, 2016; Driever *et al.*, 2017). However, the increase in SBPase activity did not significantly increase rice yield, although rice became more resilient to abiotic stresses (Feng *et al.*, 2007a; Feng *et al.*, 2007b). These contradictory findings suggest that manipulation of photoprotective mechanisms may not have identical effects on different species in different environments. Moreover, many studies using genetically modified plants are still limited to controlled environments and have not been rigorously validated in the large-scale field (Khaipho-Burch *et al.*, 2023).

As described above, photosynthesis is a complex system operating in extremely variable environments (**Section 1.1**) with multiple regulatory mechanisms operating at different time and spatial scales (**Section 1.2**) to maintain robustness, improve photosynthetic efficiency and enhance photoprotection (**Section 1.3**). Existing measurement techniques have their own limitations (**Section 1.4**), making it difficult to clarify the limiting factors of photosynthesis under dynamic conditions (Kaiser *et al.*, 2019). It is also challenging to identify the regulatory mechanisms at play and to quantify their contributions to photosynthetic dynamics in highly fluctuating environments (Eberhard *et al.*, 2008).

1.5 Frequency-domain-based method: Harmonically oscillating light

A technical breakthrough could exist in the utilization of frequency-domain measurements on photosynthesis, i.e., exposing plants to harmonically oscillating light at varying frequencies. Frequency-domain measurements, which are widely employed in physics and engineering to analyze complex systems (Dentino *et al.*, 1978; Kundert & Sangiovanni-Vincentelli, 1986; Keesman, 2011; Pintelon & Schoukens, 2012; Broughton & Bryan, 2018) were introduced to photosynthesis research in 2002 (Nedbal & Březina, 2002). This method revealed that plants, when subjected to oscillating irradiance, exhibit complex periodic patterns of ChlF. The ChlF signal can be deconvoluted into a fundamental component that is modulated at the irradiance frequency, and at least two upper harmonic components (Nedbal & Březina, 2002). Subsequent studies in 2005 identified the strongly non-linear and hysteresis-driven nature of oscillating light-induced signals (Nedbal *et al.*, 2005). These non-linear signals are presumed to reflect the dynamic regulation of photosynthesis under non-steady-state conditions, although systematic studies of these non-linear dynamic signals under harmonically oscillating light are still lacking. Recent attention and development in this method prompted Nedbal and Lazár (2021) to revisit the dynamics of ChlF in green alga *Chlorella* by applying oscillating light with a broad frequency range between 1000 Hz and 0.001 Hz. Their experiments and proposed mathematical models suggested that the occurrence of upper harmonic modulations reflects non-linear phenomena, including photosynthetic dynamic regulation.

Interpreting signals driven by harmonically oscillating light is not as intuitive as traditional time-domain measurements (Boashash, 2015). For instance, in classical induction measurements of photosynthesis starting from darkness, the dynamics can be seen as a series of redox reactions over time from the onset of light. The interpretation of the parameters obtained from time-domain measurements is much more straightforward than the interpretation of the varying parameters of oscillatory modulated reactions driven by harmonically oscillating light (Nedbal & Lazár, 2021). However, the potential of this method lies in its ability to distinguish and perceive responses or regulatory processes within specific ranges of time constants due to the characteristics of frequency-domain-based measurements (Schwartz, 2008; Boashash, 2015).

Any object has its inherent frequency of vibration (Rittweger & Taiar, 2020). When the external vibration frequency corresponds to the entity's inherent frequency, a phenomenon known as resonance occurs (Rittweger & Taiar, 2020). Resonance, a widespread natural phenomenon, manifests from the universe to micro-matter: orbital resonance of celestial bodies (Peale, 1976), resonance of the basilar membrane of the ear and the vocal cords of an animal (Lombard & Hetherington, 1993), acoustic resonance of musical instruments (Wolfe *et al.*, 2009), and resonance of atomic nuclei (Bertsch, 1983; Bortignon *et al.*, 2019), electrons (Ando *et al.*, 1982) and photons (Burke, 1965), etc. When a system is excited externally and forced to vibrate, if the frequency of the external excitation is close to the system's own frequency, the amplitude of the forced vibration can reach a very large value due to the resonance. This particular frequency is called the resonance frequency (Vistnes, 2018; Rittweger & Taiar, 2020). For the photosynthesis systems described above, each step from light absorption to CO_2 assimilation has its specific reaction time constant. In addition, dynamic regulatory processes consisting of multiple components and reactions have their own time constants of activation and deactivation (**Section 1.2**). Therefore, it can be hypothesized that significantly amplified signal dynamics will be exhibited when the frequency of the applied external input (e.g., sinusoidal light oscillation frequency) matches the frequency of intrinsic response or regulation of photosynthesis systems. This could facilitate identification of the frequency ranges in which specific regulatory processes react, or the frequency limit beyond which they cannot react. How, then, does this promote studying the dynamics and regulation of photosynthesis under fluctuating light?

Any random fluctuation of light can be reproduced by superimposing harmonic functions, each determined by the period and amplitude of a sinus and cosinus oscillation (Schwartz, 2008). **Figure 1.3** shows an example of a square sunfleck, e.g., in a forest canopy, that is approximated by seven harmonic components. Natural light fluctuations do not have perfectly sharp edges and the number of contributing harmonic components would be therefore lower than in **Figure 1.3**. Once natural fluctuating light is deconvoluted into its characteristic frequency components, one can ask if the photosynthetic regulatory processes can respond to all of them or if some frequencies are outside the operating range of the regulatory processes and cannot be followed by their response. This can be probed in the laboratory by exposing plants to harmonically oscillating light of a particular frequency and amplitude. I therefore performed frequency-domain analysis in the present thesis focusing

on the frequencies from 1 s^{-1} to 1 / (8·60) s^{-1}, i.e., the oscillation periods from 1 s to 8 min, which correspond to the frequencies of natural sunflecks as introduced in **Section 1.1**.

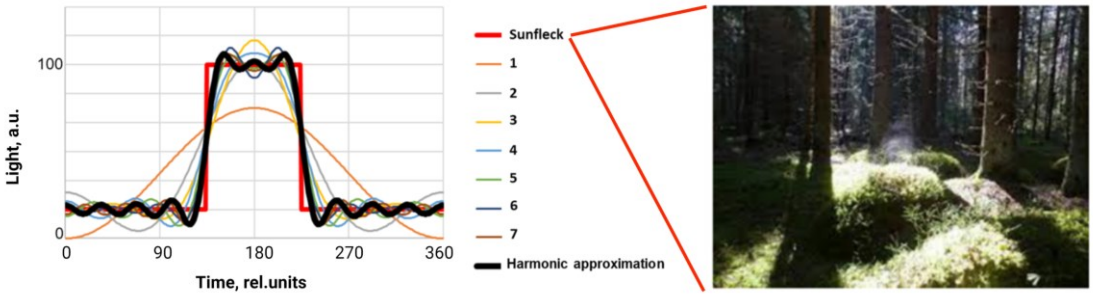

Figure 1.3 An approximation (thick black line) of a square sun fleck (thick red line) by seven harmonic components. The thin colored lines show how the approximation is improving when the number of contributing harmonic component increases from one (orange, 1st -order) to seven (dark brown, 7th -order).

The rate of photosynthesis is linearly proportional to the light intensity only until the constituent redox reactions become saturated (**Figure 1.2**, blue curve source: Tracy Lawson *et al*., 2012). This means that small increases in light intensity would result in proportional increases in photosynthetic electron transfer. If this linear relationship would hold not only in constant light but also in oscillating light, one could simulate photosynthetic response to an arbitrary light fluctuation by the sum of photosynthetic responses to characteristic harmonic components that form the fluctuation. This would mean that the photosynthetic activity occurring during the light fleck in **Figure 1.3** would be modeled by adding photosynthetic responses to the elemental light oscillations shown by the thin lines. Knowing photosynthetic reactions for all frequencies appearing in nature would then allow the prediction of photosynthetic dynamics in any light patterns that can occur in the natural canopy.

This linear approach is limited to very small variations of light intensity under non-saturating conditions in which nothing limits the photosynthetic reactions. Larger increases in light intensity result in non-linearity for two main reasons. First, downstream reactions tend to become saturated at high light, leading to the well-known light saturation (**Figure 1.2**, blue curve source: Tracy Lawson *et al*., 2012). The second type of non-linearity is caused by regulatory processes, such as rapidly reversible NPQ, CET, and photosynthesis control, or by the onset of metabolic limitations (**Section 1.2** & **Section 1.3**). Given that

responses to oscillating light are influenced by non-linear processes (Nedbal & Březina, 2002; Nedbal *et al.*, 2003; Nedbal *et al.*, 2005; Nedbal & Lazár, 2021; Niu *et al.*, 2023), exploring operational frequency ranges of specific molecular processes involves scanning through light oscillation frequencies and identifying the frequencies at which dynamics of the reporter signal (e.g., ChlF) abruptly change between wild-types and the mutants in which those molecular processes are affected. This study investigated the operational frequency ranges of the different regulatory processes by comparing the dynamics of the signals between mutants and their wild-types (**Chapter 2** & **Chapter 4**).

Experimental techniques applied in the frequency-domain are well established, e.g., in time-resolved fluorometry (Lakowicz, 1994). The frequency-domain data are usually measured directly with dedicated instrumentation that scans across the frequency range and applies synchronous detection, yielding amplitudes and phases of the reporter signal as functions of the frequency. Lacking such dedicated instrumentation, I used harmonically oscillating light, recorded the data in time over several periods of light modulation, and recovered the information about amplitudes and phases from time series by a computer de-convolution (**Chapter 2**).

Plants are more complex than linear systems probed by the established techniques. The homologies between various types of complex systems can serve to establish a methodic toolbox for frequency-domain characterization of plants, provided that essential differences between linear and non-linear systems (Leontaritis & Billings, 1985; Regan & Regan, 1988; Billings & Tsang, 1989) are considered:

• The response to harmonic forcing cannot be reduced in plants to the amplitude and phase of a single harmonic component. Several upper harmonic components contribute to the response of plants and their amplitudes and phase shifts should be analyzed (Nedbal *et al.*, 2005; Nedbal & Lazár, 2021).

• Plants are adjusting to their light environment by acclimation. Attention must be paid to the capacity of plants to acclimate not only to the intensity of the light but also to the frequency of the light modulation. In the present study, I limit this kind of "memory effect" by applying only several oscillation periods, just enough to reach the first stationary response pattern (see Materials and Methods in **Chapter 2** & **Chapter 4**).

• The response of plants to light is non-linear and, thus, the time- and frequency-domain characteristics are not necessarily linked by the Fourier transform as common in simpler,

linear systems. Information obtained from time- and frequency-domain measurements may complement each other.

1.6 Aims of this thesis

This thesis aims to systematically investigate the dynamics of plant photosynthesis in response to light oscillations with varying frequencies and amplitudes. By exposing *A. thaliana* wild-type plants and mutants to harmonically oscillating light, the operational frequency ranges of multiple photoprotective mechanisms determined by specific molecular processes have been investigated, thereby elucidating their roles in regulating responses to light fluctuations across different time scales in natural environments. In addition, this thesis also aims to improve the frequency-domain-based harmonically oscillating light method and demonstrate its potential to study the dynamics of photosynthesis. The main research questions are as follows:

- Can the harmonically oscillating light approach effectively identify and distinguish characteristic frequencies of different photoprotective processes that are differentially operating in mutants and wild-types?
- What are the operational frequency ranges or frequency limits of different rapidly reversible NPQ processes and pathways of CET in response to oscillating light?
- How do the different mechanisms of rapidly reversible NPQ and pathways of CET react to light oscillations of distinct amplitudes ranging from limited to saturating light?
- Can frequency-domain dynamic signals be explained by information obtained from time-domain measurements? What unique insights into photosynthetic dynamics that are not attainable through time-domain measurements can be gained from dynamic signals in the frequency domain?

The thesis is organized into five chapters: a general introduction (**Chapter 1**, this chapter), three research chapters (**Chapters 2-4**), and a general discussion (**Chapter 5**).

In **Chapter 2**, the operational frequency ranges of multiple photoprotective mechanisms in light-adapted *A. thaliana* plants were experimentally investigated. Dynamic signals of ChlF yield and the redox changes of key components of the photosynthetic electron transport were monitored under different frequencies of oscillating light in wild-type plants and the

mutants that are deficient in different NPQ processes and CET pathways. The results showed specific operational frequency ranges for rapidly reversible NPQ processes and CET pathways. The experiments in this chapter demonstrated that harmonically oscillating light is a powerful tool to characterize the dynamics of different regulatory processes and to identify their operational frequency ranges.

In **Chapter 3**, I aimed to investigate the roles of rapidly reversible NPQ and CETs in coping with light oscillations with different amplitudes, namely in the limiting light, medium light, and saturating light intensity ranges. Additionally, saturation pulses were superimposed on harmonically oscillating light to link the dynamic signals recorded in harmonically oscillating light (investigated in **Chapter 2**) to widely used ChlF parameters related to photosynthetic quantum yields. The experiments in this chapter highlighted distinct dynamics of the PGR5/PGRL1-dependent CET and the NDH-like complex-dependent CET in responding to different amplitudes of light oscillations, suggesting complementary roles of multiple CETs as well as NPQ mechanisms. Not all dynamic features observed in the frequency-domain measurements could be probed by the corresponding time-domain measurement parameters.

In **Chapter 4**, I focused on characterizing the non-linear relationship between ChlF yield and light intensity under harmonically oscillating light conditions with different frequencies. Based on changing patterns of this relationship in the wild-type and the mutants under harmonically oscillating light with the three amplitude ranges used in **Chapter 3**, different types of non-linear responses were identified and categorized into constitutive and regulatory non-linear responses.

Chapter 5 presents a general discussion summarizing the main findings of the thesis. The two most important notions I postulate are: (1) multiple regulatory processes respond to light fluctuations of different frequencies and amplitudes, thus playing complementary roles, and (2) the harmonically oscillating light approach has a great potential for further development for a wide range of applications in plant photosynthesis research and optical sensing.

Chapter 2

Plants cope with fluctuating light by frequency-dependent non-photochemical quenching and cyclic electron transport

Yuxi Niu [1], Dušan Lazár [2], Alfred R. Holzwarth [3], David M. Kramer [4], Shizue Matsubara[1], Fabio Fiorani[1], Hendrik Poorter[1,5], Silvia D. Schrey[1], Ladislav Nedbal[1,2,6*]

Published as

Niu Y, Lazár D, Holzwarth AR, Kramer DM, Matsubara S, Fiorani F, Poorter H, Schrey SD, Nedbal L. 2023. Plants cope with fluctuating light by frequency-dependent nonphotochemical quenching and cyclic electron transport. *New Phytologist* **239**(5): 1869-1886.

I completed 70 % of the research design and planning and carried out all the experiments. I contributed 75 % of the data analysis and 50 % of the data interpretation. My contribution to the final writing was 50 %.

Abstract

In natural environments, plants are exposed to rapidly changing light. Maintaining photosynthetic efficiency while avoiding photodamage requires equally rapid regulation of photoprotective mechanisms. We asked what the operation frequency range of regulation is in which plants can efficiently respond to varying light.

Chlorophyll fluorescence, P700, plastocyanin, and ferredoxin responses of wild-type *Arabidopsis thaliana* were measured in oscillating light of various frequencies. We also investigated the *npq1* mutant lacking violaxanthin de-epoxidase, the *npq4* mutant lacking PsbS-protein, and the mutants *crr2-2*, and *pgrl1ab* impaired in different pathways of the cyclic electron transport.

The fastest was the PsbS-regulation responding to oscillation periods longer than 10s. Processes involving violaxanthin de-epoxidase dampened changes of chlorophyll fluorescence in oscillation periods of 2 min or longer. Knocking out the PGR5/PGRL1-dependent pathway strongly reduced variations of all monitored parameters, probably due to congestion in the electron transport. Incapacitating the NDH-like complex-dependent pathway only slightly changed the photosynthetic dynamics.

Our observations are consistent with the hypothesis that non-photochemical quenching in slow light oscillations involves violaxanthin de-epoxidase to produce, presumably, a largely stationary level of zeaxanthin. We interpret the observed dynamics of Photosystem I components as being formed in slow light oscillations partially by thylakoid remodeling that modulates the redox rates.

Keywords: cyclic electron transport, frequency analysis, non-photochemical quenching, photosynthetic oscillation, regulation

2.1 Introduction

Plants grow in dynamic environments and can thrive also in rapidly fluctuating light (Müller *et al.*, 2001; Külheim *et al.*, 2002; Long *et al.*, 2022). Repeated filling and emptying of the biochemical pools in fluctuating light may cause damage by generating transient imbalances between tightly coupled redox reactions, potentially producing noxious reactive oxygen species (Pospíšil, 2009; Kono *et al.*, 2014; Kono & Terashima, 2014). Plants limit the damage and optimize their photosynthetic performance in fluctuating light by various regulatory mechanisms that operate with different activation and deactivation rates, which constrain the range of frequencies to which the regulation can effectively respond. Illustrative analogies are the range of audio frequencies that a human ear can hear or visible light range that the human eye can see. Here, we report on the limits of the operation range of photosynthetic non-photochemical quenching and cyclic electron transport in the frequency domain.

Light fluctuations in nature may occur with a wide range of characteristic frequencies. Transient gaps in the upper canopy (Chazdon & Pearcy, 1991), wind-induced canopy movement (Peressotti *et al.*, 2001), and intermittent cloudiness (Knapp & Smith, 1987) give rise to irregular light patterns within canopies (Way & Pearcy, 2012; Smith & Berry, 2013; Kaiser *et al.*, 2018). According to the categorization of light fluctuations in canopy of higher plants established by Smith and Berry (2013), sunflecks were classified as light fluctuations with periods below 8 min, which is also the upper limit of periods investigated here. The short period limit of 1 s of our experiments was dictated by the capacity of the used instrument to generate fast light oscillations.

Complex dynamic light changes occurring in natural environment can be simulated in laboratory by the Dynamic Environmental Photosynthetic Imager (Cruz *et al.*, 2016). The forced oscillations methodology presented here uses a contrasting approach in which the response of plants is stimulated by a light that follows a single sinusoidal variation. The difference between investigating plant's response to complex light patterns and to single sinusoidal variation is analogous to probing absorption by a broad-band and by monochromatic light. Such approaches reveal, in a different way, phenomena that do not appear under artificially static conditions and can thus identify photosynthetic processes important for dynamic responses. The method for investigating irregular or periodic stimulation has long been established in physics (Pintelon & Schoukens, 2012) and the used

terminology is summarized here in **Table 2.1**. Based on universal and widely applied mathematical principles, random fluctuation of light can be reproduced as a superposition of harmonic functions, each determined by the period and amplitude of sinus and cosinus oscillations (Schwartz, 2008). If some of the characteristic elemental oscillations are, for example, too fast and thus outside of the operation range, then, the photosynthetic regulation may be less effective. Similarly, when the operation range is reduced, e.g., by a mutation, one can expect different dynamic responses in elemental oscillating light in the wild-type and in the mutant. The essentials of the frequency-domain analysis are summarized in **Chapter 1** - **Section 1.5**, and *Supplementary materials* ***Figures-SM 2.1***, and in further detail available in Nedbal and Březina (2002); Nedbal *et al.* (2005); Nedbal and Lazár (2021) and Lazár *et al.* (2022). Nedbal and Lazár (2021) looked for the abrupt, qualitative changes in photosynthetic responses to oscillating light that would signal potential limits of operation frequency range in the green alg *Chlorella sorokiniana*. The experiments included light oscillations with periods ranging from 1 ms to 512 s and identified four frequency domains (α_1, β_1, α_2, and β_2), in which oxygenic photosynthesis of the alga exhibited contrasting dynamic features. In the two α domains, the amplitudes of the chlorophyll fluorescence (ChlF) oscillations were found to decrease in algae when the light oscillation was slower. The trend was opposite in the two β domains.

Due to an instrument limitation, a narrower range of light oscillations with periods between 1 s and 8 min was in our focus in this study on higher plants. Two major domains of contrasting dynamics were identified that are labelled here for simplicity without indices: α and β. Detailed measurements in the narrow range revealed an interesting dynamic behavior also in the α/β boundary.

Arabidopsis thaliana is exposed to fluctuating light due to intermittent cloudiness and canopy movements in monoculture as well as natural mixed plant communities (Mitchell-Olds, 2001; Pantazopoulou *et al.*, 2021). It is a model plant that represents well regulation in higher plants and is available with a wide range of well-defined mutations. We used elemental oscillating light with various periods to study its response to light fluctuations in the laboratory. Here, we focus on the responses of various components in the photosynthetic electron transport chain to fluctuating light (**Figure 2.1** a), in particular, on non-photochemical quenching (NPQ) and cyclic electron transport (CET) and their dynamics in fluctuating light (Holzwarth *et al.*, 2009; Ruban, 2016; Yamamoto & Shikanai, 2019; Murchie & Ruban, 2020). The rapidly reversible component of NPQ protects the plant from

transient excess light by sensing the high-light-induced acidification of the thylakoid lumen and reducing the flow of excitation energy to PSII reaction centers (Demmig-Adams *et al.*, 2014a; Ware *et al.*, 2015). This NPQ involves protonation of the PsbS protein (Li *et al.*, 2002a; Roach & Krieger-Liszkay, 2012; Ruban, 2016) and the de-epoxidation of violaxanthin to zeaxanthin by the violaxanthin de-epoxidase enzyme (VDE) (**Figure 2.1** b) (Gilmore, 1997; Jahns & Holzwarth, 2012). In fluctuating light, NPQ deficiency reduced plant's fitness (Külheim *et al.*, 2002) while enhanced NPQ response caused higher photosynthetic efficiency and better growth (Kromdijk *et al.*, 2016; De Souza *et al.*, 2022). Kinetics of NPQ/xanthophyll cycle induction and relaxation in dark-light-dark transitions have been identified, e.g., in Frommolt *et al.* (2001); Wehner *et al.* (2006) and Nilkens *et al.* (2010).

CETs mediate the electron transport from the reduced ferredoxin (Fd) at the acceptor side of PSI *via* plastoquinone pool, Cyt b_6f and PC back to the donor side of PSI (**Figure 2.1** c). By the proton-coupled electron transport, CETs contribute to the proton motive force for ATP synthesis, thus adjusting the ATP/NADPH ratio for downstream carbon assimilation. The CET-induced lumen acidification also contributes to NPQ, and regulates electron transport (Wang *et al.*, 2015), protecting both PSII and PSI (Suorsa *et al.*, 2012; Suorsa *et al.*, 2013; Yamori *et al.*, 2016; Shimakawa & Miyake, 2018; Nakano *et al.*, 2019; Yamamoto & Shikanai, 2019). As in other angiosperms, *A. thaliana* plants possess two CET pathways (Shikanai, 2014). One involves the Proton Gradient Regulation 5 (PGR5) and Proton Gradient Regulation-like 1 (PGRL1) proteins (Munekage *et al.*, 2002; DalCorso *et al.*, 2008; Hertle *et al.*, 2013; Sugimoto *et al.*, 2013) whereas in the other, the electron is transported from Fd to plastoquinone *via* the NADH dehydrogenase-like complex (NDH-like) (**Figure 2.1** c) (Yamamoto *et al.*, 2011; Peltier *et al.*, 2016). This latter pathway acidifies the thylakoid lumen not only by the plastoquinone/plastoquinol proton transport, but the NDH-like complex operates also as an energy-coupled proton pump (Kouřil *et al.*, 2014; Strand *et al.*, 2017; Laughlin *et al.*, 2020). Fluctuating light damaged PSI in plants with a CET deficiency (Suorsa *et al.*, 2012; Kono *et al.*, 2014; Yamori *et al.*, 2016) causing decreased photosynthesis control on the PSI donor side and reduced function of the PSI acceptor side (Yamamoto & Shikanai, 2019).

The first of the objectives of the present study was to identify the limiting frequencies at which the rapidly reversible NPQ responds and beyond which it ceases responding, i.e., to determine the rapidly reversible NPQ operation range. In contrast to the response times

obtained from activation during a dark-to-light induction, e.g., in Wehner *et al.* (2004) and Nilkens *et al.* (2010), the limits of the NPQ operation range in oscillating light depend on an interplay of the activation and deactivation processes that both contribute to plant response to fluctuating light. Towards this goal, we explored the responses to oscillating light of the wild-type, the *npq1* mutant, which cannot convert violaxanthin into zeaxanthin by VDE (Niyogi *et al.*, 1998), and of the *npq4* mutant that lacks the PsbS protein (Li *et al.*, 2000).

The second objective was to discriminate between the roles played in an oscillating light by the two parallel pathways of CET. For this, we contrasted the *pgrl1ab* mutant that lacks the PGR5/PGRL1-dependent pathway (DalCorso *et al.*, 2008), and the *crr2-2* mutant impaired in the NDH-like complex-dependent pathway (Hashimoto *et al.*, 2003) with their respective wild-types.

Understanding of the dynamics in complex systems like plants photosynthesis system requires simultaneous measurements of multiple system variables (Ganusov, 2016; Nedbal & Lazár, 2021) that would enable building robust mathematical models in the future (Kitano, 2001). Towards this third objective, we studied the dynamics of ChlF, and redox changes in P700, plastocyanin (PC), and ferredoxin (Fd) appearing in plants exposed to light that oscillated between light-limited and saturating intensities with periods changing between 1 s and 8 min. Two frequency domains and the boundary range between them were, in this way, characterized by highly contrasting dynamic behavior of NPQ and CET.

By characterizing the operational frequency ranges of the various processed by which plants protect themselves from dynamic changes in their light environment, we will better understand how plants utilize seemingly redundant regulatory processes to maintain the integrity of their photosynthetic machinery in such conditions, without compromising too much on their photosynthetic performance. This research provides the basis for development of novel frequency domain methodologies and instruments in the field of plant science, which will reveal phenomena that do not appear under artificially static conditions.

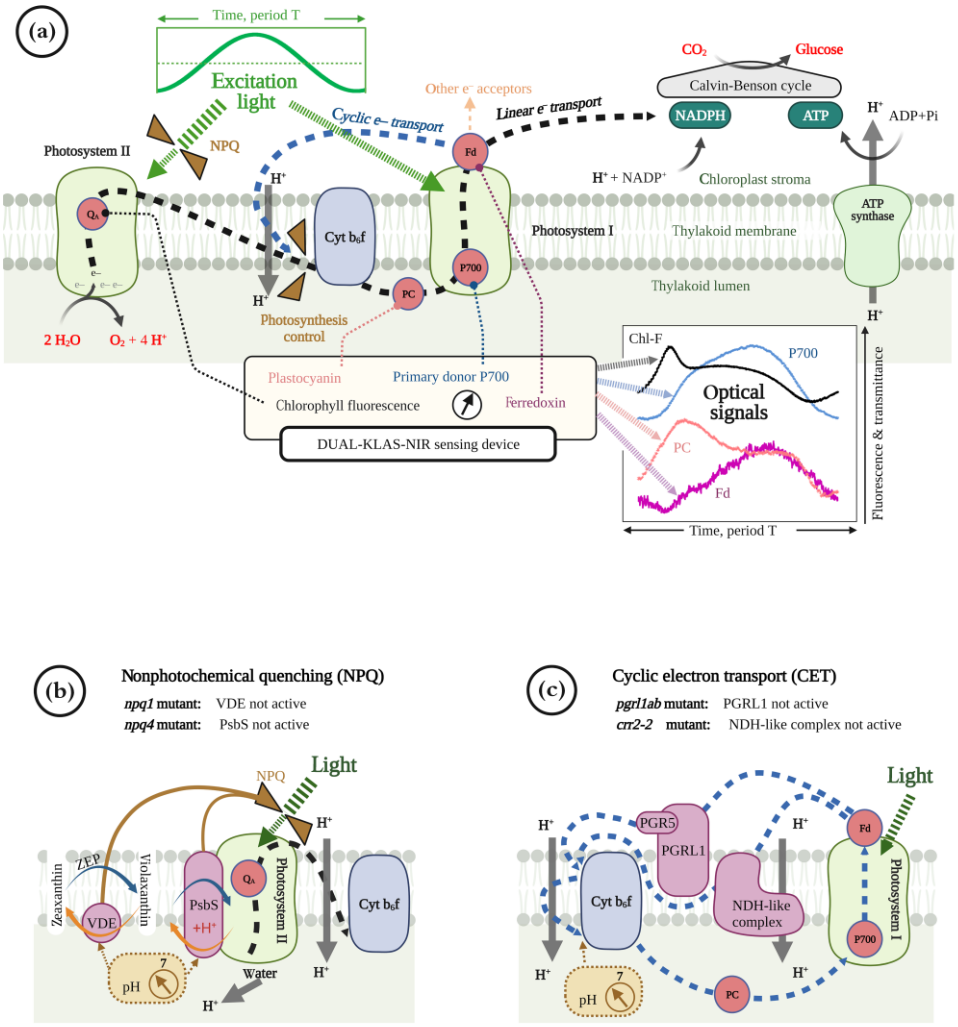

Figure 2.1 a A scheme of the photosynthetic apparatus in *A. thaliana* showing the linear electron transport from water to $NADP^+$ by the black dashed line and the part of the cyclic electron transport around PSI by the blue dashed line. The components that are monitored by the measured optical proxies (bottom right) were: the Q_A redox state determining largely the chlorophyll fluorescence yield (ChlF), plastocyanin (PC), primary donor of PSI (P700), and ferredoxin (Fd). The lumen pH-controlled regulation of PSII light harvesting efficiency (NPQ) and of the electron flow from Cyt b_6/f (photosynthesis control) are indicated by the brown valve symbol. The harmonically modulated light is represented by one period (green line top left). The optical signals measured (bottom right) by the Dual-KLAS-NIR instrument are described in Materials and Methods.

2.1 b The violaxanthin de-epoxidase (VDE) and PsbS protein constitute rapidly reversible NPQ mechanisms that are reducing the excitation of PSII. The zeaxanthin epoxidase (ZEP) is relaxing the quenching. Both mechanisms are induced by low luminal pH. The cycles with blue- and orange-colored arrows represent transitions between low- and high-light states and back that occur periodically during the light oscillations. Orange arrows indicate NPQ induction processes, triggered by increasing ΔpH, while blue arrows indicate the corresponding NPQ relaxation processes.

2.1 c The cyclic electron transport proceeds by two parallel pathways: one *via* the Proton Gradient Regulation 5 (PGR5) and Proton Gradient Regulation-like 1 (PGRL1) complexes and the other *via* the NADH dehydrogenase-like complex (NDH-like) complex. The mutant *pgrl1ab* lacks PGR5/PGRL1-dependent pathway, whereas *crr2-2* lacks the pathway that depends on the NDH-like complex. Both CET pathways lower the luminal pH by the proton-coupled electron transport (Shikanai, 2014).
In all schemes, the down-pointing gray arrows represent all processes leading to the accumulation of protons in the lumen relative to the stroma. The up-pointing gray arrow shows the dissipation of this potential difference by ATP-synthase.

2.2 Materials and Methods

2.2.1 Plant Material and Growth Conditions

Arabidopsis thaliana wild-type Col-0, trichome-lacking wild-type Col-*gl1*, and the mutants affected in NPQ (*npq1, npq4*) and in CET pathways (*pgrl1ab, crr2-2*) were used in the study. Col-0 was the background of the *npq1*, *npq4,* and *pgrl1ab* mutants, and the Col-*gl1* was the background of *crr2-2*. The mutant *crr2-2* was kindly provided by Toshiharu Shikanai, Kyoto University, Japan and *pgrl1ab* by Dario Leister, Ludwig Maximilian University München, Germany. Seeds were sown in commercial substrate (Pikier, Balster Einheitserdewerk, Fröndenberg, Germany). After 3 days of stratification in a 4°C dark room, the seedlings were transferred to a climate chamber with a light intensity of approx. 100 µmol photons·m^{-2}·s^{-1}, 12 h/12 h light/dark photoperiod, 26°C/20°C day/night air temperature, and 60 % relative air humidity. On the 15th day after sowing, the seedlings were transferred to 330 ml pots, one plant per pot filled with a commercial substrate (Lignostrat Dachgarten extensive, HAWITA, Vechta, Germany). The environmental conditions in the climate chamber remained the same as for the seedlings. The plants were watered every day from the bottom to keep soil moisture approximately constant throughout the cultivation and during the experiments.

2.2.2 Chlorophyll fluorescence and KLAS-NIR measurements

In the sixth week after sowing, chlorophyll fluorescence yield and redox changes of PC, P700, and Fd were measured simultaneously using a Dual-KLAS-NIR spectrophotometer with a 3010 DUAL leaf cuvette (Heinz Walz GmbH, Effeltrich, Germany). Red actinic light (630 nm) was applied to both sides of the leaf. The pulse-amplitude-modulated green light (540 nm, 6 µmol photons·m^{-2}·s^{-1}) was applied to the abaxial side of the leaf to excite chlorophyll.

In addition to chlorophyll fluorescence yield, the Dual-KLAS-NIR allows to measure four dual-wavelength difference signals of transmittance simultaneously in the near-infrared part of the spectrum using 780-820, 820-870, 870-965, and 840-965 nm wavelength pairs (Klughammer & Schreiber, 2016; Schreiber & Klughammer, 2016). Four difference signals of transmittance can be deconvoluted into contributions corresponding dominantly to redox

changes of ferredoxin (Fd), primary donor of PSI (P700), and plastocyanin (PC). The deconvolution relies on the selective differential transmittance spectra of P700, PC and Fd for the four wavelength pairs, which were determined by the routine called Differential Model Plots (Klughammer & Schreiber, 2016; Schreiber & Klughammer, 2016). The plots were always constructed with 2-3 replicates. The Differential Model Plot was in this way determined for each genotype and used for the respective spectral deconvolution.

Plants were dark adapted overnight and then remained in darkness until their dynamic properties were investigated by the Dual-KLAS-NIR measurement with constant and oscillating actinic light, all at room temperature of 20°C and in air of natural composition. The measurement started with the NIR-MAX routine on a dark-adapted plant to estimate the maximum oxidation of PC and P700 (100%), and maximum reduction of Fd (-100%) as described in Klughammer and Schreiber (2016). The deconvolution of the overlapping optical transmission signals in near-infrared and the subsequent quantitative interpretation may, to some extent, be compromised by long measuring times, during which the initial deconvolution and min-max parameters may drift due to changing optical properties of the leaf. This would be of utmost importance in long conventional time-domain measurements that rely on stable reference signals, as time-domain measurements are difficult to correct for drift. With harmonically modulated light, one measures relative changes of the redox states of P700, PC, and Fd that are induced by oscillating light and this method is less sensitive to slowly drifting reference levels. The redox changes are quantified here relative to the value found at the trough of the oscillation, i.e., when the light intensity reaches its minimum. The minimum PAR was always 100 μmol photons·m^{-2}·s^{-1}. By using a reference level taken in every oscillation period, we reduced or eliminated the influence of signal drift that may occur over long experimental periods. The dynamic trends occurring during the oscillations were, in this way, assessed using relative changes of the optical proxies named: apparent relative P700 and PC oxidation, and Fd reduction.

It is worth noting specific methodological aspects of the Fd signal. The implicit assumption of the NIR-MAX routine is that Fd is fully oxidized in darkness. This may not be always correct, because Fd can be reduced by multiple pathways, even in the absence of light. This potential caveat may result in an incorrect calibration of the optical proxy and in an apparent drift of the optical signal that is ascribed to fully oxidized Fd. In this situation, Fd-reduction may exceed the expected range of 0 to -100%. Therefore, we shall not base any conclusions here on the absolute numerical values of the Fd-redox state but rather focus on trends in the

Fd-reduction dynamics relative to the value found at the minimum PAR (100 μmol photons·m^{-2}·s^{-1}). Further, it is worth noting that when the charge separation induced by light occurs in the PSI core complex, electron transfer from P700 to Fd occurs in a series of rapid redox reactions through A0 (the monomeric form of Chl *a*) and A1 (phylloquinone) to the [4Fe-4S] clusters (FX, FA, and FB), and ultimately to Fd [2Fe-2S] (Schreiber & Klughammer, 2016). In the case of *in vivo* measurements, distinguishing the absorption changes of Fd from that of the other FeS proteins is practically impossible, as the NIR differential spectrum of FA-FB is similar to that of the Fd (Sétif *et al.*, 2019), and much larger absorption changes caused by other components can influence the signal deconvolution of different FeS proteins. Therefore, the "Fd" signal used in this study is a mixture of signals of FeS components at the PSI acceptor side.

2.2.3 Actinic light protocols

Forced oscillations with changing frequencies

Following induction in constant actinic light of 450 μmol photons·m^{-2}·s^{-1} (630 nm) that lasted 10 min, the plants were exposed to light that was oscillating around this level, between 100-800 μmol photons·m^{-2}·s^{-1}. The frequency (periods) and the number of periods of sinusoidal light were set in the KLAS-100 software (Heinz Walz, GmbH, Effeltrich, Germany). The periods were changing in a single continuous sequence: three periods of 8 min, five periods of each 4 min, 2 min, 1 min, 30 s, and 10 s, and finally ten periods of 5 s and 1 s (*Supplementary Materials* ***Figure-SM 2.2***). The order in which the periods were changing was not affecting our conclusions and the same results were obtained when the periods were in an increasing sequence (*Supplementary Materials* ***Figures-SM 2.4-2.7***). Three biological replicates of each *A. thaliana* genotype were examined.

Analysis of the signals induced by oscillating light

The first period of 8 mins oscillation was largely influenced by the transition from constant to oscillating light and the first two periods of the other oscillations were influenced by the change of light frequency. Because of these reasons, they were not analyzed (one example is offered in *Supplementary Materials* ***Figure-SM 2.2***). The later signals were already periodic and were used to extract the respective dynamic features by numeric analysis. The data representing each respective frequency in multiple replicated plants were averaged to improve the signal-to-noise ratio. The signal averages were then numerically approximated

by a function $Fit(t)$, consisting of a fundamental mode and of 3 upper harmonic modes as described in Nedbal and Lazár (2021):

$$Fit(t) = A_0 + A_1 \cdot \sin[\mathbf{1} \cdot \frac{2\pi(t-\tau_1)}{T}] + A_2 \cdot \sin[\mathbf{2} \cdot \frac{2\pi(t-\tau_2)}{T}] + A_3 \cdot \sin[\mathbf{3} \cdot \frac{2\pi(t-\tau_3)}{T}] + A_4 \cdot \sin[\mathbf{4} \cdot \frac{2\pi(t-\tau_4)}{T}] \quad \text{(Eqn.1)}$$

The least-square fitting procedure was done in MS Excel and the fit yielded the stationary component A_0, and the amplitudes and phase shifts $\{A_1, \tau_1\}$ for the fundamental harmonics, $\{A_2, \tau_2\}$, $\{A_3, \tau_3\}$, $\{A_4, \tau_4\}$ for the upper harmonic components. Typically, no more than 2 upper harmonics were needed as adding the third upper harmonic mode did not improve χ^2 of the fit. The fitted signals of P700, PC, and Fd apparent redox changes were normalized by dividing by the signals obtained at the minimum light level (100 μmol photons·m^{-2}·s^{-1}) as explained above.

2.3 Results

2.3.1 Chlorophyll fluorescence emission

Eight different oscillation periods of light were sequentially applied to identify the characteristic frequency limits of NPQ, and CET. Plants responded to the light changes by ChlF that was alternating in oscillations between minima and maxima around a stationary level A_0 (Eqn.1). Examples of raw data obtained with this protocol are shown in ***Figure-SM 2.2***. The information obtained in these experiments is condensed and represented by simple maximum-minimum differences and by the stationary component in **Figure 2.2**.

The oscillatory ChlF component was calculated as the difference between the respective minimum and maximum of ChlF during one cycle. The stationary as well as oscillatory ChlF components (**Figure 2.2**) were dependent on the frequency of light oscillations in three contrasting ways that can be categorized in the α (frequencies 1 - 1/10 s^{-1}), and β (frequencies 1/120 - 1/480 s^{-1}) domains, and α/β boundary domain whose frequencies 1/30 and 1/60 s^{-1} lead to a distinct resonance in ChlF. The corresponding periods were: 1 - 10 s in the α domain, 30 - 60 s in the α/β boundary domain, and 2 - 8 min in the β domain

(summarized in *Supplementary Materials* in ***Figure-SM 2.1***). The categorization of the frequency domains is compatible with that introduced for green algae in Nedbal and Lazár (2021).

The domain α included the shortest periods of light oscillations. Although the differences between the genotypes were large, the α domain can be defined by ChlF response remaining for each particular genotype largely the same, no matter if the period was 1, 5, or 10 s (**Figure 2.2**). In the boundary α/β domain, the oscillatory ChlF component was typically higher than in the neighboring domains α and β (**Figure 2.2**). This local maximum was reported earlier (Nedbal & Březina, 2002) and attributed to a resonance due to a regulatory feedback. This feature, pronounced in wild-types, was absent in the *npq4* PsbS-deficient mutant and was damped, probably by electron transport limitation, in the *pgrl1ab* mutant (see arguments below).

One should note that the stationary component of ChlF does not exhibit the resonance feature in the α/β boundary domain. It is because the stationary component integrates effects of light that are averaged over many periods and are, thus, frequency independent.

Both the stationary and oscillatory components of the ChlF yield were increasing in the β domain in the *npq1*, *npq4*, and *pgrl1ab* mutants when the period increased from 2 min to 8 min (**Figure 2.2**). This trend was absent in wild-types and *crr2-2*.

The oscillatory components of ChlF in the α, α/β, and β domains are characterized in **Figure 2.2** only by the difference between the minima and maxima. These extremes often appear before or after the minima and maxima of light and **Figure 2.2** does not show the respective phase shift of ChlF. We therefore present additional information about the phase shift of the ChlF extremes and further dynamic details in **Figure 2.3**. This figure shows by a color code the entire dynamics of the oscillatory ChlF signal as it develops with the phase of the light oscillation along the abscissa axis and how it depends on the period of the oscillation along the ordinate axis. The ChlF signal was mostly more complex than a simple sinusoidal variation, containing also strong harmonic components with periods two or more times shorter than the period of the oscillating light. These components are called upper harmonics and are known from other oscillating systems, most illustratively from musical instruments where they determine the timbre. In plants, these upper harmonics are responsible for local rapid ChlF decreases in increasing light and *vice versa* or, in other words, for changes of ChlF response that are much faster than the changing light.

The changes of the ChlF yield in **Figure 2.3** were always induced by the same light pattern (top green line), oscillating between 100 μmol photons·m^{-2}·s^{-1} and 800 μmol photons·m^{-2}·s^{-1}. The line shows the true light pattern that was slightly shifted in phase against the instrument protocol that aimed at generating the light minima at 0° and 360° and maximum at 180°. This instrumental deficiency had no impact on our conclusions.

The data show that both the stationary (**Figure 2.2**) as well as the oscillatory part of the ChlF (**Figures 2.2** & **2.3**) were strongly reduced in WT relative to the *npq1* and *npq4* mutants that lack VDE- and PsbS- dependent NPQ mechanisms, respectively. The most contrasting with WT was the *npq4* PsbS-deficient mutant exhibiting high amplitude ChlF variations that followed closely the light intensity suggesting dominance of photochemical quenching with little interference of NPQ. The ChlF was simply increasing due to reducing of the plastoquinone pool in increasing light and decreasing when the pool became more oxidized in the decreasing phase of the light oscillation. The amplitude of the ChlF oscillations in *npq4* was monotonously increasing from shorter to longer periods.

Unlike the *npq4* PsbS-deficient mutant, the *npq1* VDE-deficient mutant responded to the oscillating light with an overall phase-period pattern that was more complex than in *npq4* and not too different from WT (compare **Figure 2.3** c with a). The ChlF yield maximum in the α/β boundary was found in both *npq1* and WT (**Figure 2.2** c and **Figure 2.3** c). Only the amplitude of ChlF oscillations and the stationary ChlF component were higher in *npq1* than in WT, yet lower than in *npq4* (compare **Figure 2.2** c with a and e). Another difference between *npq1* and WT was found when the period of the oscillating light increased from 60 s to 2 min and longer (β domain). When the periods increased from 2 to 8 minutes, the oscillatory part of the ChlF yield was largely quenched and not changing in the WT (**Figure 2.2** a and **Figure 2.3** a) while it increased by ca. 29% in the VDE-deficient *npq1* mutant (**Figure 2.2** c and **Figure 2.3** c). We conclude that, in the light that was oscillating with increasingly long periods, the VDE-dependent NPQ in WT was able to respond whereas ChlF oscillations appeared with increasing amplitudes in the VDE-deficient mutant. In contrast to this NPQ response, the stationary component of ChlF yield was quenched in the WT when compared to the *npq1* mutant to a level that was about the same in all tested periods (**Figure 2.2** and *Supplementary Materials* ***Figure-SM 2.3***). We conclude that the VDE-dependent NPQ is largely responsible for protection in static or slowly changing light.

The distinct ChlF maximum in the α/β boundary found in all biological replicates of all genotypes that were competent in the PsbS-dependent NPQ mechanism, including WT and *npq1*, was supressed in the *npq4* PsbS-deficient mutant. This PsbS-dependent resonance maximum occurred with the 30 s period in both wild types at 130° phase, that is, ca. 10.8 s after the light started rising from its minimum and, with the 60 s period, at 90° phase, that is, ca. 15 s after the light minimum. The phase shift indicates that the plants and their PsbS-dependent NPQ mechanism required 10 - 20 s to change the trend from rising to declining ChlF in the ascending light phase. More on the resonance phenomenon is available in **Chapter 1** - **Section 1.5** and in *Supplementary materials.* This observed dynamics can be explained by the PsbS protein being necessary for rapid NPQ regulation in light that was oscillating with periods as short as 30 s.

A unique response to oscillating light was found in the *pgrl1ab* mutant that is impaired in the PGR5/PGRL1-dependent pathway. The stationary part of ChlF was much less suppressed in *pgrl1ab* than in WT or in the *crr2-2* mutant (**Figure 2.2**, *Supplementary Materials* ***Figure-SM 2.3***) while the variations around this stationary level that were caused by the light oscillations were by far smallest among all the tested genotypes (**Figure 2.3**). The high stationary and low oscillatory ChlF components can signal congestion of the electron transport chain on the acceptor side of PSII. Unlike in WT and in the *crr2-2* mutant, the variations of ChlF yield in the *pgrl1ab* mutant exposed to long-period light oscillations (β) were stronger than in the short-period oscillations (α) indicating that NPQ became less effective when the periods were long. The dynamic features found in the *pgrl1ab* mutant cannot be attributed solely to impairment of one of the CET pathways. It is likely that the mutation impaired also the linear electron transport and affected induction of NPQ and photosynthesis control (DalCorso *et al.*, 2008; Suorsa *et al.*, 2016; Wada *et al.*, 2021).

The ChlF patterns found with the *crr2-2* mutant were like WT (**Figure 2.2** & **2.3**) suggesting that the response to oscillating light was only marginally affected by knocking out of the NDH-like complex-dependent pathway of CET.

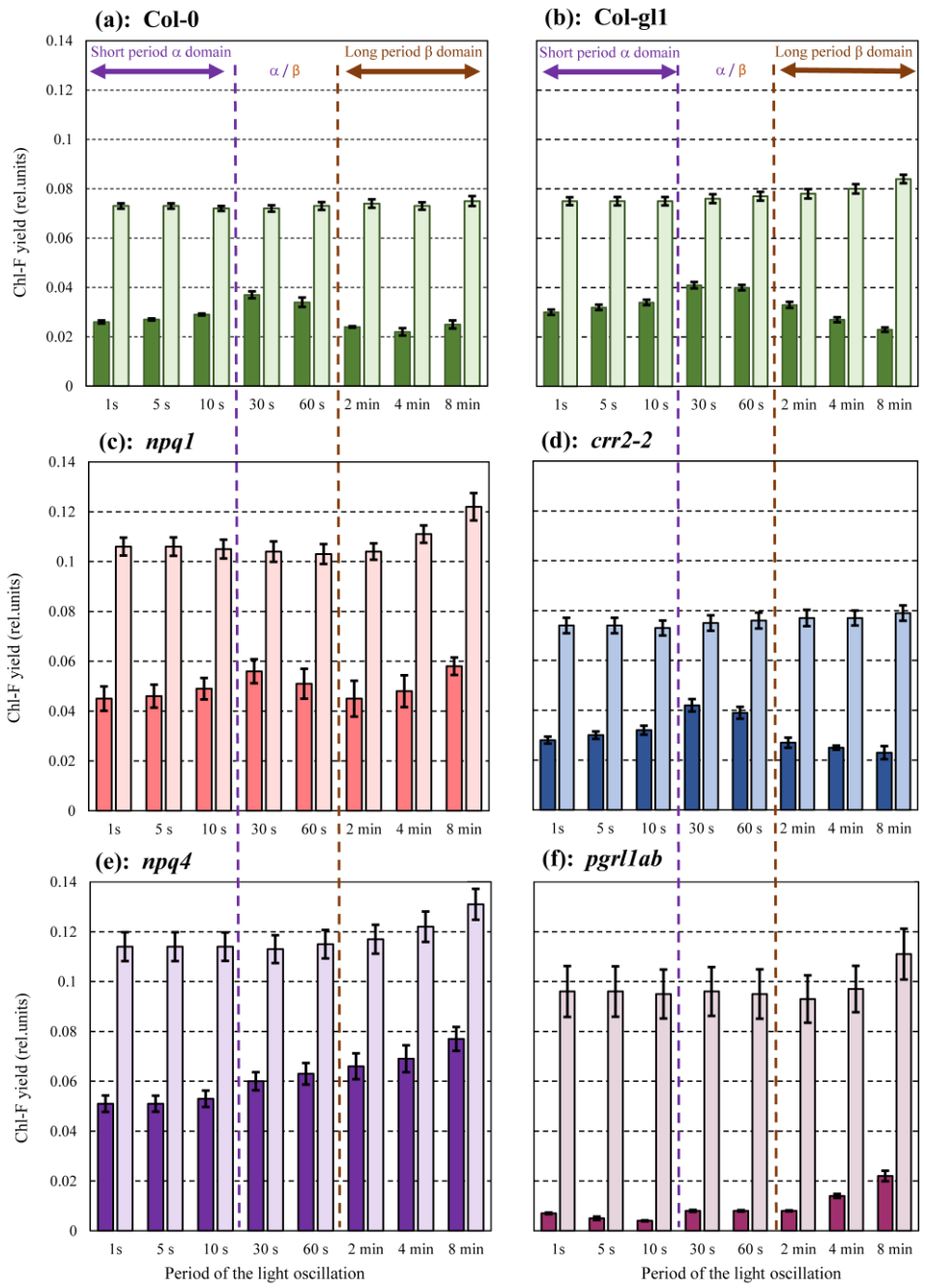

Figure 2.2 The stationary (light-shaded) and oscillatory (dark-shaded) components of ChlF yield measured in 6 genotypes of *A. thaliana* (n=3): (a) wild-type Col-0, (b) wild-type Col-*gl1*, (c) *npq1*, (d) *crr2-2*, (e) *npq4*, (f) *pgrl1ab*. The actinic light was oscillating with short periods of 1, 5, and 10 s (α domain), with periods of 30 and 60 s (boundary α/β domain), and with long periods of 2, 4, and 8 min (β domain). The raw data from which this condensed information was extracted is shown in ***Figure-SM 2.2***. The oscillatory component was calculated as a difference between maximum and minimum of ChlF in one light period. The error bars represent standard errors obtained from three biological replicates.

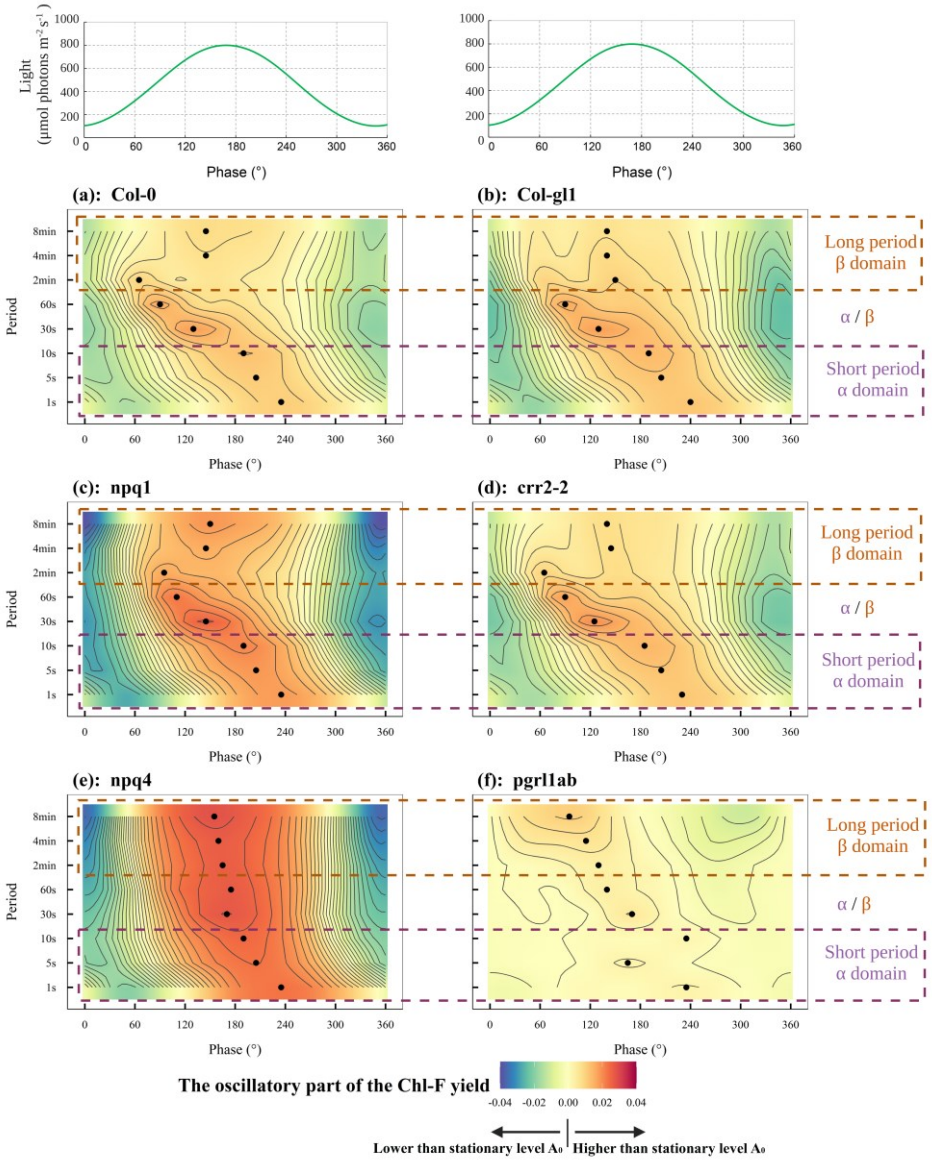

Figure 2.3 Oscillatory part of the relative chlorophyll fluorescence (ChlF) yield. The green line in the top panel represents light that was oscillating between 100 and 800 µmol photons·m^{-2}·s^{-1} with periods in the range of 1 s to 8 min. The progress of the light oscillation and of ChlF response is shown by the phase between 0 and 360°, so that the abscissa is the same for all periods of oscillations that were applied. The other six panels show the oscillatory part of the ChlF yield induced in 6 genotypes of *A. thaliana* (n=3): (a) wild-type Col-0, (b) wild-type Col-*gl1*, (c) *npq1*, (d) *crr2-2*, (e) *npq4*, (f) *pgrl1ab*. Blue colors indicate signals that were below the stationary ChlF yield, representing negative difference in the relative ChlF yield. Red colors represent oscillatory signals above the stationary ChlF yield. The black dots indicate the phase at which maximum ChlF yield at the given period occurred. The contour lines separate signal ranges of 0.0025 of relative units. The brown dashed rectangles indicate long periods of 2, 4 and 8 min (β domain), and the purple dashed rectangles indicate short periods of 1, 5, and 10 s (α domain).

2.3.2 Transmission proxies of PC, P700, and Fd redox states

The frequency responses of apparent relative oxidation/reduction of P700 (**Figure 2.4**), PC (**Figure 2.5**), and Fd (**Figure 2.6**) in oscillating light revealed diverging dynamics of components operating close to Photosystem I. The P700 oxidation was, in all genotypes except the *pgrl1ab* mutant, closely following the oscillating light (**Figure 2.4**). The amplitude of the P700 oscillations was relatively constant for periods shorter than 60 s (α and α/β) but increasing with long periods from 2 to 8 min (β). Compared to other genotypes tested, the *pgrl1ab* mutant showed qualitatively different frequency responses, in which the P700 redox state was largely independent of the oscillating light (**Figure 2.4** f). This lack of variability of the P700 redox state signaled slowing or blockage of electron flow on the acceptor side of PSI in the *pgrl1ab* mutant (Shimakawa & Miyake, 2018). This presumed congestion in the linear electron transport may extend back to PSII and also explain the lack of variability of ChlF that was described above.

The frequency responses of the apparent relative PC oxidation (**Figure 2.5**) depended strongly on the oscillation periods in all genotypes. In a rapidly oscillating light (α), PC was more oxidized in the high light phase than around the light minima. Slow light oscillations (β) elicited a distinct phase dependence, in which PC was increasingly oxidized only in the first phase of the rising light. This trend was changed at a later ascending phase of the oscillation, when the PC oxidation dropped despite light still increasing and a saddle-type depression occurred around the light maximum.

The apparent relative Fd redox states (**Figure 2.6**) were, in WT and the *npq1* and *npq4* mutants, hardly changing between the light minima and light maxima of the rapid light oscillations (α). The NPQ limitations in the *npq1* and *npq4* mutants had only a minor effect on the redox state dynamics of the PSI primary donor P700 and on the PC and Fd dynamics. In the CET mutants, particularly in the *pgrl1ab* mutant, the apparent relative Fd proxy was signaling increasing reduction on the acceptor side of PSI in the strong light relative to the light minima. An apparent Fd reduction was occurring in the *crr2-2* mutant with the periods of 30 and 60 s, i.e., in the α/β boundary (**Figure 2.6** d), where the ChlF yield exhibited a resonance feature in all PsbS-competent genotypes (**Figure 2.3**) including *crr2-2*. In the slow light oscillations (β), the apparent relative Fd-proxy signaled a high oxidation on the acceptor side of PSI around the light maxima relative to light minima in all genotypes except the *pgrl1ab* mutant.

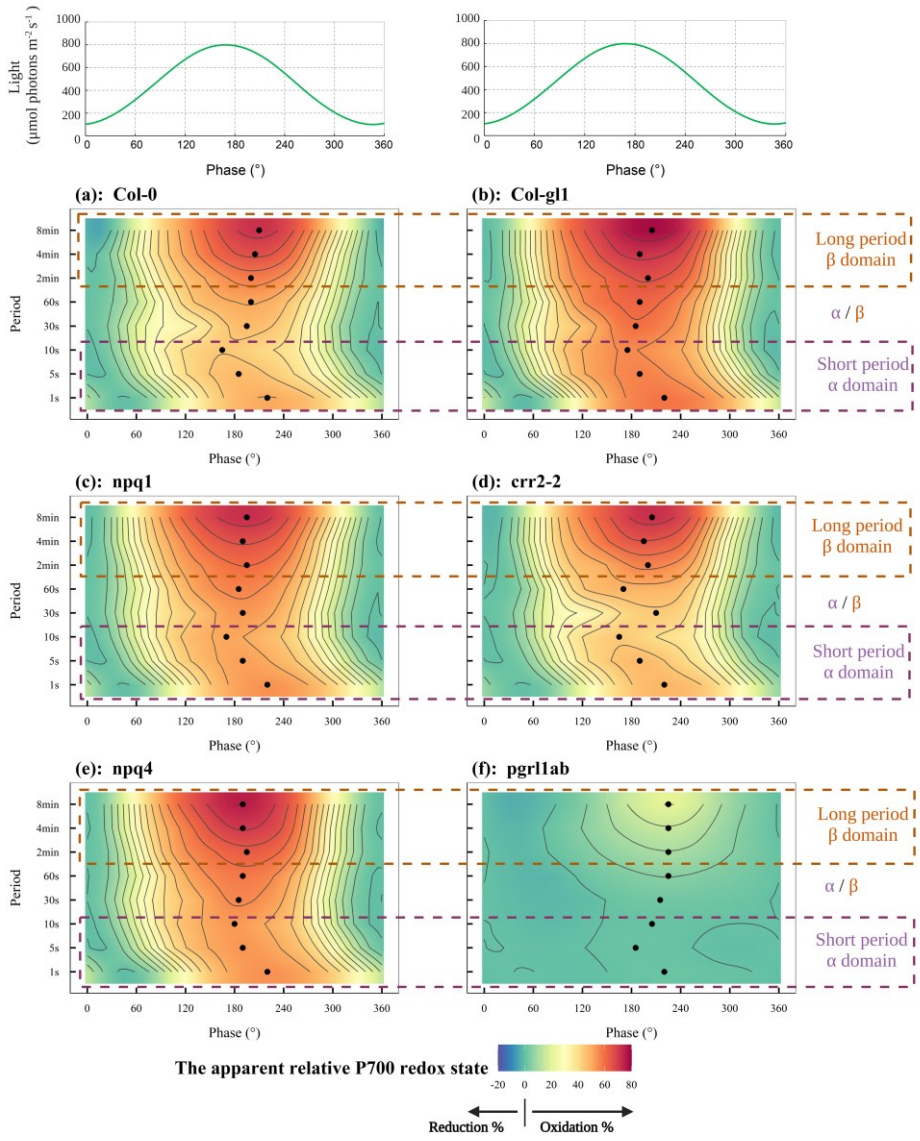

Figure 2.4 Dynamics of primary donor of PSI (P700) in light that was oscillating as shown by the green line in the top panels. The abscissa shows always the phase of the light oscillation. The six other panels show the apparent changes in the P700 redox state in 6 genotypes of *A. thaliana* (n=3): (a) wild-type Col-0, (b) wild-type Col-*gl1*, (c) *npq1*, (d) *crr2-2*, (e) *npq4*, (f) *pgrl1ab*. The dynamics were induced by light oscillating between 100 and 800 µmol photons·m^{-2}·s^{-1} with periods in the range of 1 s to 8 min. The black dots indicate at which phase the maximum of the apparent P700 oxidation at a given period occurred. The color scale ranges from blue to red and represents the apparent oxidation of P700 relative to the state at minimum light level 100 µmol photons·m^{-2}·s^{-1} from low to high. Blue indicates that P700 was more reduced than at the light minimum, while red indicates that P700 was more oxidized than at the light minimum. The contour lines separate signal ranges of 5% of oxidation-reduction. The brown dashed rectangles indicate long periods of 2, 4 and 8 min (β domain), and the purple dashed rectangles indicate short periods of 1, 5, and 10 s (α domain).

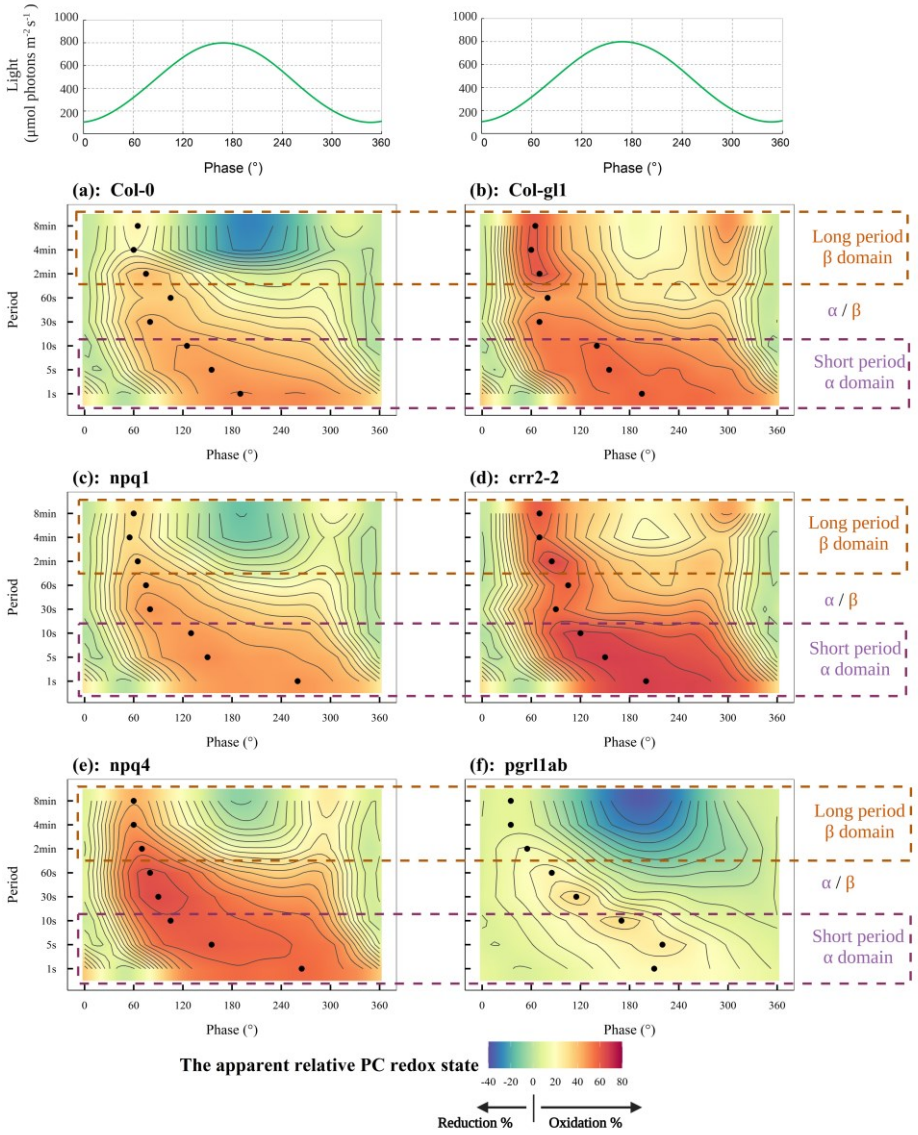

Figure 2.5 Plastocyanin (PC) dynamics in light that was oscillating as shown by the green line in the top panels. The abscissa shows always the phase of the light oscillation. The six other panels show the apparent changes in the PC redox state in 6 genotypes of *A. thaliana* (n=3): (a) wild-type Col-0, (b) wild-type Col-*gl1*, (c) *npq1*, (d) *crr2-2*, (e) *npq4*, (f) *pgrl1ab*. The dynamics were induced by light oscillating between 100 and 800 µmol photons·m^{-2}·s^{-1} with periods in the range of 1 s to 8 min. The black dots indicate at which phase the maximum of the apparent PC oxidation at a given period occurred. The color scale ranges from blue to red and represents the apparent oxidation of PC relative to the state at minimum light level 100 µmol photons·m^{-2}·s^{-1} from low to high. Blue indicates that PC was more reduced than at the light minimum, while red indicates that PC was more oxidized than at the light minimum. The contour lines separate signal ranges of 5% of oxidation-reduction. The brown dashed rectangles indicate long periods of 2, 4 and 8 min (β domain), and the purple dashed rectangles indicate short periods of 1, 5, and 10 s (α domain).

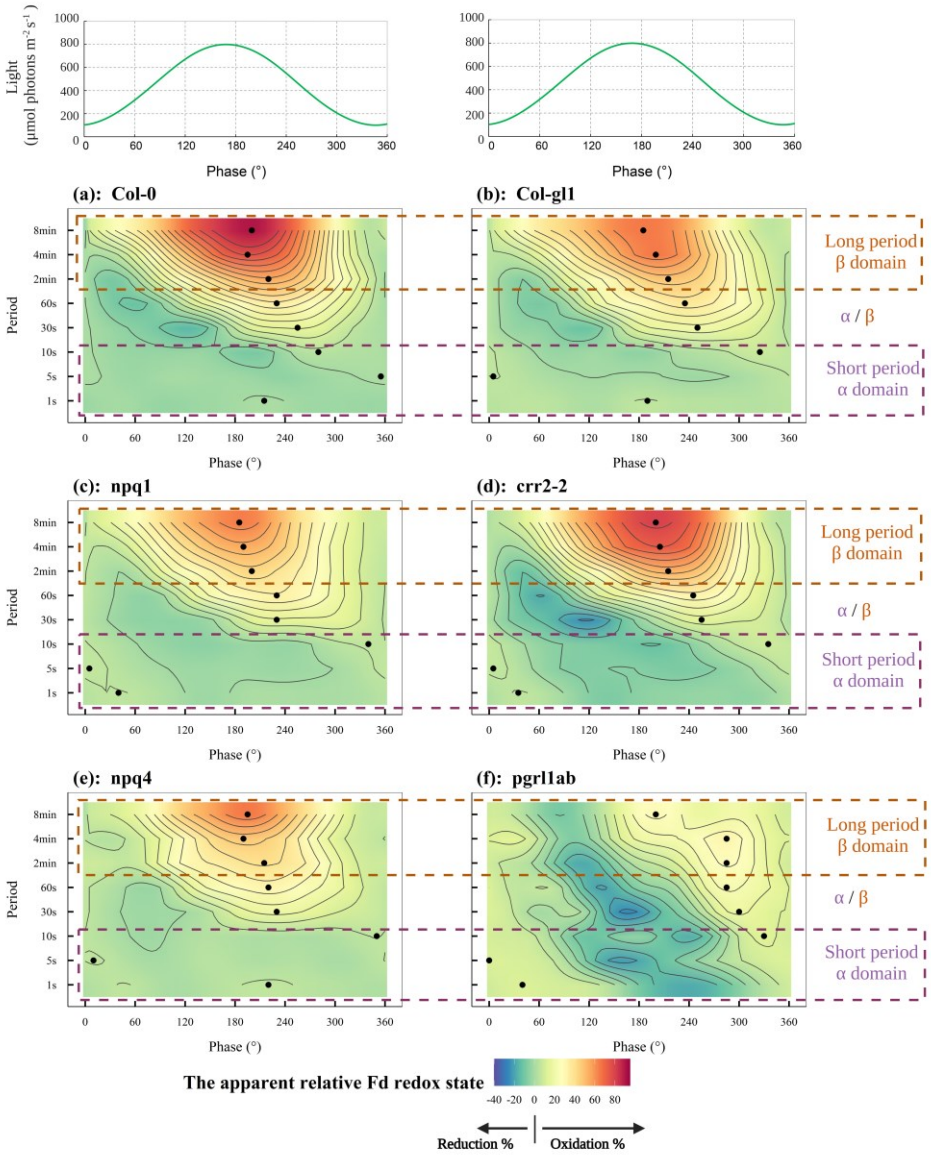

Figure 2.6 The ferredoxin (Fd) dynamics in light that was oscillating as shown by the green line in the top panels. The six other panels show the apparent changes in the Fd redox state in 6 genotypes of *A. thaliana* (n=3): (a) wild-type Col-0, (b) wild-type Col-*gl1*, (c) *npq1*, (d) *crr2-2*, (e) *npq4*, (f) *pgrl1ab*. The dynamics were induced by light oscillating between 100 and 800 µmol photons·m^{-2}·s^{-1} with periods in the range of 1 s to 8 min. The black dots indicate at which phase the maximum of the apparent Fd oxidation at a given period occurred. The color scale ranges from blue to red and represents the apparent oxidation of Fd relative to the state at minimum light level 100 µmol photons·m^{-2}·s^{-1} from low to high. Blue indicates that Fd was more reduced than at the light minimum, while red indicates that Fd was more oxidized than at the light minimum. The contour lines separate signal ranges of 5% of oxidation-reduction. The brown dashed rectangles indicate long periods of 2, 4 and 8 min (β domain), and the purple dashed rectangles indicate short periods of 1, 5, and 10 s (α domain).

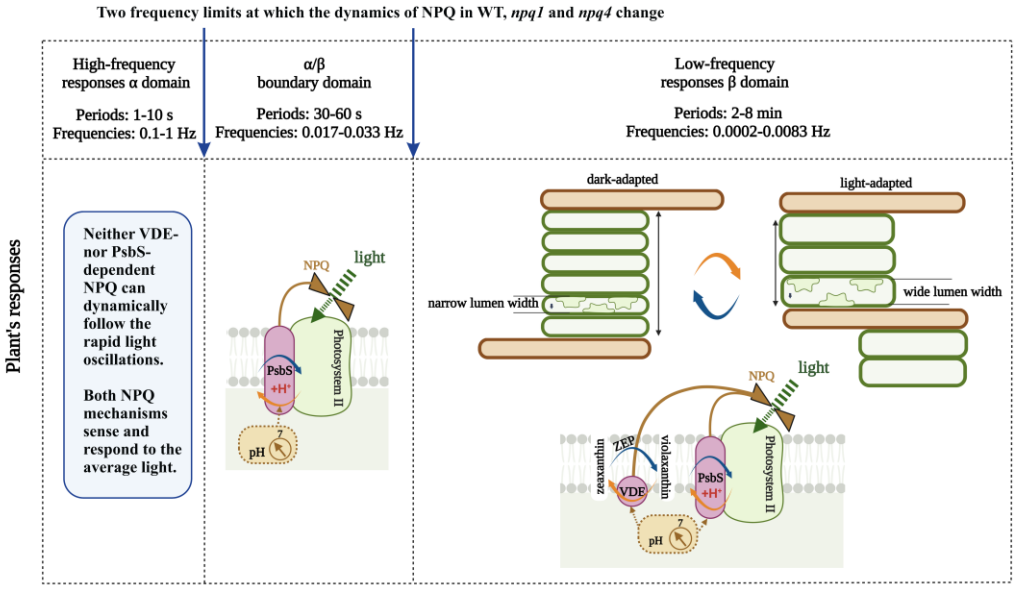

Figure 2.7 Elemental harmonic components contributing to the natural fluctuations are classified into three frequency domains in which distinct dynamic responses occur (α, α/β, β). The scheme here represents a hypothesis that is proposed to explain the observed frequency responses of wild-types and *npq1* and *npq4* genotypes in these three domains. The NPQ response in the α/β boundary domain is proposed to be PsbS-dependent. The response to slow oscillations in the β-domain is in addition formed also by VDE-dependent NPQ that is tentatively proposed to occur with periodic reorganization of the thylakoid membrane. The dark- or low-light-adapted thylakoids are organized in large grana with narrow lumen space, reducing the area of contact between the grana membranes (green ellipses) and stromal lamellae (brown ellipses). With increasing the light intensity towards the maximum of the oscillation in our study, the thylakoids were proposed (Wood *et al.*, 2018; Johnson & Wientjes, 2020) to be reorganized into numerous smaller grana, creating a larger area of contact between the grana membranes (green ellipses) and stromal lamellae (brown ellipses). Thylakoid lumen volume is proposed to expand with increasing light intensity and shrink when the light is decreasing (Kirchhoff *et al.*, 2011). The lumen pH-controlled regulation of PSII light harvesting efficiency (NPQ) is indicated by the brown valve symbol. The cycles with orange- and blue-colored arrows represent transitions between low- and high-light states and back that may occur periodically during the light oscillations. Orange arrows indicate NPQ induction processes, triggered by increasing ΔpH, while blue arrows indicate the corresponding NPQ relaxation processes. ZEP, zeaxanthin epoxidase.

2.4 Discussion

The regulation of plant photosynthesis has its operating frequency range in which the contributing molecular mechanisms can function. This study employed harmonically oscillating light with different frequencies to identify the frequency limits of multiple photosynthetic regulatory processes. When the light oscillations exceed these limits being, e.g., faster than the limit, the regulation responds only to the average of the light but cannot compensate for the rapidly changing light intensity. The transition at the limiting frequency of the operating range was manifested here by the changing dynamic response of plant photosynthesis, here ChlF, and the PC, P700, and Fd proxies, to light oscillations.

This work identified three types of plant responses that occurred in three frequency domains of light oscillations (α, α/β, β) that often occur in plant canopies. The three domains are separated from each other by two frequency limits that were identified here by qualitatively changing NPQ dynamics in wild-type and the *npq1* and *npq4* mutants (**Figure 2.3**). This led us to formulate the hypotheses on two frequency limits of PsbS- and VDE-dependent NPQ that limit the operation range in natural fluctuating light: the first separating the domain α from α/β at about 1/10 - 1/30 s^{-1} and the second between the domains α/β and β, by the separating limit at about 1/60 - 1/120 s^{-1} (**Figure 2.7**). The contrasting responses of the *crr2-2* and *pgrl1ab* CET mutants also supported the hypothesis that parallel pathways or mechanisms acting towards the same function respond differently in the α, α/β, and β domains of the oscillating light.

2.4.1 Light oscillations in the α domain were too fast to be followed by NPQ

The light oscillations in the α domain were rapid and NPQ, being unable to follow the fast changes, responded mainly to the average irradiance. This static NPQ response reduced both stationary as well as oscillatory components of ChlF and was strongest in wild-type's that were competent both in the PsbS- as well as VDE-dependent quenching and it was weakest in the *npq4* PsbS-deficient mutant. The PC, P700, and Fd proxies were also following the rapid light modulation in the α domain with a small delay which can be expected for the unregulated system of reactant pools that are filled and emptied by photosynthetic light reactions (**Figures 2.4 - 2.6**). The delay was larger for the faster light oscillations indicating

inertia of the pools. The only exception was the *pgrl1ab* mutant in which the electron transport was presumably congested, eliminating largely any variability (Shimakawa & Miyake, 2018).

2.4.2 Light frequencies in the boundary domain α/β elicited resonant enhancement of ChlF oscillations

The boundary α/β domain, represented here by the periods 30 and 60 s, was characterized by a crest maximum of ChlF that was found in plants competent in the PsbS-dependent NPQ and was absent in the *npq4* mutant missing PsbS (Li *et al.*, 2000). This dynamic feature can be assigned to the onset of the PsbS-dependent NPQ in light periods as short as 30 s. We propose that with these short periods, the VDE-dependent NPQ was unable to respond fast enough and the PsbS-dependent NPQ defined the plant's dynamic response in this domain alone (**Figure 2.7**). The PsbS-dependent regulation activated in the α/β domain, marked by an increase of ChlF may thus be responsible for the resonance identified earlier (Nedbal & Březina, 2002) and also may play a role in the spontaneous oscillations in plants that also occur with a period around 60 s (Delieu & Walker, 1983; Lazár *et al.*, 2005), i.e., within the α/β domain. More on the resonance and spontaneous oscillations is available in *Supplementary Materials - Connection between forced and spontaneous oscillations and the resonance phenomenon*. Despite the striking similarity between the resonance frequency and the frequency of spontaneous oscillations, involvement of PsbS-dependent regulation in the spontaneous oscillations of plants remains to be tested by future direct experiments that would also clarify if there were a synergy with activation of the Calvin-Benson cycle (Kaiser *et al.*, 2016; Graham *et al.*, 2017).

2.4.3 The slow light oscillations in the β domain permitted a complex plant response

The oscillatory component of the ChlF yield was in the β domain in wild-type strongly suppressed by PsbS- as well as VDE-dependent NPQ. The redox changes near PSI that were induced by slowly oscillating light occurred in wild-type, however, with high amplitudes despite the efficient NPQ. The contrast between the PC and P700 redox changes during the slow light oscillations (**Figures 2.4** & **2.5**) was found also in the *crr2-2* and *pgrl1ab* mutants that were impaired in the CET pathways. We propose that the contrasting dynamic behavior

of the PSI components might be caused by a periodic light-induced reorganization of the thylakoids that may differently affect PC and P700 (Ruban & Johnson, 2015; Ünnep *et al.*, 2017; Johnson & Wientjes, 2020; Li *et al.*, 2020; Hepworth *et al.*, 2021). Other alternative explanations for the observed slow changes could be the activation and de-activation of the Calvin-Benson cycle (Kaiser *et al.*, 2016; Graham *et al.*, 2017), malate shuttle (Thormählen *et al.*, 2017), chloroplast movements (Kihara *et al.*, 2020), or changing stomata conductance (Matthews *et al.*, 2018; Li *et al.*, 2021). The last two alternative mechanisms are however unlikely because we have not used blue light excitation that is known to elicit chloroplast movements and the light changes were in our experiments too fast to be followed by the stomata aperture. Based on our results, slow light oscillations up to the period of 8 min are proposed to elicit periodic changes of PsbS-and VDE-dependent NPQ together with periodically changing thylakoid organization (**Figure 2.7**). The effect of such a concerted regulation is small in the PsbS-impaired *npq4* mutant and limited in the VDE-impaired *npq1* mutant, indicating that PsbS, VDE, and thylakoid reorganization (Horton & Ruban, 2005) are required for fully functional regulation in the slowly oscillating light.

According to this model (**Figure 2.7**), the PsbS-dependent NPQ plays an indispensable role in the plant's response to light that oscillates in the α/β and β domains. The *npq4* mutant impaired in this function will, in a natural fluctuating light with a range covering 30 s to 8 min, experience largely undamped oscillations in its electron transport chain and, most likely suffer from a dynamic load stress even though PAR may remain in the oscillations far below high levels that would cause photoinhibition in a static light.

2.4.4 On the complementarity of the time- and frequency-domain experiments

It is important to note that the widely explored dark-to-light induction yields information that is not equivalent to the information obtained from plant response to oscillating light or to natural fluctuating light. Namely, rate constants obtained in dark-to-light induction experiments may co-determine the frequency limits in a, potentially, complex way. The rate constant of antheraxanthin accumulation 1/130 – 1/260 s^{-1} reported in Wehner *et al.* (2006) for different lhcb complexes is not far from the lower frequency limit that we found separating the α/β domain from β (1/60 - 1/120 s^{-1}). Other work (Nilkens *et al.*, 2010) characterized the NPQ response by two characteristic time constants. In wild-type, they

found a fast component with 70% relative contribution responding with a characteristic time of 60 s and a slower 30% component with 570 s. In mutant plants, the components were 50% and 50% and appeared with characteristic times of 460 and 2600 s in *npq4* and 9 and 1600 s in *npq1*. We underline however that the experimental protocol in Nilkens *et al.* (2010) is fundamentally different compared to ours because dark-to-light experiments map the entire transition of plants from neutral pH in lumen (no NPQ) to acidic pH in lumen (active NPQ). The oscillating light in our experiments, however, never dropped below 100 μmol photons·m^{-2}·s^{-1} and pH in the thylakoid lumen was likely also oscillating in already acidic range and NPQ was already largely activated. The dynamic response of NPQ in our experiments reflected coupling of oscillating light and pH changes in the acidic range and further to activation and de-activation of molecular processes that involve PsbS and VDE and that control antenna excitation and, eventually, ChlF. One can further illustrate the difference between the rate constants measured in dark-to-light induction experiments and the frequency limits identified here using the VDE-dependent NPQ. The conventional time-domain induction experiments reveal dominantly the de-epoxidation of violaxanthin into antheraxanthin and zeaxanthin whereas the frequency limit found in the oscillating light would depend both on the de-epoxidation dominating in the rising light and the relatively slow epoxidation in the declining light. We propose that antheraxanthin and zeaxanthin produced during the pre-illumination and high-light phases of the oscillation did not significantly decline during the relatively short periods of low light during the oscillation. This could change in higher temperatures at or above 25°C when the epoxidation is faster (von Bismarck *et al.*, 2021). Our hypothesis about stationary concentrations of antheraxanthin and zeaxanthin in fluctuating light needs to be further tested also by experiments in which the xanthophyll concentrations in the leaves would be directly measured during the light oscillation. The methodology described in Nilkens *et al.* (2010) cannot however be used for the range of periods applied here and, therefore, methods with a higher time resolution will need to be applied. This future development is required to test the hypothesis that the VDE-dependent oscillatory NPQ in the tested frequency range requires zeaxanthin or antheraxanthin to be present, but that the respective NPQ periodic changes are not caused directly by oscillating xanthophyll concentrations.

2.4.5 Outlook

Experiments using the KLAS-NIR spectrometer also revealed that the redox changes in and near PSI that were induced by oscillating light remained highly dynamic despite effective NPQ regulation in WT plants. The dynamic changes around PSI were largely independent of the mutations affecting NPQ. In the slow oscillation β domain, the dynamics of P700 were profoundly different from those of PC (**Figures 2.4** & **2.5**). This may seem contradictory to the close interaction between the two redox components, with PC shuttling electrons from Cyt b_6/f to P700. We propose that unlike P700 dynamics, the PC dynamics is modulated by a factor that connects both photosystems, such as photosynthesis control (Suorsa *et al.*, 2013; Colombo *et al.*, 2016; Johnson & Berry, 2021) and/or systemic properties such as changing thylakoid topology (Ünnep *et al.*, 2017; Johnson & Wientjes, 2020; Li *et al.*, 2020; Hepworth *et al.*, 2021) that affects PC diffusion (Kirchhoff *et al.*, 2011). The remodeling of the thylakoid membrane structure in slowly oscillating light may affect pronouncedly the heterogeneity of the plastoquinone pool and Cyt b_6/f in granal and stromal segments of the thylakoid membranes (Joliot *et al.*, 1992; Kirchhoff *et al.*, 2000; Malone *et al.*, 2021). The PQ pool in the grana thylakoid domains participates in the linear electron transport from PSII to Cyt b_6/f whereas the PQ pool in the stromal thylakoid domains serves primarily for CET (see **Figure 2.1**). Further, one ought to consider that PC transports electrons from Cyt b_6/f to P700 over long distance (Höhner *et al.*, 2020), presumably with a low probability of backward electron transfer from P700 to PC and is subject to photosynthesis control (Johnson & Berry, 2021). The proposed effect of the thylakoid remodeling on the photosynthetic dynamics needs to be further examined because it may entail fundamental consequences for studies that are based on the dark-to-light transitions in the time domain. Unlike these traditional experimental protocols, the frequency-domain experiments employing oscillating light are applied to light-adapted plants rather than to plants that change from dark-adapted to light-adapted state.

Identifying and quantifying frequency limits for operation of regulatory mechanisms and alternative pathways in plants exposed to oscillating light holds promise for improvements of photosynthetic efficiency in nature under fluctuating light. This may parallel the tremendous success of applying frequency domain analysis in engineering and other fields of science (Ogata, 2010). At the molecular level, our work is broadly important in directly supporting the discovery of processes responsible for the regulation of photosynthetic electron fluxes and redox homeostasis in fluctuating light environments mimicking natural

conditions. We also anticipate that at the leaf tissue level new insights will be gained regarding the coupling of electron transfer with stomatal conductance and photosynthetic rates and the acclimation of these processes to fluctuating light environments (Matthews *et al.*, 2018).

Based on these considerations, novel screening assays could be devised to characterize physiological manifestations of mutations and genetically diverse germplasm. These assays could detect altered metabolic control networks and support the identification of genetic mechanisms controlling dynamic responses to fluctuating environmental conditions. The potential applications of the methodologies presented here range from the integration in automated plant phenotyping platforms in controlled environments and greenhouses to the use in plant agro-ecological research through newly designed portable devices.

Table 2.1: Glossary of terms	
amplitude	the maximum deviation from a mean; in the case of harmonically modulated light, it is one half of the difference between the light intensity maximum and minimum
angular frequency ω	the parameter of light modulation or of plant response that defines how many times a full cycle (360° in angle degrees or 2π in radian units) is completed in a unit of time. It is related to the period T as: $\omega = \frac{2\pi}{T}$
fluctuating light	randomly changing light: its intensity pattern thus cannot be predicted
forced oscillation	a repeating variation pattern of plant photosynthesis that is sustained in time by a *periodic* energy supply, here *harmonically modulated light*
frequency-domain measurement	the measurement of plant activity applying *harmonically modulated light* with *period*/*frequency* of the light modulation changing over a wide range; plant response(s) are measured as a function of the light modulation *frequency*
harmonically modulated light	the light intensity that consists of a variable part that is changing as a harmonic function $$a * \sin\left(\frac{2\pi}{T} \cdot t\right) + b * \cos\left(\frac{2\pi}{T} \cdot t\right)$$, where t stands for time, T is the *period*, $\frac{2\pi}{T}$ the *angular frequency* of the light variation, and a, b are parameters that define together the *amplitude* and *phase* of the light modulation.
oscillation	a repeating variation pattern of light or plant activity
period T	the time after which a process is repeated, here it applies both to the light modulation as well as to plant response elicited by the modulated excitation light
periodic	Repeating
oscillation phase	the parameter defining the progress of a periodic process: e.g., phase 0 is the origin, the phase $\frac{1}{4} \cdot 2\pi$ represents one-quarter of the full cycle, phase 2π represents the full cycle
resonance	a phenomenon of the increased *amplitude* of a measured response that occurs when the *frequency* of external forcing agrees with an internal characteristic *frequency* of the examined plant (sometimes called eigen-frequency)
spontaneous oscillation	the *oscillation* of plant activities that sometimes appear in response to an abrupt change of external conditions; spontaneous oscillations of plants are fading over time
time-domain measurement	the meaning common in fluorometry or spectroscopy of plants: the plant response to an aperiodic light change; mostly a stepwise dark-to-light or light-to-dark transition, often also the response to a short light flash measured as a function of time

Acknowledgements

Y.N., S.D.S., and L.N. gratefully acknowledge the financial support from the Federal Ministry of Education and Research of Germany (BMBF) in the framework of the YESPVNIGBEN project (03SF0576A).
D.L. and L.N. were supported by the European Regional Development Fund project "Plants as a tool for sustainable global development" (CZ.02.1.01/0.0/0.0/16_019/0000827).
D.L., S.M., and L.N. gratefully acknowledge the financial support by HORIZON-EIC-2021-PATHFINDER OPEN project DREAM (grant agreement No 101046451)
Work by DMK was supported by the U.S. Department of Energy (DOE), Office of Science, Basic Energy Sciences (Kok) under Award no. DE-SC0007101.

Author Contribution

YN, SM and LN planned and designed the research. YN performed experiments. YN, SDS, and LN analyzed data. YN, DL, ARH, DMK, SM, SDS, and LN interpreted the results. YN, DL, ARH, DMK, SM, FF, HP, SDS, and LN wrote the manuscript.

Supplementary materials

Plants grow in light that often fluctuates. The frequencies of the light fluctuations can be categorized in domains in which plants respond similarly. The concept of frequency domains was introduced for green algae in Nedbal & Lazár (2021). The ***Figure-SM 2.1*** below illustrates a schematic representation of the three domains investigated in this study in higher plants.

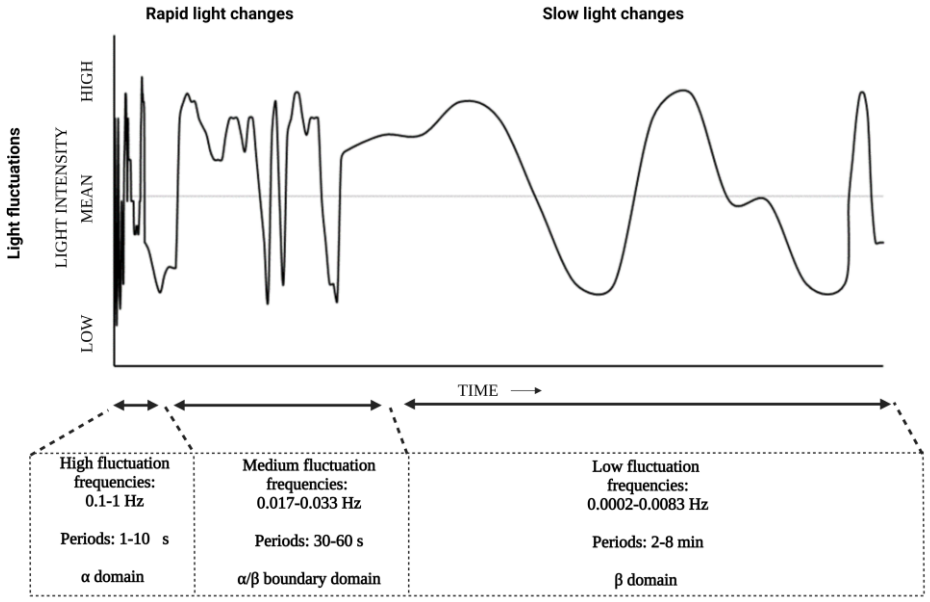

Figure-SM 2.1 Schematic representation of natural light fluctuations occurring within plant canopies, often caused by transient gaps in the upper canopy, wind induced canopy movement and intermittent cloudiness. The elemental harmonic components contributing to the natural fluctuations are classified into three frequency domains in which distinct dynamic responses occur using nomenclature introduced in Nedbal & Lazár (2021).

Connection between forced and spontaneous oscillations and the resonance phenomenon

Some systems, including plants, oscillate spontaneously even without a periodic stimulation. This phenomenon is sometimes also called autonomous oscillation or self-oscillation. It is the generation and maintenance of a (semi)periodic motion by a source of power that lacks any corresponding periodicity. A very simple example is the classical pendulum. Applying an initial disturbing force results in an extended oscillation behavior with a characteristic natural frequency, sometimes called eigenfrequency. The amplitude of the oscillation damps over time but the natural frequency remains almost constant. This also happens in plants

when the air CO_2 concentration or light intensity abruptly changes (e.g., in Ferimazova *et al.* (2002)). The plants then start to oscillate with a period of ca. 60 s and the oscillations are damped over ca. 10-15 minutes.

The analogy with a pendulum shows an important relation between the spontaneous oscillations that fade away and the oscillations that are forced and sustained by periodic stimulation. If the pendulum is a part of a clock, there is a mechanism that forces the oscillation to persist over time. This mechanism stimulates the oscillations exactly at the natural frequency of the pendulum. The stimulation would be less effective if the forcing frequency were slower or faster than the natural frequency of the pendulum. The agreement between the natural frequency and the forcing frequency is called resonance. The amplitude of the forced oscillations is always highest when the forcing frequency is in resonance.

Knowing that plants exhibit spontaneous oscillations with a period of around 60 s, one can expect that oscillations forced by oscillating light of the same period will increase the amplitude of, e.g., ChlF. This was exactly the case shown in **Figures 2.2** & **2.3**.

Raw ChlF-yield data

The periods of light oscillations were changing from 8 min to 1 s (green line in ***Figure-SM 2.2***). The first three oscillations had a period of 8 minutes. The ChlF pattern in the first period was strongly marked by the influence of the pre-illumination in constant light and only the two later 8 min periods were used for the data analysis. Similarly, in all shorter periods (4 min to 1 s), the first two oscillations were influenced by the change in the period and not analyzed. The last three oscillations representing the given period were analyzed. Some of the analyzed time intervals are marked in ***Figure-SM 2.2*** by the dashed squares.

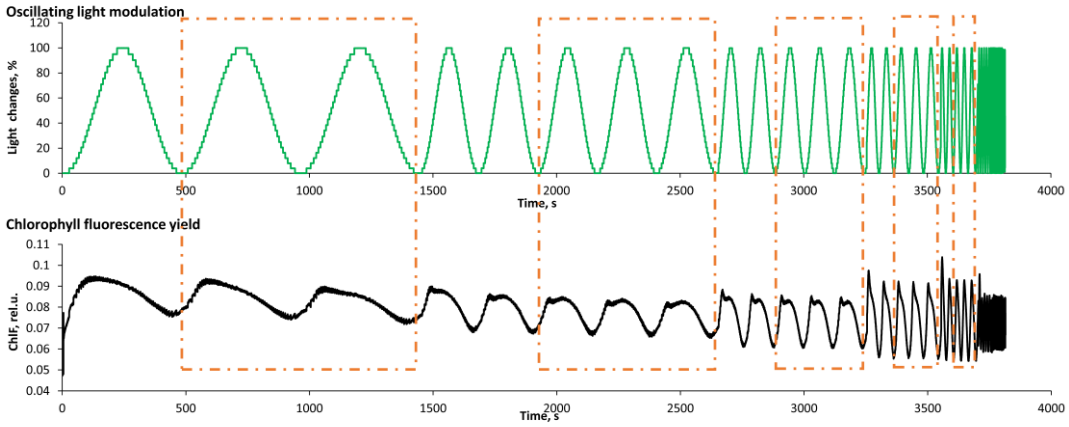

Figure-SM 2.2 Light (green line) and ChlF yield response (black line) obtained with the protocol described in Materials and methods. The orange dashed squares mark the later periods of 8min, 4min, 2 min, 60 s, 30 s oscillations that were used for data analysis. Cycle selection in 10 s, 5 s and 1 s /periods are not shown but was done in the same way.

ChlF-yield data shown without separating the oscillatory and stationary components

The oscillatory part of the ChlF yield is represented in detail in **Figure 2.2**. Below, we show also the total ChlF yield as measured in our experiments, i.e., without separating the stationary and oscillatory components, in ***Figure-SM 2.3***.

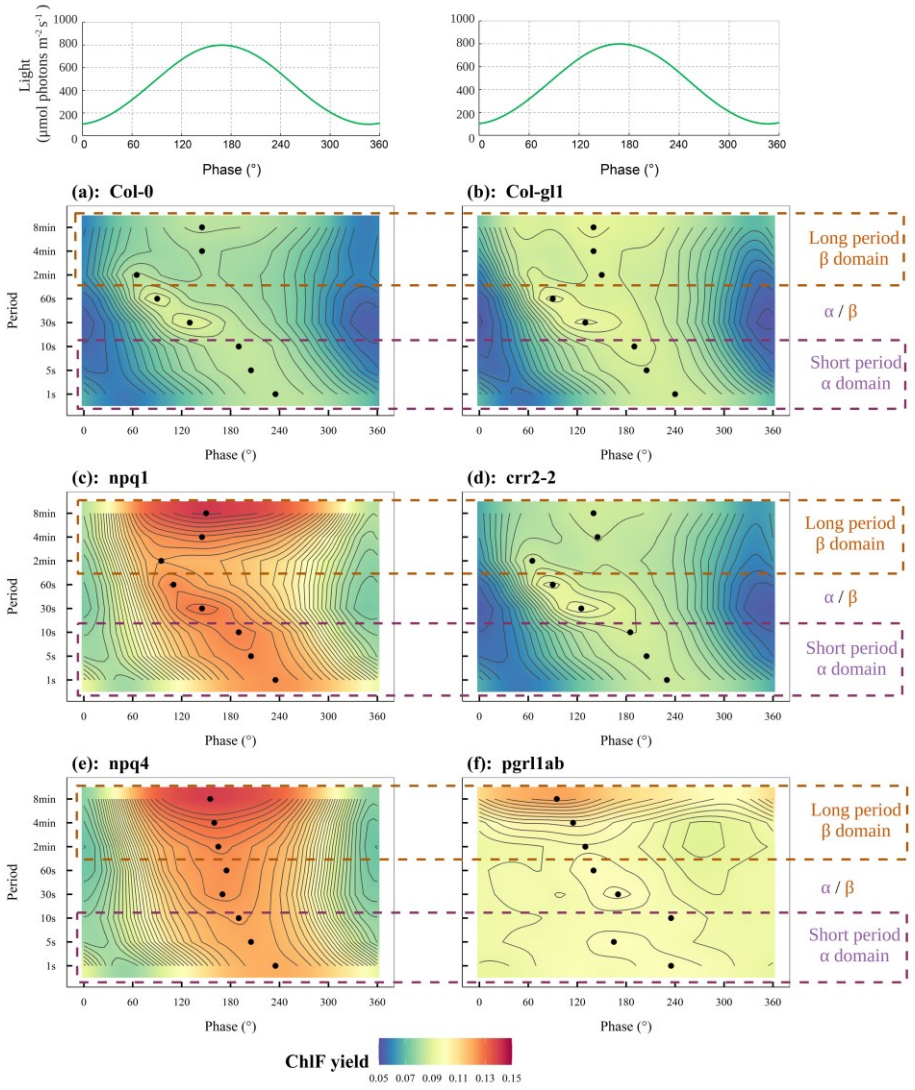

Figure-SM 2.3 Dynamics of the total chlorophyll fluorescence (ChlF) yield (including the stationary and oscillatory components). The green line in the top panel represents light that was oscillating between 100 and 800 µmol photons·m^{-2}·s^{-1} with periods in the range of 1 s to 8 min. The progress of the light oscillation and of ChlF response are shown by the phase between 0 and 360°, so that the abscissa is the same for all periods of oscillations that were applied. The other six panels show the oscillatory part of the ChlF yield induced in 6 genotypes of *A. thaliana* (n=3): (a) wild-type Col-0, (b) wild-type Col-*gl1*, (c) *npq1*, (d) *crr2-2*, (e) *npq4*, (f) *pgrl1ab*. The black dots indicate the phase at which maximum ChlF yield at the given period occurred. The colors ranging from blue to red represent the amplitude of ChlF signals from low to high. The contour lines separate signal ranges of 0.0025 of relative units. The brown dashed rectangles indicate long periods of 2, 4 and 8 min (β domain), and the purple dashed rectangles indicate short periods of 1, 5, and 10 s (α domain).

Influence of light history on the signal patterns

The pre-illumination of the measured leaves by constant light and the changes in the period of light oscillations influenced the dynamic patterns that we measured during the first oscillations following the respective transition (***Figure-SM 2.2***). The shape of the signal patterns then converged to a largely stationary pattern in the successive two or three cycles of the same frequency, marked by the dashed squares in ***Figure-SM 2.2***, that were then analyzed.

This convergence does not exclude however that the signal patterns change over longer periods of time and that the signals would be, e.g., dependent on the order in which the periods changed. This was checked in the experiments shown in ***Figures-SM 2.4*** to ***2.7*** that compared signals recorded with the periods decreasing from 8 minutes to 1 second with those obtained for the periods increasing from 1 second to 8 minutes.

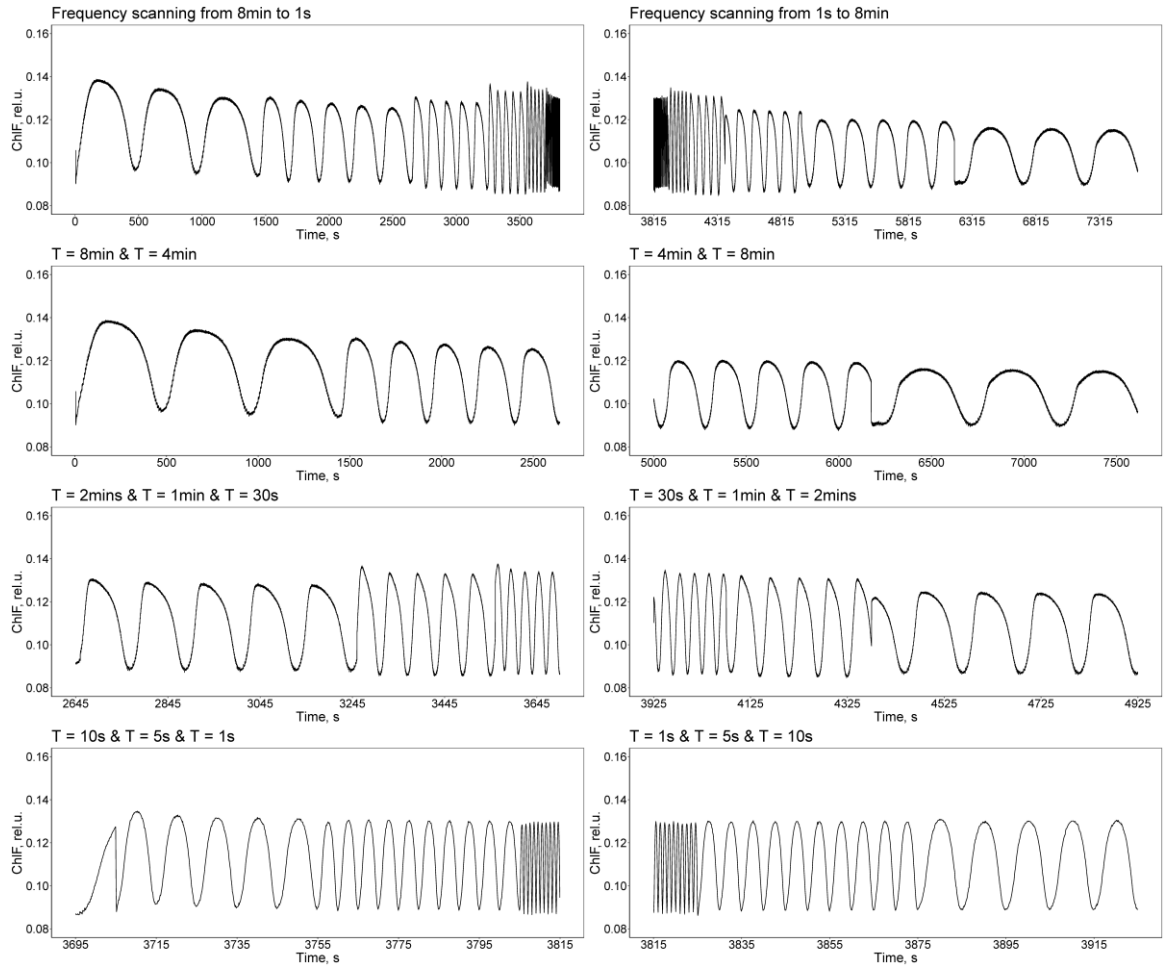

Figure-SM 2.4 Effects of the period-scanning direction on the Chl-F responses. The top-left panel shows the ChlF signals obtained with the protocol described in Materials and Methods, i.e., with periods decreasing from 8 min to 1 s. The top-right panel depicts the ChlF signals responding to periods /changing in the opposite direction, i.e., increasing 1 s to 8 min. The second, third, and fourth rows show the comparisons in detail. The data show responses of the *npq1* mutant. Similar tests were performed with the other genotypes used in this study.

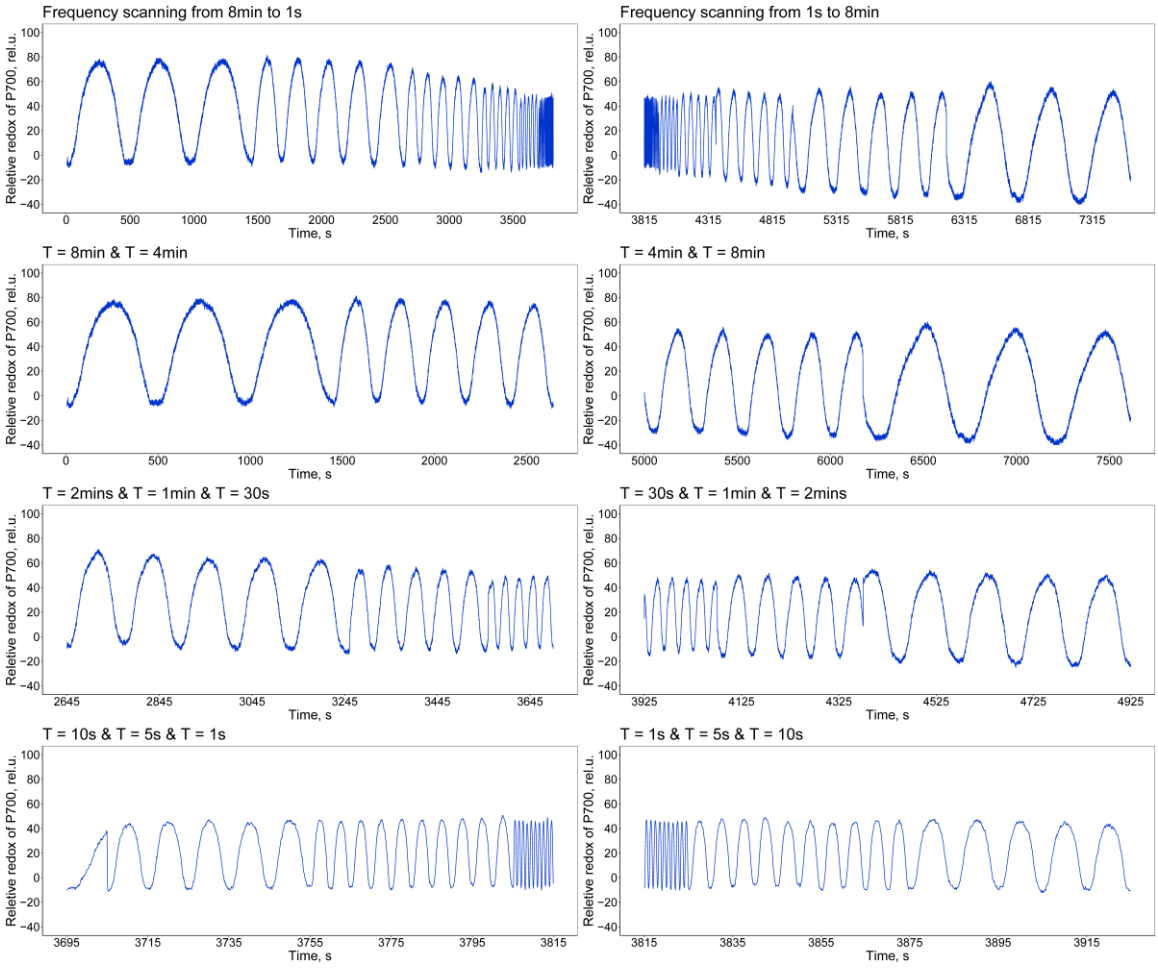

Figure-SM 2.5 Effects of the period-scanning direction on the relative P700 redox responses. The top-left panel shows the P700 redox signals obtained with the protocol described in Materials and Methods, i.e., with periods decreasing from 8 min to 1 s. The top-right panel depicts the P700 redox signals responding to periods /changing in the opposite direction, i.e., increasing 1 s to 8 min. The second, third, and fourth rows show the comparisons in detail. The data show responses of the *npq1* mutant. Similar tests were performed with the other genotypes used in this study.

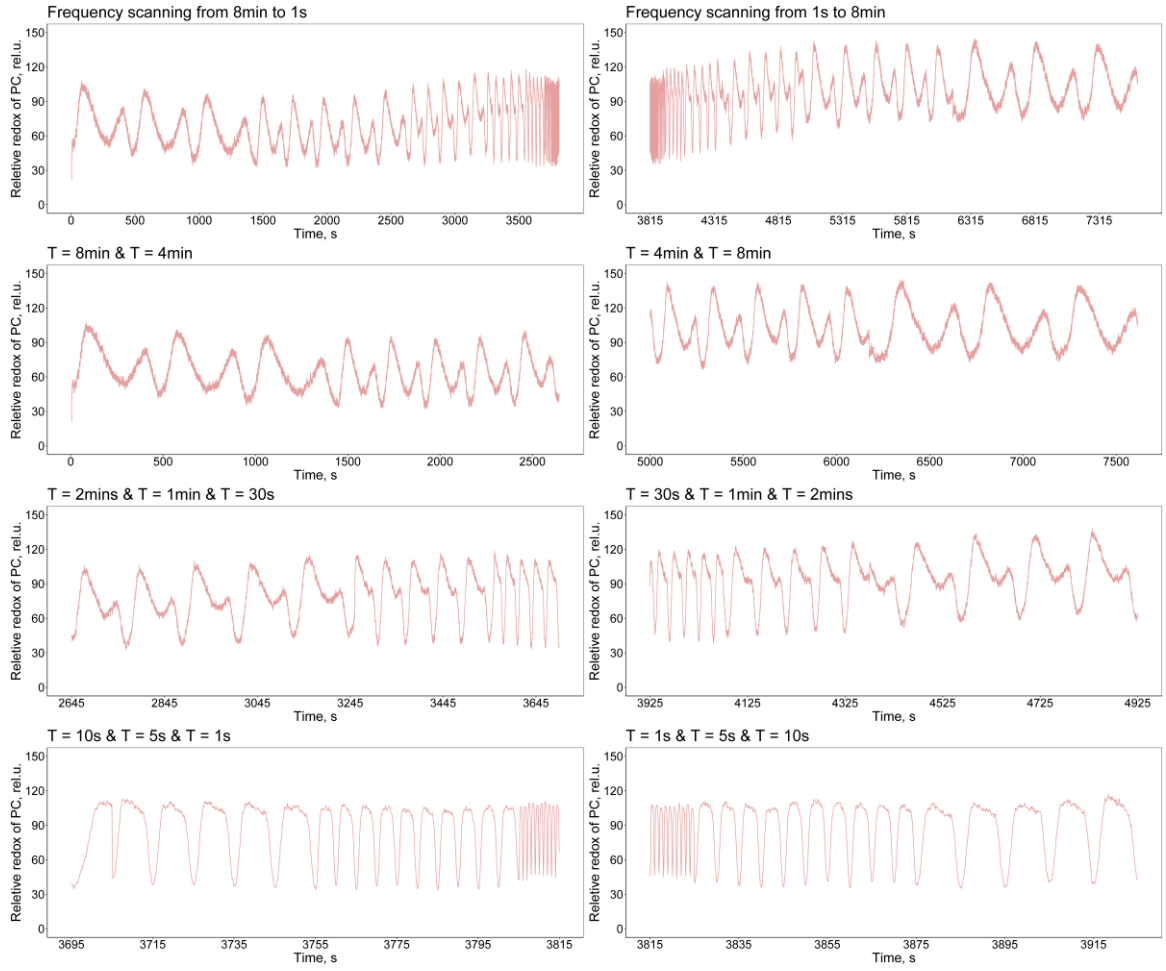

Figure-SM 2.6 Effects of the period-scanning direction on the PC redox responses. The top-left panel shows the PC redox signals obtained with the protocol described in Materials and Methods, i.e., with periods decreasing from 8 min to 1 s. The top-right panel depicts the PC redox signals responding to periods /changing in the opposite direction, i.e., increasing 1 s to 8 min. The second, third, and fourth rows show the comparisons in detail. The data show responses of the *npq1* mutant. Similar tests were performed with the other genotypes used in this study.

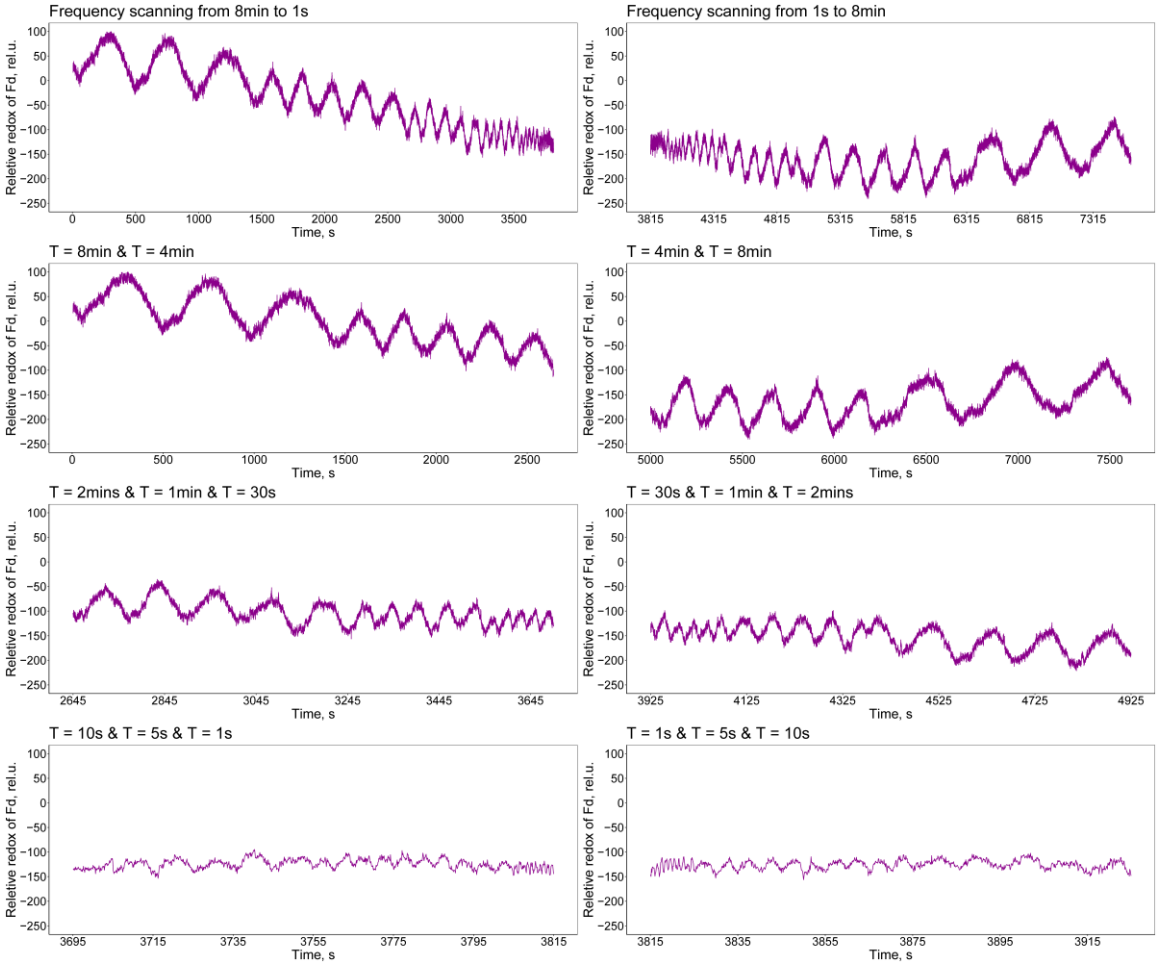

Figure-SM 2.7 Effects of the period-scanning direction on the Fd redox responses. The top-left panel shows the Fd redox signals obtained with the protocol described in Materials and Methods, i.e., with periods decreasing from 8 min to 1 s. The top-right panel depicts the Fd redox signals responding to periods /changing in the opposite direction, i.e., increasing 1 s to 8 min. The second, third, and fourth rows show the comparisons in detail. The data show responses of the *npq1* mutant. Similar tests were performed with the other genotypes used in this study.

Chapter 3

Photoprotection Dynamics and Coordination in Response to Amplitude of Light Fluctuations

Yuxi Niu[1], Shizue Matsubara[1], Ladislav Nedbal[1,2,3], Dušan Lazár[2*]

(Submitted to Plant, Cell & Environment)

I completed 80% of the research design and planning. I conducted all the experiments and analyzed the data. I contributed 70% of the data interpretation. My contribution to the final writing was 70%.

Abstract

Plants have evolved multiple regulatory mechanisms to cope with natural light fluctuations. The interplay among these mechanisms presumably leads to the resilience of plants in diverse light patterns. We investigated the rapidly reversible non-photochemical quenching (NPQ) and cyclic electron transports (CET) in light oscillating with a 60-s period and three different amplitudes. The PSI and PSII function-related quantum yields, together with redox changes of plastocyanin and ferredoxin, were measured in *Arabidopsis thaliana* wild-types and mutants with partial defects in rapidly reversible NPQ or CET. Lack of either PsbS- or violaxanthin de-epoxidase-dependent NPQ resulted in a decrease in the quantum yield of the regulated non-photochemical quenching, compensated by an increase in the quantum yield of the constitutive non-photochemical quenching. Under high amplitudes of light oscillations, the mutant lacking NDH-like complex-dependent CET experienced a transiently evidential PSI acceptor side limitation during the light increasing phase. Regardless of oscillation amplitudes, the mutant lacking PGR5/PGRL1-dependent CET restricted electron flows and failed to induce effective photosynthesis control. These results suggest the importance of PGR5/PGRL1-dependent CET in regulating PSI function at various amplitudes of light oscillation, while the NDH-like complex-dependent CET acts as a safety valve under light oscillations with high amplitude. The study proposed interplays among multiple regulatory mechanisms in photosynthesis.

Keywords: fluctuating light, rapidly reversible non-photochemical quenching, cyclic electron transport, alternative electron transports

3.1 Introduction

Plants grow in light that is perpetually changing due to diurnal and seasonal alternations, varying cloudiness, moving canopy, and other factors (Smith & Berry, 2013; Morales & Kaiser, 2020). Light fluctuations have a wide range of characteristic frequencies and irradiance levels. For instance, the frequency caused by wind-driven leaf flutter (Roden & Pearcy, 1993) is several orders of magnitude higher than the frequency caused by moving clouds or the sun´s position in the sky relative to gaps in the vegetation (Chazdon & Pearcy, 1991; Way & Pearcy, 2012). To maintain photosynthesis efficiency in such diverse fluctuating light environments, plants have developed multiple regulatory mechanisms (Kono & Terashima, 2014; Allahverdiyeva *et al.*, 2015; Kaiser *et al.*, 2018; Gjindali *et al.*, 2021). These mechanisms enable plants to adjust their photosynthetic apparatus and energy metabolism to a wide range of changes in light quantity and duration.

An important role is played by the rapidly reversible component of non-photochemical quenching (NPQ) that protects Photosystem II (PSII) by mitigating overexcitation (Roach & Krieger-Liszkay, 2012; Demmig-Adams *et al.*, 2014a; Ware *et al.*, 2015; Kromdijk *et al.*, 2016; Ruban, 2016). The importance of NPQ-dependent protection has also been demonstrated in fluctuating light conditions (Müller *et al.*, 2001; Külheim *et al.*, 2002; Ikeuchi *et al.*, 2014; Steen *et al.*, 2020). The rapidly reversible NPQ relies on two protective responses: one involving the violaxanthin de-epoxidase (VDE) (Demmig-Adams, 1990; Gilmore, 1997; Niyogi *et al.*, 1998; Jahns & Holzwarth, 2012), and the other involving protonation of the PsbS protein (Li *et al.*, 2000; Li *et al.*, 2002a). Both mechanisms are induced by low luminal pH.

Cyclic electron transport around PSI (CET) also plays an important role in coping with fluctuating light by regulating electron transport and trans-thylakoid proton motive force (pmf) (Wang *et al.*, 2015; Strand *et al.*, 2017; Nakano *et al.*, 2019), thereby inducing NPQ in PSII, photosynthesis control in the cytochrome (Cyt) b6/f complex and, most importantly, balancing ATP/NADPH ratio (Shikanai, 2007; Johnson, 2011; Suorsa *et al.*, 2012; Yamori *et al.*, 2015). Two CET pathways have been identified in angiosperms (Shikanai, 2014): the Proton Gradient Regulation 5 and Proton Gradient Regulation-like 1 proteins-dependent pathway (PGR5/PGRL1-dependent CET) (Munekage *et al.*, 2002; DalCorso *et al.*, 2008; Hertle *et al.*, 2013; Sugimoto *et al.*, 2013) and the NADH dehydrogenase-like complex-dependent pathway (NDH-like complex-dependent CET) (Yamamoto *et al.*, 2011; Peltier

et al., 2016). The absence of PGR5/PGRL1-dependent CET leads to a significant PSI reduction and photoinhibition under excessive light of constant intensity (Munekage *et al.*, 2002; DalCorso *et al.*, 2008; Suorsa *et al.*, 2012; Kono & Terashima, 2016; Yamori *et al.*, 2016). In contrast, the absence of NDH-like complex-dependent CET has little effect on steady-state photosynthesis under constant high light intensity (Sazanov *et al.*, 1998; Hashimoto *et al.*, 2003). Recent studies (Kono *et al.*, 2014; Kono & Terashima, 2016; Yamori *et al.*, 2016; Yamamoto & Shikanai, 2019; Zhou *et al.*, 2022) have shown that both CET pathways contribute to P700 oxidation under fluctuating light preventing PSI photoinhibition.

Tremendous knowledge of photosynthetic regulation was accumulated by close-proximity measurements of chlorophyll fluorescence (ChlF) and transmittance using pulse-modulated measuring light (PAM), exposing plants to actinic light (AL) of constant intensity, and applying multiple-turnover saturation pulses (SPs) (Schreiber, 2004). However, constant light or sudden dark-to-light transitions are rare in nature, where photosynthetic organisms are typically exposed to fluctuating light.

To investigate plant dynamics in fluctuating light conditions, the probing actinic light can be modulated as a sinus function of varying frequency and amplitude. Such a harmonically modulated light was proposed for studying the dynamics of photosynthesis by Nedbal and Březina (2002); Nedbal *et al.* (2003) and Nedbal *et al.* (2005). The early studies conducted on tobacco (*Nicotiana tabacum*) and cyanobacterium *Synechocystis sp. PCC 6803* and later on other organisms revealed that photosynthetic apparatus excited by harmonically oscillating irradiance responds by an information-rich periodic pattern of ChlF emission (Nedbal & Březina, 2002; Nedbal *et al.*, 2003; Nedbal *et al.*, 2005). The response was strongly non-linear and could be deconvoluted into a fundamental component, which was modulated with the same frequency as the irradiance and a small number of upper harmonic components (Nedbal & Březina, 2002; Nedbal *et al.*, 2003). Using a mathematical model (Nedbal *et al.*, 2005), this complex modulation of ChlF emission was interpreted as reflecting non-linear processes, particularly photosynthetic regulation. Recently, Nedbal and Lazár (2021) further strengthened this concept by detecting the dynamics of ChlF in the green alga *Chlorella sorokiniana* in a broad range of light frequencies (1000-0.001 Hz) and supporting the proposed interpretation with new mathematical models.

Further insights into the response dynamics of photosynthetic apparatus were obtained by changing the color of the oscillating light and by measuring the response in CO_2 assimilation rate, F_V'/F_M' and NPQ parameters, and Δ820 transmission signal (Nedbal *et al.*, 2003). The period of light oscillations in this study was 60 s, and the light oscillated with two amplitudes: between 20 and 200 and between 20 and 400 μmol photons·m^{-2}·s^{-1}, conditions like in the present study.

Multiple reporter signals, namely ChlF, I830, and P515 transmittance, were also measured in pea (*Pisum sativum*) under oscillating light with a frequency range of 1 Hz to 1/300 Hz (Lazár *et al.*, 2022). To access the function of PSI, PSII, and pmf at thylakoid membrane in the light oscillating with 1/60 Hz frequency (60 s period), the authors applied the SPs (for ChlF and I830) or a short switching off of the light (for P515). The measurements of several signals with the given approach provided new insights into the dynamic regulation of photosynthetic light reactions (Lazár *et al.*, 2022). In a recent study, mutants of *Arabidopsis thaliana* that are defective in NPQ and CET were first used to identify the operational frequency range of the regulatory mechanisms by applying harmonically oscillating light with frequencies ranging from 1 Hz to 1/480 Hz (Niu *et al.*, 2023). It proposed that the PsbS-dependent NPQ responds to periods of oscillating light over 10 s (frequency < 0.1 Hz), while the VDE-dependent NPQ operates when the period is over 1 min (frequency < 1/60 Hz). Further, it experimentally demonstrated that the upper harmonic modulation of signals induced by the regulatory processes of the light-dependent photosynthetic reactions (Niu *et al.*, 2023).

This study offers principally new insight into photosynthetic dynamic regulation in oscillating light by combining SPs with harmonically oscillating light of various amplitudes and 1/60 Hz frequency. Application of the SPs enables calculation of the quantum yields and fractions of reduced (oxidised) forms of electron carriers. The 1/60 Hz frequency was selected because it characterizes the spontaneous oscillations occurring in plants (Delieu & Walker, 1983; Ferimazova *et al.*, 2002; Lazár *et al.*, 2005) and corresponds to a photosynthetic resonance that was identified in Nedbal and Březina (2002) and Lazár *et al.* (2022). The light oscillated with three different amplitudes, ranging from light-limited to saturated. The interpretation of the results was strengthened by simultaneously measuring multiple optical proxies (ChlF, redox changes of plastocyanin, P700, and ferredoxin) and comparing the dynamics in wild-type plants of *A. thaliana* with mutants. The dynamics of rapidly reversible NPQ-related regulatory processes were studied in the *npq1* mutant

(Niyogi *et al.*, 1998), lacking VDE-dependent NPQ, and the *npq4* mutant (Li *et al.*, 2000), lacking PsbS-dependent NPQ. The operation of CET pathways was inspected in the *crr2-2* mutant (Hashimoto *et al.*, 2003), which is incompetent in the NDH-like complex-dependent CET pathway, and the *pgrl1ab* mutant (DalCorso *et al.*, 2008), which is defective in the PGR5/PGRL1-dependent CET pathway.

3.2 Materials and Methods

3.2.1 Plant materials and growth conditions

Six genotypes of *A. thaliana* plants, including wild-type Col-0 (Columbia-0, the background of *npq1*, *npq4,* and *pgrl1ab*), wild-type Col-*gl1* (trichome-lacking *glabrous 1*, the background of *crr2-2*), *npq1* (VDE-deficient), *npq4* (PsbS-deficient), *pgrl1ab* (lacking the PGR5/PGRL1-dependent pathway of CET), and *crr2-2* (lacking the NDH-like complex-dependent pathway of CET) were grown under controlled climate conditions. All seeds were first sown in the commercial substrate (Pikier, Balster Einheitserdewerk, Fröndenberg, Germany). After three days of stratification in a dark room at 4°C, sowing panels were moved to a climate chamber at a photoperiod of 12 h/12 h light/dark, a day/night temperature of 26°C/20°C, and a constant relative air humidity of 60%. The photosynthetic photon flux density (PPFD) of growth light (Fluora L 58W/77; Osram, Munich, Germany) was approximately 100 μmol photons·m^{-2}·s^{-1}. Two weeks after sowing, the seedlings were transplanted into pots (7 × 7 × 8 cm, one plant per pot) filled with commercial substrate (Lignostrat Dachgarten extensiv, HAWITA, Vechta, Germany). Plants were watered from the bottom to maintain soil moisture. Measurements were started on the 36th day after sowing; by this time, mature leaves were large enough to cover the entire measurement area of the DUAL-KLAS-NIR instrument (see below).

3.2.2 Instrument setting of chlorophyll fluorescence and KLAS-NIR measurements

The DUAL-KLAS-NIR spectrophotometer (Heinz Walz GmbH, Effeltrich, Germany) with a 3010-DUAL leaf cuvette was used for monitoring the ChlF yield and relative redox changes of the primary donor of PSI (P700), plastocyanin (PC) and ferredoxin (Fd)

simultaneously. The KLAS-100 software (Heinz Walz GmbH) was used to implement the measurement and record the data. The red light (630 nm) was applied from both sides of the leaf as AL. The pulse-amplitude-modulated green light (540 nm, 6 μmol photons·m^{-2}·s^{-1}) was applied from the abaxial side of the leaf as measuring light (ML) of ChlF yield. In parallel with the ChlF detection, four dual-wavelength difference transmittance signals in near-infrared (780-820, 820-870, 870-965, and 840-965 nm wavelength pairs; NIR-ML) were measured and deconvoluted into relative redox changes of P700, PC and Fd. The deconvolution depends on the selective differential transmission spectra of P700, PC, and Fd at these four wavelength pairs, called "Differential Model Plots", which were determined a priori on overnight dark-adapted plants following the default procedures provided by the KLAS-100 software (Klughammer & Schreiber, 2016). Specific differential model plots were determined for each genotype and used for subsequent measurements for all plants of the same genotype grown under the same environments.

3.2.3 Light response curve measurement

Overnight dark-adapted plants were taken out of the climate chamber at the end of the dark period of the day/night regime and kept in the darkness until the measurements began in the laboratory. The maximum oxidation of P700 (P_m) and PC (PC_m), and the maximum reduction of Fd (Fd^-_m) were determined for each dark-adapted plant by performing the NIR-MAX routine before starting the measurements (Klughammer & Schreiber, 2016). Subsequently, the rapid light response curve was measured for each plant by increasing the AL intensity in eight steps: 67, 99, 133, 182, 247, 425, 671, 1049 μmol photons·m^{-2}·s^{-1}. The light remained constant at each intensity for 60 s (the instrument pre-defined protocol). The first multiple-turnover SP (630 nm, 300 ms duration, 3700 μmol photons·m^{-2}·s^{-1}) was given in the dark to determine the maximum yield of ChlF, F_m, to estimate the maximum quantum yield of PSII photochemistry. After a 40-s delay, the AL was switched on and increased in eight steps as described above. High-intensity SP (630 nm, 300 ms duration, 17000 μmol photons·m^{-2}·s^{-1}) was given at the end of each light step to estimate the quantum yields of PSI and PSII and the apparent relative oxidation/reduction of PC and Fd. Three to seven plants were measured as biological replicates of each genotype.

3.2.4 Harmonically oscillating light measurement with saturation pulse analysis

The NIR-MAX routine was performed for each plant as described above to determine the P_m, PC_m, and Fd^-_m before measurements. After that, the measurement combining harmonically oscillating light with SPs was conducted. The first SP (630 nm, 300 ms duration, 3700 µmol photons·m^{-2}·s^{-1}) was given in the dark to determine the F_m. Then, with a 25-s delay, the oscillating AL with 1/60 Hz (= period of 60 s) was triggered and continued for 40 cycles. The first 10 cycles were applied without SPs to establish a stationary dynamic pattern and to allow the dark-adapted leaf to adapt to light. During these 10 cycles, the four dynamic signals (PSII ChlF and relative redox changes of PSI, PC, and Fd) were recorded under oscillating light without any interference from SPs. Starting from the 11^{th} cycle, a high-intensity SP (630 nm, 300 ms duration, 17000 µmol photons·m^{-2}·s^{-1}) was triggered during each cycle (one SP per cycle) at different phases of AL oscillation to cover the entire period of oscillation within 30 cycles (*Supplementary materials* ***Figure-SM*** **3.1** *A*). Therefore, the maximum ChlF yield (F_m') at different phases of AL oscillation, as well as the maximum oxidation of P700, PC (P_m', PC_m'), and the maximum reduction of Fd (Fd^-_m'), can be quantified. For detailed descriptions of the combined measurement of photosynthetic efficiency under oscillating light, see Lazár *et al.* (2022). Three different amplitudes of AL oscillation were implemented, covering different light ranges on the light response curves: 100-200, 100-400, and 100-800 µmol photons·m^{-2}·s^{-1}. Due to the limitations of the DUAL-KLAS-NIR instrument in adjusting the light intensity levels, the oscillating AL was modulated incrementally rather than smoothly. The real light modulation was compared with the expected light modulation in *Supplementary materials* ***Figure-SM 3.1*** *B*. Three to seven plants were measured as biological replicates for each genotype in each amplitude of oscillation. Based on the values of ChlF and dual-wavelength difference transmittance signals measured in the dark-adapted state with and without the SP, and in the light-adapted state with the SP and just before application of the SP, quantum yields of PSI and PSII and apparent relative redox states of PC and Fd were estimated (Schreiber & Klughammer, 2016; Lazár *et al.*, 2022).

3.3 Results

3.3.1 Rapid light response curves

The experiments started with measuring the rapid light response curves with 60 s dwell time at each light intensity step (**Figure 3.1**). The light intensities used were from the ranges of light oscillations in the second phase of the experiments, as indicated by the arrows in **Figure 3.1** C. The rapid light response curves show that the intensity of the low-amplitude oscillations (LL) varied largely in the linear part of the rapid light response curves, whereas the high-amplitude oscillations (HL) reached, at their maxima, into the saturation range of all probed signals.

The graphs represent wild-types (Col-0 and Col-*gl1*), NPQ mutants (*npq1, npq4*), and CET mutants (*crr2-2, pgrl1ab*) of *A. thaliana* with different colors. The transmittance measurements were used to determine PSI quantum yields: the effective photochemical quantum yield of PSI, Y(I) in **Figure 3.1** A; the quantum yield of non-photochemical energy dissipation in PSI due to donor side limitation, Y(ND) in **Figure 3.1** B; and the quantum yield of non-photochemical energy dissipation in PSI due to acceptor side limitation, Y(NA) in **Figure 3.1** C. The PSII-related parameters were calculated from the ChlF measurements: the effective photochemical quantum yield of PSII, Y(II) in **Figure 3.1** D; the quantum yield of the regulated non-photochemical quenching in PSII, Y(NPQ) in **Figure 3.1** E; and the quantum yield of the constitutive non-photochemical quenching in PSII, Y(NO) in **Figure 3.1** F. The coefficient of photochemical quenching qP in **Figure 3.1** G was also evaluated from the ChlF measurements and served further as a proxy for a fraction of open PSII centres (with Q_A oxidized). This interpretation of qP is based on the puddle model of PSII units (Stirbet, 2013). The apparent relative oxidation of PC (PC Ox) and apparent relative reduction of Fd (Fd Red) shown in **Figure 3.1** H and I were also estimated from transmittance measurements.

The rapid light response curves were different for different reporter signals. On the extremes, the optical proxy of Fd reduction state and PC oxidation state were increasing with the constant light only below 200 µmol photons·m^{-2}·s^{-1}, whereas the yields of Y(I), Y(II), Y(NPQ) reached stationary levels in all tested genotypes only above 500 µmol photons·m^{-2}·s^{-1}. The curves representing quantum yields related to the PSI function, Y(I), Y(NA), and Y(ND) (**Figure 3.1** A-C) were similar across all genotypes except for the

pgrl1ab. When PAR rose from low levels, Y(NA) of all genotypes (**Figure 3.1** C), except *pgrl1ab*, decreased rapidly as downstream reactions at the PSI acceptor side were activated by light, and Y(ND) was subsequently enhanced (**Figure 3.1** B). In the *pgrl1ab* mutant, however, the Y(NA) largely increased with rising light intensity while Y(ND) stayed low at all light intensities.

The dynamics of Y(ND) and Y(NA) (**Figure 3.1** B, C) were consistent with the redox states of PC at the donor side of PSI and Fd at its acceptor side (**Figure 3.1** H, I). In the Col-0, PC rapidly reached a fully oxidized state at AL intensity of about 200 μmol photons·m^{-2}·s^{-1} and higher (**Figure 3.1** H), while Fd was partially reduced with increasing light and then remained relatively stable (**Figure 3.1** I). In contrast, *pgrl1ab* showed a substantially higher reduction level of Fd (**Figure 3.1** I) and a decreased level of PC oxidation (i.e., higher PC reduction) than Col-0 (**Figure 3.1** H). The electron congestions at the acceptor side of PSI appeared to limit the efficiency of electron transport throughout the entire electron transport chain in *pgrl1ab*, as indicated by the lower fraction of the open PSII reaction centres (proxied by qP) in this mutant (**Figure 3.1** G). The changes in Y(I), Y(NA), and Y(ND) in the other CET mutant, *crr2-2*, were identical to its wild-type Col-*gl1* in constant light illumination (**Figure 3.1** A-C) except at the low light intensities in which Fd was less reduced in *crr2-2* than in Col-*gl1* (**Figure 3.1** I). The *npq1* and *npq4* mutants were largely comparable with Col-0 in the PSI-related quantum yields (**Figure 3.1** A-C) and the redox changes of PC and Fd (**Figure 3.1** H, I), although Fd tended to stay more oxidized in *npq1* than the others.

Y(II) was generally comparable among the genotypes, with a slightly lower value in the *prgl1ab* mutant (**Figure 3.1** D). Y(NPQ) of both *npq1* and *npq4* was considerably lower than that of Col-0 (**Figure 3.1** E) due to the rapidly reversible NPQ deficiency (Li *et al.*, 2000; Niyogi, 2000). The lower level of Y(NPQ) in the *npq1* and *npq4* was compensated by a higher level of Y(NO) (**Figure 3.1** F), resulting in the same sum of Y(NPQ) and Y(NO) for the NPQ mutants and Col-0 (since Y(II) + Y(NPQ) + Y(NO) = 1). The *pgrl1ab* mutant also had lower Y(NPQ) than Col-0 (**Figure 3.1** E), consistent with the role of the PGR5/PGRL1-dependent CET in lumen acidification and thus the NPQ induction (Munekage *et al.*, 2002; DalCorso *et al.*, 2008). Contrary to *pgrl1ab*, Y(NPQ) of the *crr2-2* mutant was the same as that of Col-*gl1*, supporting the notion that the NDH-like complex-dependent CET may not be essential for the regulation of rapidly reversible NPQ and electron transport in relatively constant excess light conditions (Hashimoto *et al.*, 2003).

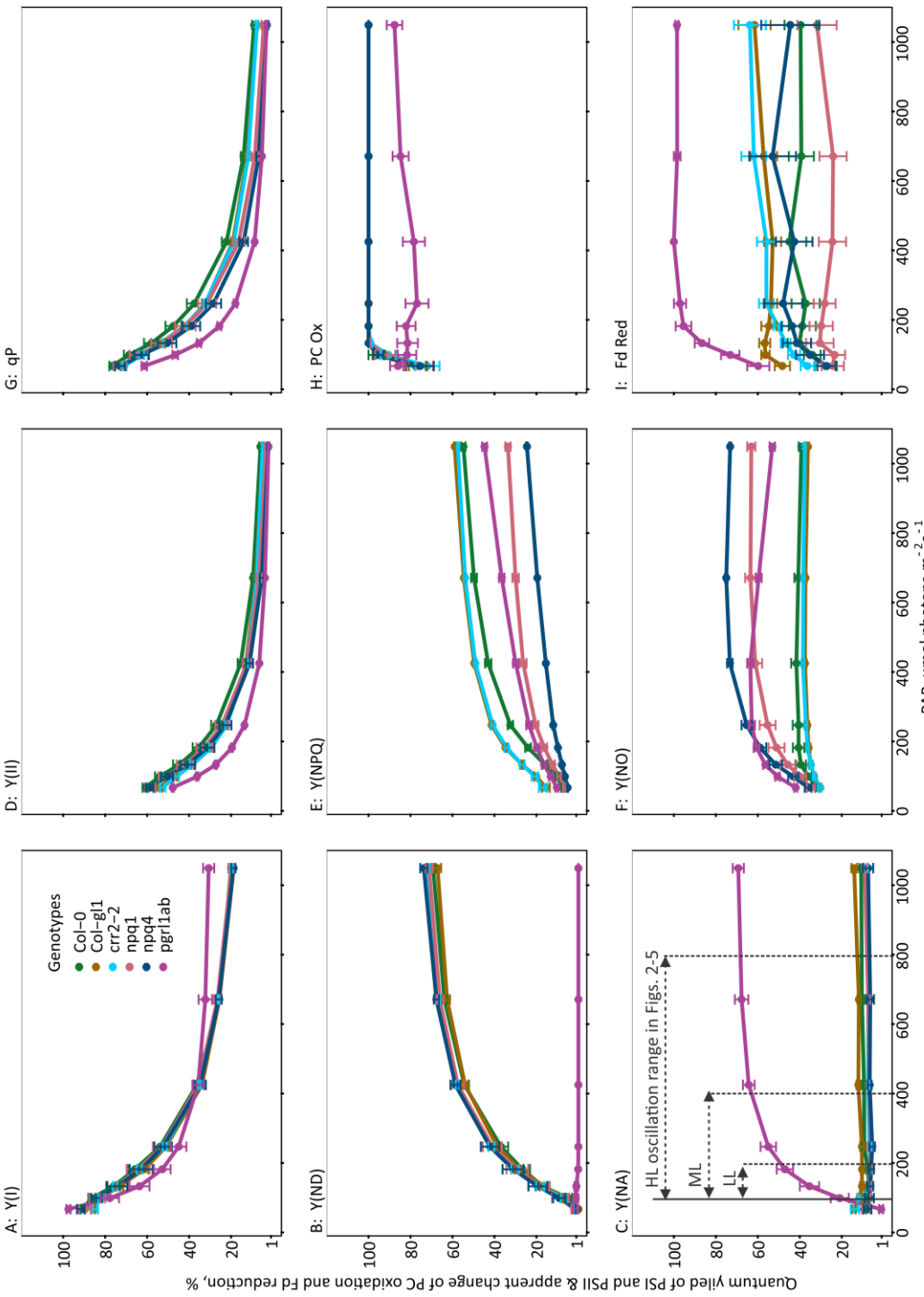

Figure 3.1 The quantum yields of photosystems and redox states of electron carriers were evaluated in rapid light response curves with six genotypes of *A. thaliana:* Col-0, Col-*gl1*, *npq1*, *npq4*, *crr2-2*, and *pgrl1ab* (see legend in panel A). The quantum yields of PSI and PSII functions are shown from panels A to F, the apparent oxidation/reduction changes of PC and Fd are shown in panels H and I, and panel G shows changes of qP. The error bars represent the standard error (n = 3-7). The horizontal dashed arrows in panel C indicate the ranges of light intensity oscillation that were used in further experiments: low-light oscillations (LL, 100-200 µmol photons·m^{-2}·s^{-1}), medium-light oscillations (ML, 100-400 µmol photons·m^{-2}·s^{-1}), and high-light oscillations (HL, 100-800 µmol photons·m^{-2}·s^{-1}).

The effects of lacking different protective mechanisms on the induction of rapidly reversible NPQ can also be visualized by the commonly used NPQ parameter, which equals to Y(NPQ)/Y(NO), see review in Lazár (2015). Therefore, changes in the NPQ parameter (*Supplementary materials* ***Figure-SM 3.2*** *A*) can be expected based on the values of Y(NPQ) and Y(NO) shown in **Figure 3.1** E & F.

The Y(I)-Y(II) parameter (Miyake *et al.*, 2005; Huang *et al.*, 2011; Yamori *et al.*, 2011; Sagun *et al.*, 2019) (*Supplementary materials* ***Figure-SM 3.2*** *B*) was used to estimate the quantum yield of CET. The Y(I)/Y(II) parameter (Miyake *et al.*, 2005; Yamori *et al.*, 2011; Kono *et al.*, 2014) (*Supplementary materials* ***Figure-SM 3.2*** *C*) represents the relative quantum yield of CET. While Y(I)/Y(II) showed a seeming advantage for discriminating differences among the genotypes, it is important to keep in mind that a high value of Y(I)/Y(II) might simply be caused by unchanged Y(I) with Y(II) approaching zero, as is the case in the *pgrl1ab*, *npq1* and *npq4* mutants (cf. **Figure 3.1** A, D and *Supplementary materials* ***Figure-SM 3.2*** *C*). Notably, the absence of the PGR5/PGRL1-dependent CET did not result in a low level of Y(I)-Y(II) or Y(I)/Y(II), as the *pgrl1ab* mutant showed high levels of both parameters (*Supplementary materials* ***Figures-SM 3.2*** *B, C*). We note that unspecified effects caused by mutations other than those related to the PGRL1A and PGRL1B proteins, as was found for the *pgr5-1* mutant (Wada *et al.*, 2021), can be ruled out in the *pgrl1ab* mutant, since the *pgr5*^{hope1} mutant lacking only the PGR5 protein has the same phenotype as *pgrl1ab* mutant (Wada *et al.*, 2021).

In summary, the *pgrl1ab*, *npq1*, and *npq4* mutants showed altered phenotypes compared to their wild-type Col-0 when exposed to AL of 60 s constant intensity during the light response curve measurements, whereas the *crr2-2* mutant was largely indistinguishable from its wild-type Col-*gl1*. These results confirm the previously described phenotypes of these mutants (Niyogi *et al.*, 1998; Li *et al.*, 2000; Hashimoto *et al.*, 2003; DalCorso *et al.*, 2008).

3.3.2 Saturation pulse analysis under light oscillating with frequency of 1/60 Hz (period of 60 s)

Three different amplitudes, low-light (LL, 100-200 µmol photons·m^{-2}·s^{-1}), medium-light (ML, 100-400 µmol photons·m^{-2}·s^{-1}), and high-light oscillations (HL, 100-800 µmol photons·m^{-2}·s^{-1}) were applied to study plant dynamics reaching from light-limited to light-

saturated levels (**Figure 3.1** C, *Supplementary materials* ***Figure-SM 3.1*** *B*). A single frequency of 1/60 s^{-1} of the light modulation was applied in this study (other frequencies were explored in **Chapter 2**). The quantum yields and redox-proxy signals were probed by SPs of light, one pulse per period, that were given on top of the AL oscillations, always slightly phase-shifted. In this way, the dynamics of the measured signals were probed with minimal disruption along the entire period (see Materials and Methods and *Supplementary materials* ***Figure-SM 3.1*** *A*).

The results were presented in **Figures 3.2 - 3.5** in a condensed way, where the response to individual SP was plotted relative to the phase of the light oscillation at which the pulse was applied. Namely, the phases 0° and 360° represent SPs that were applied at the minimum of the light oscillation, 60 s apart. Phase 180° represents a SP that was given at the maximum of the light period, 30 s from the light minima. Circles, triangles, and squares represent the LL, ML, and HL oscillations, respectively. Different colors denote plant genotypes, as explained in legends placed in one of the figure panels.

The Col-0 wild-type and NPQ mutants

The oscillating light-induced modulations in the PSI- and PSII-related quantum yields were generally small in LL oscillation but became larger as the light oscillation amplitudes increased (except Y(NA), **Figure 3.2** C). Notably, the changes in Y(I) (**Figure 3.2** A), Y(II) (**Figure 3.2** D), and Y(ND) (**Figure 3.2** B) show nearly symmetrical patterns closely mirroring the light modulation. The minimum of Y(I) and Y(II), and the maximum of Y(ND) coincided with the maximum of light oscillations (phase 180°). A contrasting response to the light oscillations was found with Y(NA) in **Figure 3.2** C, which remained below 20% across all genotypes and light intensities, essentially unaffected by the light oscillations. The trend of Y(ND) (**Figure 3.2** B) complements that of Y(I) (**Figure 3.2** A). These phenomena held true for the wild-type Col-0 and both NPQ mutants.

Another contrasting dynamic response was found with Y(NPQ) in **Figure 3.2** E. The minima and maxima of Y(NPQ) were delayed by approximately 45° phase (7.5 s) relative to the course of HL oscillation, reflecting the time necessary to activate and deactivate the regulatory rapidly reversible NPQ. The strength of the regulatory response increased with the amplitude of light oscillations and was, understandably, stronger in the Col-0 wild-type (green lines and symbols) compared to the NPQ-impaired mutants *npq1* (pink lines and

symbols) and *npq4* (dark blue lines and symbols). The NPQ response was weaker in *npq4* than in *npq1*.

The weak Y(NPQ) responses in the NPQ mutants were compensated by increased levels and modulation of the quantum yield of the constitutive non-photochemical quenching in PSII, Y(NO) in **Figure 3.2** F. As a result, the sum of Y(NPQ) and Y(NO) was about the same for Col-0 and the *NPQ* mutants for the given range of the sinusoidal illumination, as deduced from roughly the same magnitudes of Y(II) (**Figure 3.2** D) in all three (with slightly lower values in the mutants compared to Col-0 in ML and HL oscillations) and considering that Y(II) + Y(NPQ) + Y(NO) = 1. Interestingly, the strongest response of Y(NO) in the Col-0 wild-type (green, **Figure 3.2** F) during the rising phase of the light oscillation, between 90° and 180°, again complemented for the delayed Y(NPQ) (green, **Figure 3.2** E). This qualitative pattern was also found in both mutants with HL (squares) and ML oscillations (triangles). The LL oscillations (circles) were not strong enough to elicit similar response in the mutants.

It should be noted that the NPQ parameter (= Y(NPQ)/Y(NO)) of both *npq1* and *npq4* displayed roughly monotonically increasing trends in all oscillating light amplitudes (*Supplementary materials* ***Figure-SM 3.3*** *A*). However, it is premature to conclude that rapidly reversible NPQ of both mutants does not respond to oscillating light illumination based solely on this parameter. Such a conclusion is not supported by the courses of Y(NPQ), and Y(NO) (**Figure 3.2** E, F).

Generally, in comparison to wild-type Col-0, the *npq1* and *npq4* mutants displayed little difference in their responses concerning PSI-related quantum yields, Y(I), Y(ND), and Y(NA) (**Figure 3.2** A-C). This implies that the defects in rapidly reversible NPQ processes had barely any impact on PSI functionality, encompassing both its donor and acceptor sides. Regarding PSII-related quantum yields, while an apparent reduction of Y(NPQ) was shown in mutants (**Figure 3.2** E), the trend in Y(II) (**Figure 3.2** D) was similar between the NPQ mutants and wild-type Col-0. Minor differences occurred primarily in the ML and HL oscillations (**Figure 3.2** D), where the mutants displayed slightly lower Y(II) than wild-type Col-0, with *npq4* exhibiting lower values than *npq1*. This suggests that the ability of the NPQ mutants to maintain PSII efficiency under oscillating light illumination was slightly restricted compared to their wild-type Col-0, with the *npq4* performing worse than the *npq1* (**Figure 3.2** D).

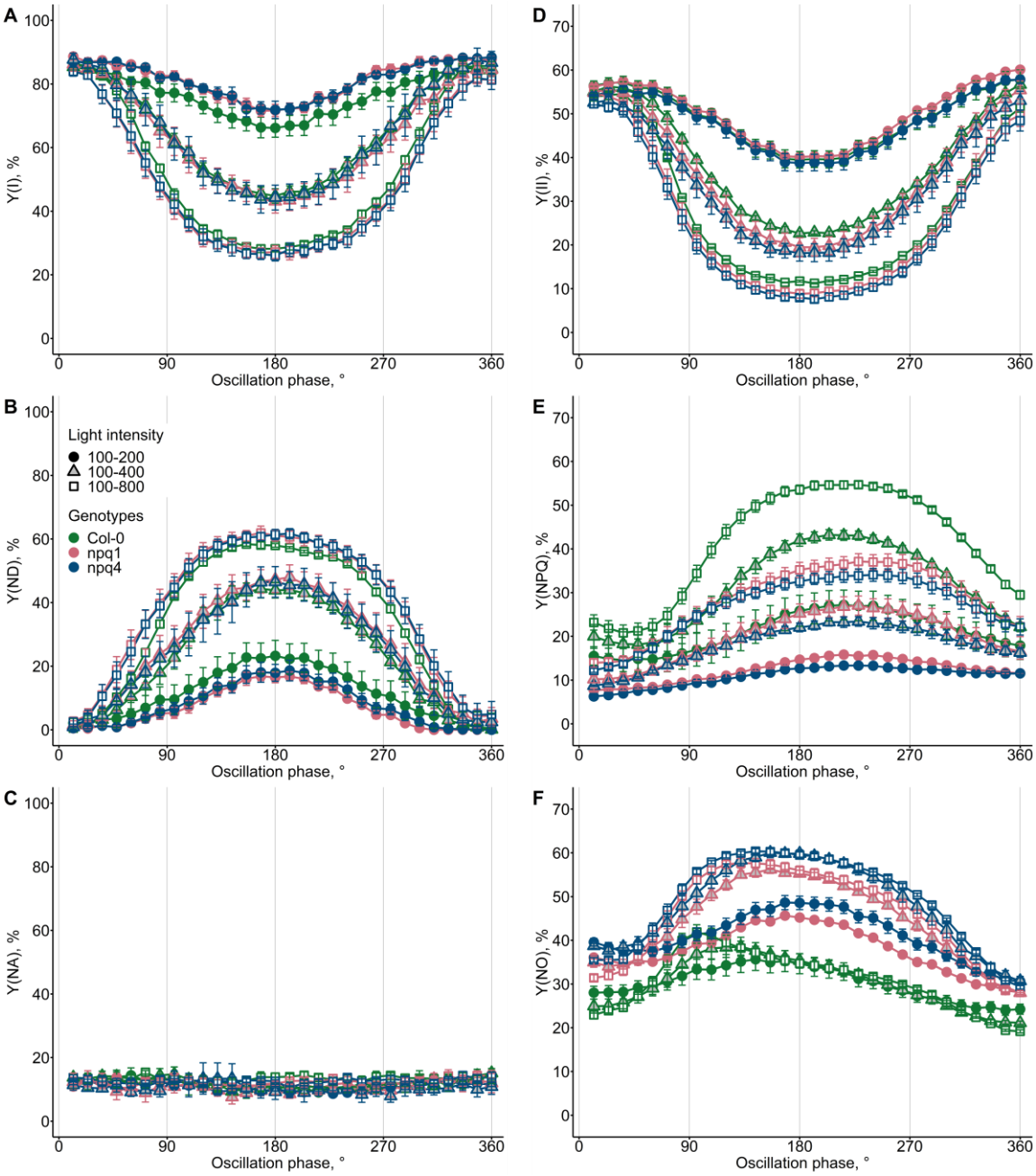

Figure 3.2 Changes in PSI- and PSII-related quantum yields of the three NPQ-related genotypes of *A. thaliana*, Col-0, *npq1*, and *npq4*, under three different amplitudes of oscillating light ranging from 100 to 200 µmol photons·m^{-2}·s^{-1}, 100 to 400 µmol photons·m^{-2}·s^{-1}, and 100 to 800 µmol photons·m^{-2}·s^{-1}. The error bars represent the standard error (n = 3-7).

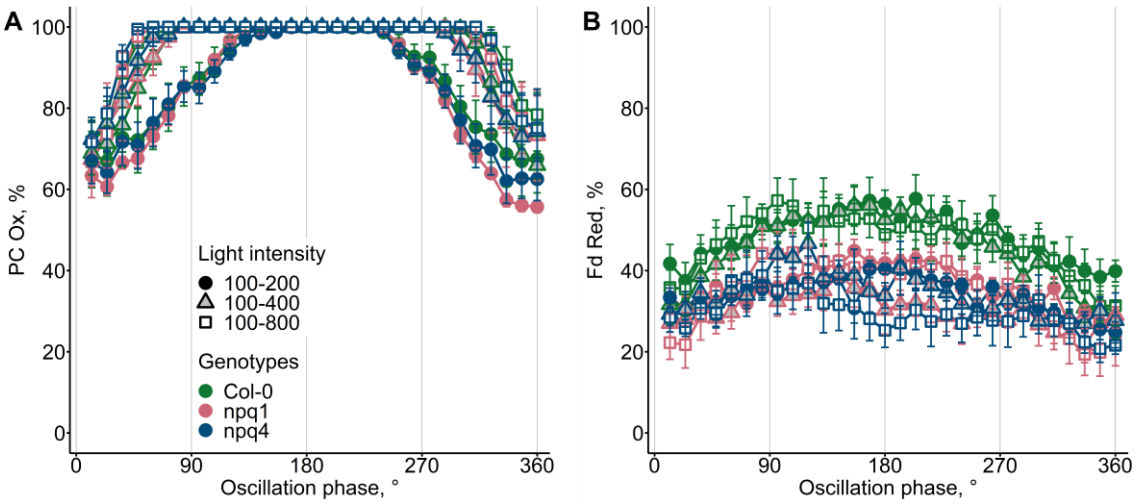

Figure 3.3 Changes of the apparent relative oxidation of PC (PC Ox) and reduction of Fd (Fd Red) in response to three different amplitudes of oscillating light for the three NPQ-related genotypes of *A. thaliana*, Col-0, *npq1*, and *npq4*. The oscillating light amplitudes range from 100 to 200 µmol photons·m^{-2}·s^{-1}, from 100 to 400 µmol photons·m^{-2}·s^{-1}, and from 100 to 800 µmol photons·m^{-2}·s^{-1}. The error bars represent the standard error (n = 3-7).

For the NPQ mutants and their corresponding wild-type Col-0, the oxidation process of PC under LL oscillation (cycles, **Figure 3.3** A) closely followed the course of the light intensity changes. However, it stayed at the maximal oxidation even prior to and following the maximum of the oscillating light intensity (spanning phases approximately from 135° to 225°). Under ML and HL oscillations (triangles and squares, **Figure 3.3** A), the saturation of PC oxidation was more pronounced, maintaining maximum oxidation between phases approximately from 90° to 270°. In contrast, the redox state of Fd exhibited limited alignment with light oscillations, irrespective of the genotype or light oscillation amplitude (**Figure 3.3** B). Notably, *npq4* and *npq1* consistently exhibited lower levels of Fd reduction compared to Col-0 across all oscillating light amplitudes.

In addition, the impact of the rapidly reversible NPQ deficiency on CET in oscillating light was elucidated in *Supplementary materials* ***Figure-SM 3.3***. Both NPQ mutants had elevated quantum yields of CET, Y(I)-Y(II), in comparison to Col-0 under LL and ML oscillations but showed similar levels as Col-0 under HL oscillations (*Supplementary materials* ***Figure-SM 3.3*** *B*). A more dramatic contrast appeared in the relative quantum yields of CET, Y(I)/Y(II), which followed the course of light oscillations with more substantial modulations in HL oscillation and fewer changes in LL oscillation (*Supplementary materials* ***Figure-SM 3.3*** *C*). Both NPQ mutants exhibited higher Y(I)/Y(II) than Col-0,

with the *npq4* showing the highest values. These results suggest that a potential enhancement of CET might occur in NPQ mutants as a mechanism to alleviate the pressure on the electron transport chain under oscillating light conditions. This may partly explain the lower reduction of Fd in NPQ mutants than in Col-0 (**Figure 3.3** B).

The CET mutants

The wild-type Col-*gl1* (background of *crr2-2*) behaved in much the same way as the wild-type Col-0 (background of *pgrl1ab*) in terms of the dynamics of all tested photosynthetic parameters under light oscillations (cf. green symbols and lines in **Figure 3.2** and gold symbols and lines in **Figure 3.4**).

Regarding the changes in Y(I) and Y(II) of *crr2-2* in oscillating light, they were roughly similar to those of Col-*gl1*, with some differences (light blue compared with gold symbols and lines, **Figure 3.4** A, D). Y(I) and Y(II) were slightly lower in *crr2-2* than in Col-*gl1* under LL oscillation. Under ML oscillations, *crr2-2* showed constrained recovery of Y(I) and Y(II) as the light approached the lowest intensity, particularly around phases 0°-60° and 300°-360°. During HL oscillation, Y(I) (**Figure 3.4** A), but not Y(II) (**Figure 3.4** D) in *crr2-2* was higher than in Col-*gl1* around the maximum intensity of oscillating light. The most distinctive feature of the *crr2-2* mutant, in contrast to Col-*gl1*, was its smaller donor side limitation of PSI (Y(ND), **Figure 3.4** B) but higher acceptor side limitation of PSI (Y(NA), **Figure 3.4** C) under ML and HL oscillations. This contrast was especially evident during the ascending phase of HL oscillation, where Y(NA) of *crr2-2* exhibited a peak at approximately 90° phase (squares with light blue in **Figure 3.4** C) accompanied by a shallow depression phase of Y(ND) (**Figure 3.4** B). These results suggest that the absence of NDH-like complex-dependent CET might diminish the capacity of the PSI acceptor side to relieve electron pressure in the initial rising phase of HL oscillation.

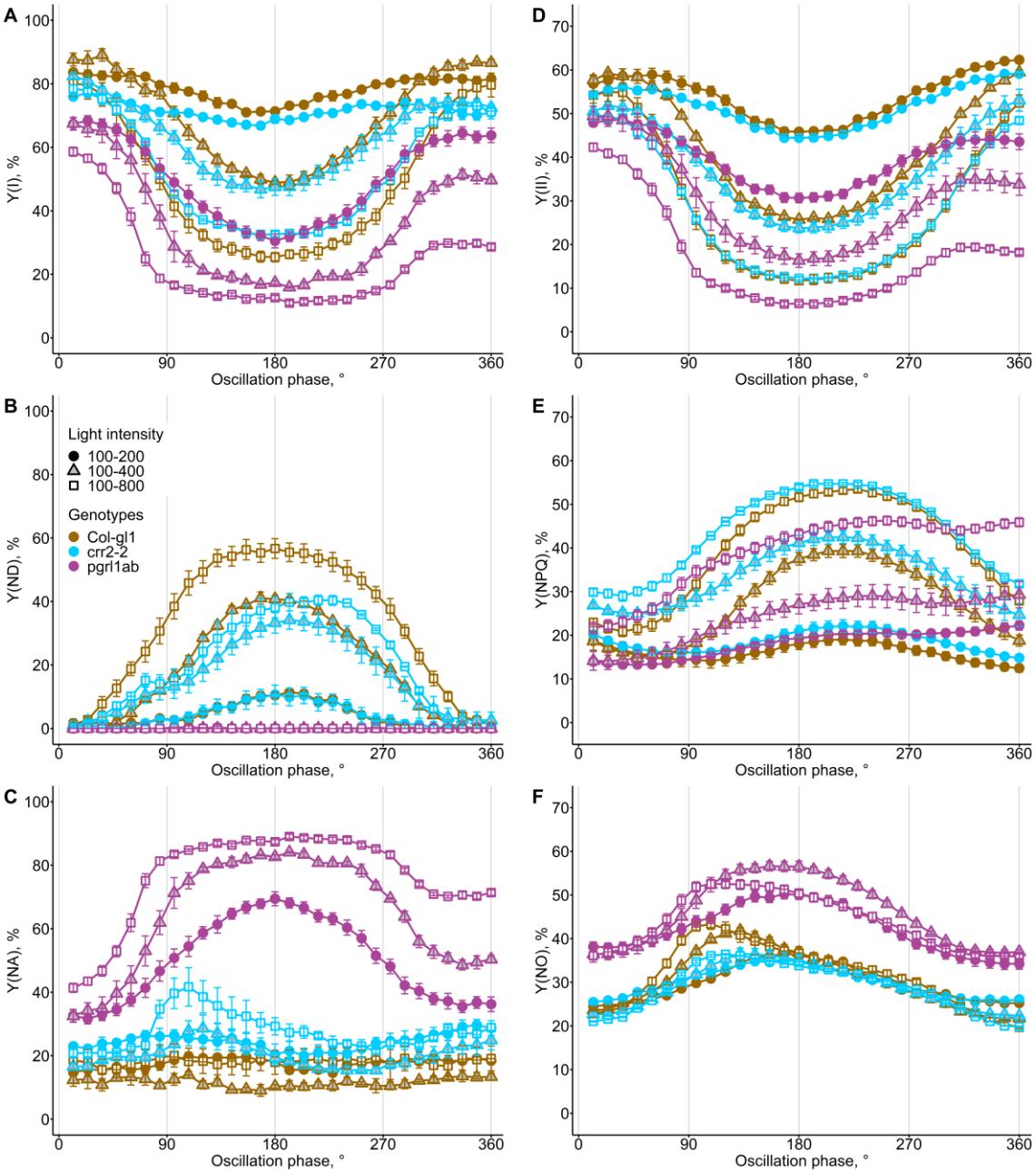

Figure 3.4 Changes in PSI- and PSII-related quantum yields of the three CET-related genotypes of *A. thaliana*, Col-*gl1*, *crr2-2*, and *pgrl1ab*, under three different amplitudes of oscillating light ranging from 100 to 200 µmol photons·m^{-2}·s^{-1}), from 100 to 400 µmol photons·m^{-2}·s^{-1}, and from 100 to 800 µmol photons·m^{-2}·s^{-1}. The error bars represent the standard error (n = 3-7).

The *pgrl1ab* mutant had considerably lower photochemical efficiencies of both PSI and PSII (magenta symbols and lines in **Figure 3.4** A, D) when compared to Col-0 (green symbols and lines in **Figure 3.2** A, D) and the other plants, regardless of the oscillation amplitude. Under all oscillation amplitudes, this mutant consistently displayed notably

higher Y(NA) (**Figure 3.4** C), while Y(ND) was absent (**Figure 3.4** B). These data highlight the essential role of PGR5/PGRL1-dependent CET in facilitating electron release at the PSI acceptor side and oxidation at the PSI donor side under oscillating light, regardless of the amplitude.

Notably, mutants with CET defects exhibited variations in their NPQ-related parameters compared to their respective wild-types, with two mutants showing entirely distinct behaviors. The *crr2-2* mutant had the same course and slightly higher values of Y(NPQ) as Col-*gl1* under LL oscillations, with notably higher values at the beginning and end phases of the oscillation period under ML and HL oscillations (**Figure 3.4** E). Conversely, in comparison to Col-0 (green, **Figure 3.2** E), Y(NPQ) of the *pgrl1ab* mutant (magenta, **Figure 3.4** E) was lower at the beginning but higher at the end phase of the oscillation period, indicating that the course of Y(NPQ) in *pgrl1ab* did not follow the course of the oscillating light intensity. Apparent differences between CET mutants and their respective wild-types were also observed in the NPQ parameter (*Supplementary materials* ***Figures-SM 3.4*** *A* and ***SM 3.3*** *A*). The NPQ parameter in *crr2-2* followed a similar pattern to Col-*gl1* but with remarkably higher values in all amplitudes of light oscillation (***Figure-SM 3.4*** *A*). Conversely, NPQ values of *pgrl1ab* were much lower (***Figure-SM 3.4*** *A*) than those of Col-0 and followed the same courses as seen in both *npq1* and *npq4* mutants in all oscillation amplitudes (***Figure-SM 3.3*** *A*). The delay in Y(NPQ) minima and maxima relative to light oscillations, previously observed in Col-0 wild-type and NPQ mutants (**Figure 3.2** E), was also present in the *crr2-2* mutant and Col-*gl1* wild-type (approx. 45° phase delay relative to the course of HL oscillation, 7.5 s) (**Figure 3.4** E). In the case of NPQ parameter, a similar delay was observed in *crr2-2* and Col-*gl1* (***Figure-SM 3.4*** *A*), but it was more pronounced to approx. 90° (15 s) phase delay relative to the course of HL oscillation. In the *pgrl1ab* mutant (**Figure 3.4** E), there was still an observable delay of Y(NPQ), but overall upward trend highly overshadowed it.

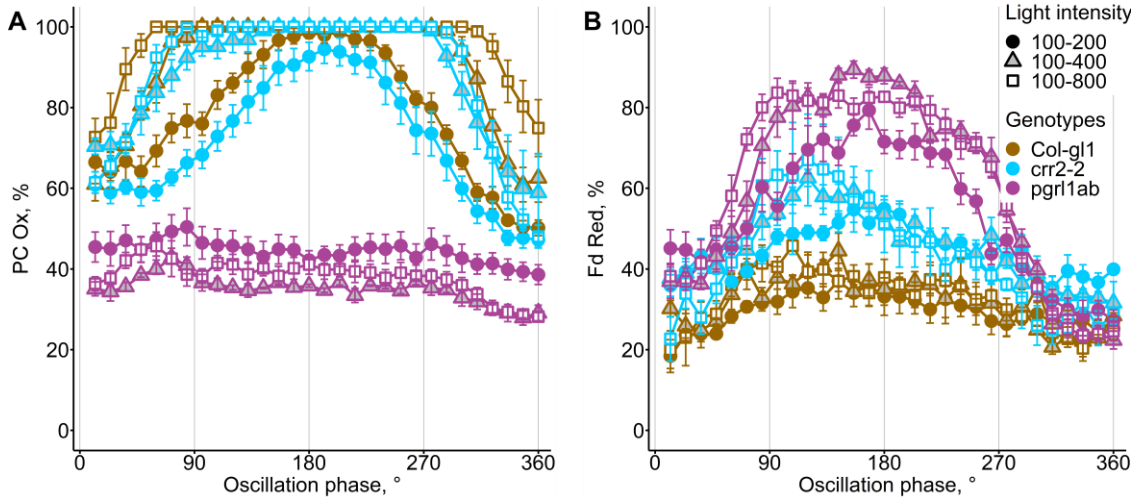

Figure 3.5 Changes of the apparent relative oxidation of PC (PC Ox) and reduction of Fd (Fd Red) in response to three different amplitudes of oscillating light for the three CET-related genotypes of *A. thaliana*, Col-*gl1*, *crr2-2*, and *pgrl1ab*. The oscillating light amplitudes range from 100 to 200 µmol photons·m^{-2}·s^{-1}, from 100 to 400 µmol photons·m^{-2}·s^{-1}, and from 100 to 800 µmol photons·m^{-2}·s^{-1}. The error bars represent the standard error (n = 3-7).

In Col-*gl1* and both CET mutants, the Y(NO) courses aligned with the light intensity changes in LL oscillation (**Figure 3.4** F). However, this alignment was substantially distorted in ML and HL oscillations of Col-*gl1*, as well as in HL oscillation of both CET mutants. The delayed responses of Y(NPQ) (**Figure 3.4** E) seem to be partially complemented by the increased levels and modulation of Y(NO) (**Figure 3.4** F). For LL oscillation, Y(NO) of *crr2-2* closely resembled that of Col-*gl1* (**Figure 3.4** F), whereas Y(NO) of *pgrl1ab* was much higher than that of Col-0 (**Figure 3.2** F). For ML and HL oscillations, Y(NO) of *crr2-2* was lower than Y(NO) of Col-*gl1* in the raising phase of the light oscillation, whereas Y(NO) of *pgrl1ab* remained well above Y(NO) of Col-0 (**Figures 3.4** F and **3.2** F). Similar to the NPQ mutants (**Figure 3.2** E, F), the consistently enhanced Y(NO) in *pgrl1ab* may act to partially compensate for the lower Y(NPQ) (**Figure 3.4** E, F). Considering again that Y(II) + Y(NPQ) + Y(NO) = 1, the sum of Y(NPQ) and Y(NO) was slightly higher for *crr2-2*, but considerably higher for *pgrl1ab* than in their respective wild-types (**Figures 3.4** D and **3.2** D).

The PC oxidation in *crr2-2* was smaller than in Col-*gl1* during LL oscillation and smaller at the beginning and the end phases of oscillation in ML and HL oscillations (**Figure 3.5** A). Regarding the PSI acceptor side, Fd (**Figure 3.5** B) in *crr2-2* was more reduced than in Col-*gl1*, especially evident in ML and HL oscillations where a peak can be observed in *crr2-2* at roughly 90° phase. The lower oxidation of PC (**Figure 3.5** A) and higher reduction

of Fd in *crr2-2* (**Figure 3.5** B) compared to Col-*gl1* were consistent with a smaller Y(ND) (**Figure 3.4** B) and a larger Y(NA) (**Figure 3.4** C) in this mutant, further confirming that the absence of NDH-like complex-dependent CET caused PSI acceptor side limitation, particularly in ML and HL oscillations.

On both the PSI donor and acceptor sides, the *pgrl1ab* mutant (**Figure 3.5**) had dramatic differences from its wild-type Col-0 (**Figure 3.3**). The mutant exhibited markedly higher Fd reduction (**Figure 3.5** B) and consistently low and relatively stable PC oxidation (**Figure 3.5** A), irrespective of the amplitude of the oscillating light. These findings were in line with the strong Y(NA) (**Figure 3.4** C) and zero Y(ND) (**Figure 3.4** B) observed in *pgrl1ab* and provided further indication that electron congestion occurred in the PSI acceptor side of *pgrl1ab* in all intensities of oscillating light.

An intriguing phenomenon that occurred in *pglr1ab* was that certain parameters showed different values at the beginning and end of the oscillation period, namely Y(I), Y(NA), Y(II), Y(NPQ) (**Figure 3.4** A, C, D, E), and Fd reduction (**Figure 3.5** B). The lower values of Y(II) and Y(I) at the end than at the beginning of the light oscillation period were counterbalanced by higher values of Y(NPQ) and Y(NA), respectively. This was consistently observed in *pgrl1ab* and was more pronounced in HL than in ML oscillations. This behavior occurred only in the *pgrl1ab* mutant, so it reflects its functional characteristics rather than measurement errors.

In terms of the quantum yield of the CET (*Supplementary materials* ***Figure-SM 3.4*** *B*), Y(I)-Y(II) in *crr2-2* was lower in LL oscillations but higher in HL oscillations when compared to Col-*gl1*. For the relative quantum yield of the CET, Y(I)/Y(II), *crr2-2* also displayed higher values than Col-*gl1* under HL oscillations (*Supplementary materials* ***Figure-SM 3.4*** *C*). In contrast, for the *pgrl1ab* mutant, both Y(I)-Y(II) (***Figure-SM 3.4*** *B*) and Y(I)/Y(II) (***Figure-SM 3.4*** *C*) showed lower values than in Col-0 (*Supplementary materials* ***Figure-SM 3.3*** *B, C*) in all oscillation amplitudes. Notably, the Y(I)/Y(II) of *pgrl1ab* showed a bumpy pattern in HL oscillation, with distinct decreases at about 70° and 280° phases but a peak at approximately 180° phase (***Figure-SM 3.4*** *C*).

3.4 Discussion

3.4.1 Regulation of rapidly reversible NPQ occurs at all tested intensity range of oscillating light

Both the VDE- and PsbS-dependent rapidly reversible NPQ are indispensable in dealing with fluctuating light (Külheim *et al.*, 2002; Külheim & Jansson, 2005; Sylak-Glassman *et al.*, 2014). The PsbS-protein governs the rate of NPQ quenching induction, but the amount of energy that can be quenched is determined by both PsbS- and VDE-dependent processes (Sylak-Glassman *et al.*, 2014). Our results here in a 60 s period of oscillation support these previous findings: Y(NPQ) of the *npq1* and *npq4* mutants was consistently lower than that of Col-0 across all amplitudes of oscillating light (**Figure 3.2** E). Thus, both VDE- and PsbS-dependent processes contribute to the NPQ in all intensities of light oscillations studied here.

Both NPQ mutants show increased CET (*Supplementary materials* ***Figure-SM 3.3*** *B*, *C*), which aligns with less reduction of Fd in these mutants than in Col-0 (**Figure 3.3** B). This finding suggests that increased CET in the NPQ mutants (*Supplementary materials* ***Figure-SM 3.3*** *B*, *C*) may represent a compensatory defence mechanism to counteract their inability to quench effectively. However, this increased CET in the NPQ mutants does not lead to increased photosynthesis control. If such control was present, it would be reflected in elevated Y(ND) (**Figure 3.2** B) and increased PC oxidation (**Figure 3.3** A) in the NPQ mutants compared to Col-0. Therefore, the increase in CET, evaluated as Y(I) - Y(II) and Y(I)/Y(II), might be unreal and alternative electron transport routes (e.g., Mehler-ascorbate-peroxidase reaction) might contribute to the evaluated CET. Contribution of AET to the evaluated CET is expected owing to i) the existing lateral heterogeneity of PSII and PSI (e.g., Tikhonov, (2023)) and the fact that ii) turnover time of PSII is about one order of magnitude slower (milliseconds; Crofts & Wraight, (1983); Ananyev & Dismukes, (2005)) than that of PSI (a hundred of microseconds; Bottin & Mathis, (1985); Setif & Bottin, (1995)). With respect to i), electrons from PSIs located in stroma lamellae can flow to AET and thus increase Y(I) but not affecting Y(II). With respect to ii), faster turnover time of PSI, even if PSIs are located in the same thylakoid membrane of a granum as PSIIs, enables electron flow from PSIs to AET without affecting Y(II).

3.4.2 The quantum yield of constitutive non-photochemical quenching is not constant and depends on the intensity of actinic light

The changes in the amplitude of Y(NPQ) in the NPQ mutants (**Figure 3.2** E) were accompanied by compensative quantitative changes of Y(NO) for all amplitudes of light oscillations (**Figure 3.2** F). Similar changes were also observed for Y(NO) and Y(NPQ) in the *pgrl1ab* mutant (**Figure 3.4** E, F). Moreover, the course of Y(NO) of both wild-types in ML and HL oscillations, as well as that of the *pgrl1ab* and *crr2-2* mutants in HL oscillations (**Figures 3.2** F and **3.4** F), deviated from the course of light oscillation and compensated to some extent for the delayed response of Y(NPQ) (**Figures 3.2** E and **3.4** E). It means that the quantum yield of constitutive non-photochemical quenching of excitation energy, Y(NO), which includes deactivation of the excitation energy *via* ChlF and *via* constitutive heat dissipation, is not constant at different light intensities and non-linearly depends on light intensities. The fact that Y(NO) is not constant and appears to be "regulated" has been noticed before (Han *et al.*, 2022; Lazár *et al.*, 2022). The simplest explanation for observed changes of Y(NO) might be attributed to the light-induced changes in Y(II) and Y(NPQ) since Y(NO) = 1 - Y(II) - Y(NPQ). However, it has been reported that changes in Y(NO) qualitatively agree with changes in ChlF signal during light oscillations and that thylakoid membrane voltage-dependent non-radiative charge recombination is probably involved in modulating the ChlF signal, and consequently, Y(NO) (Lazár *et al.*, 2022). Thus, the quantum yield of constitutive non-photochemical quenching, Y(NO), also denoted as Y(f,D) (Lazár, 2015), seems to be also regulated.

3.4.3 The PGR5/PGRL1 dependent-CET is crucial in oscillating light of different amplitudes

Light changes with large magnitude were typically employed to investigate the role of CETs in response to light fluctuations (Kono *et al.*, 2014; Kono & Terashima, 2016; Yamori *et al.*, 2016; Yamamoto & Shikanai, 2019; Zhou *et al.*, 2022), most of which can even lead to partial photoinhibition in wild-type organisms. In this study, we examined the physiological roles of PGR5/PGRL1-dependent CET and NDH-like complex-dependent CET in regulating photosynthesis under different amplitudes of light oscillations while applying the SPs during the oscillations. This way, we were able to explore the effects of these two CET pathways in detail during both the rising and declining phases of light intensity changes.

Regardless of the amplitudes of the light oscillations, the *pgrl1ab* mutant showed a striking contrast to Col-0. It displayed higher Y(NA), lower Y(I) and Y(II), while Y(ND) remained at zero (**Figure 3.4**). This supports earlier findings that the absence of PGR5/PGRL1-dependent CET causes severe PSI acceptor side limitation, leading to a substantial reduction in the efficiency of both PSI and PSII under fluctuating light conditions (Suorsa *et al.*, 2012; Suorsa *et al.*, 2013; Yamori *et al.*, 2016; Shimakawa & Miyake, 2018; Yamamoto & Shikanai, 2019). The marked reduction of Fd (**Figure 3.5** B) and PC (**Figure 3.5** A) further supports the notion that the entire electron transport chain is substantially reduced in the absence of PGR5/PGRL1-dependent CET.

Interestingly, the *pgrl1ab* mutant shows lower values of Y(I), Y(II) (**Figure 3.4** A, D) and a more reduced Fd (**Figure 3.5** B), and higher values of Y(NA) and Y(NPQ) (**Figure 3.4** C, E) at the end than at the beginning of the HL, and also the ML oscillations. If rapidly reversible NPQ is responsible for the higher values of Y(NPQ) (**Figure 3.4** E) at the end than in the beginning of the oscillations, a decreased proton efflux via ATP-synthase (Avenson *et al.*, 2005; Degen *et al.*, 2023) when PGR5/PGRL1-dependent CET is malfunctioned, can be the reason for accumulation of protons in lumen. However, it is more likely that the lower values of Y(I), Y(II) (**Figure 3.4** A, D) and the higher values of Y(NPQ) (**Figure 3.4** E) at the end than at the beginning of the oscillations reflect photoinhibition of PSI and PSII, induing photoinhibitory NPQ - qI, rather than rapidly reversible NPQ. The lack of rapidly reversible NPQ in the *pgrl1ab* mutant is also supported by the significant contribution of PGR5/PGRL1-dependent CET to lumen acidification compared to NDH-like complex-dependent CET (Wang *et al.*, 2015; Kawashima *et al.*, 2017; Degen *et al.*, 2023). Thus, in agreement with the literature (Kono *et al.*, 2014; Kono & Terashima, 2016; Yamori *et al.*, 2016; Yamamoto & Shikanai, 2019; Zhou *et al.*, 2022), our data indicates that PGR5/PGRL1-dependent CET protects plants from photodamage in light fluctuations.

The decreased PC oxidation (**Figure 3.5** A), absence of Y(ND) (**Figure 3.4** B), and the decoupling of P700 redox state from PSII reduction found in *pgrl1ab* (*Supplementary materials* ***Figure-SM 3.5*** *A-C*) collectively indicate that photosynthesis control at Cyt b_6/f does not operate effectively in the absence of PGR5/PGRL1-dependent CET, leading to electron congestion around PSI (Suorsa *et al.*, 2012; Yamori & Shikanai, 2016). In wild-type plants, PGR5/PGRL1-dependent CET plays a role in generating a pH difference across the thylakoid membrane (Wang *et al.*, 2015; Kawashima *et al.*, 2017; Wolf *et al.*, 2020), which is critical for supplying ATP required for downstream carbon fixation and for preventing

photodamage (Ma *et al.*, 2021a). This is accomplished in wild-types by inducing excess energy dissipation, as reflected in Y(NPQ) (**Figure 3.4** E) (Müller *et al.*, 2001; Johnson *et al.*, 2014), and by regulating the rate of electron transport via photosynthesis control (*Supplementary materials* ***Figure-SM 3.5*** *A-C*) (Suorsa *et al.*, 2012; Yamori & Shikanai, 2016). However, neither of these mechanisms is functioning well in *pgrl1ab*. Lumen acidification in *pgrl1ab* was limited (Wolf *et al.*, 2020), resulting in impaired photosynthesis control (*Supplementary materials* ***Figure-SM 3.5*** *A-C*) and restricted rapidly reversible NPQ (**Figure 3.4** E).

3.4.4 The NDH-like complex-dependent CET acts as a safety valve to protect PSI in light oscillations of high amplitude

Despite significant advances in understanding its structure (Peltier *et al.*, 2016; Ma *et al.*, 2021b), the physiological role of NDH-like complex still needs to be understood. The absence of NDH-like complex-dependent CET led to a diversity of behaviors under different environmental stresses in different species (Yamori & Shikanai, 2016; Ma *et al.*, 2021b). Previous studies in *A. thaliana* showed mixed results regarding the impact of NDH-like complex-dependent CET deficiency on photosynthetic performance under fluctuating light conditions. Some studies reported no significant difference compared to the wild-types (Suorsa *et al.*, 2012; Kono *et al.*, 2014), while others found that the lack of NDH-like complex-dependent CET limited PSI oxidation (Kono & Terashima, 2016; Shimakawa & Miyake, 2018; Zhou *et al.*, 2022). The concept of NDH-like complex-dependent CET as a safety valve was proposed previously based on the observation that double mutants defective in both PGR5/PGRL1-depednet CET and NDH-like complex-dependent CET exhibited larger suppression of pmf accumulation, P700 oxidation, and lower electron transport efficiency than single mutants lacking PGR5/PGRL1-dependent CET (Munekage *et al.*, 2004; Wang *et al.*, 2015; Nakano *et al.*, 2019). Here, we directly demonstrated the safety valve function of NDH-like complex-dependent CET by comparing the performance of multiple components in the electron transport chain between the *crr2-2* mutant and its wild-type Col-*gl1*, under different amplitudes of light oscillations.

In the present study *crr2-2* exhibited limitations on the PSI acceptor side, particularly pronounced during the light increasing phase of HL oscillation (**Figures 3.4** C and **3.5** B), whereas the PSI donor side was less limiting than in Col-*gl1* (**Figures 3.4** B and **3.5** A).

These differences were observed under ML and HL oscillations but not during the light response curve measurements (**Figure 3.1** B, C, H, I). In the case of HL oscillation, we noted that the initial increase in Y(NA) (**Figure 3.4** C), accompanied by a shallow depression phase of Y(ND) (**Figure 3.4** B), was partly alleviated as the intensity of oscillating light approached its maximum at a 180° phase. Such dynamic redox changes in the PSI donor and acceptor sides are difficult to monitor in a rectangular light condition, where light intensity fluctuates abruptly (Kono & Terashima, 2016; Zhou *et al.*, 2022). The decline of Y(NA) at the phase of maximal light intensity in HL oscillation may reflect enhancement of PGR5/PGRL1-dependent CET (*Supplementary materials* ***Figure-SM 3.4*** *B, C*) or AETs (see the reasoning above), such as the Mehler-ascorbate-peroxidase reaction, which could compensate for the NDH-like complex-dependent CET defect.

Interestingly, the *crr2-2* mutant showed consistently higher Y(NPQ) and NPQ than Col-*gl1* at all oscillating light conditions (**Figure 3.4** E and *Supplementary materials* ***Figure-SM 3.4*** *A*). This was also observed by Shimakawa and Miyake (2018) under oscillating light with the same period but higher amplitude (30 - 1970 µmol photons m^{-2} s^{-1}), whereas it was not the case under rectangular light changes, where Y(NPQ) in *crr2-2* was roughly the same as in its wild-type (Kono & Terashima, 2016; Zhou *et al.*, 2022). The NDH-like complex is able to transport electrons from Fd to plastoquinone while simultaneously causing accumulation of protons in lumen, not only via oxidation of reduced plastoquinone molecules at Cyt b6/f but also by transporting protons from stroma to lumen by itself (Kouřil *et al.*, 2014; Strand *et al.*, 2017; Laughlin *et al.*, 2020). Despite this superior proton transport ability of the NDH-like complex, its absence does not apparently impair the induction of rapidly reversible NPQ, suggesting a low turnover rate of the NDH-like complex-dependent CET (Okegawa *et al.*, 2008; Trouillard *et al.*, 2012). Linear electron transport and the PGR5/PGRL1-dependent CET, along with other AETs, may already be sufficient to reduce luminal pH and induce rapidly reversible NPQ (Nakano *et al.*, 2019), especially for light intensities exceeding 200 µmol photons m^{-2} s^{-1}.

To further elucidate the impact of the absence of NDH-like complex-dependent CET on luminal pH, we also assessed the correlation between qP and P700 reduction (*Supplementary materials* ***Figure-SM 3.5*** *A-C*), which mirrors the state of photosynthesis control. Under HL oscillation, *crr2-2* had a more reduced PSI compared to Col-*gl1* while maintaining the same PSII openness (***Figure-SM 3.5*** *A*); this effect was, however, not visible in ML and LL oscillations (***Figure-SM 3.5*** *B, C*). It seems that the absence of NDH-

like complex-dependent CET may moderately retard lumen acidification and, consequently, the induction of photosynthesis control under HL oscillation. However, this absence does not appear to affect the induction of rapidly reversible NPQ (**Figure 3.4** E). This agrees with the facts that pmf is only slightly lower in mutants lacking NDH-like complex-dependent CET compared to wild-type (Wang *et al.*, 2015) and that NDH-like complex-dependent CET contributes only by about 5% to the total ΔpH across the thylakoid membrane (Kawashima *et al.*, 2017). It is also consistent with the fact that rapidly reversible NPQ requires less acidified lumen than photosynthesis control does (Schansker, 2022).

These findings collectively suggest that the NDH-like complex-dependent CET may function as a safety valve when the amplitude of light oscillations is high, alleviating the electron pressure on the PSI acceptor side and enhancing ΔpH formation across the thylakoid membrane, thereby effectively inducing photosynthesis control. Furthermore, under conditions where photosynthesis control was less obvious, such as in LL and ML oscillations (*Supplementary materials* ***Figure-SM 3.5*** *B, C*), the absence of NDH-like complex-dependent CET in *crr2-2* resulted in more reduced PSI donor and acceptor sides (**Figure 3.5**) and slightly lower Y(I) and Y(II) (**Figure 3.4** A, D). This suggests that NDH-like-CET may contribute to the maintenance of efficient linear electron transport under these conditions. While not indispensable, the NDH-like complex-dependent CET does support the dynamic regulations in response to oscillating light, which is essential for optimizing photosynthesis in dynamically changing light environments.

3.4.5 Complementary effects among multiple protective regulatory mechanisms

Long-term acclimation to fluctuating light involves alterations in gene expression and protein abundance (Barker *et al.*, 1997; Alter *et al.*, 2012; Caliandro *et al.*, 2013; Gjindali *et al.*, 2021; Wei *et al.*, 2021), resulting in enhanced regulatory mechanisms. Plants grown in fluctuating light have increased rapidly reversible NPQ, attributed to higher amounts of PsbS protein and enzymes involved in the xanthophyll cycle, compared to plants grown under constant light (Alter *et al.*, 2012; Caliandro *et al.*, 2013; Schneider *et al.*, 2019; Wei *et al.*, 2021). Some genes and proteins associated with NDH-like complex-dependent CET and PGR5/PGRL1-dependent CET are also upregulated in response to long-term fluctuating light (Suorsa *et al.*, 2012; Schneider *et al.*, 2019; Niedermaier *et al.*, 2020).

In this study, plants were grown under constant low light and were exposed to oscillating light only during measurements. These short-term light oscillations revealed the complementary responses among different protective mechanisms, particularly pronounced in mutants lacking one or the other regulatory mechanisms. Further studies are required to explore these interactions. Here is a brief summary of observed complementary phenomena in tested oscillating light conditions:

- The complementary effect between Y(NPQ) and Y(NO) as discussed above can be observed in all tested genotypes (**Figures 3.2** E, F and **3.4** E, F).
- Although the decrease of Y(NPQ) in the NPQ-deficient mutants was largely counteracted by increased Y(NO) under oscillating light (**Figure 3.2** E, F), there was still a slight reduction in PSII efficiency in these mutants (**Figure 3.2** A). However, these defects had little impact on PSI efficiency (**Figure 3.2** A), even in HL oscillation. This may be attributed to an increased efficiency of CET in NPQ mutants, evident via higher Y(I)-Y(II) and Y(I)/Y(II) levels (*Supplementary materials* ***Figure-SM 3.3*** *B, C*), as well as less reduced Fd (**Figure 3.3** B) compared to the wild-type. It is possible that AET also contributes to this.
- In HL oscillations, the PSI acceptor side limitation of *crr2-2* was temporarily induced during the light ascending phase (**Figures 3.4** C and **3.5** B). We speculate that PGR5/PGRL1-dependent CET or other AETs, e.g., the malate shuttle or the Mehler-ascorbate-peroxidase reaction (Lazár *et al.*, 2022), might alleviate this limitation on the acceptor side of PSI, causing it to diminish within seconds of its induction (*Supplementary materials* ***Figure-SM 3.4*** *C*).
- The *crr2-2* mutant had higher levels of Y(NPQ) and NPQ parameter than Col-*gl1* at all tested oscillation amplitudes (**Figure 3.4** E and *Supplementary materials* ***Figure-SM 3.4*** *A*), likely to prevent over-excitation of photosystems.

In this study, we delved into the dynamics of two short-term regulatory mechanisms, rapidly reversible NPQ and CETs, in response to different amplitudes of oscillating light. Their interplays are already dazzling. However, they constitute only part of the intricate regulatory networks adjusting and optimizing photosynthesis, which operate across a wide range of timescales. Gaining a deeper understanding of this complexity in natural environments necessitates studying the dynamic response of photosynthesis and its regulation to fluctuating light or, more broadly, to a dynamically changing environment (Gjindali *et al.*, 2021). Many experimental investigations have been conducted under well-defined light

conditions, drastically differing from natural light environments. Therefore, it is crucial to explore novel approaches for systematically investigating the dynamics of photosynthesis in changing light environments. Our findings highlight the potential of harmonically oscillating light approach in advancing the study of the dynamics of photosynthesis.

Acknowledgments

DL and LN were supported by the European Regional Development Fund project 'Plants as a tool for sustainable global development' (no. CZ.02.1.01/0.0/0.0/16_019/0000827) and the Horizon Europe, European Innovation Council Pathfinder Open 2021 project 'DREAM' (no. 101046451). SM was also supported by the Horizon Europe, European Innovation Council Pathfinder Open 2021 project 'DREAM' (no. 101046451). YN gratefully acknowledge the financial support from the Federal Ministry of Education and Research of Germany (BMBF) in the 'YESPVNIGBEN' project (no. 03SF0576A).

The authors thank Dr. Benjamin Bailleul for his comments. The authors thank Toshiharu Shikanai of Kyoto University, Japan for kindly providing seeds of the *crr2-2* mutant of *Arabidopsis thaliana* and Dario Leister in Ludwig Maximilian University München, Germany for providing seeds of the *pgrl1ab* mutant.

Author contributions

YN, SM, and LN planned and designed the research. YN conducted the experiments and analysed the data. YN, DL, and SM interpreted the results. YN, DL, SM, and LN wrote the manuscript.

Supplementary material

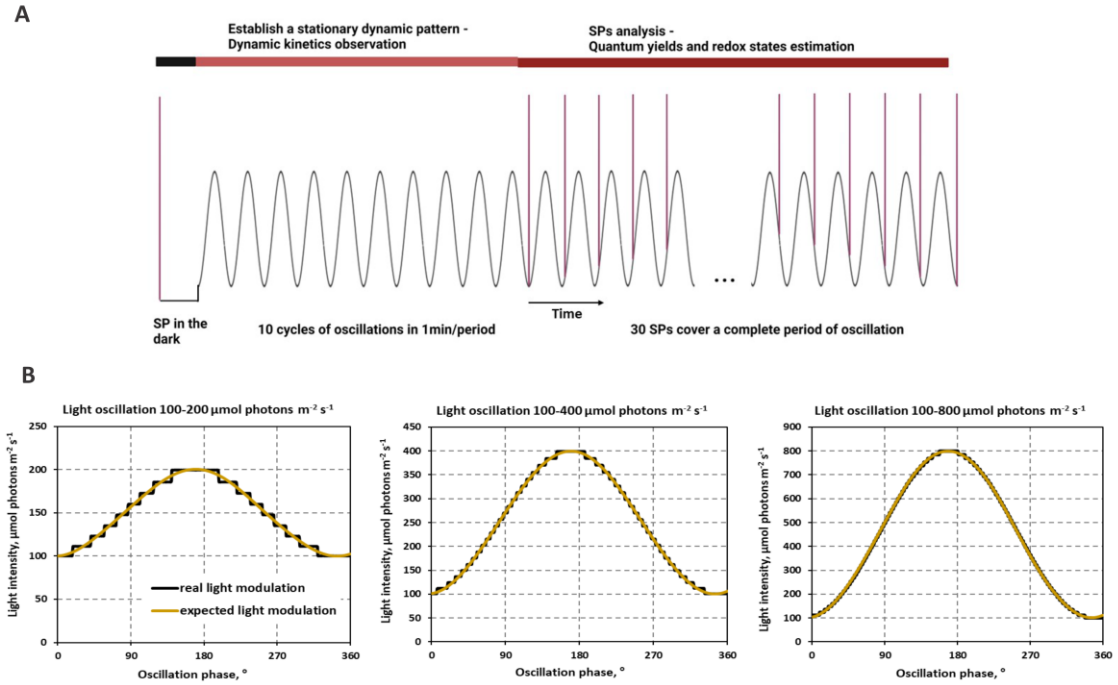

Figure-SM 3.1 A diagram illustrates the flow of measurements under harmonically oscillating light, which includes the establishment of a stationary dynamic pattern and the SPs analysis. The black curve represents the course of the AL light, and the vertical magenta lines represent the SPs. The top color bars indicate the light conditions: the dark bar represents darkness, the red bar represents oscillating AL on, and the dark red bar contains oscillating AL and SPs. The first SP was given to the dark-adapted plants to obtain maximum efficiency of PSII photochemistry in darkness. After a 25-s delay, the first 10 cycles of light oscillations were performed without SPs to establish a stationary dynamic pattern. Then, each cycle triggered an SP with a 2-s phase shift to assess the quantum yields of photosystems and the redox states of electron carriers under light oscillations. A total of 30 SPs were applied, one SP in each oscillation period, covering a complete 60 s light period. In panel B, the difference between the actual (black curve) and simulated (yellow line) light oscillations of different amplitudes (100-200, 100-400, and 100-800 µmol photons·m^{-2}·s^{-1}) is shown. The real light applied was modulated in a stepwise ascending/descending manner rather than in a smooth sinusoidal manner due to the limitations of the commercial instrument.

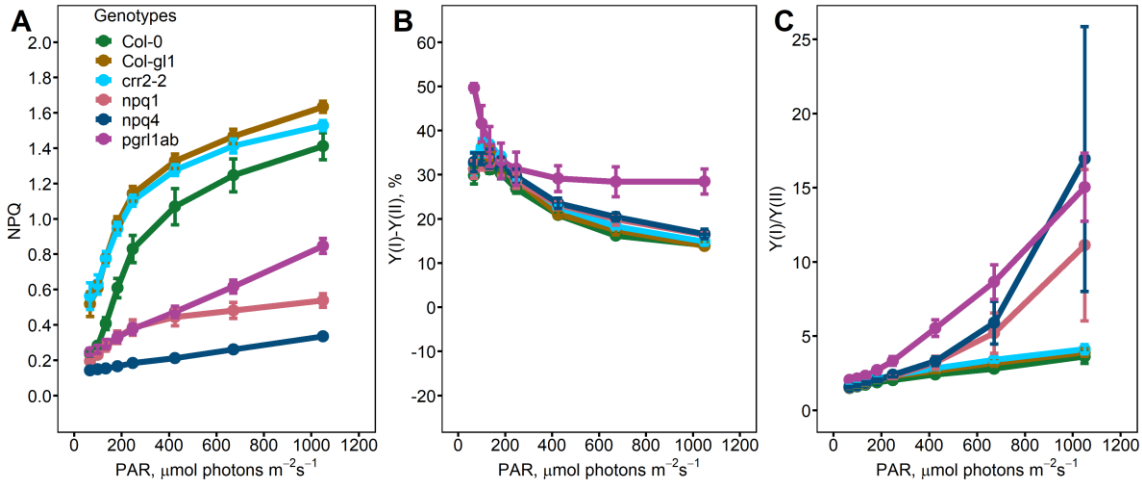

Figure-SM 3.2 The non-photochemical quenching parameter, NPQ (A), and the efficiency of CETs (B, C) were assessed in light response curves with six genotypes of A. thaliana (see the legend). The Y(I)-Y(II) represents the estimation of the quantum yield of CET. The Y(I)/Y(II) represents the estimation of the relative quantum yield of CET. The error bars represent the standard error (n=3-7).

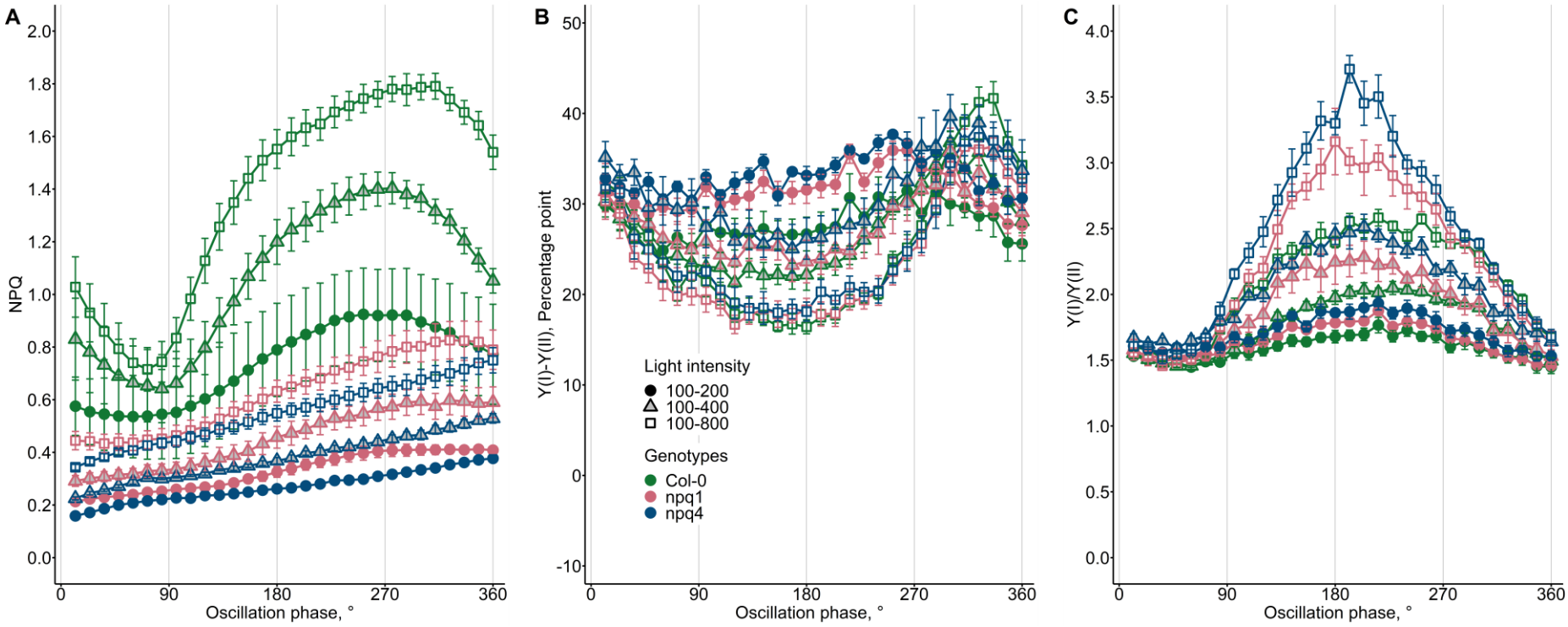

Figure-SM 3.3 The non-photochemical quenching parameter, NPQ (A), and two proxies used to estimate the efficiency of CETs: the difference (B) and the ratio (C) of the effective quantum yield of PSI and PSII photochemistry, were assessed under oscillating light with three different amplitudes in three genotypes of *A. thaliana* including Col-0, *npq1*, and *npq4* (see the legend). The error bars represent the standard error (n=3-7).

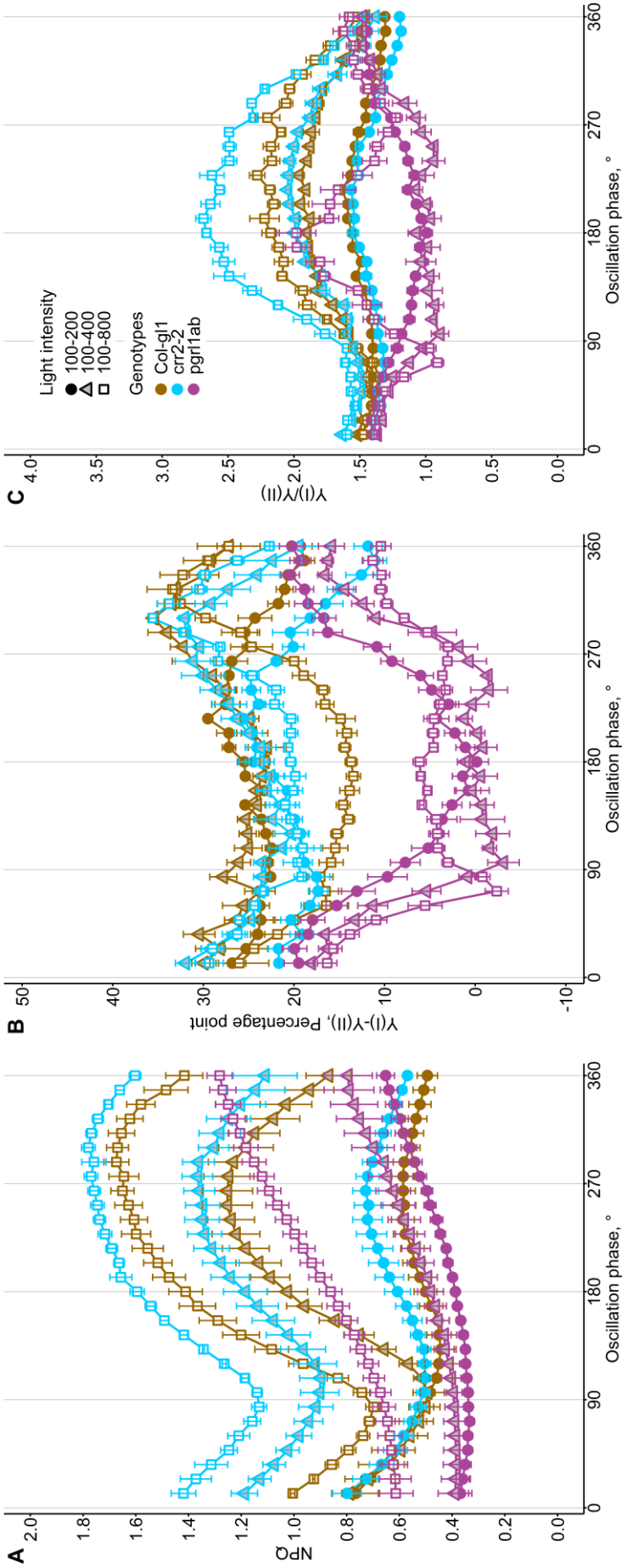

Figure-SM 3.4 The non-photochemical quenching parameter, NPQ (A), and two proxies used to estimate the efficiency of CET: the difference (B) and the ratio (C) of the effective quantum yield of PSI and PSII photochemistry, were assessed under oscillating light with three different amplitudes in three genotypes of *A. thaliana* including Col-*gl1*, *crr2-2*, and *pgrl1ab* (see the legend). The error bars represent the standard error (n=3-7).

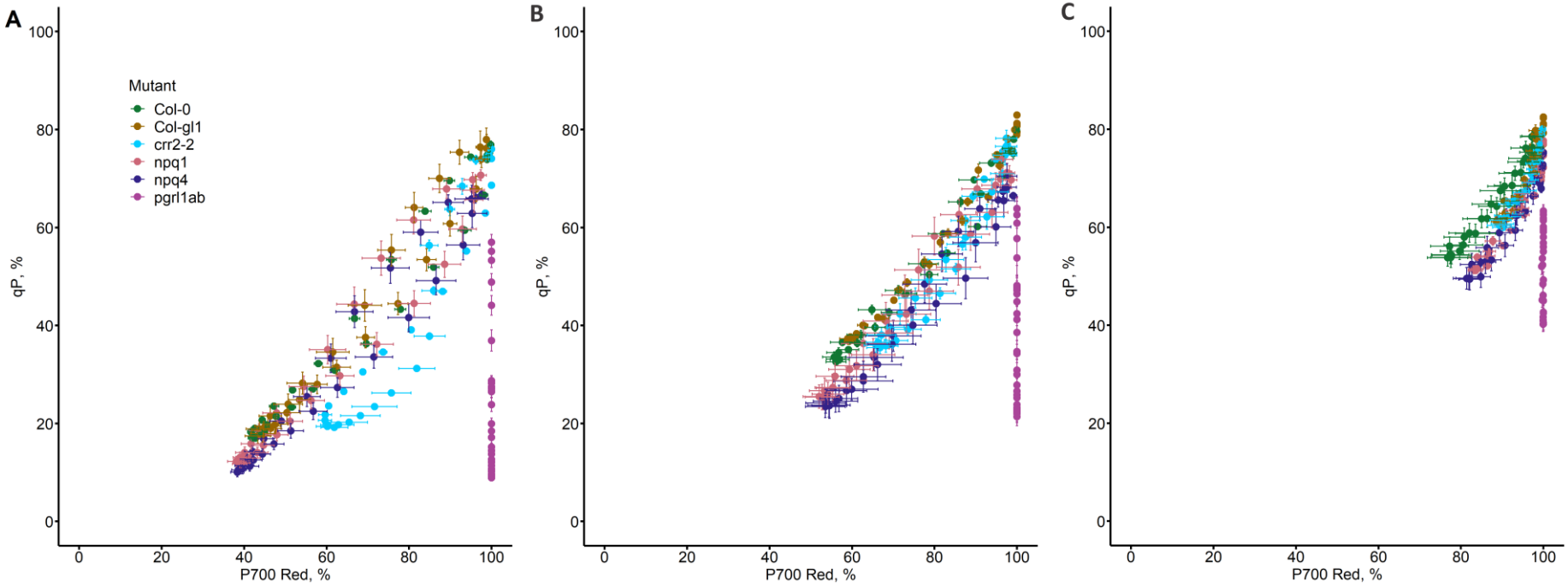

Figure-SM 3.5 Relationships between qP and P700 Red for estimating photosynthesis control in Cyt b6/f complex were obtained from SP analysis of all six genotypes of *A. thaliana* (see in the elegend) under three different amplitudes of oscillating light: 100-800 µmol photons·m^{-2}·s^{-1} (A), 100-400 µmol photons·m^{-2}·s^{-1} (B), 100-200 µmol photons·m^{-2}·s^{-1} (C). The error bars represent the standard error (n=3-7).

Chapter 4

The Non-linear Responses of Chlorophyll Fluorescence to Oscillating Light

Yuxi Niu[1], Shizue Matsubara[1], Ladislav Nedbal[1,2,3*]

(in preparation)

I completed 80% of the research design and planning. I conducted all the experiments and analyzed the data. I contributed 90% of the data interpretation. My contribution to the final writing was 90%.

Abstract

The stationary photosynthesis increases proportionally to low light intensity and saturates in high light. This simple relationship becomes intriguingly complex when the light oscillates. The dynamic fingerprint of photosynthesis is characterized here by changes in ChlF yield that follow the light that oscillated with three amplitudes ranging from the linear part of the photosynthetic light response curve to the saturation.

Experiments with wild-type *Arabidopsis thaliana* and mutants with incapacitated rapidly reversible NPQ (qE) revealed that the response in the fast oscillation frequencies can be explained solely by the constitutive non-linearity due to saturation of photosynthetic pathways or to filling and emptying of the photosynthetic reactant pools. The response is then delayed after the light oscillation and tends to saturate in high light, characterized by a counterclockwise input-output dynamic fingerprint. The dominating effect of qE appears only in the slow oscillation periods 30 s and longer and is characterized by a clockwise input-output dynamic fingerprint with a distorted loop trajectory, i.e., ChlF decreases with increasing light intensity. The stationary state of photosynthesis under oscillating light occurs only in wild-type plants when the oscillation period is long enough, and the amplitude is large enough to induce a highly efficient qE.

Four different types of non-linear dynamics of ChlF yield observed include delayed response, saturation trend, distorted loop trajectory and stationary state, which are categorized as constitutive and regulatory non-linearities.

Keywords: Photosynthesis systems, Constitutive non-linearity, Regulatory non-linearity, Delayed response, Saturation, distorted loop trajectory, Stationary state

4.1 Introduction

The stimulus-response relationship is a fundamental concept in biology, characterizing the extent to which an organism responds to the duration or doses of exposure to a stimulus (Calabrese & Baldwin, 2003; Mattson, 2008; Pinheiro & Duffull, 2009). In plant research, this concept is commonly applied to assess optimal growth conditions and plant resistance to stress (Berry & Bjorkman, 1980; Idso & Idso, 1994; Lee *et al.*, 2007; Dusenge *et al.*, 2019). One widely used stimulus-response relationship is the photosynthetic light response curve (P-I curve) (Evans *et al.*, 1993; Ralph & Gademann, 2005; Hogewoning *et al.*, 2010; Flood *et al.*, 2011), which depicts the relationship between the assimilation rate and the intensity of photosynthetically active radiation (PAR).

A typical P-I curve exhibits three distinct phases. At low light intensities, the rate of photosynthetic assimilation is linearly proportional to the intensity level as it is primarily limited by the availability of light. The slope of this linear phase of the P-I curve depends on the functional absorption cross-section and the number of functional reaction center units (Kiss *et al.*, 2008; Krah & Logan, 2010; Murchie & Niyogi, 2011; Hasan & Cramer, 2012). As the light intensity increases, the rate of photosynthetic assimilation rises less steeply, eventually reaching saturation. At this phase, the light availability is no longer a limiting factor, and instead, the electron transport and reaction rates in the Calvin-Benson cycle limit photosynthesis at saturating light intensity (Murchie & Niyogi, 2011; Hasan & Cramer, 2012; Hoh *et al.*, 2023). As the light intensity continues to rise, the assimilation rate may decline due to photoinhibition.

The P-I curve of photosynthesis can be measured by net CO_2 uptake or net O_2 evolution in incrementally adjusted light intensities (Evans *et al.*, 1993; Ögren & Evans, 1993). An alternative proxy estimating the rate of photosynthesis in relation to light intensity is the relative electron transport rate (ETR) of photosystem II (PSII), which can be estimated by examining the Chlorophyll fluorescence (ChlF) yield (Schreiber, 2004). Calculating PSII ETR directly from ChlF yield measurements requires employing the Pulse-Amplitude-Modulation (PAM) technique in conjunction with saturation pulses (Schreiber, 2004). Studies have demonstrated a strong correlation between the estimated ETR and the rates of photosynthesis determined through O_2 evolution or CO_2 uptake in gas exchange measurements (Beer *et al.*, 1998; Beer *et al.*, 2001; Ralph & Gademann, 2005). Therefore,

ChlF yield measurement offers a simple and fast method for assessing P-I curves of photosynthesis.

The ChlF yield is influenced by an interplay of two major processes in PSII: photochemical quenching and NPQ (Baker, 2008). Photochemical quenching is closely tied to the redox state of the primary quinone acceptor of PSII (QA). At low light intensities, photochemical quenching decreases with increasing light due to an increase in PSII reaction centers with reduced QA, meaning that ChlF yield increases linearly with increasing light intensity. At high light intensity, PQ becomes largely reduced and cannot efficiently re-oxidize QA, resulting in a sustained low photochemical quenching and high ChlF yield. The situation is more complicated, however, when NPQ is present.

NPQ is a regulatory mechanism that prevents PSII from being over-excitation in high light by decreasing the functional cross-section of PSII and dissipating excess photo-excitation energy as heat (Roach & Krieger-Liszkay, 2012; Demmig-Adams *et al.*, 2014a; Ware *et al.*, 2015; Kromdijk *et al.*, 2016; Ruban, 2016). It reduces the flow of electrons from PSII into PQ, and ChlF yield decreases with increasing NPQ. The induction of NPQ in land plants primarily depends on two processes triggered by low luminal pH (Külheim *et al.*, 2002; Horton & Ruban, 2005; Ruban *et al.*, 2007): protonation of PsbS protein in PSII (Li *et al.*, 2000; Li *et al.*, 2002b) and enzymatic conversion of violaxanthin to zeaxanthin, catalyzed by violaxanthin de-epoxidase enzyme (VDE) (Demmig-Adams, 1990; Gilmore, 1997; Niyogi *et al.*, 1998; Jahns & Holzwarth, 2012). TheseΔpH-dependent NPQ components are rapidly developing and relaxing, commonly referred to as qE (Jahns & Holzwarth, 2012), and are also termed rapidly reversible NPQ in this paper. Importantly, zeaxanthin also plays roles in the slowly developing and slowly relaxing component of NPQ, qZ, as well as in photoinhibition-related quenching, qI (Nilkens *et al.*, 2010; Jahns & Holzwarth, 2012) (**Chapter 1 - Section 1.2**).

The relationship between photosynthesis and light intensity becomes much more complex when light fluctuates. In fact, solar irradiance in nature is highly dynamic, changing on different timescales and intensities (Way & Pearcy, 2012; Smith & Berry, 2013; Kaiser *et al.*, 2018) (**Chapter 1 - Section 1.1**). With the aim of characterizing the relationships between photosynthesis and light intensity in dynamically changing light conditions, we simulated natural light conditions in the laboratory by exposing plants to harmonically

oscillating light with varying frequencies/periods and amplitudes, while using ChlF yield as a reporter proxy to monitor dynamics of photosynthesis.

To better interpret the ChlF signals obtained under changing light conditions, in addition to wild-type plants of *Arabidopsis thaliana*, we also characterized the relationship between photosynthesis and changing light in mutants that lack different NPQ processes: the *npq1* mutant (Niyogi *et al.*, 1998) lacking VDE-dependent NPQ and the *npq4* mutant (Li *et al.*, 2000) lacking PsbS-dependent NPQ.

The results highlighted non-linear dynamics of photosynthesis under harmonically oscillating light, which can be characterized by four different types of non-linearity: delayed responses, saturation, distorted loop trajectory and stationary state. Two of these can be considered constitutive non-linearity that arises from the primary function of photosynthetic apparatus, while the other two are of regulatory nature.

4.2 Materials and Methods

Three genotypes of *Arabidopsis thaliana* were grown in the climate chamber under light intensity of approx. 100 µmol photons·m^{-2}·s^{-1}, including wild-type Col-0, the *npq1* mutant that cannot convert violaxanthin into zeaxanthin (Niyogi *et al.*, 1998), and the *npq4* mutant that is deficient in PsbS protein (Li *et al.*, 2000). Plants were cultivated under controlled environmental conditions with a 12/12-hour light/dark photoperiod and a day/night air temperature of 26/20°C. Relative air humidity was maintained at 60%. Measurements were taken between 38 and 43 days after sowing.

The Dual-KLAS-NIR spectrophotometer with a 3010-DUAL leaf cuvette (Heinz Walz GmbH, Effeltrich, Germany) was used for detecting the dynamics of ChlF yield (Klughammer & Schreiber, 2016; Schreiber & Klughammer, 2016). The kinetic data were detected every 5 ms and 20 points were averaged, resulting in data recording of every 0.1 s. Red actinic light (630 nm) was applied to both the abaxial and adaxial sides of the leaf. The pulse-amplitude-modulated measuring light was green light (540 nm) with an intensity of 6 µmol photons·m^{-2}·s^{-1}, and it was applied only to the abaxial side of the leaf. The plants were removed from the climate chamber before the end of the dark photoperiod and kept in darkness until measurement. Prior to the oscillating light measurements, each dark-adapted plant was initially exposed to a 10-min constant red actinic light (630 nm) for photosynthetic

induction. The intensity of the constant light was set as the average of the subsequently given oscillating light. Thus, plants that were later exposed to light oscillating between 100 and 200 µmol photons·m^{-2}·s^{-1} (low light, LL) were initially subjected to a constant light intensity of 150 µmol photons·m^{-2}·s^{-1}, while those exposed to oscillations ranging from 100 to 400 µmol photons·m^{-2}·s^{-1} (medium light, ML) were initially subjected to a constant light of 250 µmol photons· m^{-2}·s^{-1}. Similarly, a constant light intensity of 450 µmol photons·m^{-2}·s^{-1} was used for plants that were later exposed to oscillations between 100-800 µmol photons·m^{-2}·s^{-1} (high light, HL).

Following induction in constant actinic light, plants were then exposed to sinusoidally oscillating light with different amplitudes: 100-200, 100-400 and 100-800 µmol photons·m^{-2}·s^{-1}. The response of plants to the largest oscillation amplitude of 100-800 µmol photons·m^{-2}·s^{-1} has been reported in our previous study in **Chapter 2** (Niu *et al.*, 2023). In the present study, we additionally measured the response of plants to the medium and low amplitudes of oscillating light and analyzed all data in an input-output format. The sequence of oscillating light periods was as previously described in **Chapter 2** (Niu *et al.*, 2023), consisting of eight different periods that varied continuously from 8 min to 1 s: three oscillation cycles with 8 min period, five cycles each with 4 min, 2 min, 1 min, 30 s and 10 s period, and finally ten cycles with 5 s and 1 s periods. The light was controlled by an 8-bit DA-converter, yielding 256 light levels to cover the amplitude range of the light intensities. The "sinusoidal" light changes were thus occurring in discrete steps rather than smoothly: the oscillations were approximated by 8 light intensity steps for 100-200 µmol photons·m^{-2}·s^{-1}, 22 light intensity steps for 100-400 µmol photons· m^{-2}·s^{-1}, and 49 light intensity steps for 100-800 µmol photons·m^{-2}·s^{-1}. To minimize the interference of stepwise increases/decreases in illumination on the dynamic response of ChlF to oscillating light, the data were fitted to the harmonics function Fit(t) (Eqn. 1) described in Nedbal and Lazár (2021). This allowed us to diminish noise without compromising the dynamic characteristics of ChlF signals. The original dynamics are presented in the *Supplementary materials* ***Figure-SM 4.1*** to ***Figure-SM 4.3*** for each of the three genotypes. The discrete character of the light changes did not affect the prevailing dynamics of extracted ChlF signals. Three biological replicates of each *A. thaliana* genotype were measured in three oscillating light conditions.

$$Fit(t) = A_0 + A_1 \cdot \sin[\mathbf{1} \cdot \frac{2\pi(t-\tau_1)}{T}] + A_2 \cdot \sin[\mathbf{2} \cdot \frac{2\pi(t-\tau_2)}{T}] + A_3 \cdot \sin[\mathbf{3} \cdot \frac{2\pi(t-\tau_3)}{T}] + A_4 \cdot \sin[\mathbf{4} \cdot \frac{2\pi(t-\tau_4)}{T}]$$

(Eqn.1)

As dynamic patterns of ChlF signals changed during the first one or two cycles following a shift in oscillation periods, only stationary response patterns that emerged in later cycles were used for the analysis. Specifically, the first cycle of the 8 min oscillation and the first two cycles of the other oscillation periods were thus excluded. The signals in the periodically dynamic stationary cycles were averaged for each plant and fitted to Eqn. 1 (Nedbal & Lazár, 2021; Niu *et al.*, 2023). The least-square fitting was done by Microsoft Excel to obtain the offset A_0 as well as the amplitudes (A_1, A_2, A_3, A_4) and phase shifts $(\tau_1, \tau_2, \tau_3, \tau_4)$ of multiple harmonic components. Lastly, the fitted data of the three biological replicates were averaged for each oscillation period. The values of offset A_0 and amplitudes of fundamental (A_1) as well as upper harmonics (A_2, A_3, A_4) of ChlF signals under different frequencies of oscillating light were presented in *Supplementary materials* ***Figure-SM 4.4***.

4.3 Results

4.3.1 ChlF response to oscillating light is frequency- and amplitude-dependent

The Input-output diagram in **Figure 4.1** shows the relationships between the ChlF yield and harmonically oscillating light intensity. The light was oscillating with eight periods ranging from 1 s to 8 min (**Figure 4.1**, panels A to H) and three amplitudes including 100-200 (LL), 100-400 (ML), and 100-800 (HL) μmol photons·m^{-2}·s^{-1} (**Figure 4.1**, denoted by black, dark-blue, and light-blue curves, respectively).

The dynamic response of the ChlF yield to oscillating light was manifested as signal loops (**Figure 4.1**). The orientation of the loops varied at different oscillation frequencies. In rapid oscillations with periods equal to or shorter than 10 s, the response of ChlF yield was delayed compared to the light oscillation, and the signal loops were always in a counterclockwise orientation, as indicated by the yellow arrows in the top corner of each

plot (**Figure 4.1** A-C). Using the 10-s period as an example (**Figure 4.1** C), the ChlF yield resembled a typical P-I curve, changing linearly with light intensity at low light intensities and nearly saturating at high light intensities. However, this relationship was not identical in the increasing and decreasing phases of oscillating light; the increasing phase induced slightly higher ChlF signals than the decreasing phase, resulting in the elliptical loops in a counterclockwise orientation. Hereafter, this phenomenon is referred to as delayed response, which typically signifies a lag between the input stimulus and output responses (Mayergoyz, 2003).

The ChlF dynamics changed strikingly in longer oscillation periods. In the 30 s period, the signal loops were distorted and no longer resembled a typical P-I curve in ML and HL oscillations (**Figure 4.1** D, dark-blue and light-blue curves). Importantly, the orientation of signal loops was reversed to give rise to a clockwise trajectory (**Figure 4.1** D, marked with purple arrows). The light input changes induced a stronger response of ChlF yield during the increasing phase than during the decreasing phase, leading to a distorted loop trajectory. The difference between the increasing and decreasing phases grew larger in the 1 min period (**Figure 4.1** E), with a clear decline of ChlF yield prior to the decline in light intensity. The expansion of the loop area in LL, albeit smaller, was also evident in the 1 min oscillation (**Figure 4.1** E black curve).

For oscillation periods longer than 1 min, the signal loops were consistently in a clockwise orientation (**Figure 4.1** F-H). A new feature emerged in these longer periods, with ChlF yield becoming largely independent of the light intensity in the ML and HL oscillations. In the 2 min period, for example, it occurred in the HL oscillation when the light intensity exceeded approximately 600 μmol photons·m^{-2}·s^{-1} (**Figure 4.1** F, light-blue curve). For the 4- and 8-min periods of the HL oscillation, the ChlF yield reached a stationary state already at the onset of the light increasing phase and further increase in light intensity hardly affected the ChlF yield (**Figure 4.1** G, H light-blue curves). This stationary state of ChlF yield was maintained even when the light intensity started to decline. This stationary state was less pronounced in the ML oscillations (**Figure 4.1** F-H, dark-blue curves) and absent in the LL oscillations (**Figure 4.1** F-H, black curves).

Another noteworthy feature in the signal loops was the variability of ChlF yield at the same light intensity in the same oscillation frequency. The same light intensity can trigger higher ChlF yield in the LL oscillations than in the ML and HL oscillations (**Figure 4.1** black

curves compared to dark-blue and light-blue curves). Likewise, higher ChlF yield was measured at the same light intensity in the ML oscillations than in the HL oscillations. The slopes of the signal changes were generally steeper in the smaller amplitudes of oscillation. These patterns were consistent across the different light oscillation frequencies. Thus, in combination with the effects of the oscillation period (frequency) described above, the amplitude of oscillating light also plays a role in shaping the dynamic response patterns of ChlF yield.

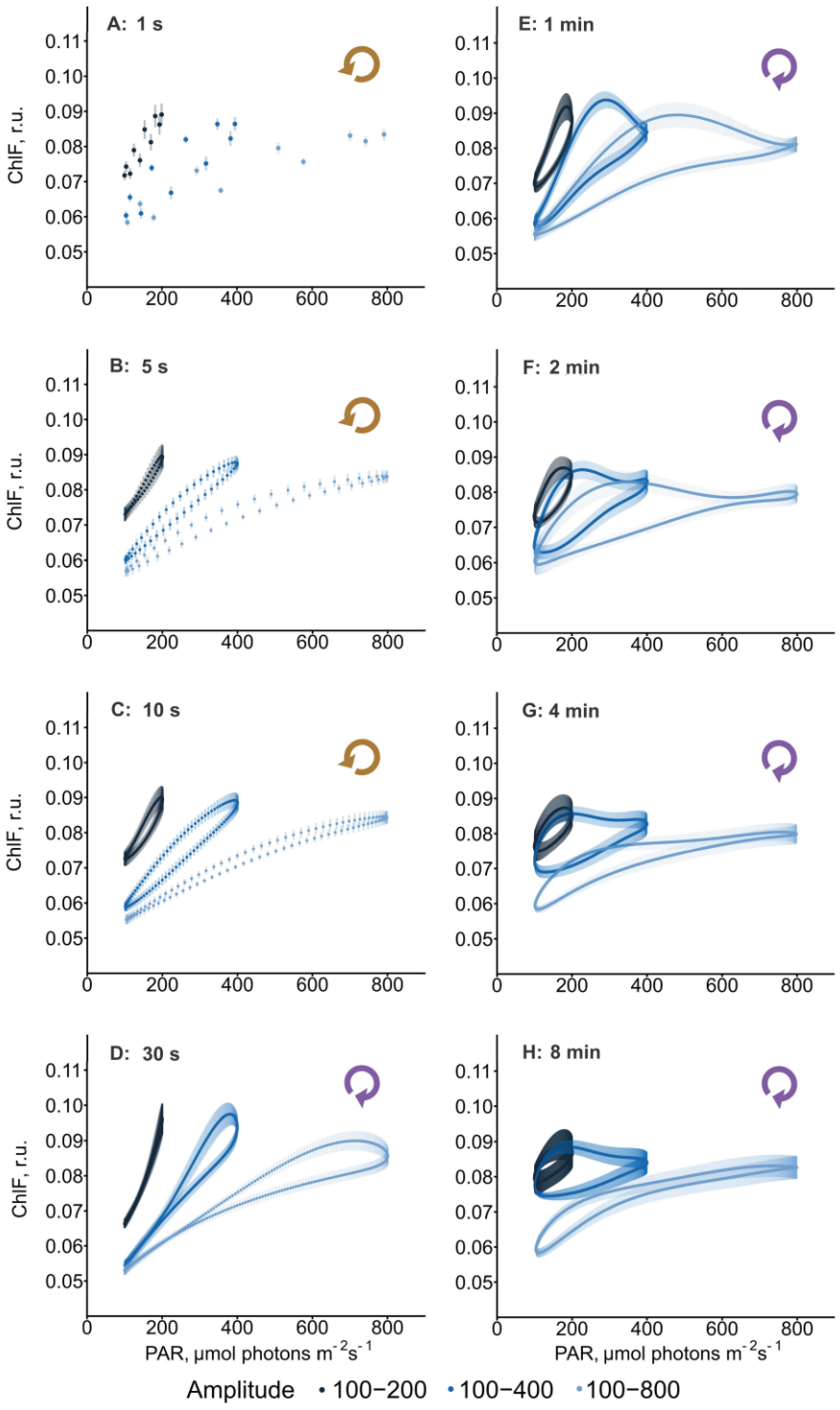

Figure 4.1 Input-output diagrams demonstrate the ChlF yield (fitted data) of wild-type *A. thaliana* Col-0 as a function of photosynthetically active radiation (PAR) changes induced by oscillating light with varied amplitudes. Three amplitude ranges were tested: 100-200 µmol photons·m^{-2}·s^{-1} (black), 100-400 µmol photons·m^{-2}·s^{-1} (dark-blue), and 100-800 µmol photons·m^{-2}·s^{-1} (light-blue). Eight different oscillation periods were executed, ranging from 1 s to 8 min. The left column of panels shows the results for periods from 1s to 30 s, while the right column (E-H) shows the results for periods from 1 min to 8 min. The colored arrows denote the orientations of the ChlF changes following the oscillating light, with purple arrows representing clockwise changes and yellow arrows representing counterclockwise changes.

4.3.2 The distorted loop trajectory reflects the regulatory processes of rapidly reversible NPQ (qE)

In the following, we examined the assumptions we made in interpreting the dynamic fingerprints observed in wild-type *A. thaliana* under oscillating light. We initially assumed that delayed response in fast periods might reflect an inherent lag in the primary photosynthetic reactions, unrelated to regulatory processes. The orientation reversal with a distorted loop trajectory emerging during the light oscillation might be associated with the onset of regulatory processes within the photosynthesis systems. We also hypothesized that the stationary state reached during long oscillation periods with ML and HL amplitude might indicate regulatory processes that can effectively cope with the light intensity changes to keep ChlF yield nearly constant. To test these, we compared the differences in ChlF dynamics in response to oscillating light between two NPQ mutants, *npq1* and *npq4*, and wild-type *A. thaliana* in **Figure 4.2**. Given the similarity in the dynamics of ChlF yield for fast oscillation periods shorter than 10 s and slow oscillation periods longer than 2 min, we selected one period each for these fast and slow ranges in addition to an intermediate period of 1 min. **Figure 4.2** displays the comparison of ChlF dynamics in three *A. thaliana* genotypes for the three oscillation periods: 10 s (Panels A-C), 1 min (Panes D-F), and 4 min (Panels G-I). The data of the NPQ mutants in other oscillation periods are shown in *Supplementary materials* ***Figures-SM 4.5*** *and* ***SM 4.6***.

In rapid oscillations (**Figure 4.2** A-C), the dynamic patterns were similar between the mutants and the wild-type despite the lack of feedback mechanisms related to NPQ in the mutants. Even though the amplitudes of ChlF changes were consistently bigger in the mutants than in the wild-type, the signal loops of the mutants resembled that of the wild-type in both shape and orientation, varying linearly at low light and saturating at high light. Hence, the occurrence of non-linearity under rapidly oscillating light (i.e., delayed response and saturating trend) is not attributable to NPQ regulation but mainly determined by the inherent properties of primary photosynthetic reactions. This finding aligns with our assumption.

Over the course of the 1 min oscillation, the response *of* the *npq4* mutant (**Figure 4.2** E) clearly differed from that of the wild-type (**Figure 4.2** D). While the wild-type exhibited loop orientation reversal, the response of the *npq4* mutant still resembled a P-I curve like seen in the fast oscillations. The ChlF signal in *npq4* still followed light changes linearly at

low light but tended to saturate at high light, whereas increasing light intensity induced a decline in the ChlF signal in the wild-type. In the *npq4* mutant, the orientation of signal loops remained counterclockwise in the 1 min LL and ML oscillations, whereas the loop shape became like an eight (8) in the HL oscillation (**Figure 4.2** E). These results indicate that the reversal of loop orientation with a distorted loop trajectory seen in the wild-type in the 30 s to 1 min oscillations (**Figure 4.1** D, E) is related to PsbS-dependent qE process.

In contrast, the *npq1* mutant (**Figure 4.2** F) exhibited pronounced changes in the loop features in the 1 min oscillations, as was observed in the wild-type (**Figure 4.2** D), although the overall amplitudes of ChlF changes were greater in *npq1*. The orientation of signal loops in *npq1* was the same as in the wild-type, and a decrease in ChlF yield was observed before reaching the light intensity peak in both ML and HL oscillations (**Figure 4.2** F, dark-blue and light-blue curves). The VDE-dependent NPQ (qE) is therefore not needed to induce the reversal of loop orientation in the 1 min oscillations.

In the 4 min oscillations, the wild-type plants displayed marked flattening of the loops in long oscillation periods (**Figure 4.2** G), suggesting a stationary state, while such a feature was completely absent in the *npq4* mutant (**Figure 4.2** H). While the orientation of the signal loops changed clockwise in the *npq4* mutant (**Figure 4.2** H), the signals induced by increasing and decreasing light intensity were still largely overlapping, and ChlF yield declined only with decreasing light intensity. As a result, the overall patterns were similar to those in the shorter periods. Likewise, the occurrence of the stationary state was barely noticeable in *npq1* in the 4 min oscillations (**Figure 4.2** I). The distorted loop trajectory of ChlF decline with increasing light intensity was not evident in *npq1* in the 4 min oscillations (**Figure 4.2** I), although it was manifested in the 1 min ML and HL oscillations (**Figure 4.2** F). In long oscillation periods, the ChlF signal patterns of *npq1* were much closer to those of *npq4* (**Figure 4.2** H) than the wild-type (**Figure 4.2** G). From these observations, it seems that the absence of VDE-dependent NPQ (qE) largely affects the dynamic NPQ regulation in long periods of light oscillations, such as 4 min oscillations. The PsbS-dependent NPQ (qE) plays an essential role in dynamic regulation of photosynthesis in response to oscillating light with periods exceeding 10 s. These results are consistent with our previous findings in these genotypes under oscillating light (Niu *et al*., 2023).

The saturation trends observed in the wild-type under rapid HL oscillations (**Figure 4.1** A-C, **Figure 4.2** A, light-blue curves) were observed in the *npq4* mutant in all oscillation frequencies when light intensity exceeded approximately 400 µmol photons m^{-2} s^{-1} (**Figure 4.2** B, E, H, light-blue curves). Similarly, the *npq1* mutant exhibited saturation trends in fast oscillations shorter than 10 s (**Figure 4.2** C) and in long period 4 min oscillations (**Figure 4.2** I, light-blue curve), but not in the 1 min oscillations (**Figure 4.2** F). The absence of PsbS- or VDE-dependent rapidly reversible NPQ likely leads to increased QA reduction as light intensity increases. Thus, ChlF yield remains high and saturates with increasing light.

An intriguing phenomenon appeared in the LL oscillations when the period exceeded 1 min (**Figure 4.1** E-H, black curves). In the wild-type, the distance between the rising and descending phases of the ChlF signal loops widened compared to shorter periods (**Figure 4.1** A-D, black curves). This suggests that the frequency-dependent changes in the loop features observed under the ML and HL oscillations may also occur in the LL oscillations with longer periods, albeit not as clearly as in the ML and HL oscillations. However, as illustrated in *Supplementary Materials* ***Figures-SM 4.5*** and ***SM 4.6***, this phenomenon was absent in both *npq1* and *npq4* mutants. In these mutants, ChlF yield was a linear function of light intensity in LL oscillations. Accordingly, the non-linear dynamics in the LL oscillations seem to necessitate both PsbS- and VDE-dependent NPQ processes.

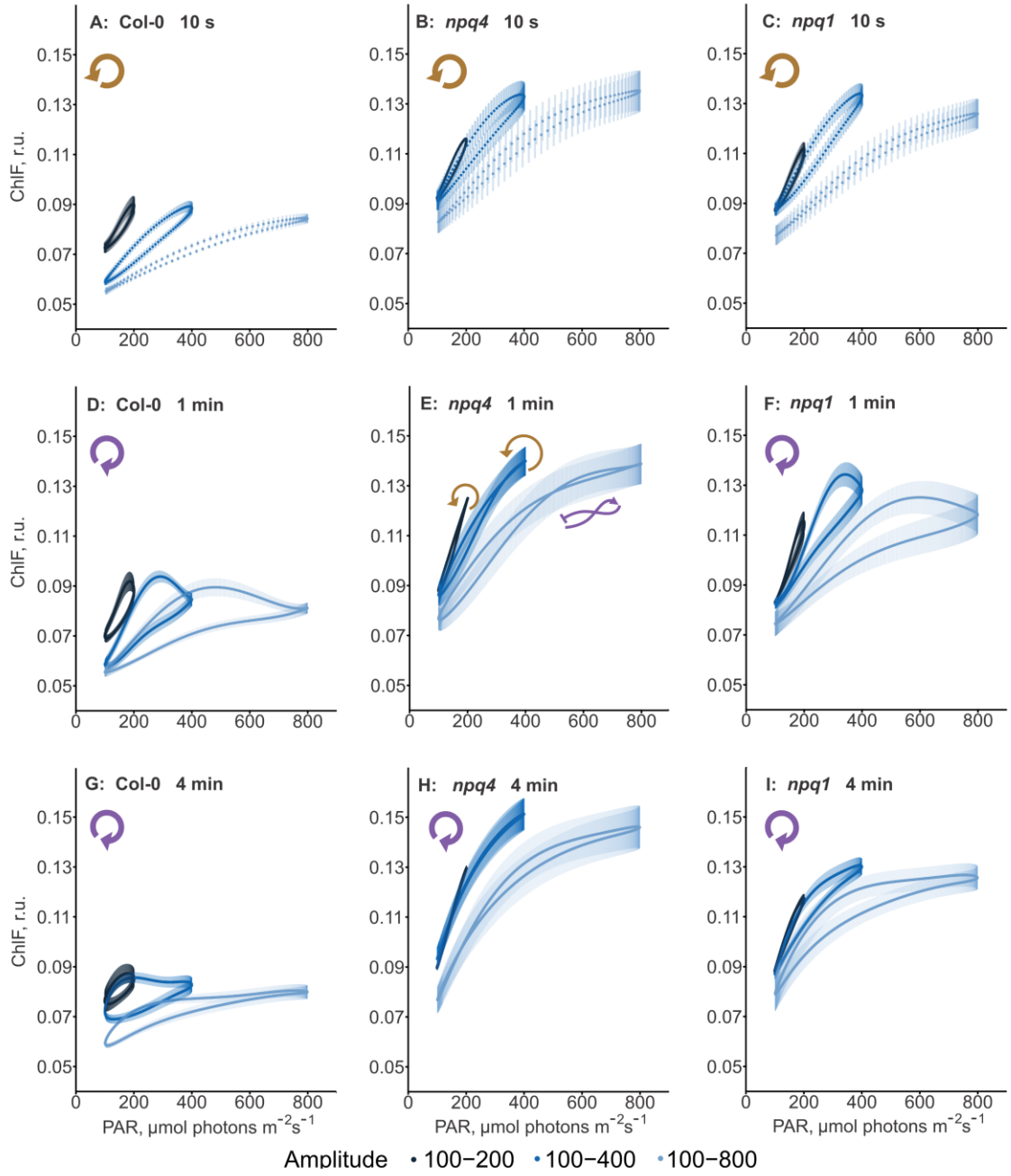

Figure 4.2 Input-output diagrams demonstrate the dependence of the ChlF yield (fitted data) on changes in photosynthetic active radiation (PAR) in wild-type A. thaliana Col-0 (Panels A, D, G) and non-photochemical quenching mutants npq4 (Panels B, E, H) and npq1 (Panels C, F, I). The light oscillates with three different amplitudes, including 100-200 µmol photons·m^{-2}·s^{-1} (black), 100-400 µmol photons·m^{-2}·s^{-1} (dark blue), and 100-800 µmol photons·m^{-2}·s^{-1} (light blue). The dynamics of the ChlF in response to three specific periods of oscillation were shown, including 10 s (top row), 1 min (middle row), and 4 min (bottom row). The purple arrow indicates that the signal changed in a clockwise manner, and the yellow arrow indicates that the signal changed counterclockwise. The npq4 mutant exhibited a distinctive 8-shaped signal under 1 min period of oscillating light (Panel E).

4.4. Discussion

4.4.1 Multiple non-linear responses of ChlF yield are categorized as constitutive and regulatory non-linearities.

The dynamic responses of ChlF to light oscillations in wild-type *A. thaliana* can be characterized by several non-linear phenomena. Specifically, our analysis revealed the following: (1) a delayed response of ChlF to rapidly oscillating light shorter than 30 s, characterized by counterclockwise signal loops (**Figure 4.1** A-C); (2) a saturation trend of ChlF at high light intensities in rapid oscillations (**Figure 4.1** A-C); (3) the emergence of a distorted loop trajectory, starting at the 30 s period and becoming more pronounced at the 1 min period, persisting in longer periods (**Figure 4.1** D-H); and (4) the attainment of stationary state in long periods of oscillating light with high amplitude (**Figure 4.1** F-H).

The delayed responses observed in both wild-type and NPQ mutants under rapidly oscillating light (**Figure 4.2** A-C) suggest that this type of phase delay is not linked to the regulation of rapidly reversible NPQ (qE). Instead, it can be mainly ascribed to the constitutive non-linearity of the primary photosynthetic reactions, determined by the sizes of photosynthetic reactant pools and the reaction rates within the electron transport chain (Nedbal & Koblížek, 2006; Rascher & Nedbal, 2006; Kalaji *et al.*, 2012). This delayed response is frequency-dependent and approaches zero as the frequency decreases (Bertotti, 1998).

In wild-type plants, a saturation of the ChlF yield occurred in rapid oscillations (**Figure 4.1** A-C, light-blue curves), in which regulatory processes of rapidly reversible NPQ (qE) are unable to keep pace with light changes. Increasing closure of PSII reaction centers leads to the saturation trend of ChlF emission. Saturation may also occur in the wild-type under slow oscillations when light-induced over-excitation exceeds the capacity of NPQ regulation. The mutants have limited NPQ capacities compared to those of the wild-type, and thus, the ChlF yield also tended to saturate under slowly oscillating light. In the case of *npq4*, ChlF saturated at HL regardless of the oscillation frequency (**Figure 4.2** B-H and *Supplementary Materials* ***Figure-SM 4.5***), suggesting that the absence of the PsbS-dependent qE leads to an inability to effectively mitigate the PSII over-excitation caused by the HL oscillations in all tested frequency ranges. In long periods above 2 min, ChlF yield remained high and tended to saturate at HL in both *npq4* and *npq1* mutants (**Figure 4.2** H, I, light-blue curves;

Supplementary Materials ***Figure-SM 4.5 & SM 4.6***), suggesting that the remaining NPQ mechanisms in these mutants are insufficient to cope with the PSII over-excitation in such conditions (**Figure 4.2** H, I). It can be considered that ChlF yield then saturates when the operational frequency (**Chapter 2**) of the regulatory process is lower than the frequency of the light perturbation, rendering the regulated processes inoperable, or when, despite the operating frequency being higher than the frequency of the light perturbation the regulatory process is insufficient to compensate for over-excitation caused by excessive changes in light intensities. The saturation process is influenced by the inherent capacities of photosynthesis and its regulation, as a consequence of developmental acclimation, including factors like the light-harvesting capacity, the pool sizes of redox active components in the electron transport chain, the capacity of NPQ, as well as the strength of electron and energy sinks in the Calvin-Benson cycle and alternative pathways (Chow *et al.*, 1990; Walters & Horton, 1995; Dietzel *et al.*, 2008; Eberhard *et al.*, 2008; Schöttler & Tóth, 2014; Schöttler *et al.*, 2015; Miller *et al.*, 2017; Schneider *et al.*, 2019; Niedermaier *et al.*, 2020). Therefore, we classified the saturation trend as constitutive non-linearity. Long-term plant acclimation to environmental conditions can alter these inherent capacities (Schöttler & Tóth, 2014; Schöttler *et al.*, 2015; Niedermaier *et al.*, 2020). Studies have shown that plants that are acclimated to fluctuating light, as opposed to static light, exhibit a more rapid engagement of NPQ and, in some cases, a higher NPQ capacity (Külheim *et al.*, 2002; Demmig-Adams *et al.*, 2014b; Murchie & Ruban, 2020) . In this study, we applied only a few cycles of oscillations for each frequency and captured the first stationary response patterns. Therefore, we expect limited effects of long-term acclimation.

The distorted loop trajectory, as observed in ChlF yield, refers to a phenomenon in which the ChlF dynamics in the ascending light phase substantially differ from those in the descending light, typically manifested by a clockwise loop with partial signal decline during the light intensity increase. This feature emerged in the 30 s period and was strongly amplified in the 1 min period (**Figure 4.1** D, E), which aligns with the time periods of the resonance peaks observed in oscillating light in wild-type *A. thaliana* (**Chapter 2**; Niu *et al.* (2023)). It is likely that the occurrence of this distorted loop trajectory is not solely influenced by photochemical reactions but reflects the interplay of photochemical and non-photochemical quenching.

By comparing the mutants to the wild-type (**Figure 4.2**), it becomes evident that the distorted loop trajectory in ChlF signals at the tested oscillating frequencies is dominated

by rapidly reversible NPQ (qE), specifically, the PsbS-dependent qE (**Figure 4.2** D-F, *Supplementary Materials* ***Figures-SM 4.5*** and ***SM 4.6***). Therefore, the distorted loop trajectory is different from the delayed response and saturation (constitutive non-linearity). Instead, it most likely represents dynamic regulation within the system (regulatory non-linearity). It occurs when the regulation of qE is active (like in wild-type plants) and the oscillation period is long enough for qE processes to kick in.

The last non-linear phenomenon is characterized by the stationary state observed in the wild-type under long periods of ML and HL oscillations (periods > 2 min, **Figure 4.1** F-H). The distorted loop trajectory induced by regulatory processes in the 30 s and 1 min periods (**Figure 4.1** D, E) in the wild-type was attenuated in these conditions. The damped and stable ChlF signals suggest that a dynamic equilibrium in the photosynthesis systems might be reached and maintained. This means that efficient regulatory processes of rapidly reversible NPQ (qE) can be triggered and can effectively mitigate over-excitation in slow light oscillations, especially in HL oscillations where the luminal pH is low. The absence of the stationary state in both mutants proved this (**Figure 4.2** H, I; *Supplementary Materials* ***Figures-SM 4.5*** and ***SM 4.6***). Therefore, the stationary state that arises in long periods of oscillations can be considered a consequence of effective regulatory processes and falls under the category of regulatory non-linearity.

To summarize, we observed the four types of non-linear ChlF dynamics in response to oscillating light and classified them into constitutive non-linearity and regulatory non-linearity. The occurrence and dynamic fingerprints of these non-linearities in photosynthesis largely depend on the amplitude and frequency of light oscillations.

4.4.2 The reversal of loop orientation indicates the onset of PsbS-dependent qE

The non-linearity related to the distorted loop trajectory was absent in oscillation periods shorter than 10 s (**Figure 4.1** A-C, all curves) and was attenuated in periods longer than 2 min (**Figure 4.1** F-H, light-blue curves). It seems that the distorted loop trajectory diminishes in conditions in which regulatory processes of NPQ cannot be triggered or are effective in maintaining the system in a stationary state. The period at which the distorted loop trajectory is most pronounced presumably corresponds to the time to activate specific

NPQ regulatory processes, but their effectiveness in counteracting the impact of external disturbances remains limited.

The distorted loop-type non-linearity seen in ChlF dynamics within the tested frequency ranges was manifested as a shift in the orientation of the signal loops. This reversal of loop orientation in the 30 s period oscillation was observed in both wild-type and *npq1* plants (**Figure 4.1** D and *Supplementary materials* ***Figure-SM 4.6*** *D*) but not in the *npq4* mutant (*Supplementary materials* ***Figure-SM 4.5*** *D*), demonstrating that the PsbS-dependent qE dominates the response to the 30 s light oscillation. In contrast, the loop orientation of the *npq4* mutant reversed around the 2 min oscillation period (*Supplementary materials* ***Figure-SM 4.5*** *F*), but the distorted loop-type non-linearity was absent. I hypothesize that this loop reversal in *npq4* mutant is caused by VDE-dependent qE, as this is consistent with the identified operating frequency of VDE-dependent qE (1/60 - 1/120 Hz) (**Chapter 2**; Niu *et al.* (2023)), and is also comparable to a retarded VDE-dependent qE induction in *npq4* mutant (50% of total NPQ induced in 460 s) (Nilkens *et al.*, 2010). As ChlF yield was not quenched and remained highly saturated, there was insufficient evidence to prove this; thus, measurements of the pigment compositions of xanthophylls under oscillating light conditions in future experiments are warranted.

Notably, the other components of NPQ (**Chapter 1** - **Section 1.2**) may also affect the ChlF quenching in oscillating light conditions, e.g., zeaxanthin-dependent sustained quenching component qZ (Nilkens *et al.*, 2010). However, I assume that dynamic changes of ChlF induced by qZ per se in a single oscillation cycle cannot spoil the qE-dominated signal patterns. It is because the formation (rising time 10 - 15 mins) and relaxation (lifetime 10 - 15 mins or longer) times of qZ proposed are longer than the longest oscillation period we tested (8 min per period, with 4 min rise and fall in light intensity). Also, these times were determined by Nilkens *et al.* (2010) in a higher light intensity (900 µmol photons·m^{-2}·s^{-1}) and complete darkness, whereas our maximum oscillation light intensity was 800 µmol photons·m^{-2}·s^{-1} and there was no darkness (minimal light intensity at 100 µmol photons·m^{-2}·s^{-1}). It has also been demonstrated that there is a delay (> 2 min) in the reduction of zeaxanthin when switching instantaneously from high to low light (15 µmol photons·m^{-2}·s^{-1}) and that this delay increases with the duration of high light due to a decrease in the rate of zeaxanthin epoxidation (Gilmore & Björkman, 1994; Jahns, 1995; Jahns & Holzwarth, 2012). Although for the above reasons, I assume that qZ cannot substantially affect the dynamic signals of a single oscillation cycle, this is not to say that qZ is not present

in oscillating light. On the contrary, in genotypes with VDEs, prolonged measurements (10 min pre-illumination for induction plus 63 mins oscillations) can result in zeaxanthin accumulation, and thus qZ should be present, especially in HL oscillations. The effect of this accumulated zeaxanthin on the dynamic ChlF signals may arise from the influence of the exiting zeaxanthin on the qE responses (Horton *et al.*, 2000; Pérez-Bueno *et al.*, 2008; Jahns & Holzwarth, 2012) (see also **Section 4.4.4** below). The reason for the formation of the stationary state during long-period oscillations in the wild-type cannot be excluded as a possible facilitation of the qE response by accumulated zeaxanthin.

4.4.3 NPQ enhances the robustness of the photosynthesis system and enriches its dynamic behavior

As defined by Bich *et al.* (2016), regulatory processes should be carried out by sub-systems outside the constitutive regime, and should sense and respond to external perturbations to adjust the system's response in an efficient manner. It improves the ability of the biological system to cope with perturbations and enriches its functional dynamic behavior. The induction of qE involves protonation of the PsbS proteins (Li *et al.*, 2000; Li *et al.*, 2002b) and de-epoxidation of violaxanthin to zeaxanthin (Demmig-Adams, 1990; Gilmore, 1997; Niyogi *et al.*, 1998; Jahns & Holzwarth, 2012), both executed by sub-systems outside the constitutive photosynthesis system. The much stronger changes in ChlF yield observed in the NPQ mutants compared to the wild-type, and the absence of stationary states in both mutants indicate that the PsbS- and VDE-dependent NPQ regulatory processes enhance the photosynthesis system's capacity to cope with light perturbations, possibly leading to increased robustness in dynamic environments (Külheim *et al.*, 2002; Külheim & Jansson, 2005). The absence of the distorted loop trajectory and the lack of dynamic equilibrium in the mutants demonstrate that regulatory processes of NPQ enriches the dynamic behavior of the photosynthesis system.

4.4.4 The presence of zeaxanthin enables rapid qE induction at high luminal pH

In the wild-type, the distorted loop trajectory was also observed in the LL oscillations when the period exceeded 1 min (**Figure 4.1** E-H, dark curves), but not in either mutant (*Supplementary materials* ***Figures-SM 4.5*** and ***SM 4.6****, E-H, dark curves*). The *npq4*

showed no distorted loop trajectory in all tested oscillation amplitudes (*Supplementary materials* ***Figure-SM 4.5***), while the *npq1* exhibited distorted loop trajectories in the ML and HL oscillations but not in the LL oscillations (***Figure-SM 4.6*** *E-H*). The remaining PsbS-dependent qE in the *npq1* mutant could not be induced by the LL oscillations despite its presumed functionality for oscillation periods longer than 30 s. The distinct responses of the wild-type and the *npq1* to the LL oscillations might be attributed to zeaxanthin accumulation in the wild-type but not in *npq1*. The presence or absence of zeaxanthin is known to influence the relationship between qE and the luminal pH (Noctor *et al.*, 1991; Noctor *et al.*, 1993). Specifically, when zeaxanthin is present, qE can be induced at higher luminal pH, allowing it to be triggered in the LL oscillations, in which a less acidic luminal pH is expected compared to the HL oscillations. Previous *in vitro* studies in chloroplasts have shown that the presence of zeaxanthin is able to shift the pK of qE from 4.5 to at least 6.5 (Horton *et al.*, 2000; Ruban *et al.*, 2001; Pérez-Bueno *et al.*, 2008; Murchie & Ruban, 2020). Our results are consistent with the previous reports that zeaxanthin itself plays a regulatory role in activating qE, and the relationship between qE and ΔpH is non-linear and dynamically altered (Noctor *et al.*, 1991). Parallel measurements of the xanthophyll composition and the proton motive force could demonstrate dynamic changes in zeaxanthin accumulation and the sensitivity of qE to luminal pH under oscillating light conditions.

4.4.5 Future outlook

The diverse non-linear dynamic responses observed in ChlF yield under harmonically oscillating light can be challenging to discern by measuring conventional P-I curves. The complexity of regulatory networks and the inherent non-linearity of photosynthesis systems highlight the importance of studying photosynthesis from a dynamic perspective. Dynamic fingerprints of photosynthesis in oscillating light are highly non-linear and rich in information, with the extent and type of non-linearity being dependent on the amplitude and frequency of light perturbations. By sensing and analyzing these non-linear dynamics using multiple frequencies and/or amplitudes of harmonically oscillating light, we will be able to gain valuable insights into different regulatory processes and pathways that operate and function under dynamically changing light environments.

Acknowledgement

Y.N., and L.N. gratefully acknowledge the financial support from the Federal Ministry of Education and Research of Germany (BMBF) in the framework of the YESPVNIGBEN project (03SF0576A).
D.L. and L.N. were supported by the European Regional Development Fund project "Plants as a tool for sustainable global development" (CZ.02.1.01/0.0/0.0/16_019/0000827).
D.L., S.M., and L.N. gratefully acknowledge the financial support by HORIZON-EIC-2021-PATHFINDER OPEN project DREAM (grant agreement No 101046451)

Author contribution

YN, SM and LN designed the research. YN performed experiments. YN, and LN analyzed data. YN, LN and DL interpreted the results. YN, DL, SM and LN wrote the manuscript.

Supplementary materials

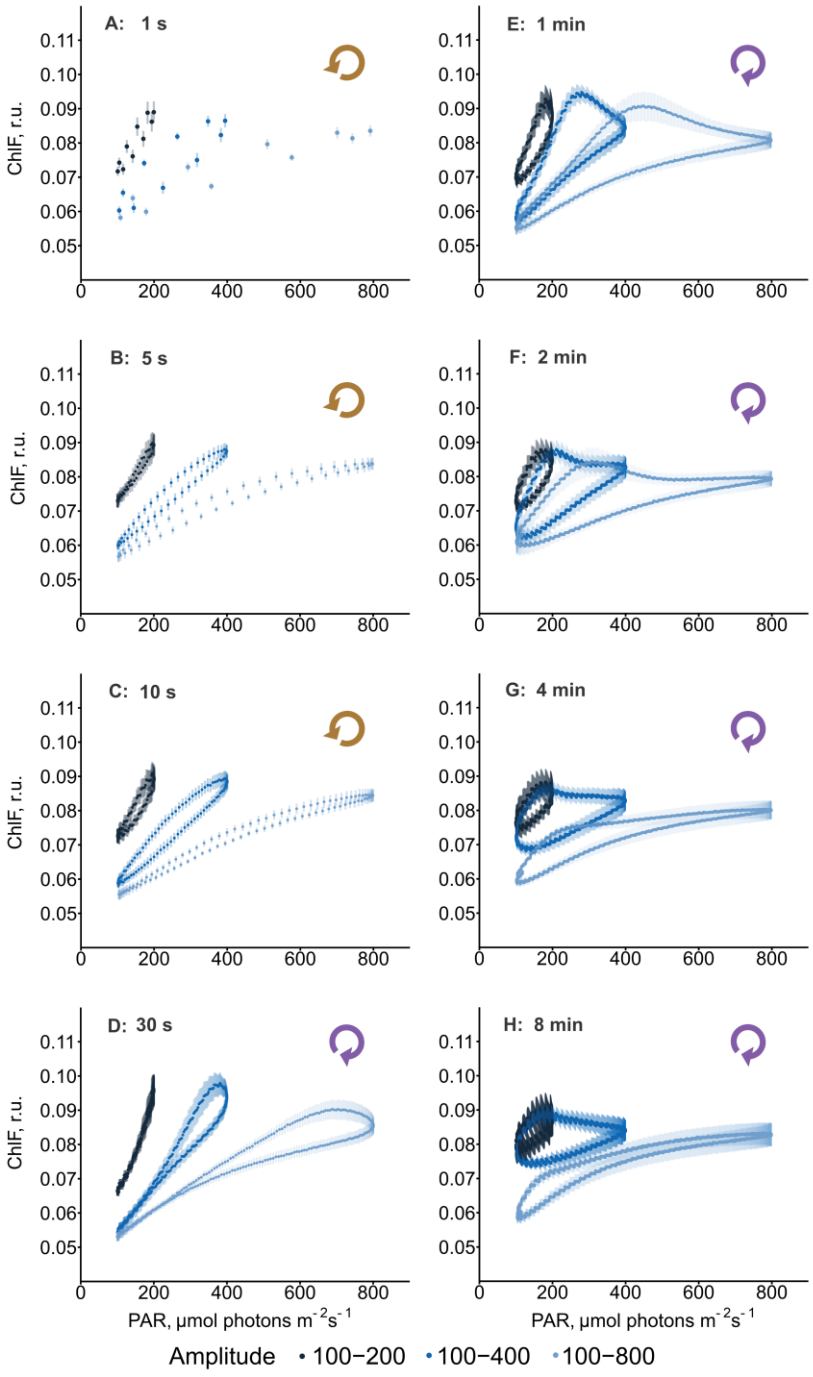

Figure-SM 4.1 Input-output diagrams demonstrate the dependence of the original data of the ChlF yield of wild-type *A. thaliana* Col-0 on changes in photosynthetic active radiation (PAR). The implemented oscillating light had three different amplitudes, including oscillations between 100 to 200 µmol photons·m^{-2}·s^{-1} (black), 100 to 400 µmol photons·m^{-2}·s^{-1} (dark blue), and 100 to 800 µmol photons·m^{-2}·s^{-1} (light blue). Eight different oscillation periods were executed, from 1 s to 8 min, with the left column (Panels A-D) for periods from 1 s to 30 s and the right column (Panels E-H) for periods from 1 min to 8 min. The colored arrows denote the orientations of the signal following the oscillating light, where the purple arrow indicates that the signal changed in a clockwise manner and the yellow arrow indicates that the signal was counterclockwise changed.

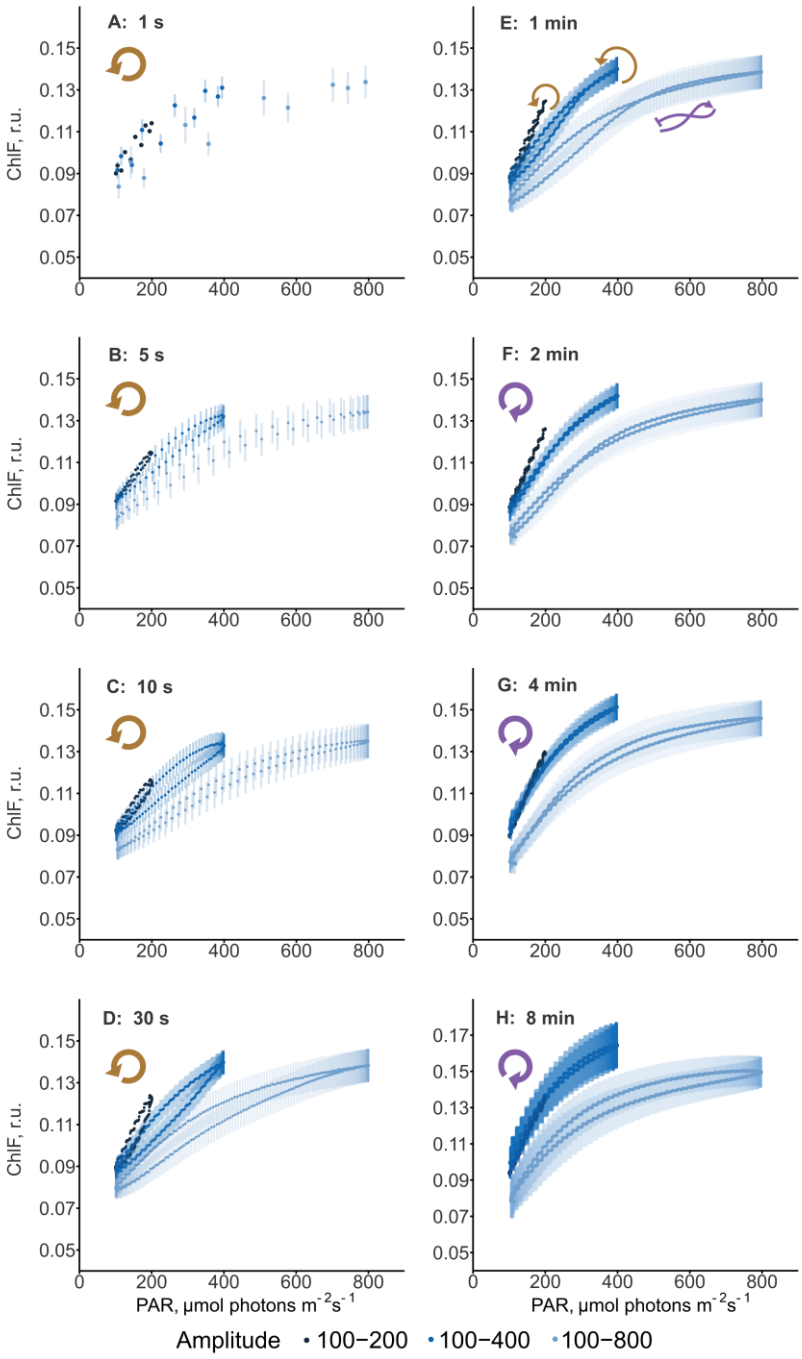

Figure-SM 4.2 Input-output diagrams demonstrate the dependence of the original data of the ChlF yield of *npq4* mutant *of A. thaliana* on changes in photosynthetic active radiation (PAR). The implemented oscillating light had three different amplitudes, including oscillations between 100 to 200 µmol photons·m^{-2}·s^{-1} (black), 100 to 400 µmol photons·m^{-2}·s^{-1} (dark blue), and 100 to 800 µmol photons·m^{-2}·s^{-1} (light blue). Eight different oscillation periods were executed, from 1 s to 8 min, with the left column (Panels A-D) for periods from 1 s to 30 s and the right column (Panels E-H) for periods from 1 min to 8 min. The colored arrows denote the orientations of the signal following the oscillating light, where the purple arrow indicates that the signal changed in a clockwise manner and the yellow arrow indicates that the signal was counterclockwise changed. A distinctive 8-shaped signal appeared under 1 min period of oscillating light (Panel E).

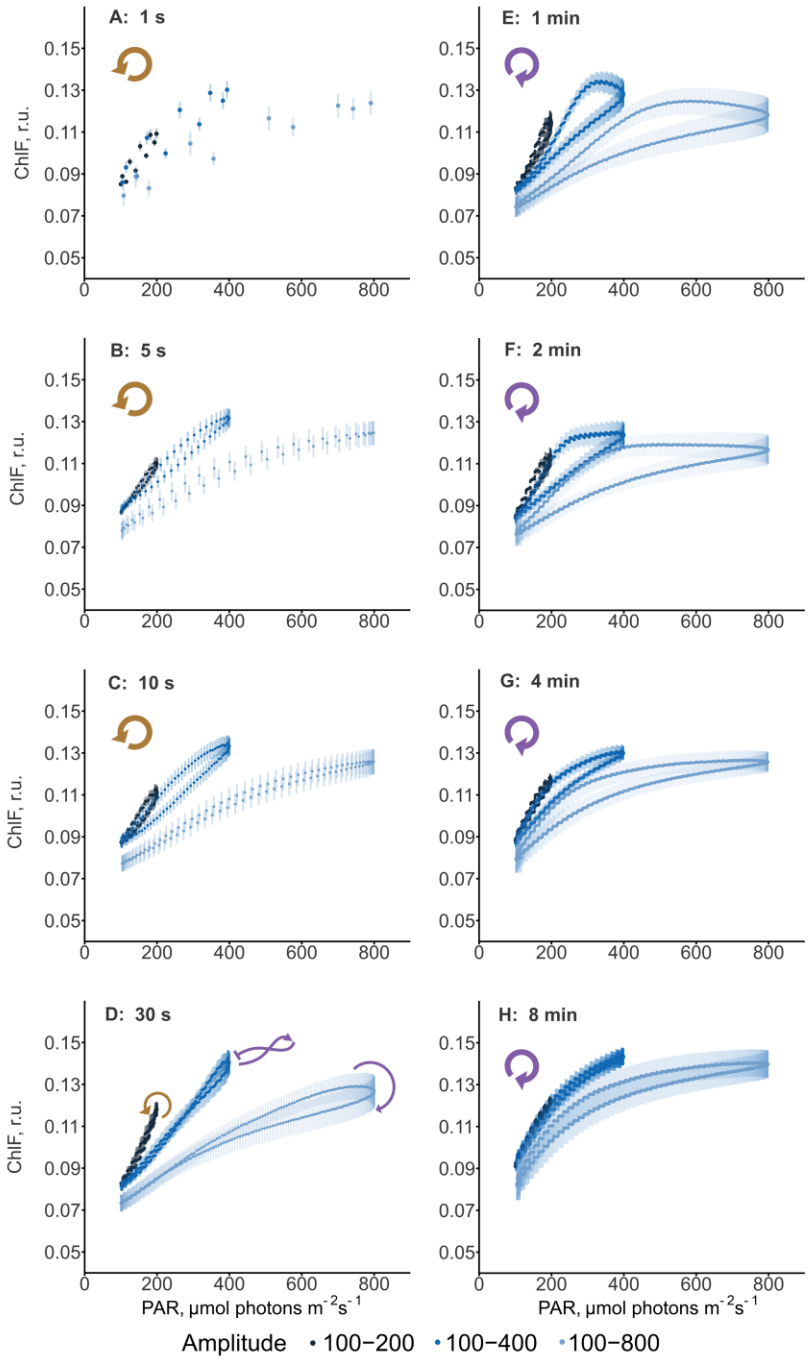

Figure-SM 4.3 Input-output diagrams demonstrate the dependence of the original data of the ChlF yield of *npq1* mutant *of A. thaliana* on changes in photosynthetic active radiation (PAR). The implemented oscillating light had three different amplitudes, including oscillations between 100 to 200 µmol photons·m^{-2}·s^{-1} (black), 100 to 400 µmol photons·m^{-2}·s^{-1} (dark blue), and 100 to 800 µmol photons·m^{-2}·s^{-1} (light blue). Eight different oscillation periods were executed, from 1 s to 8 min, with the left column (Panels A-D) for periods from 1 s to 30 s and the right column (Panels E-H) for periods from 1 min to 8 min. The colored arrows denote the orientations of the signal following the oscillating light, where the purple arrow indicates that the signal changed in a clockwise manner and the yellow arrow indicates that the signal was counterclockwise changed. A distinctive 8-shaped signal appeared under 30 s period of oscillating light (Panel D).

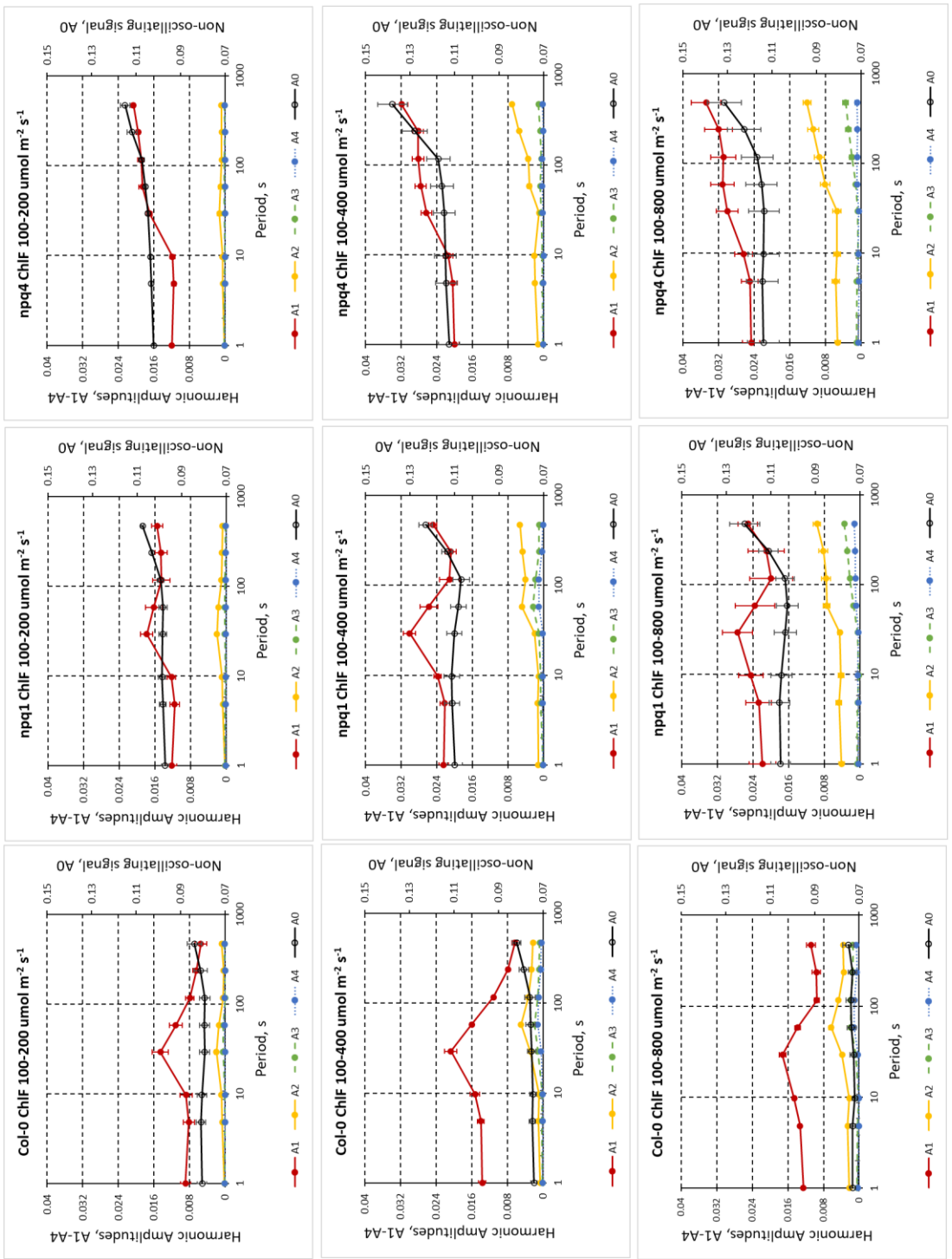

Figure-SM 4.4 The averaged ChlF signals in each frequency were fitted with the $Fit(t)$ function as shown in Materials and Methods Eqn.1. The least-square fitting procedure was done in MS Excel and the fit yielded the offset A_0, as well as the amplitudes (A_1, A_2, A_3, A_4), and phase shifts $(\tau_1, \tau_2, \tau_3, \tau_4)$ of multiple harmonic components. The offset A_0, (black symbols and lines corresponding to the right y-axis), amplitudes of fundamental harmonics A_1, (red symbols and lines corresponding to the left y-axis) and upper harmonics A_2, A_3, A_4, (yellow, green, blue symbols and lines respectively, corresponding to the left y-axis) of ChlF signals under different frequencies of oscillating light were shown. Parameters changes in response to three different amplitudes were listed in three rows: 100-200 (top row), 100-400 (medium row) and 100-800 (bottom row) µmol photons·m^{-2}·s^{-1}. The parameters estimated for wild-type were demonstrated in left column, the estimation of *npq1* mutant was shown in medium column, and *npq4* was in right column.

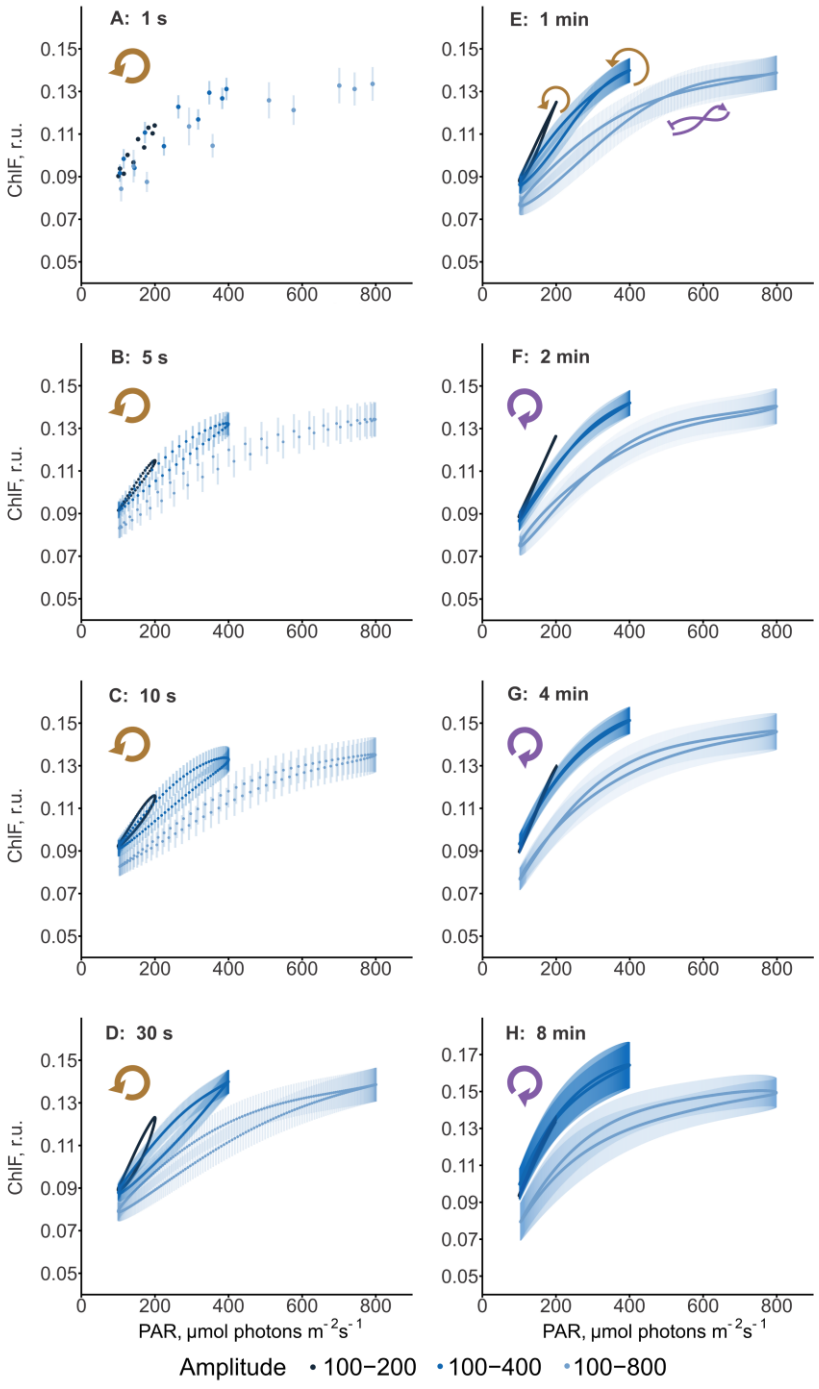

Figure-SM 4.5 Input-output diagrams demonstrate the dependence of the ChlF yield (Fitted data) of *npq4* mutant *of A. thaliana* on changes in photosynthetic active radiation (PAR). The implemented oscillating light had three different amplitudes, including oscillations between 100 to 200 µmol photons·m^{-2}·s^{-1} (black), 100 to 400 µmol photons·m^{-2}·s^{-1} (dark blue), and 100 to 800 µmol photons·m^{-2}·s^{-1} (light blue). Eight different oscillation periods were executed, from 1 s to 8 min, with the left column (Panels A-D) for periods from 1 s to 30 s and the right column (Panels E-H) for periods from 1 min to 8 min. The colored arrows denote the orientations of the signal following the oscillating light, where the purple arrow indicates that the signal changed in a clockwise manner and the yellow arrow indicates that the signal was counterclockwise changed. A distinctive 8-shaped signal appeared under 1 min period of oscillating light (Panel E).

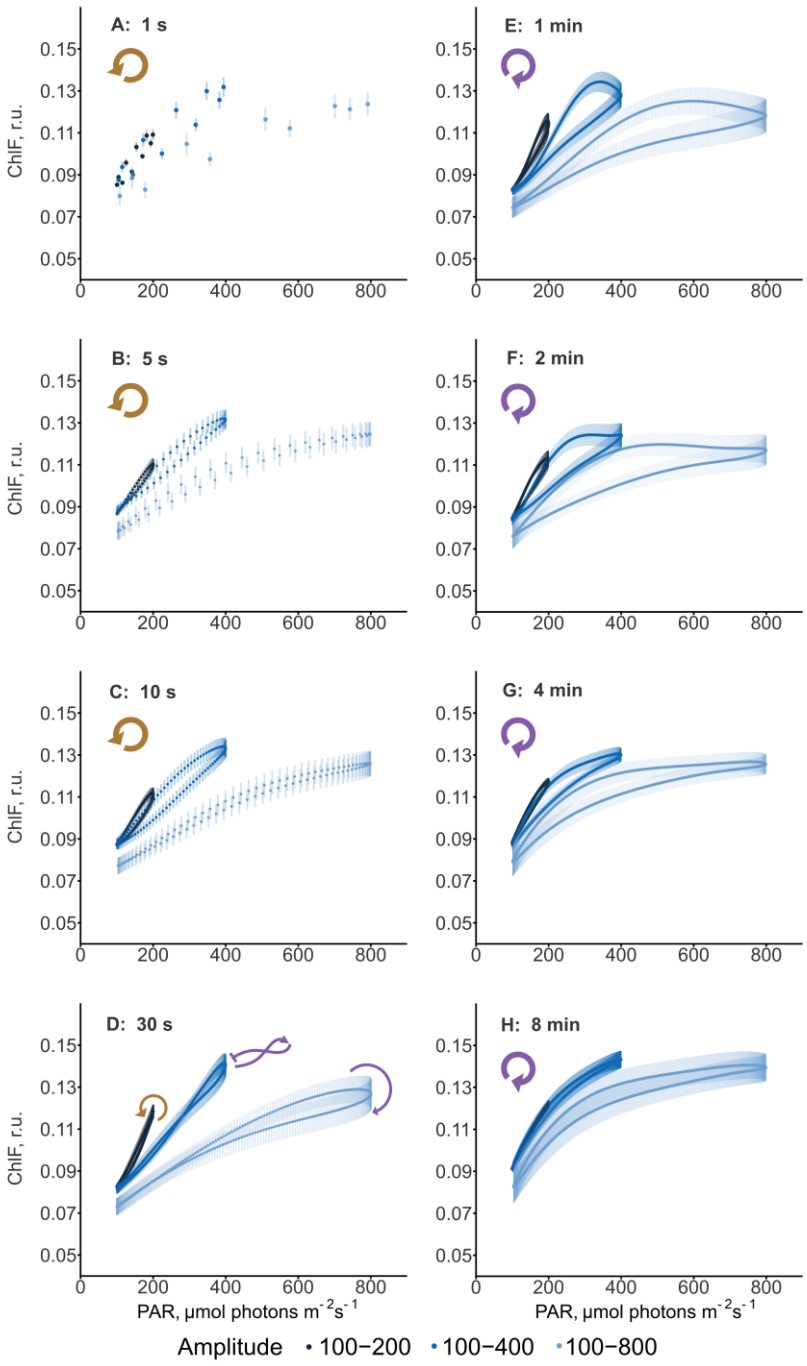

Figure-SM 4.6 Input-output diagrams demonstrate the dependence of the ChlF yield (fitted data) of *npq1* mutant *of A. thaliana* on changes in photosynthetic active radiation (PAR). The implemented oscillating light had three different amplitudes, including oscillations between 100 to 200 µmol photons·m^{-2}·s^{-1} (black), 100 to 400 µmol photons·m^{-2}·s^{-1} (dark blue), and 100 to 800 µmol photons·m^{-2}·s^{-1} (light blue). Eight different oscillation periods were executed, from 1 s to 8 min, with the left column (Panels A-D) for periods from 1 s to 30 s and the right column (Panels E-H) for periods from 1 min to 8 min. The colored arrows denote the orientations of the signal following the oscillating light, where the purple arrow indicates that the signal changed in a clockwise manner and the yellow arrow indicates that the signal was counterclockwise changed. A distinctive 8-shaped signal appeared under 30 s period of oscillating light (Panel D).

Chapter 5

General Discussion

Chapter 5

In this PhD thesis, I pursued two primary objectives. First, I employed a frequency-domain-based optical sensing method, known as the harmonically oscillating light method, to explore its capabilities in studying photosynthetic dynamics. Second, I utilized this method to examine the responses of multiple photoprotective mechanisms, with a particular focus on rapidly reversible NPQ (qE) and CETs under oscillating light conditions of varying intensities and frequencies. The experiments were carried out on wild-types plants of *Arabidopsis thaliana* and mutants with partial deficiencies in qE and CETs.

In **Chapter 2**, I sought to distinguish the roles played by different mechanisms of rapidly reversible NPQ and CET in response to varying frequencies of oscillating light (ranging from 1 Hz to 1/480 Hz) and determined the frequency at which particular regulatory processes begin to respond. The results revealed that different regulatory mechanisms have their own operational frequency ranges. While the onset of the PsbS-dependent qE was at a frequency range of about 1/10 Hz - 1/30 Hz, the VDE-dependent qE started at a slower frequency range of about 1/60 Hz - 1/120 Hz. The PGR5-dependent CET pathway played an indispensable role in coping with oscillating light at all frequencies, whereas the role of NDH-like complex-dependent CET had a more limited impact, transiently influencing the redox state of the PSI acceptor side at around 1/30 Hz - 1/60 Hz.

To gain a deeper understanding of the dynamic response to oscillating light, I incorporated the saturation pulses into harmonically oscillating light. This allowed me to estimate the quantum yields of photosystems and the redox states of other components of the electron transport chain under oscillating light conditions (**Chapter 3**). Here, the focus was on the responses of different photoprotective processes to oscillating light of different amplitudes at the same frequency (1/60 Hz). The absence of qE had minimal effects on PSI quantum yield and only modestly affected PSII quantum yield. The effects of lacking qE (lower Y(NPQ)) were primarily compensated by the constitutive components of NPQ (higher Y(NO)). The PGR5/PGRL1-dependent CET seemed to contribute to protecting photosynthesis against light oscillations of varying intensities, while the NDH-like complex-dependent CET may act as a safety valve to optimize photosynthesis under light oscillations with large amplitudes.

In **Chapter 4**, I characterized different types of non-linear responses of ChlF yield to oscillating light of multiple frequencies and amplitudes. I categorized these responses into constitutive and regulatory non-linearity, following the principles from system biology. The

results confirmed the non-linear nature of photosynthetic dynamics under fluctuating light and highlighted the importance of amplitude and frequency of light oscillation in shaping the photosynthetic responses. Using harmonically oscillating light to sense and analyze non-linear dynamics provides valuable insights into the operations and roles of different regulatory processes of photosynthesis under dynamically changing environments.

In this general discussion (**Chapter 5**), I first provided a comprehensive discussion of what information related to the dynamic regulation of photosynthesis can be extracted from the signal fingerprints obtained by using the harmonically oscillating light method and whether this information can be explained by knowledge obtained from the conventional methods. Hypotheses were proposed for interpreting dynamic features, and some suggestions were made regarding follow-up experiments for further validation. Then, I discussed the dynamic regulation of photosynthesis from a systems perspective and explained how frequency-domain sensing methods can contribute to a more comprehensive understanding of the dynamics of photosynthesis systems. Finally, I shared thoughts on the possible future developments and applications of frequency-domain sensing techniques.

5.1 Signal fingerprints in oscillating light characterize the dynamic regulation of photosynthesis

5.1.1 Resonance peaks and distorted loop trajectory reflect the onset of qE

In the wild-type plants, resonance peaks in ChlF yield appeared at oscillating frequencies around 1/30 to 1/60 Hz (contour map plot, **Figures 2.2** & **2.3**). This local maximum of ChlF yield was reported earlier (Nedbal & Březina, 2002). These resonance peaks corresponded to frequencies at which we noted a distorted loop trajectory in ChlF signals (input-output diagram, **Figure 4.1**), signified by a shift from counterclockwise to clockwise signal loop orientation. The coincidence of the distorted loop trajectory and the appearance of the resonance peaks is not accidental but carries important information about the onset of dynamic qE adjustment. This was proved by the comparison of the wild-type with the NPQ mutants. In both wild-type and *npq1* mutant, the shift of signal loop orientation occurred at approximately 1/30 Hz and was more prominent at 1/60 Hz with a noticeable decline of ChlF yield in the light intensity increasing phase (**Figures 4.1** & **4.2**, ***Figure-SM 4.6***). The resonance peaks were also observed in the *npq1* mutant (**Figures 2.2** & **2.3**). In contrast, the resonance peaks in this frequency range disappeared in the *npq4* mutant (**Figures 2.2** & **2.3**). This mutant displayed a shift in the orientation of signal loops at a lower oscillation frequency of about 1/120 Hz, but the distorted loop trajectory was absent (**Figure 4.2**, ***Figure-SM 4.5***). In addition, when considering the PSII-related quantum yields at 1/60 Hz oscillation, the Y(NPQ) of the wild-type began to rise in a phase close to 90° (**Figure 3.2**). This phase was consistent with the phase of the resonance peak in the wild-type at 1/60 Hz oscillation (**Figure 2.3**), and ChlF signals started to decline after this point (**Figure 2.3**). This delay of Y(NPQ) in the wild-type relative to the oscillatory changes in light intensity reflects the time necessary to activate and deactivate the qE. Based on our findings, it can be concluded that the distorted loop trajectory with reversal orientation of ChlF signal loops and the emergence of ChlF resonance peaks within the oscillation frequency range around 1/30 Hz to 1/60 Hz indicate the onset of dynamic NPQ adjustment, specifically, the dynamic changes in the PsbS-dependent qE in response to oscillating light.

In general, the resonance phenomenon is supposed to reflect operational frequencies of various regulatory processes of photosynthesis that operate on different time scales. These processes may encompass feedback and feedforward mechanisms within the primary

photochemical reactions and the Calvin-Benson cycle (Scheibe *et al.*, 2005; Horton, 2012; Kaiser *et al.*, 2016; Graham *et al.*, 2017), as well as the regulatory processes such as NPQ (Horton *et al.*, 1996; Li *et al.*, 2004; Murchie & Niyogi, 2011; Ruban, 2018; Ruban & Wilson, 2021), photosynthesis control (Rumberg & Siggel, 1969; Tikhonov *et al.*, 1981; Colombo *et al.*, 2016), the Mehler reaction (Asada, 1999), malate valves (Thormählen *et al.*, 2017), thylakoid rearrangement (Horton & Ruban, 2005), and stomatal conductance changes (Matthews *et al.*, 2018; Li *et al.*, 2021). Each regulatory mechanism has its own time constant to respond to external stimuli (**Chapter 1** - **Section 1.2**) and, thus, operates within its specific frequency limits. A dynamic regulatory process occurs when its operational frequency is able to keep pace with the frequency of oscillating light. In the context of qE, the PsbS-dependent qE mechanism seems to function at a frequency of approximately 1/10 Hz - 1/30 Hz, while the frequency limit of the VDE-dependent qE may be around 1/60 Hz - 1/120 Hz.

A point of clarification is that the discussion focuses on the qE component of NPQ (the ΔpH-regulated rapidly reversible component of NPQ), as it is assumed that other components of NPQ, such as qZ (zeaxanthin-dependent sustained quenching component), based on its slow induction (10 - 30 min) and relaxation (10 - 60 min) (Nilkens *et al.*, 2010; Jahns & Holzwarth, 2012; Kress & Jahns, 2017), might have difficulty in influencing the dynamic signal patterns of each oscillatory cycle (rise and fall of up to 4 min). However, it does not mean that qZ is absent in oscillating light or that qZ has no effect on signals at all. Instead, qZ can be induced by long-term oscillating light measurement, especially in HL oscillations. The influence of the accumulated zeaxanthin on qE should not be overlooked. It has been shown that zeaxanthin is an allosteric modulator of qE that controls its efficiency and kinetics, and shifts the apparent pK of qE from 4.5 to 6.5 or an even more alkaline pH (Crouchman *et al.*, 2006; Johnson *et al.*, 2008; Pérez-Bueno *et al.*, 2008; Johnson *et al.*, 2009; Johnson & Ruban, 2009). High levels of zeaxanthin can accelerate or enhance the qE formation and delay its relaxation (Niyogi *et al.*, 1998; Johnson *et al.*, 2008; Nilkens *et al.*, 2010; Jahns & Holzwarth, 2012). Thus, the distinct dynamics of *npq1* from the wild-type due to the absence of the VDE may be caused not solely by the VDE-dependent qE, but also by the accumulation of zeaxanthin (qE or qE plus qZ) in the wild-type that affects the efficiency and kinetics of its qE. Additionally, the re-conversion of zeaxanthin to violaxanthin in darkness depends on the intensity of the pre-illumination; the higher the light intensity, the slower the re-conversion (Jahns, 1995; Jahns & Holzwarth, 2012; Kress

& Jahns, 2017). This is in line with our hypothesis in **Chapter 2** (HL oscillations) that the zeaxanthin produced during the pre-illumination and high-light phases of the oscillation may not apparently decline during the relatively short periods of low light during the oscillation. However, this may not be the case for the LL oscillations (**Chapter 4**). Under low light conditions, when light intensity is insufficient to saturate photosynthesis, the xanthophyll cycle (de-epoxidation and epoxidation) seems to operate in both directions in response to changes in ΔpH (Jahns, 1995), leading zeaxanthin concentration to be dynamically changed. Thus, changes in VDE-dependent qE in the LL oscillations may be directly related to the dynamic changes in zeaxanthin concentration. The dynamics of VDE-dependent qE in oscillating light involve the interaction with other NPQ components and become complex, requiring further studies to elucidate the mechanisms.

Furthermore, as manifested in the *crr2-2* mutant, ChlF may not be sensitive enough to detect the operation of certain regulatory mechanisms (**Figure 2.3**), highlighting the need to probe multiple signals at different steps of the electron transport chain and downstream processes. The results of dynamic redox signals of P700, PC, and Fd, suggested that the PGR5/PGRL1-dependent CET operates faster than the fastest frequency tested in this study (1 Hz). The dynamics of the signals in the mutant *pgrl1ab* contrasted with those of the wild-type at all frequencies tested (**Figures 2.3 - 2.6**). The NDH-like complex-dependent CET, on the other hand, may operate at frequencies around 1/30 Hz, judging from the resonance phenomenon of Fd redox states seen in the *crr2-2* mutant at 1/30 Hz and 1/60 Hz (**Figure 2.6**). Although the reduction resonance of Fd was not strong in the *crr2-2* mutant compared to its wild-type, this was evidenced by the increase in Fd reduction at the same phase of saturation pulse analysis at 1 min oscillation (**Figure 3.5**) as well as the transient increase in PSI acceptor side limitation (**Figure 3.4**). The contribution of the NDH-like complex to CET is questionable because of its low stoichiometric ratio (1:100) to PSI (Burrows *et al.*, 1998). If the NDH-like complex is relied upon to maintain the rate of cyclic electron flow (up to 100 s^{-1}) (Joliot *et al.*, 2004; Joliot & Johnson, 2011; Nawrocki *et al.*, 2019), then the NDH-like complex turnover should be at a rate of approximately 10^4 s^{-1}. However, the turnover rate of NDH-like complex proposed in vivo is about 0.1 s^{-1} (Trouillard *et al.*, 2012; Nawrocki *et al.*, 2019). This rate proposed is not far from the 1/30 Hz proposed here. The photoprotective function of NDH-like complex-dependent CET under high amplitude light oscillations was experimentally demonstrated. It can alleviate PSI acceptor side limitation

and promote efficient electron transfer under oscillating light conditions, although its role is not decisive but auxiliary.

5.1.2 Dynamic NPQ adjustment in oscillating light differs from NPQ induction during dark-to-light transition

It is important to clarify that the onset of dynamic NPQ adjustment refers to the ability of regulatory processes to keep pace with light intensity oscillations, which is not the same as the NPQ induction during the dark-to-light transition. The absence of dynamic adjustment does not imply that no regulatory processes have been activated or that there is a complete absence of regulatory intervention. In oscillating light, even if rapidly reversible NPQ (qE) cannot precisely follow the light intensity changes in high-frequency oscillations (1 Hz - 0.1 Hz), the regulatory processes can still respond to the integrated average of light intensity. This is manifested by the overall lower ChlF yield of the wild-type compared to the NPQ mutants under these fast oscillations (**Figure 2.3** & **Figure 4.2**). This distinctive feature of oscillating light may explain why the operating frequencies of specific regulatory processes determined in oscillating light, such as for the PsbS-dependent qE and the VDE-dependent qE (**Figure 2.3** & **Figure 4.2**), are not equivalent to the time constants of the same processes determined in time-domain induction or relaxation measurements (Nilkens *et al.*, 2010).

The responses of photosynthesis induced by induction or relaxation measurement differ from those under harmonically oscillating light measurements. In the case of photosynthesis induction, the transition from darkness to light simultaneously triggers the activation of both photosynthesis and photoprotection. This includes the activation of enzymes in the Calvin-Benson cycle (Buchanan, 1980; Edwards & Walker, 1983; Woodrow & Berry, 1988; Andersson, 2008), particularly the activation of FBPase, SBPase (Kirschbaum & Pearcy, 1988; Sassenrath-Cole *et al.*, 1994; Kaiser *et al.*, 2015) and Rubisco (Mott & Woodrow, 2000; Kaiser *et al.*, 2015), stomatal opening (Lawson *et al.*, 2010; Lawson *et al.*, 2012; Lawson & Blatt, 2014), establishment of trans-thylakoid photochemical potential (Rumberg & Siggel, 1969; Tikhonov *et al.*, 1981; Colombo *et al.*, 2016), alterations in protein conformations and the activation of photoprotection-related processes (Kereïche *et al.*, 2010; Correa-Galvis *et al.*, 2016; Sacharz *et al.*, 2017; Tutkus *et al.*, 2019), and so on. In contrast, under harmonically oscillating light, the photosynthesis systems are not in a dark-adapted

state. Enzymes associated with carbon assimilation are partially activated, while thylakoid environments and proteins are in light-adapted states. The thylakoid luminal acidity remains more acidic rather than changing from a neutral to an acidic state. As stomatal responses are relatively slow processes (Lawson *et al.*, 2010; Lawson *et al.*, 2012; Lawson & Blatt, 2014), thus they can be separated from more rapid dynamic processes occurring in relatively fast oscillations tested in this study. Therefore, oscillating light measurements can avoid drastic changes of the membrane environments and enzyme activities that occur during dark-light transitions. By choosing specific frequencies, the regulatory processes can be investigated in a more targeted manner.

During the induction or relaxation, one can only observe unidirectional reactions, such as the activation or relaxation of NPQ, respectively (Nilkens *et al.*, 2010; Kress & Jahns, 2017). Photosynthesis responds differently to an increase and a decrease in irradiance. For example, the conversion of zeaxanthin back to violaxanthin is catalyzed by ZEP but at a slower rate than the conversion of violaxanthin to zeaxanthin by VDE (Niyogi *et al.*, 1997; Nilkens *et al.*, 2010; Jahns & Holzwarth, 2012; Kress & Jahns, 2017). While the separation of induction and relaxation allows us to focus on the reactions that predominate in one of these two transition phases, it does not provide a comprehensive understanding of the dynamic responses of photosynthesis under fluctuating light. In oscillating light measurements, instead of studying processes in a single direction, integrated regulatory processes in both directions can be observed. This approach exposes plants to harmonically oscillating light comprising natural sunlight conditions.

In frequency-domain measurements using harmonically oscillating light, the main question is whether regulatory processes can respond to light oscillations and compensate for the effects caused by light perturbations. This approach is concerned with the dynamic response and regulation of the system rather than the complete shutdown or kickoff of the entire system.

The response of plants to fluctuating light is often experimentally investigated in light that is square-modulated (Kono *et al.*, 2014; Kono & Terashima, 2016; Yamori *et al.*, 2016; Yamamoto & Shikanai, 2019; Zhou *et al.*, 2022). Here, I clarify the differences and advantages of the harmonically oscillating light approach compared to square-modulated light. **Figure 5.1** shows changes in light intensity (red line) that are square-modulated with a period of 1.5-min high light and 1.5-min low light. These changes in light intensity can be

approximated by a sum of four harmonics (thin colored lines), as shown in **Figure 5.1**. The approximated sum is shown by the dashed black line. The component with the fundamental harmonic period of 3 min contributes the most. The second most contributing is the first upper harmonic component with a period of 1 min. The amplitude of the first upper harmonic component (1 min) is three times lower than that of the fundamental harmonic (3 min), but its influence on plant photosynthesis can be enhanced by the resonance described above that occurs for periods of around 1 min. Accordingly, the plant responses to a square-modulated period of 3 min may well involve an amplified resonance response of the investigated plant to the 1-min upper harmonic component. This, however, is not the case in harmonically modulated light regimes with a period of 3 min. Follow-up experiments are required to test the differences between the dynamics induced by square-modulated light and the integration of the dynamics induced by its Fourier decomposed-harmonic light.

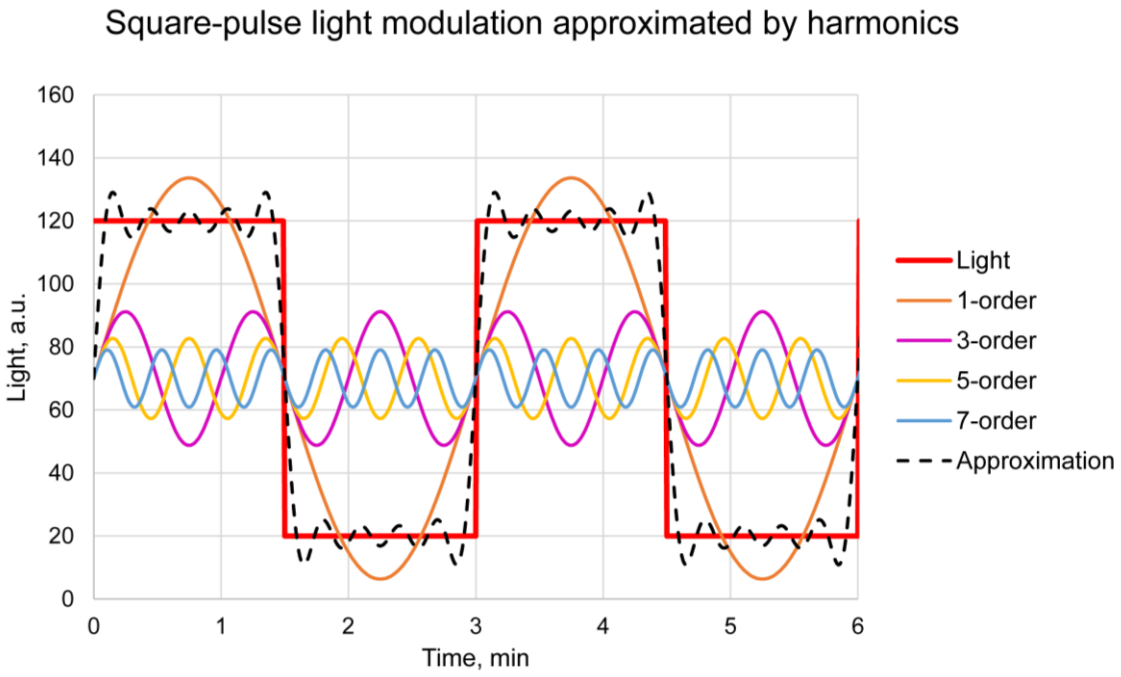

Figure 5.1 An approximation (dashed black line) of a square-modulated light (thick red line) by four harmonic components. The thin colored lines show the contributing harmonic components with periods of 3 min (orange, 1st -order), 1 min (magenta, 3rd -order), 3/5 min (yellow, 5th -order), and 3/7 min (blue, 7th -order).

5.1.3 Possible ways to quantify the dynamic signals

In this study, I focused on qualitatively characterizing the dynamic signals obtained in frequency-domain measurements and interpreting them by comparing the differences in the responses of wild-type and mutant plants. However, further research is necessary to develop quantifiable parameters for dynamic signals that can be easily compared and interpreted, similar to the ChlF parameters in time-domain measurements, such as Fv/Fm or Fv'/Fm' (Baker, 2008).

Supplementary Materials ***Figure-SM 4.4*** displays the amplitudes of different harmonics of ChlF signals. In this figure, the fundamental harmonic (A1) exhibited a clear peak at 1/30 Hz oscillation in both the wild-type and *npq1* mutant, and the first upper harmonic (A2) showed a distinct peak at 1/60 Hz in ML and HL oscillations. However, the *npq4* mutant did not display such a peak phenomenon around 1/30-1/60 Hz, and the amplitudes of both A1 and A2 continued to increase as the periods became longer. As discussed, these resonances are thought to be the onset of the PsbS-dependent qE. Based on this figure, it can be hypothesized that useful parameters may be derived by quantifying the changes in the amplitudes and phases of the signals at the frequencies identified as the characteristic frequencies of specific processes, as well as the amplitudes and phases of the corresponding harmonics.

Acquisition of accurate parameters requires a comprehensive scan of different species and genotypes under oscillating light with broader frequencies, followed by a comprehensive analysis of amplitude variations and phase shifts (Keesman, 2011; Pintelon & Schoukens, 2012). This would entail a substantial amount of work. Therefore, for this approach to be widely used in the future, it would be necessary to use mechanistic models and system identification to quantify, simulate and interpret dynamic signals.

5.1.4 Points to be verified and possible interpretations

In contour map plots (**Figures 2.4** & **2.5**), a large discrepancy between the redox states of PC and P700 was observed at oscillating frequencies lower than 1/120 Hz. While the P700 oxidation closely followed the light modulation, the PC oxidation exhibited a saddle-type depression when the light intensity was close to the maximum. In the electron transport chain, the redox state of PC is determined by both its electron donor (Cyt b_6/f) and acceptor (P700). As a mobile electron carrier, PC links the electron transfer between PSII in the grana

and PSI in the stroma lamellae (Höhner *et al.*, 2020). The pool size and distribution of PC in these thylakoid compartments and its ability to migrate between grana and stroma lamellae may jointly affect the rate of electron transport between Cyt b_6/f and P700 (Joliot *et al.*, 1992; Kirchhoff *et al.*, 2000; Kirchhoff *et al.*, 2011; Malone *et al.*, 2021). In addition, PC is involved in both linear and cyclic electron transports; hence, its redox state can be influenced collectively by both. In the context of oscillating light, energization (Suorsa *et al.*, 2013; Colombo *et al.*, 2016; Johnson & Berry, 2021) and structure (Ünnep *et al.*, 2017; Johnson & Wientjes, 2020; Li *et al.*, 2020; Hepworth *et al.*, 2021) of the thylakoid membrane may change. Therefore, in **Chapter 2**, this discrepancy between PC and P700 was attributed to the re-arrangement of the thylakoid structure. It may influence the diffusion of PC and, as a result, its interaction with Cyt b_6/f and P700, especially considering the relatively long distance a reduced PC may need to travel (Höhner *et al.*, 2020).

Since this discrepancy only occurred in the HL oscillations (results not shown, but the large discrepancy between PC and P700 observed in HL oscillations was not found in ML and the LL oscillations), another possible explanation is that HL-induced oxidative stress, leading to more calcium ion (Ca^{2+}) influx into thylakoid lumen (Sello *et al.*, 2018). This influx could, in turn, induce the phosphorylation of the PsaN subunit of PSI complex (Stael *et al.*, 2012). Given that PsaN is in close proximity to the PC binding side, PsaF, the alteration of three-dimensional structure caused by the phosphorylation of PsaN may affect the binding affinity of PC to PSI (Amunts *et al.*, 2010). These assumptions need further investigations.

In this study, photoinhibition-induced quenching, qI (Kok, 1956; Murata *et al.*, 2007; Nawrocki *et al.*, 2021), was not quantified at the end of oscillating light measurement in **Chapter 3**. However, in some cases, photoinhibition may have affected the estimated quantum yields, especially in the mutants lacking specific photoprotective mechanisms under the HL oscillation conditions (Li *et al.*, 2002b; Ware *et al.*, 2015; Yamamoto & Shikanai, 2019). A quantitative analysis of quantum yields for *pgrl1ab* mutant under the 1/60 Hz light oscillation showed differences in the values of Y(I), Y(NA), Y(II), Y(NPQ), and Fd reduction at the beginning and at the end of the oscillation cycle (**Figures 3.4** & **3.5**). Photoinhibition is likely to be one of the reasons for these differences, as it is well known that the lack of PGR5/PGRL1-dependent CET leads to photoinhibition of both PSI and PSII under fluctuating light (Suorsa *et al.*, 2012; Yamamoto & Shikanai, 2019; Barbato *et al.*, 2020; Wada *et al.*, 2021). However, the extent to which it played a role remains unknown

here. Future experiments should consider the impact of photoinhibition-induced NPQ (qI) on quantum yields estimation under oscillating light. Under the oscillating light conditions in this study, only the effects of photoinhibition on the estimation of quantum yields were considered (**Chapter 3**), while its effects on the dynamic signals were not taken into account (**Chapter 2** & **Chapter 4**). Since the qI is a slowly inducible quenching process (> 30 min) and the relaxation of qI is also slowly developing and energy-consuming (tens of minutes to days) (Kok, 1956; Murata *et al.*, 2007; Murchie & Niyogi, 2011; Jahns & Holzwarth, 2012; Kaiser *et al.*, 2019; Nawrocki *et al.*, 2021), possible effects of photoinhibition on dynamic signals caused by prolonged exposure to oscillation light measurements, such as signal drifting, can be eliminated by normalizing the signal to the value at the minimal light intensity in each oscillation cycle.

When light oscillation conditions that differ from those tested here are implemented, contributions of other NPQ components like qT (Haldrup *et al.*, 2001; Allen, 2003; Dietzel *et al.*, 2008), qZ (Jahns *et al.*, 2009; Nilkens *et al.*, 2010; Dall'Osto *et al.*, 2012; Jahns & Holzwarth, 2012; Kress & Jahns, 2017), qH (Malnoë, 2018; Malnoë *et al.*, 2018) as well as qI to dynamic ChlF signal in oscillating light should also be considered accordingly. For example, if the light oscillates from darkness or very low intensity, the contribution of qT should be clarified. Likewise, if the oscillation period is long enough, the slowly inducing and relaxing components of NPQ, qI, qZ, or qH may also contribute to ChlF dynamic signals.

As discussed in **Chapter 2**, the hypothesis regarding stable levels of zeaxanthin during HL oscillations needs to be experimentally validated. In **Chapter 2**, it was assumed that the levels of zeaxanthin produced during the pre-illumination and high-light phases of oscillations remained stable during the relatively short periods of low light during the light oscillations. To test this, experiments should be conducted to measure xanthophyll concentrations in the leaves during light oscillations. The destructive analysis method (Nilkens *et al.*, 2010) may not be suitable for the oscillation frequencies tested in this study, as it is time-consuming and not applicable to high-frequency oscillations. Therefore, non-destructive methods with high resolution will be needed for future study.

5.2 The operation and interaction of multiple regulatory processes in dynamically changing environments

5.2.1 Understanding dynamic regulation of photosynthesis from a systems perspective

Photosynthesis systems share some similarities with complex physical systems. Both exhibit varying degrees of complexity. The complexity of physical systems can range from simple mechanical devices to highly complex systems, while photosynthesis systems, being biological, are notably more intricate. Modularity makes it feasible to manage complexity in both cases, and feedback regulations between modules are common, contributing to systems' robustness. When systems exceed their operating limits, they become fragile and prone to cascading failures.

The dynamics of photosynthesis in oscillating light, as observed in this study, can be partially explained by the concept of system frequency response (Smith, 1997). If the external stimulus frequency is too high, the system struggles to keep pace with the rapid changes of the external force, and might diminish response or even respond to the average of the stimulus (Nedbal *et al.*, 2005; Nedbal & Lazár, 2021). This could explain why the wild-type exhibited lower ChlF yields compared to the NPQ mutants at the fast frequencies of oscillations, 1 Hz - 0.1 Hz (**Figure 2.3** & **Figure 4.2**), in which the regulatory processes of qE find it difficult to keep pace with the light intensity changes. Conversely, when the stimulus frequency slows down, the system could synchronize its response with the stimulus as it has ample time to respond to each force cycle. This synchronization might explain the stationary states (dynamic homeostasis) of ChlF observed in the wild-type plants during low-frequency oscillations, 1/240 Hz - 1/480 Hz (**Figure 4.1**). When the frequency of external stimulus coincides with the system's inherent frequency, resonance occurs, leading to amplified responses (Dau & Hansen, 1989; Nedbal & Březina, 2002; Vistnes, 2018; Rittweger & Taiar, 2020). Accordingly, the emergence of resonance peaks at particular frequencies could reflect the onset of specific regulatory processes that have the matching inherent frequencies within the photosynthesis systems (**Chapter 2**). The resonance peaks occur because the frequency of oscillating light matches or approaches the internal

frequencies of the regulatory processes, triggering large modulations of signals (Vistnes, 2018; Rittweger & Taiar, 2020).

However, analogies to physical systems cannot fully explain the signal dynamics of photosynthesis systems. Physical systems often have clear and predictable frequency responses that are characterized by their inherent frequencies and linear behaviors. In contrast, photosynthesis systems operate across multiple temporal and spatial scales and are equipped with multiple regulatory mechanisms (**Chapter 1 - Section 1.2**). The inherent complexity and non-linearity of the photosynthesis systems lead to complex frequency responses that are influenced by regulatory processes and can vary depending on physiological or environmental conditions (Bich *et al.*, 2016). Importantly, photosynthesis systems are highly adaptive (Walters, 2005; Athanasiou *et al.*, 2010; Schöttler & Tóth, 2014; Dyson *et al.*, 2015; Morales & Kaiser, 2020; Gjindali *et al.*, 2021). The extent of its influence on dynamic responses under oscillating light remains a subject of future research.

The complexity of interpreting signals of photosynthetic dynamics also arises from technical limitations in sensing signals. For example, regulatory processes like NPQ were not directly detected but inferred from the ChlF signals. The ChlF reflects an interplay between photochemical and non-photochemical quenching, challenging signal interpretation. When ChlF yields remain stable, it may indicate efficient energy dissipation by NPQ, as seen in the wild-type under low-frequency oscillations (**Figure 2.3** & **Figure 4.1**). In high-frequency oscillations, however, it may signify saturation of ChlF yields (**Figure 2.3** & **Figure 4.1**). This study obtained information on regulatory processes by comparing dynamic signals between the wild-types and the mutants. Additionally, simultaneous measurements of dynamic responses of various photosynthetic components helped to interpret the regulatory information.

When plants are exposed to oscillating light, the ChlF response does not follow a linear pattern. Instead, the signal responses are distorted by upper harmonics. These harmonics-related distortions are thought to carry valuable information about the system's response to oscillating light, such as regulatory processes and time constraints (Dau & Hansen, 1989; Nedbal & Březina, 2002; Nedbal *et al.*, 2005; Nedbal & Lazár, 2021). Experiments in algae and mathematical models have further supported this point (Nedbal & Lazár, 2021). In this thesis, through a comparative analysis of dynamics of ChlF and redox components in response to multi-frequency oscillating light in the wild-type and the mutant plants lacking

specific regulatory mechanisms, I experimentally demonstrated that these distorted, highly non-linear signals with upper harmonics are indeed the result of dynamic regulatory processes of photosynthesis.

In summary, the dynamics of photosynthesis systems are highly non-linear, featuring a multitude of feedback and feedforward reactions as well as various regulatory processes to ensure robustness (Nedbal *et al.*, 2005; Bich *et al.*, 2016; Nedbal & Lazár, 2021; Lazár *et al.*, 2022). Comprehending the dynamic signals of intricate biological photosynthesis systems demands extensive experimental investigations and modelling studies.

5.2.2 Oscillating light has the potential to differentiate regulatory mechanisms and contributes to studying their implementation in dynamically changing environments

As improving photosynthetic efficiency is considered an effective way to increase crop production, more and more studies have focused on photosynthetic efficiency under natural or fluctuating light conditions in the last decades (Zhu *et al.*, 2008; Zhu *et al.*, 2010; Long *et al.*, 2015). Significant progress has been made in enhancing photosynthetic efficiency and even yields in some species through genetic engineering to manipulate critical regulatory reactions in photoprotection or major rate-limiting steps in the Calvin-Benson cycle (Harrison *et al.*, 1997; Harrison *et al.*, 2001; Lefebvre *et al.*, 2005; Lawson *et al.*, 2006; Feng *et al.*, 2007a; Feng *et al.*, 2007b; Feng *et al.*, 2009; Rosenthal *et al.*, 2011; Rojas-González *et al.*, 2015; Ding *et al.*, 2016; Kromdijk *et al.*, 2016; Driever *et al.*, 2017; De Souza *et al.*, 2022). These advances hold promise for improving crop photosynthesis to meet increasing food demands (Zhu *et al.*, 2010; Long *et al.*, 2015). Many studies on photosynthetic dynamics have focused on how photosynthesis systems adjust to external perturbations. However, there is limited understanding of how those adjustments are actually triggered and implemented in naturally fluctuating environments. In other words, the mechanisms and capacities of regulatory processes in photosynthesis systems have been extensively revealed under various conditions, but more explorations can be made to discern how exactly these regulatory adjustments operate and achieve under dynamically changing environments. It would be unwise to evaluate the capabilities of photosynthesis without considering the operational environments. Observations in controlled environments like laboratories or greenhouses may not necessarily be translated to field conditions (Khaipho-

Burch *et al.*, 2023). Therefore, it is crucial to study the onset and implementation of these regulatory mechanisms and their interactions in dynamically changing environments. This will contribute to the successful validation of laboratory results in the field.

Understanding the mechanisms behind dynamic regulatory adjustments remains a challenge due to a wide array of regulation-induced processes in photosynthesis systems and the limitations of non-destructive sensing techniques (**Chapter 2**).

The frequency-domain-based approach, as used in this PhD study, offers a workable way to investigate how different regulatory mechanisms are implemented in dynamically changing light conditions. By analyzing those responses to changes in the frequency of light intensity oscillation, we can determine frequency limits within which different regulatory processes are engaged (**Chapter 2**). Specifically, when the frequency of light oscillations exceeds the limit at which a specific regulatory process can respond, that process fails to modulate photosynthesis in response to changes in light. Conversely, when the light frequency falls below the frequency limit, the specific regulatory process is able to respond to the light changes. In **Chapter 2**, I found that different regulatory mechanisms have distinct frequency limits. For instance, the PsbS-dependent NPQ (qE) can respond to an upper frequency limit of around 1/10 Hz - 1/30 Hz, while the VDE-dependent NPQ (qE) can only counteract in slower light oscillations of about 1/60 Hz - 1/120 Hz (**Figures 2.2** & **2.3**). In addition to identifying the frequencies at which the specific regulatory processes can operate, it is also possible to find the frequencies at which certain regulatory processes are effective in maintaining the dynamic equilibrium of the photosynthesis systems to cope with external fluctuations. In wild-type plants, rapidly reversible NPQ (qE) is activated at the frequency of about 1/30 Hz. However, the frequency at which the rapidly reversible NPQ (qE) can maintain the system in dynamic homeostasis is much lower, around 1/240 or 1/480 Hz (**Figure 2.3** & **Figure 4.1**).

5.2.3 Dynamic complementarity among multiple regulatory mechanisms becomes visible in oscillating light

In harmonically oscillating light, the signal dynamics reflect not only how regulatory mechanisms respond to external fluctuations but also the complementary effects among different regulatory mechanisms.

In NPQ mutants, the constitutive non-photochemical quenching (Y(NO)) largely compensated for the lack of rapidly reversible NPQ (**Figure 3.2**). The fact that Y(NO) is not always constant and appears to be "regulated", has been noticed before (Han *et al.*, 2022; Lazár *et al.*, 2022) (**Chapter 3**). The presence of other regulatory processes, including the CET pathways or probably the AET pathways (***Figure-SM 3.3***) may also contribute to compensating for the absence of NPQ, thereby stabilizing PSI.

In the HL oscillations, resonance peaks were observed in Fd signals at the PSI acceptor side in the *crr2-2* mutant. These peaks occurred at around 120° phase with a frequency of 1/30 Hz and 60° phase with a frequency of 1/60 Hz (**Figure 2.6**). Analysis of quantum yields revealed that during these corresponding phases of Fd resonance peaks, there were transiently increased limitations on the PSI acceptor side (Y(NA), between approximately 60°-120°) and decreased limitations on the PSI donor side (Y(ND)) (**Figure 3.4**). Furthermore, the redox states of Fd, as examined by saturation pulses, again displayed a transient reduction peak at similar phases (**Figure 3.5**). These effects were not so prominent in the corresponding wild-type (**Figure 2.6** & **Figures 3.4**, **3.5**). It is therefore that in the *crr2-2* mutant, temporary limitations on the PSI acceptor side occurred in the light increasing phase of oscillations, resulting from the absence of the NDH-like complex-dependent CET. These limitations, however, were only transient and could be swiftly alleviated by other photoprotective mechanisms.

Previous studies have shown that under constant light conditions, double mutants lacking both NDH-like complex-dependent CET and PGR5/PGRL1-dependent CET exhibit more pronounced PSI acceptor side limitations and experience more severe photoinhibition compared to single mutants lacking the PGR5/PGRL1-dependent CET (Munekage *et al.*, 2004; Wang *et al.*, 2015; Nakano *et al.*, 2019). This illustrates the role of the NDH-like complex-dependent CET in PSI photoprotection. However, when the PGR5/PGRL1-dependent CET is functional, the absence of the NDH-like complex-dependent CET alone has a minimal impact on photosynthesis (Suorsa *et al.*, 2012; Kono *et al.*, 2014). Our observations in the *crr2-2* mutant under oscillating light align with these findings and highlight the difficulty in detecting the limitations imposed by the absence of the NDH-like complex-dependent CET under steady-state conditions, possibly because other functional regulatory mechanisms can rapidly compensate for these limitations. In contrast, when the PGR5/PGRL1-dependent CET is absent, PSI experienced a substantial reduction with severe acceptor-side limitations (**Figures 2.4**, **2.6** & **Figures 3.4**, **3.5**). The large

contribution of PGR5/PGRL1-dependent CET to lumen acidification (Wang *et al.*, 2015; Kawashima *et al.*, 2017; Degen *et al.*, 2023) causes its absence essentially restricts the ΔpH-dependent photoprotective regulatory processes, including the NPQ induction and photosynthesis control. Thus, the other photoprotective mechanisms cannot effectively compensate for the absence of the PGR5/PGRL1-dependent CET (Munekage *et al.*, 2002; Suorsa *et al.*, 2012; Yamamoto & Shikanai, 2019; Ma *et al.*, 2021a). Notably, the limitation caused by the absence of the NDH-like complex-dependent CET was pronounced in the HL oscillations (**Figures 3.4** & **3.5**). The results presented in **Chapter 3** indicated that the PGR5/PGRL1-dependent CET can protect photosystems against light fluctuations of varying amplitudes, while the NDH-like complex-dependent CET may act as a safety valve to balance the electron transports in light fluctuations with large intensity changes. Overall, complementary effects existing among multiple regulatory mechanisms in response to dynamically changing light environments can be reflected by harmonically oscillating light measurements.

5.3 Perspectives for future research

The potential for the application of different frequencies of oscillating light to probe the dynamics of plant photosynthesis should be further explored in the following ways:

1) The correlation between plant responses to randomly fluctuating light (**Table 1**) and responses to harmonically oscillating light should be investigated. The superposition of multiple sinusoidal modes may not necessarily elicit a response to the arithmetic sum of the responses to the constituent single oscillatory modes. The extent to which the superposition of multiple sinusoidal modes provides a good approximation of natural dynamics of fluctuating light needs to be determined experimentally.

2) In the same direction, due to the inherent non-linearity of photosynthesis, plant responses may differ between a dark-to-light transition and the superposition of harmonic oscillatory modes representing the Fourier decomposition of the elements of such a dark-to-light transition. If this difference is negligible, then the frequency-domain-based method presented in this and earlier studies (Nedbal & Březina, 2002; Nedbal *et al.*, 2003; Nedbal *et al.*, 2005; Nedbal & Lazár, 2021; Lazár *et al.*, 2022) will yield the same information as dark-to-light transition measurements, albeit without the need for dark adaptation and higher

sensitivity. If large differences are found, dark-to-light transition measurement and harmonically oscillating light method will provide complementary information.

3) The detection of photosynthesis by harmonic modulation of irradiance can benefit from the fact that the frequency of the plant's response is correlated with the frequency of oscillating light. Such priori knowledge can be used to reduce noise from irregular dynamics. This is a well-documented principle of simultaneous detection in electronics, which was also applied earlier to the measurement of fluorescence lifetimes (Lakowicz, 2013). Considering signals in the framework of information theory leads to the same conclusion: by using the available additional information about the dynamic properties of the signal, it is possible to reduce noise in the signal. The extent to which this potential can actually improve photosynthesis detection in noisy environments such as fields, greenhouses, or phenotyping platforms remains to be tested experimentally.

4) Possible opportunities in plant growth environments can be explored by improved frequency-domain real-time sensing technologies combined with artificial intelligence to control greenhouse lighting, temperature, and other factors that are decisive for crop yield and economics. Oscillating light may not only provide new opportunities for sensing regulatory processes, but using the resonant frequencies thus determined (Nedbal *et al.*, 2005), it may also disturb equilibrium and manipulate stress responses to improve the production of valuable secondary metabolites or other high-value plant products.

5) The ChlF-based early detection of stress symptoms has been explored previously (Matous *et al.*, 2006; Berger *et al.*, 2007; Pineda *et al.*, 2008). Harmonically oscillating light may have the potential to be applied to the early detection of plant stresses, because it is possible to discriminate among the operating frequencies of different regulatory mechanisms. By providing light stimuli at specific frequencies, signals of stress-related regulatory processes can be triggered in a targeted manner. This would require extensive frequency scanning under different stress conditions.

6) While this study focused on monochromatic light, the impacts of light oscillations of different spectra (Nedbal *et al.*, 2003) as well as the modulation-mediated activities of different photoreceptors, e.g. blue light-mediated chloroplast movement (Kagawa *et al.*, 2001; Sakai *et al.*, 2001; Banaś *et al.*, 2012), can be investigated.

7) Photoreceptors and photosynthesis-mediated signaling synergistically influence the expression of specific genes, enabling acclimation of plant growth and function to changes

in environmental conditions, including alterations in nutrient levels, temperature and light quality or intensity. The long-term acclimation, in turn, impacts the capabilities of photosynthesis and its regulations in the short term. It remains to be experimentally verified whether the short-term dynamic regulatory mechanisms of plants have consistent frequency characteristics under different long-term adaptation conditions.

8) Frequency domain sensing has the potential to outperform traditional time-domain sensing when it comes to monitoring photosynthetic regulatory processes and capacities. Through the application of frequency-domain sensing techniques, it becomes feasible to phenotype natural variations in photosynthetic capacities and their regulation-related traits across different plant species and genotypes. When combined with advanced genetic techniques like next-generation sequencing and QTL analyses, the potential for targeted-breeding to improve the efficiency and dynamic regulation of photosynthesis under fluctuating light becomes feasible. As growth conditions for plants become more diverse, with huge differences in light between field, greenhouse and vertically farmed growing environments, the development of crop varieties suited to different environmental conditions will be crucial for future breeding efforts to improve yields. Effective quantitative signal analysis methods and high-throughput frequency domain sensing techniques are powerful tools to achieve these.

Abbreviations and symbols

Abbreviation	Description
AET	Alternative electron transport
AL	Actinic light
ATP	adenosine triphosphate
CET	Cyclic electron transport
Chl	Chlorophyll
ChlF	Chlorophyll fluorescence
Cyt b_6/f	Cytochrome b6f complex
FBPase	Fructose-1,5-bisphosphatase
Fd	Ferredoxin
Fd^-_m	Maximum reduction of ferredoxin
HL	High light oscillation
LHCII	Light-harvesting complex of Photosystem II
LL	Low light oscillation
NADPH	Reduced nicotinamide adenine dinucleotide phosphate
NIR	Near-infrared light
NPQ	Non-photochemical quenching. Multiple molecular mechanisms lead to the lowering of emission of Chl fluorescence in high light. Here we use the term referring to mechanisms that are reversible on the scale of seconds to minutes and that involve PsbS and/or VDE proteins
NDH-like	Chloroplast NAD(P)H dehydrogenase-like complex
ML	Medium light oscillation
P700	Primary electron donor in the reaction centre of photosystem I
P_m	Maximum oxidation of P700
PC	Plastocyanin
PC_m	Maximum oxidation of plastocyanin
PSI	Photosystem I
PSII	Photosystem II
PGR5	Proton Gradient Regulation 5 protein
PGRL1	Proton Gradient Regulation-like 1 protein
pmf	Proton motive force
PsbS	Chloroplastic 22 kDa Photosystem II protein involved in NPQ
qI	Photoinhibition-induced non-photochemical quenching
qP	The coefficient of photochemical quenching, estimating the fraction of open PSII centres (with Q_A oxidized) based on a puddle model for the photosystem II units
qT	State transitions
PTOX	Plastid terminal oxidase
qZ	Zeaxanthin-dependent sustained quenching components
ROS	Reactive oxygen species
RuBisCO	Ribulose-1,5-bisphosphate carboxylase/oxygenase
RuBP	Ribulose 1,5-bisphosphate
Fd Red	Apparent relative reduction of ferredoxin
SBPase	Sedoheptulose-1,7-bisphosphatase

Abbreviation	Description
SP	Multiple-turnovers saturation pulse
VDE	Violaxanthin de-epoxidase enzyme
WWC	Water-water cycle, also known as the Mehler-ascorbate-peroxidase reactions
Y(I)	The effective photochemical quantum yield of photosystem I
Y(ND)	The quantum yield of non-photochemical energy dissipation in photosystem I due to donor side limitation
Y(NA)	The quantum yield of non-photochemical energy dissipation in photosystem I due to acceptor side limitation
Y(II)	The effective photochemical quantum yield of photosystem II
Y(NPQ)	The quantum yield of the regulated non-photochemical quenching
Y(NO)	The quantum yield of the constitutive non-photochemical quenching
ZEP	Zeaxanthin epoxidase enzyme
α frequency domain	The domain with periods shorter than 30 s was identified by a specific dynamic behavior of ChlF
β frequency domain	Another domain of distinct dynamics with periods longer than 1 min and shorter than 8 min

Bibliography

Ahn TK, Avenson TJ, Ballottari M, Cheng Y-C, Niyogi KK, Bassi R, Fleming GR. 2008. Architecture of a charge-transfer state regulating light harvesting in a plant antenna protein. *Science* **320**(5877): 794-797.

Allahverdiyeva Y, Suorsa M, Tikkanen M, Aro E-M. 2015. Photoprotection of photosystems in fluctuating light intensities. *Journal of Experimental Botany* **66**(9): 2427-2436.

Allen JF. 1992. Protein phosphorylation in regulation of photosynthesis. *Biochimica et Biophysica Acta (BBA) - Bioenergetics* **1098**(3): 275-335.

Allen JF. 2002. Photosynthesis of ATP—electrons, proton pumps, rotors, and poise. *Cell* **110**(3): 273-276.

Allen JF. 2003. State transitions--a question of balance. *Science* **299**(5612): 1530-1532.

Allen JF, Bennett J, Steinback KE, Arntzen CJ. 1981. Chloroplast protein-phosphorylation couples plastoquinone redox state to distribution of excitation-energy between photosystems. *Nature* **291**(5810): 25-29.

Alter P, Dreissen A, Luo F-L, Matsubara S. 2012. Acclimatory responses of Arabidopsis to fluctuating light environment: comparison of different sunfleck regimes and accessions. *Photosynthesis Research* **113**(1): 221-237.

Amthor JS. 2010. From sunlight to phytomass: on the potential efficiency of converting solar radiation to phyto-energy. *New Phytologist* **188**(4): 939-959.

Amunts A, Toporik H, Borovikova A, Nelson N. 2010. Structure determination and improved model of plant photosystem I. *Journal of Biological Chemistry* **285**(5): 3478-3486.

Ananyev G, Dismukes GC. 2005. How fast can photosystem II split water? Kinetic performance at high and low frequencies. *Photosynthesis Research* **84**(1): 355-365.

Andersson I. 2008. Catalysis and regulation in Rubisco. *Journal of Experimental Botany* **59**(7): 1555-1568.

Ando T, Fowler AB, Stern F. 1982. Electronic properties of two-dimensional systems. *Reviews of Modern Physics* **54**(2): 437-672.

Asada K. 1999. The water-water cycle in chloroplasts: scavenging of active oxygens and dissipation of excess photons. *Annual Review of Plant Physiology and Plant Molecular Biology* **50**(1): 601-639.

Athanasiou K, Dyson BC, Webster RE, Johnson GN. 2010. Dynamic acclimation of photosynthesis increases plant fitness in changing environments. *Plant Physiology* **152**(1): 366-373.

Avenson TJ, Kanazawa A, Cruz JA, Takizawa K, Ettinger WE, Kramer DM. 2005. Integrating the proton circuit into photosynthesis: progress and challenges. *Plant, Cell and Environment* **28**(1): 97-109.

Baker NR. 2008. Chlorophyll fluorescence: A probe of photosynthesis in vivo. *Annual Review of Plant Biology* **59**: 89-113.

Ballaré CL, Pierik R. 2017. The shade-avoidance syndrome: multiple signals and ecological consequences. *Plant, Cell and Environment* **40**(11): 2530-2543.

Banaś AK, Aggarwal C, Łabuz J, Sztatelman O, Gabryś H. 2012. Blue light signalling in chloroplast movements. *Journal of Experimental Botany* **63**(4): 1559-1574.

Barbato R, Tadini L, Cannata R, Peracchio C, Jeran N, Alboresi A, Morosinotto T, Bajwa AA, Paakkarinen V, Suorsa M, et al. 2020. Higher order photoprotection mutants reveal the importance of ΔpH-dependent photosynthesis-control in preventing light induced damage to both photosystem II and photosystem I. *Scientific Reports* **10**(1): 6770.

Barker DH, Logan BA, Iii WWA, Demmig-Adams B. 1997. The response of xanthophyll cycle-dependent energy dissipation in Alocasia brisbanensis to sunflecks in a subtropical rainforest. *Functional Plant Biology* **24**(1): 27-33.

Bassi R, Croce R, Cugini D, Sandonà D. 1999. Mutational analysis of a higher plant antenna protein provides identification of chromophores bound into multiple sites. *Proceedings of the National Academy of Sciences of the United States of America* **96**(18): 10056-10061.

Beer S, Björk M, Gademann R, Ralph P 2001. Chapter 9 - Measurements of photosynthetic rates in seagrasses. *Global Seagrass Research Methods*. Amsterdam: Elsevier Science, 183-198.

Beer S, Vilenkin B, Weil A, Veste M, Susel L, Eshel A. 1998. Measuring photosynthetic rates in seagrasses by pulse amplitude modulated (PAM) fluorometry. *Marine Ecology Progress Series* **174**: 293-300.

Bellafiore S, Barneche F, Peltier G, Rochaix J-D. 2005. State transitions and light adaptation require chloroplast thylakoid protein kinase STN7. *Nature* **433**(7028): 892-895.

Berger S, Benediktyová Z, Matouš K, Bonfig K, Mueller MJ, Nedbal L, Roitsch T. 2007. Visualization of dynamics of plant–pathogen interaction by novel combination of chlorophyll fluorescence imaging and statistical analysis: differential effects of virulent and avirulent strains of P. syringae and of oxylipins on A. thaliana. *Journal of Experimental Botany* **58**(4): 797-806.

Berry J, Bjorkman O. 1980. Photosynthetic response and adaptation to temperature in higher plants. *Annual Review of Plant Physiology* **31**(1): 491-543.

Bertotti G. 1998. *Hysteresis in magnetism: for physicists, materials scientists, and engineers*: Gulf Professional Publishing.

Bertsch GF. 1983. Vibrations of the atomic nucleus. *Scientific American* **248**(5): 62-73.

Bich L, Mossio M, Ruiz-Mirazo K, Moreno A. 2016. Biological regulation: controlling the system from within. *Biology & Philosophy* **31**(2): 237-265.

Billings SA, Tsang KM. 1989. Spectral analysis for non-linear systems, Part I: Parametric non-linear spectral analysis. *Mechanical Systems and Signal Processing* **3**(4): 319-339.

Boashash B. 2015. *Time-frequency signal analysis and processing: a comprehensive reference*: Academic press.

Bonardi V, Pesaresi P, Becker T, Schleiff E, Wagner R, Pfannschmidt T, Jahns P, Leister D. 2005. Photosystem II core phosphorylation and photosynthetic acclimation require two different protein kinases. *Nature* **437**(7062): 1179-1182.

Bonente G, Howes BD, Caffarri S, Smulevich G, Bassi R. 2008. Interactions between the photosystem II subunit PsbS and xanthophylls studied in vivo and in vitro. *Journal of Biological Chemistry* **283**(13): 8434-8445.

Bortignon PF, Bracco A, Broglia RA. 2019. *Giant Resonances: Nuclear structure at finite temperature*: CRC Press.

Bottin H, Mathis P. 1985. Interaction of plastocyanin with the photosystem I reaction center: a kinetic study by flash absorption spectroscopy. *Biochemistry* **24**(23): 6453-6460.

Broughton SA, Bryan K. 2018. *Discrete Fourier analysis and wavelets: applications to signal and image processing*: John Wiley & Sons.

Buchanan BB. 1980. Role of light in the regulation of chloroplast enzymes. *Annual Review of Plant Physiology* **31**(1): 341-374.

Burgess AJ, Durand M, Gibbs JA, Retkute R, Robson TM, Murchie EH. 2021. The effect of canopy architecture on the patterning of "windflecks" within a wheat canopy. *Plant, Cell and Environment* **44**(11): 3524-3537.

Burke PG. 1965. Resonances in electron scattering and photon absorption. *Advances in Physics* **14**(56): 521-567.

Burrows PA, Sazanov LA, Svab Z, Maliga P, Nixon PJ. 1998. Identification of a functional respiratory complex in chloroplasts through analysis of tobacco mutants containing disrupted plastid ndh genes. *The EMBO Journal* **17**(4): 868-876.

Caffarri S, Croce R, Breton J, Bassi R. 2001. The major antenna complex of photosystem II has a xanthophyll binding site not involved in light harvesting. *Journal of Biological Chemistry* **276**(38): 35924-35933.

Calabrese EJ, Baldwin LA. 2003. Hormesis: The dose-response revolution. *Annual Review of Pharmacology and Toxicology* **43**(1): 175-197.

Caliandro R, Nagel KA, Kastenholz B, Bassi R, Li Z, Niyogi KK, Pogson BJ, Schurr U, Matsubara S. 2013. Effects of altered α- and β-branch carotenoid biosynthesis on

photoprotection and whole-plant acclimation of Arabidopsis to photo-oxidative stress. *Plant, Cell and Environment* **36**(2): 438-453.

Chazdon RL 1988. Sunflecks and their importance to forest understorey plants. *Advances in Ecological Research*: Academic Press, 1-63.

Chazdon RL, Pearcy RW. 1991. The importance of sunflecks for forest understory plants - photosynthetic machinery appears adapted to brief, unpredictable periods of radiation. *BioScience* **41**(11): 760-766.

Cheng YC, Fleming GR. 2009. Dynamics of light harvesting in photosynthesis. *Annual Review of Physical Chemistry* **60**: 241-262.

Chiang C, Olsen JE, Basler D, Bånkestad D, Hoch G. 2019. Latitude and weather influences on sun light quality and the relationship to tree growth. *Forests* 10(8): 610

Chow WS, Melis A, Anderson JM. 1990. Adjustments of photosystem stoichiometry in chloroplasts improve the quantum efficiency of photosynthesis. *Proceedings of the National Academy of Sciences of the United States of America* **87**(19): 7502-7506.

Colombo M, Suorsa M, Rossi F, Ferrari R, Tadini L, Barbato R, Pesaresi P. 2016. Photosynthesis control: An underrated short-term regulatory mechanism essential for plant viability. *Plant signaling and behavior* **11**(4): e1165382.

Correa-Galvis V, Poschmann G, Melzer M, Stühler K, Jahns P. 2016. PsbS interactions involved in the activation of energy dissipation in Arabidopsis. *Nature Plants* **2**(2): 15225.

Croce R. 2015. PsbS is the plants' pick for sun protection. *Nature Structural & Molecular Biology* **22**(9): 650-652.

Croce R, Weiss S, Bassi R. 1999. Carotenoid-binding sites of the major light-harvesting complex II of higher plants. *Journal of Biological Chemistry* **274**(42): 29613-29623.

Crofts AR, Wraight CA. 1983. The electrochemical domain of photosynthesis. *Biochimica et Biophysica Acta (BBA) - Reviews on Bioenergetics* **726**(3): 149-185.

Crouchman S, Ruban A, Horton P. 2006. PsbS enhances nonphotochemical fluorescence quenching in the absence of zeaxanthin. *FEBS Letters* **580**(8): 2053-2058.

Cruz JA, Savage LJ, Zegarac R, Hall CC, Satoh-Cruz M, Davis GA, Kovac WK, Chen J, Kramer DM. 2016. Dynamic environmental photosynthetic imaging reveals emergent phenotypes. *Cell Systems* **2**(6): 365-377.

DalCorso G, Pesaresi P, Masiero S, Aseeva E, Nemann DS, Finazzi G, Joliot P, Barbato R, Leister D. 2008. A complex containing PGRL1 and PGR5 is involved in the switch between linear and cyclic electron flow in Arabidopsis. *Cell* **132**(2): 273-285.

Dall'Osto L, Holt NE, Kaligotla S, Fuciman M, Cazzaniga S, Carbonera D, Frank HA, Alric J, Bassi R. 2012. Zeaxanthin protects plant photosynthesis by modulating chlorophyll triplet yield in specific light-harvesting antenna subunits. *Journal of Biological Chemistry* **287**(50): 41820-41834.

Dau H, Hansen U-P. 1989. Studies on the adaptation of intact leaves to changing light intensities by a kinetic analysis of chlorophyll fluorescence and oxygen evolution as measured by the photoacoustic signal. *Photosynthesis Research* **20**(1): 59-83.

Davis GA, Kanazawa A, Schöttler MA, Kohzuma K, Froehlich JE, Rutherford AW, Satoh-Cruz M, Minhas D, Tietz S, Dhingra A, et al. 2016. Limitations to photosynthesis by proton motive force-induced photosystem II photodamage. *eLife* **5**: e16921.

Davis GA, Rutherford AW, Kramer DM. 2017. Hacking the thylakoid proton motive force for improved photosynthesis: modulating ion flux rates that control proton motive force partitioning into $\Delta\psi$ and ΔpH. *Philosophical Transactions of the Royal Society B: Biological Sciences* **372**(1730): 20160381.

de Castro F. 2000. Light spectral composition in a tropical forest: measurements and model. *Tree Physiology* **20**(1): 49-56.

de Langre E. 2008. Effects of wind on plants. *Annual Review of Fluid Mechanics* **40**(1): 141-168.

De Souza AP, Burgess SJ, Doran L, Hansen J, Manukyan L, Maryn N, Gotarkar D, Leonelli L, Niyogi KK, Long SP. 2022. Soybean photosynthesis and crop yield are improved by accelerating recovery from photoprotection. *Science* **377**(6608): 851-854.

Degen GE, Jackson PJ, Proctor MS, Zoulias N, Casson SA, Johnson MP. 2023. High cyclic electron transfer via the PGR5 pathway in the absence of photosynthetic control. *Plant Physiology* **192**(1): 370-386.

Delieu TJ, Walker DA. 1983. Simultaneous measurement of oxygen evolution and chlorophyll fluorescence from leaf pieces. *Plant Physiology* **73**(3): 534-541.

Demmig-Adams B. 1990. Carotenoids and photoprotection in plants: A role for the xanthophyll zeaxanthin. *Biochimica et Biophysica Acta (BBA) - Bioenergetics* **1020**(1): 1-24.

Demmig-Adams B, Adams WW, Garab G, Govindjee. 2014a. *Non-photochemical quenching and energy dissipation in plants, algae and cyanobacteria preface*: Springer Netherlands.

Demmig-Adams B, Koh S-C, Cohu CM, Muller O, Stewart JJ, Adams WW 2014b. Non-photochemical fluorescence quenching in contrasting plant species and environments. *Non-Photochemical Quenching and Energy Dissipation in Plants, Algae and Cyanobacteria*. Dordrecht: Springer Netherlands, 531-552.

Demmig B, Winter K, Kruger A, Czygan FC. 1987. Photoinhibition and zeaxanthin formation in intact leaves - a possible role of the xanthophyll cycle in the dissipation of excess light Energy. *Plant Physiology* **84**(2): 218-224.

Dengel S, Grace J, MacArthur A. 2015. Transmissivity of solar radiation within a Picea sitchensis stand under various sky conditions. *Biogeosciences* **12**(14): 4195-4207.

Dentino M, McCool J, Widrow B. 1978. Adaptive filtering in the frequency domain. *Proceedings of the IEEE* **66**(12): 1658-1659.

Dietzel L, Bräutigam K, Pfannschmidt T. 2008. Photosynthetic acclimation: State transitions and adjustment of photosystem stoichiometry – functional relationships between short-term and long-term light quality acclimation in plants. *The FEBS Journal* **275**(6): 1080-1088.

Ding F, Wang M, Zhang S, Ai X. 2016. Changes in SBPase activity influence photosynthetic capacity, growth, and tolerance to chilling stress in transgenic tomato plants. *Scientific Reports* **6**(1): 32741.

Driever SM, Simkin AJ, Alotaibi S, Fisk SJ, Madgwick PJ, Sparks CA, Jones HD, Lawson T, Parry MAJ, Raines CA. 2017. Increased SBPase activity improves photosynthesis and grain yield in wheat grown in greenhouse conditions. *Philosophical Transactions of the Royal Society B: Biological Sciences* **372**(1730): 20160384.

Dusenge ME, Duarte AG, Way DA. 2019. Plant carbon metabolism and climate change: elevated CO2 and temperature impacts on photosynthesis, photorespiration and respiration. *New Phytologist* **221**(1): 32-49.

Dyson BC, Allwood JW, Feil R, Xu YUN, Miller M, Bowsher CG, Goodacre R, Lunn JE, Johnson GN. 2015. Acclimation of metabolism to light in Arabidopsis thaliana: the glucose 6-phosphate/phosphate translocator GPT2 directs metabolic acclimation. *Plant, Cell and Environment* **38**(7): 1404-1417.

Eberhard S, Finazzi G, Wollman F-A. 2008. The dynamics of photosynthesis. *Annual Review of Genetics* **42**(1): 463-515.

Edwards G, Walker D. 1983. *C three C four: mechanisms, cellular and environmental regulation of photosynthesis*: Univ of California Press.

Evans JR, Jakobsen I, Ögren E. 1993. Photosynthetic light-response curves. *Planta* **189**(2): 191-200.

Fan M, Li M, Liu Z, Cao P, Pan X, Zhang H, Zhao X, Zhang J, Chang W. 2015. Crystal structures of the PsbS protein essential for photoprotection in plants. *Nature Structural & Molecular Biology* **22**(9): 729-735.

Farquhar GD, Sharkey TD. 1982. Stomatal conductance and photosynthesis. *Annual Review of Plant Physiology* **33**(1): 317-345.

Feng L, Han Y, Liu G, An B, Yang J, Yang G, Li Y, Zhu Y. 2007a. Overexpression of sedoheptulose-1,7-bisphosphatase enhances photosynthesis and growth under salt stress in transgenic rice plants. *Functional Plant Biology* **34**(9): 822-834.

Feng L, Li H, Jiao J, Li D, Zhou L, Wan J, Li Y. 2009. Reduction in SBPase activity by antisense RNA in transgenic rice plants: Effect on photosynthesis, growth, and biomass allocation at different nitrogen levels. *Journal of Plant Biology* **52**(5): 382-394.

Feng L, Wang K, Li Y, Tan Y, Kong J, Li H, Li Y, Zhu Y. 2007b. Overexpression of SBPase enhances photosynthesis against high temperature stress in transgenic rice plants. *Plant Cell Reports* **26**(9): 1635-1646.

Ferimazova N, Küpper H, Nedbal L, Trtílek M. 2002. New insights into photosynthetic oscillations revealed by two-dimensional microscopic measurements of chlorophyll fluorescence kinetics in intact leaves and isolated protoplasts. *Photochem Photobiol* **76**(5): 501-508.

Fiorucci AS, Fankhauser C. 2017. Plant strategies for enhancing access to sunlight. *Current Biology* **27**(17): r931-r940.

Flood PJ, Harbinson J, Aarts MGM. 2011. Natural genetic variation in plant photosynthesis. *Trends in Plant Science* **16**(6): 327-335.

Foyer CH. 2018. Reactive oxygen species, oxidative signaling and the regulation of photosynthesis. *Environmental and Experimental Botany* **154**: 134-142.

Fristedt R, Carlberg I, Zygadlo A, Piippo M, Nurmi M, Aro EM, Scheller HV, Vener AV. 2009a. Intrinsically unstructured phosphoprotein TSP9 regulates light harvesting in Arabidopsis thaliana. *Biochemistry* **48**(2): 499-509.

Fristedt R, Willig A, Granath P, Crèvecoeur M, Rochaix JD, Vener AV. 2009b. Phosphorylation of photosystem II controls functional macroscopic folding of photosynthetic membranes in Arabidopsis. *Plant Cell* **21**(12): 3950-3964.

Frommolt R, Goss R, Wilhelm C. 2001. The de-epoxidase and epoxidase reactions of Mantoniella squamata (Prasinophyceae) exhibit different substrate-specific reaction kinetics compared to spinach. *Planta* **213**(3): 446-456.

Fufezan C, Simionato D, Morosinotto T. 2012. Identification of key residues for pH dependent activation of violaxanthin de-epoxidase from Arabidopsis thaliana. *PLOS ONE* **7**(4): e35669.

Ganusov VV. 2016. Strong inference in mathematical modeling: A method for robust science in the twenty-first century. *Frontiers in Microbiology* **7**: 1131.

Garcia-Molina A, Leister D. 2020. Accelerated relaxation of photoprotection impairs biomass accumulation in Arabidopsis. *Nature Plants* **6**(1): 9-12.

Gilbert ME, Zwieniecki MA, Holbrook NM. 2011. Independent variation in photosynthetic capacity and stomatal conductance leads to differences in intrinsic water use efficiency in 11 soybean genotypes before and during mild drought. *Journal of Experimental Botany* **62**(8): 2875-2887.

Gilmore AM. 1997. Mechanistic aspects of xanthophyll cycle-dependent photoprotection in higher plant chloroplasts and leaves. *Physiologia Plantarum* **99**(1): 197-209.

Gilmore AM, Björkman O. 1994. Adenine nucleotides and the xanthophyll cycle in leaves. *Planta* **192**(4): 526-536.

Gjindali A, Herrmann HA, Schwartz J-M, Johnson GN, Calzadilla PI. 2021. A holistic approach to study photosynthetic acclimation responses of plants to fluctuating light. *Frontiers in Plant Science* **12**: 668512.

Graham PJ, Nguyen B, Burdyny T, Sinton D. 2017. A penalty on photosynthetic growth in fluctuating light. *Scientific Reports* **7**(1): 12513.

Haldrup A, Jensen PE, Lunde C, Scheller HV. 2001. Balance of power: A view of the mechanism of photosynthetic state transitions. *Trends in Plant Science* **6**(7): 301-305.

Han J, Chang CYY, Gu L, Zhang Y, Meeker EW, Magney TS, Walker AP, Wen J, Kira O, McNaull S, et al. 2022. The physiological basis for estimating photosynthesis from Chla fluorescence. *New Phytologist* **234**(4): 1206-1219.

Harrison EP, Olcer H, Lloyd JC, Long SP, Raines CA. 2001. Small decreases in SBPase cause a linear decline in the apparent RuBP regeneration rate, but do not affect Rubisco carboxylation capacity. *Journal of Experimental Botany* **52**(362): 1779-1784.

Harrison EP, Willingham NM, Lloyd JC, Raines CA. 1997. Reduced sedoheptulose-1,7-bisphosphatase levels in transgenic tobacco lead to decreased photosynthetic capacity and altered carbohydrate accumulation. *Planta* **204**(1): 27-36.

Hasan SS, Cramer WA. 2012. On rate limitations of electron transfer in the photosynthetic cytochrome b6f complex. *Physical Chemistry Chemical Physics* **14**(40): 13853-13860.

Hashimoto M, Endo T, Peltier G, Tasaka M, Shikanai T. 2003. A nucleus-encoded factor, CRR2, is essential for the expression of chloroplast ndhB in Arabidopsis. *Plant Journal* **36**(4): 541-549.

Hepworth C, Wood WHJ, Emrich-Mills TZ, Proctor MS, Casson S, Johnson MP. 2021. Dynamic thylakoid stacking and state transitions work synergistically to avoid acceptor-side limitation of photosystem I. *Nature Plants* **7**(1): 87-98.

Herbstová M, Tietz S, Kinzel C, Turkina MV, Kirchhoff H. 2012. Architectural switch in plant photosynthetic membranes induced by light stress. *Proceedings of the National Academy of Sciences of the United States of America* **109**(49): 20130-20135.

Herman JR, Goldberg RA. 1978. *Sun, weather, and climate*: Scientific and Technical Information Office, National Aeronautics and Space Administration.

Hertle AP, Blunder T, Wunder T, Pesaresi P, Pribil M, Armbruster U, Leister D. 2013. PGRL1 is the elusive ferredoxin-plastoquinone reductase in photosynthetic cyclic electron flow. *Molecular cell* **49**(3): 511-523.

Hikosaka K. 2010. Mechanisms underlying interspecific variation in photosynthetic capacity across wild plant species. *Plant Biotechnology* **27**(3): 223-229.

Hogewoning SW, Trouwborst G, Maljaars H, Poorter H, van Ieperen W, Harbinson J. 2010. Blue light dose–responses of leaf photosynthesis, morphology, and chemical composition of Cucumis sativus grown under different combinations of red and blue light. *Journal of Experimental Botany* **61**(11): 3107-3117.

Hoh D, Froehlich JE, Kramer DM. 2023. Redox regulation in chloroplast thylakoid lumen: The pmf changes everything, again. *Plant, Cell and Environment* **n/a**(n/a).

Höhner R, Pribil M, Herbstová M, Lopez LS, Kunz HH, Li M, Wood M, Svoboda V, Puthiyaveetil S, Leister D, et al. 2020. Plastocyanin is the long-range electron carrier between photosystem II and photosystem I in plants. *Proceedings of the National Academy of Sciences of the United States of America* **117**(26): 15354-15362.

Holt NE, Fleming GR, Niyogi KK. 2004. Toward an understanding of the mechanism of nonphotochemical quenching in green plants. *Biochemistry* **43**(26): 8281-8289.

Holt NE, Zigmantas D, Valkunas L, Li X-P, Niyogi KK, Fleming GR. 2005. Carotenoid cation formation and the regulation of photosynthetic light harvesting. *Science* **307**(5708): 433-436.

Holzwarth AR, Miloslavina Y, Nilkens M, Jahns P. 2009. Identification of two quenching sites active in the regulation of photosynthetic light-harvesting studied by time-resolved fluorescence. *Chemical Physics Letters* **483**(4-6): 262-267.

Hope AB, Valente P, Matthews DB. 1994. Effects of pH on the kinetics of redox reactions in and around the cytochromebf complex in an isolated system. *Photosynthesis Research* **42**(2): 111-120.

Horton P. 2012. Optimization of light harvesting and photoprotection: molecular mechanisms and physiological consequences. *Philosophical Transactions of the Royal Society B: Biological Sciences* **367**(1608): 3455-3465.

Horton P, Ruban A. 2005. Molecular design of the photosystem II light-harvesting antenna: photosynthesis and photoprotection. *Journal of Experimental Botany* **56**(411): 365-373.

Horton P, Ruban AV, Rees D, Pascal AA, Noctor G, Young AJ. 1991. Control of the light-harvesting function of chloroplast membranes by aggregation of the LHCII chlorophyll-protein complex. *FEBS Letters* **292**(1-2): 1-4.

Horton P, Ruban AV, Walters RG. 1996. Regulation of light harvesting in green plants. *Annual Review of Plant Physiology and Plant Molecular Biology* **47**(1): 655-684.

Horton P, Ruban AV, Wentworth M. 2000. Allosteric regulation of the light-harvesting system of photosystem II. *Philosophical Transactions of the Royal Society of London. Series B: Biological Sciences* **355**(1402): 1361-1370.

Huang W, Zhang S-B, Cao K-F. 2011. Cyclic electron flow plays an important role in photoprotection of tropical trees illuminated at temporal chilling temperature. *Plant and Cell Physiology* **52**(2): 297-305.

Huber SC, Huber JL. 1992. Role of sucrose-phosphate synthase in sucrose metabolism in Leaves 1. *Plant Physiology* **99**(4): 1275-1278.

Idso KE, Idso SB. 1994. Plant responses to atmospheric CO2 enrichment in the face of environmental constraints: a review of the past 10 years' research. *Agricultural and Forest Meteorology* **69**(3): 153-203.

Ihnken S, Kromkamp JC, Beardall J. 2011. Photoacclimation in Dunaliella tertiolecta reveals a unique NPQ pattern upon exposure to irradiance. *Photosynthesis Research* **110**(2): 123-137.

Ikeuchi M, Uebayashi N, Sato F, Endo T. 2014. Physiological functions of PsbS-dependent and PsbS-independent NPQ under naturally fluctuating light conditions. *Plant and Cell Physiology* **55**(7): 1286-1295.

Iwai M, Roth MS, Niyogi KK. 2018. Subdiffraction-resolution live-cell imaging for visualizing thylakoid membranes. *Plant Journal* **96**(1): 233-243.

Jahns P. 1995. The xanthophyll cycle in intermittent light-grown pea plants (possible functions of Chlorophyll a/b-binding proteins). *Plant Physiology* **108**(1): 149-156.

Jahns P, Holzwarth AR. 2012. The role of the xanthophyll cycle and of lutein in photoprotection of photosystem II. *Biochimica et Biophysica Acta (BBA) - Bioenergetics* **1817**(1): 182-193.

Jahns P, Latowski D, Strzalka K. 2009. Mechanism and regulation of the violaxanthin cycle: The role of antenna proteins and membrane lipids. *Biochimica et Biophysica Acta (BBA) - Bioenergetics* **1787**(1): 3-14.

Järvi S, Suorsa M, Aro E-M. 2015. Photosystem II repair in plant chloroplasts — regulation, assisting proteins and shared components with photosystem II biogenesis. *Biochimica et Biophysica Acta (BBA) - Bioenergetics* **1847**(9): 900-909.

Johnson GN. 2011. Physiology of PSI cyclic electron transport in higher plants. *Biochimica et Biophysica Acta (BBA) - Bioenergetics* **1807**(3): 384-389.

Johnson GN, Cardol P, Minagawa J, Finazzi G. 2014. Regulation of electron transport in photosynthesis. *Plastid Biology* **5**: 437-464.

Johnson JE, Berry JA. 2021. The role of Cytochrome b6f in the control of steady-state photosynthesis: A conceptual and quantitative model. *Photosynthesis Research* **148**(3): 101-136.

Johnson MP, Davison PA, Ruban AV, Horton P. 2008. The xanthophyll cycle pool size controls the kinetics of non-photochemical quenching in Arabidopsis thaliana. *FEBS Letters* **582**(2): 262-266.

Johnson MP, Goral TK, Duffy CDP, Brain APR, Mullineaux CW, Ruban AV. 2011. Photoprotective energy dissipation involves the reorganization of photosystem II light-harvesting complexes in the grana membranes of spinach chloroplasts. *The Plant Cell* **23**(4): 1468-1479.

Johnson MP, Pérez-Bueno MaL, Zia A, Horton P, Ruban AV. 2009. The zeaxanthin-independent and zeaxanthin-dependent qE components of nonphotochemical quenching Involve common conformational changes within the photosystem II antenna in Arabidopsis *Plant Physiology* **149**(2): 1061-1075.

Johnson MP, Ruban AV. 2009. Photoprotective energy dissipation in higher plants involves alteration of the excited state energy of the emitting chlorophyll(s) in the light harvesting antenna II (LHCII). *Journal of Biological Chemistry* **284**(35): 23592-23601.

Johnson MP, Wientjes E. 2020. The relevance of dynamic thylakoid organisation to photosynthetic regulation. *Biochimica et Biophysica Acta (BBA) - Bioenergetics* **1861**(4): 148039.

Joliot P, Béal D, Joliot A. 2004. Cyclic electron flow under saturating excitation of dark-adapted Arabidopsis leaves. *Biochimica et Biophysica Acta (BBA) - Bioenergetics* **1656**(2): 166-176.

Joliot P, Johnson GN. 2011. Regulation of cyclic and linear electron flow in higher plants. *Proceedings of the National Academy of Sciences of the United States of America* **108**(32): 13317-13322.

Joliot P, Lavergne J, Béal D. 1992. Plastoquinone compartmentation in chloroplasts. I. Evidence for domains with different rates of photo-reduction. *Biochimica et Biophysica Acta (BBA) - Bioenergetics* **1101**(1): 1-12.

Kagawa T, Sakai T, Suetsugu N, Oikawa K, Ishiguro S, Kato T, Tabata S, Okada K, Wada M. 2001. Arabidopsis NPL1: a phototropin homolog controlling the chloroplast high-light avoidance response. *Science* **291**(5511): 2138-2141.

Kaiser E, Correa Galvis V, Armbruster U. 2019. Efficient photosynthesis in dynamic light environments: A chloroplast's perspective. *Biochemical Journal* **476**(19): 2725-2741.

Kaiser E, Morales A, Harbinson J. 2018. Fluctuating light takes crop photosynthesis on a rollercoaster ride. *Plant Physiology* **176**(2): 977-989.

Kaiser E, Morales A, Harbinson J, Heuvelink E, Prinzenberg AE, Marcelis LF. 2016. Metabolic and diffusional limitations of photosynthesis in fluctuating irradiance in Arabidopsis thaliana. *Scientific Reports* **6**: 31252.

Kaiser E, Morales A, Harbinson J, Kromdijk J, Heuvelink E, Marcelis LFM. 2015. Dynamic photosynthesis in different environmental conditions. *Journal of Experimental Botany* **66**(9): 2415-2426.

Kalaji HM, Goltsev V, Bosa K, Allakhverdiev SI, Strasser RJ, Govindjee. 2012. Experimental in vivo measurements of light emission in plants: A perspective dedicated to David Walker. *Photosynthesis Research* **114**(2): 69-96.

Kargul J, Barber J. 2008. Photosynthetic acclimation: Structural reorganisation of light harvesting antenna – role of redox-dependent phosphorylation of major and minor chlorophyll a/b binding proteins. *The FEBS Journal* **275**(6): 1056-1068.

Kawashima R, Sato R, Harada K, Masuda S. 2017. Relative contributions of PGR5- and NDH-dependent photosystem I cyclic electron flow in the generation of a proton gradient in Arabidopsis chloroplasts. *Planta* **246**(5): 1045-1050.

Keesman KJ. 2011. *System identification: an introduction*: Springer London.

Kenji T, Cruz JA, Kanazawa A, Kramer DM. 2007. The thylakoid proton motive force in vivo. Quantitative, non-invasive probes, energetics, and regulatory consequences of light-induced pmf. *Biochimica et Biophysica Acta (BBA) - Bioenergetics* **1767**(10): 1233-1244.

Kereïche S, Kiss AZ, Kouřil R, Boekema EJ, Horton P. 2010. The PsbS protein controls the macro-organisation of photosystem II complexes in the grana membranes of higher plant chloroplasts. *FEBS Letters* **584**(4): 759-764.

Khaipho-Burch M, Cooper M, Crossa J, de Leon N, Holland J, Lewis R, McCouch S, Murray SC, Rabbi I, Ronald P, et al. 2023. Genetic modification can improve crop yields - but stop overselling it. *Nature* **621**(7979): 470-473.

Khatoon M, Inagawa K, Pospíšil P, Yamashita A, Yoshioka M, Lundin B, Horie J, Morita N, Jajoo A, Yamamoto Y, et al. 2009. Quality control of photosystem II: Thylakoid unstacking is necessary to avoid further damage to the D1 protein and to facilitate D1 degradation under light stress in spinach thylakoids. *Journal of Biological Chemistry* **284**(37): 25343-25352.

Kihara M, Ushijima T, Yamagata Y, Tsuruda Y, Higa T, Abiko T, Kubo T, Wada M, Suetsugu N, Gotoh E. 2020. Light-induced chloroplast movements in Oryza species. *Journal of Plant Research* **133**(4): 525-535.

Kirchhoff H, Hall C, Wood M, Herbstová M, Tsabari O, Nevo R, Charuvi D, Shimoni E, Reich Z. 2011. Dynamic control of protein diffusion within the granal thylakoid lumen. *Proceedings of the National Academy of Sciences of the United States of America* **108**(50): 20248-20253.

Kirchhoff H, Horstmann S, Weis E. 2000. Control of the photosynthetic electron transport by PQ diffusion microdomains in thylakoids of higher plants. *Biochimica et Biophysica Acta (BBA) - Bioenergetics* **1459**(1): 148-168.

Kirschbaum MUF, Küppers M, Schneider H, Giersch C, Noe S. 1998. Modelling photosynthesis in fluctuating light with inclusion of stomatal conductance, biochemical activation and pools of key photosynthetic intermediates. *Planta* **204**(1): 16-26.

Kirschbaum MUF, Pearcy RW. 1988. Gas exchange analysis of the fast phase of photosynthetic Induction in Alocasia macrorrhiza 1. *Plant Physiology* **87**(4): 818-821.

Kiss AZ, Ruban AV, Horton P. 2008. The PsbS protein controls the organization of the photosystem II antenna in higher plant thylakoid membranes. *Journal of Biological Chemistry* **283**(7): 3972-3978.

Kitano H. 2001. *Foundations of systems biology*: The MIT Press Cambridge, Massachusetts London, England.

Klughammer C, Schreiber U. 2016. Deconvolution of ferredoxin, plastocyanin, and P700 transmittance changes in intact leaves with a new type of kinetic LED array spectrophotometer. *Photosynthesis Research* **128**(2): 195-214.

Knapp AK, Smith WK. 1987. Stomatal and photosynthetic responses during sun/shade transitions in subalpine plants: influence on water use efficiency. *Oecologia* **74**(1): 62-67.

Kok B. 1956. On the inhibition of photosynthesis by intense light. *Biochimica et Biophysica Acta (BBA) - Bioenergetics* **21**(2): 234-244.

Kono M, Noguchi K, Terashima I. 2014. Roles of the cyclic electron flow around PSI (CEF-PSI) and O2-dependent alternative pathways in regulation of the photosynthetic electron flow in short-term fluctuating light in Arabidopsis thaliana. *Plant and Cell Physiology* **55**(5): 990-1004.

Kono M, Terashima I. 2014. Long-term and short-term responses of the photosynthetic electron transport to fluctuating light. *Journal of Photochemistry and Photobiology B: Biology* **137**: 89-99.

Kono M, Terashima I. 2016. Elucidation of photoprotective mechanisms of PSI against fluctuating light photoinhibition. *Plant and Cell Physiology* **57**(7): 1405-1414.

Kotilainen T, Aphalo PJ, Brelsford CC, Böök H, Devraj S, Heikkilä A, Hernández R, Kylling A, Lindfors AV, Robson TM. 2020. Patterns in the spectral composition of sunlight and biologically meaningful spectral photon ratios as affected by atmospheric factors. *Agricultural and Forest Meteorology* **291**: 108041.

Kouřil R, Strouhal O, Nosek L, Lenobel R, Chamrád I, Boekema EJ, Šebela M, Ilík P. 2014. Structural characterization of a plant photosystem I and NAD(P)H dehydrogenase supercomplex. *The Plant Journal* **77**(4): 568-576.

Krah NM, Logan BA. 2010. Loss of psbS expression reduces vegetative growth, reproductive output, and light-limited, but not light-saturated, photosynthesis in Arabidopsis thaliana (Brassicaceae) grown in temperate light environments. *American Journal of Botany* **97**(4): 644-649.

Kramer DM, Avenson TJ, Edwards GE. 2004. Dynamic flexibility in the light reactions of photosynthesis governed by both electron and proton transfer reactions. *Trends in Plant Science* **9**(7): 349-357.

Kramer DM, Evans JR. 2011. The importance of energy balance in improving photosynthetic productivity. *Plant Physiology* **155**(1): 70-78.

Kress E, Jahns P. 2017. The dynamics of energy dissipation and xanthophyll conversion in arabidopsis indicate an indirect photoprotective role of zeaxanthin in slowly inducible and relaxing components of non-photochemical quenching of excitation energy. *Frontiers in Plant Science* **8**: 2094.

Kromdijk J, Głowacka K, Leonelli L, Gabilly ST, Iwai M, Niyogi KK, Long SP. 2016. Improving photosynthesis and crop productivity by accelerating recovery from photoprotection. *Science* **354**(6314): 857-861.

Külheim C, Ågren J, Jansson S. 2002. Rapid regulation of light harvesting and plant fitness in the field. *Science* **297**(5578): 91-93.

Külheim C, Jansson S. 2005. What leads to reduced fitness in non-photochemical quenching mutants? *Physiologia Plantarum* **125**(2): 202-211.

Kundert KS, Sangiovanni-Vincentelli A. 1986. Simulation of nonlinear circuits in the frequency domain. *IEEE Transactions on Computer-Aided Design of Integrated Circuits and Systems* **5**(4): 521-535.

Küpers JJ, van Gelderen K, Pierik R. 2018. Location matters: Canopy light responses over spatial scales. *Trends in Plant Science* **23**(10): 865-873.

Laisk A, Eichelmann H, Oja V, Talts E, Scheibe R. 2007. Rates and roles of cyclic and alternative electron flow in potato leaves. *Plant and Cell Physiology* **48**(11): 1575-1588.

Laisk A, Oja V. 2020. Variable fluorescence of closed photochemical reaction centers. *Photosynthesis Research* **143**(3): 335-346.

Lakowicz JR 1994. Emerging biomedical applications of time-resolved fluorescence spectroscopy. *Topics in Fluorescence Spectroscopy: Probe Design and Chemical Sensing*. Boston, MA: Springer US, 1-19.

Lakowicz JR. 2013. *Principles of fluorescence spectroscopy*: Springer science & business media.

Laughlin TG, Savage DF, Davies KM. 2020. Recent advances on the structure and function of NDH-1: The complex I of oxygenic photosynthesis. *Biochimica et Biophysica Acta (BBA) - Bioenergetics* **1861**(11): 148254-148254.

Lawson T, Blatt MR. 2014. Stomatal size, speed, and responsiveness impact on photosynthesis and water use efficiency. *Plant Physiology* **164**(4): 1556-1570.

Lawson T, Bryant B, Lefebvre S, Lloyd JC, Raines CA. 2006. Decreased SBPase activity alters growth and development in transgenic tobacco plants. *Plant, Cell and Environment* **29**(1): 48-58.

Lawson T, Kramer DM, Raines CA. 2012. Improving yield by exploiting mechanisms underlying natural variation of photosynthesis. *Current Opinion in Biotechnology* **23**(2): 215-220.

Lawson T, von Caemmerer S, Baroli I 2010. Photosynthesis and stomatal behaviour. *Progress in Botany 72*: Springer Berlin Heidelberg, 265-304.

Lazár D. 2015. Parameters of photosynthetic energy partitioning. *Journal of Plant Physiology* **175**: 131-147.

Lazár D, Kaňa R, Klinkovský T, Nauš J. 2005. Experimental and theoretical study on high temperature induced changes in chlorophyll a fluorescence oscillations in barley leaves upon 2 % CO 2. *PHOTOSYNTHETICA* **43**(1): 13-27.

Lazár D, Niu Y, Nedbal L. 2022. Insights on the regulation of photosynthesis in pea leaves exposed to oscillating light. *Journal of Experimental Botany* **73**(18): 6380-6393.

Leakey ADB, Scholes JD, Press MC. 2005. Physiological and ecological significance of sunflecks for dipterocarp seedlings. *Journal of Experimental Botany* **56**(411): 469-482.

Lee H-Y, Chow WS, Hong Y-N. 1999. Photoinactivation of photosystem II in leaves of Capsicum annuum. *Physiologia Plantarum* **105**(2): 376-383.

Lee K-S, Park SR, Kim YK. 2007. Effects of irradiance, temperature, and nutrients on growth dynamics of seagrasses: A review. *Journal of Experimental Marine Biology and Ecology* **350**(1): 144-175.

Lefebvre S, Lawson T, Fryer M, Zakhleniuk OV, Lloyd JC, Raines CA. 2005. Increased Sedoheptulose-1,7-Bisphosphatase qctivity in transgenic tobacco plants stimulates photosynthesis and growth from an early stage in development. *Plant Physiology* **138**(1): 451-460.

Lennon AM, Prommeenate P, Nixon PJ. 2003. Location, expression and orientation of the putative chlororespiratory enzymes, Ndh and IMMUTANS, in higher-plant plastids. *Planta* **218**(2): 254-260.

Leontaritis IJ, Billings SA. 1985. Input-output parametric models for non-linear systems Part I: deterministic non-linear systems. *International Journal of Control* **41**(2): 303-328.

Li M, Mukhopadhyay R, Svoboda V, Oung HMO, Mullendore DL, Kirchhoff H. 2020. Measuring the dynamic response of the thylakoid architecture in plant leaves by electron microscopy. *Plant Direct* **4**(11): e00280-e00280.

Li TY, Shi Q, Sun H, Yue M, Zhang SB, Huang W. 2021. Diurnal response of photosystem I to fluctuating light is affected by stomatal conductance. *Cells* **10**(11): 3128.

Li X-P, Björkman O, Shih C, Grossman AR, Rosenquist M, Jansson S, Niyogi KK. 2000. A pigment-binding protein essential for regulation of photosynthetic light harvesting. *Nature* **403**(6768): 391-395.

Li X-P, Gilmore AM, Caffarri S, Bassi R, Golan T, Kramer D, Niyogi KK. 2004. Regulation of Photosynthetic Light Harvesting Involves Intrathylakoid Lumen pH Sensing by the PsbS Protein. *Journal of Biological Chemistry* **279**(22): 22866-22874.

Li X-P, Gilmore AM, Niyogi KK. 2002a. Molecular and global time-resolved analysis of a psbS gene dosage effect on pH- and xanthophyll cycle-dependent nonphotochemical quenching in photosystem II. *Journal of Biological Chemistry* **277**(37): 33590-33597.

Li X-P, Müller-Moulé P, Gilmore AM, Niyogi KK. 2002b. PsbS-dependent enhancement of feedback de-excitation protects photosystem II from photoinhibition. *Proceedings of the National Academy of Sciences of the United States of America* **99**(23): 15222-15227.

Lombard RE, Hetherington TE. 1993. Structural basis of hearing and sound transmission. *The skull* **3**: 241-302.

Long SP, Marshall-Colon A, Zhu X-G. 2015. Meeting the global food demand of the future by engineering crop photosynthesis and yield potential. *Cell* **161**(1): 56-66.

Long SP, Taylor SH, Burgess SJ, Carmo-Silva E, Lawson T, De Souza AP, Leonelli L, Wang Y. 2022. Into the shadows and back into sunlight: Photosynthesis in fluctuating light. *Annual Review of Plant Biology* **73**(1): 617-648.

Ma M, Liu Y, Bai C, Yang Y, Sun Z, Liu X, Zhang S, Han X, Yong JWH. 2021a. The physiological functionality of PGR5/PGRL1-dependent cyclic electron transport in sustaining photosynthesis. *Frontiers in Plant Science* **12**: 702196.

Ma M, Liu Y, Bai C, Yong JWH. 2021b. The significance of chloroplast NAD(P)H dehydrogenase complex and its dependent cyclic electron transport in photosynthesis. *Frontiers in Plant Science* **12**: 661863.

Magyar M, Sipka G, Kovács L, Ughy B, Zhu Q, Han G, Špunda V, Lambrev PH, Shen J-R, Garab G. 2018. Rate-limiting steps in the dark-to-light transition of Photosystem II - revealed by chlorophyll-a fluorescence induction. *Scientific Reports* **8**(1): 2755.

Malnoë A. 2018. Photoinhibition or photoprotection of photosynthesis? Update on the (newly termed) sustained quenching component qH. *Environmental and Experimental Botany* **154**: 123-133.

Malnoë A, Schultink A, Shahrasbi S, Rumeau D, Havaux M, Niyogi KK. 2018. The plastid lipocalin LCNP Is required for sustained photoprotective energy dissipation in arabidopsis. *The Plant Cell* **30**(1): 196-208.

Malone LA, Proctor MS, Hitchcock A, Hunter CN, Johnson MP. 2021. Cytochrome b6f – orchestrator of photosynthetic electron transfer. *Biochimica et Biophysica Acta (BBA) - Bioenergetics* **1862**(5): 148380.

Martinsuo P, Pursiheimo S, Aro E-M, Rintamäki E. 2003. Dithiol oxidant and disulfide reductant dynamically regulate the phosphorylation of light-harvesting complex II proteins in thylakoid membranes. *Plant Physiology* **133**(1): 37-46.

Matous K, Benediktyová Z, Berger S, Roitsch T, Nedbal L. 2006. Case study of combinatorial imaging: What protocol and what chlorophyll fluorescence image to use when visualizing infection of Arabidopsis thaliana by Pseudomonas syringae? *Photosynthesis Research* **90**(3): 243-253.

Matsubara S, Chow WS. 2004. Populations of photoinactivated photosystem II reaction centers characterized by chlorophyll a fluorescence lifetime in vivo. *Proceedings of the National Academy of Sciences* **101**(52): 18234-18239.

Matthews JSA, Vialet-Chabrand S, Lawson T. 2018. Acclimation to fluctuating light impacts the rapidity of response and diurnal rhythm of stomatal conductance *Plant Physiology* **176**(3): 1939-1951.

Mattson MP. 2008. Hormesis defined. *Ageing Research Reviews* **7**(1): 1-7.

Mayergoyz ID. 2003. *Mathematical models of hysteresis and their applications*: Academic press.

Mikko T, Mirva P, Marjaana S, Sari S, Paula M, Julia V, Alexander V, Yagut A, Eva-Mari A. 2006. State transitions revisited—a buffering system for dynamic low light acclimation of Arabidopsis. *Plant Molecular Biology* **62**(4): 779-793.

Miller MAE, O'Cualain R, Selley J, Knight D, Karim MF, Hubbard SJ, Johnson GN. 2017. Dynamic acclimation to high light in Arabidopsis thaliana involves widespread reengineering of the leaf proteome. *Frontiers in Plant Science* **8**: 1239.

Mitchell-Olds T. 2001. Arabidopsis thaliana and its wild relatives: a model system for ecology and evolution. *Trends in Ecology & Evolution* **16**(12): 693-700.

Miyake C, Miyata M, Shinzaki Y, Tomizawa K-i. 2005. CO2 response of cyclic electron flow around PSI (CEF-PSI) in tobacco leaves—relative electron fluxes through PSI and PSII determine the magnitude of non-photochemical quenching (NPQ) of chl fluorescence. *Plant and Cell Physiology* **46**(4): 629-637.

Miyake C, Yonekura K, Kobayashi Y, Yokota A. 2002. Cyclic electron flow within PSII functions in intact chloroplasts from spinach leaves. *Plant and Cell Physiology* **43**(8): 951-957.

Morales A, Kaiser E. 2020. Photosynthetic acclimation fluctuating irradiance in plants. *Frontiers in Plant Science* **11**: 268-268.

Mott KA, Woodrow IE. 2000. Modelling the role of Rubisco activase in limiting non-steady-state photosynthesis. *Journal of Experimental Botany* **51**(suppl_1): 399-406.

Müller P, Li X-P, Niyogi KK. 2001. Non-photochemical quenching. A response to excess light energy. *Plant Physiology* **125**(4): 1558-1566.

Munekage Y, Hashimoto M, Miyake C, Tomizawa K-I, Endo T, Tasaka M, Shikanai T. 2004. Cyclic electron flow around photosystem I is essential for photosynthesis. *Nature* **429**(6991): 579-582.

Munekage Y, Hojo M, Meurer J, Endo T, Tasaka M, Shikanai T. 2002. PGR5 is involved in cyclic electron flow around photosystem I and is essential for photoprotection in Arabidopsis. *Cell* **110**(3): 361-371.

Murata N, Takahashi S, Nishiyama Y, Allakhverdiev SI. 2007. Photoinhibition of photosystem II under environmental stress. *Biochimica et Biophysica Acta (BBA) - Bioenergetics* **1767**(6): 414-421.

Murchie EH, Niyogi KK. 2011. Manipulation of photoprotection to improve plant photosynthesis. *Plant Physiology* **155**(1): 86-92.

Murchie EH, Pinto M, Horton P. 2009. Agriculture and the new challenges for photosynthesis research. *New Phytologist* **181**(3): 532-552.

Murchie EH, Ruban AV. 2020. Dynamic non-photochemical quenching in plants: from molecular mechanism to productivity. *Plant Journal* **101**(4): 885-896.

Nakano H, Yamamoto H, Shikanai T. 2019. Contribution of NDH-dependent cyclic electron transport around photosystem I to the generation of proton motive force in the weak mutant allele of pgr5. *Biochimica et Biophysica Acta (BBA) - Bioenergetics* **1860**(5): 369-374.

Nandha B, Finazzi G, Joliot P, Hald S, Johnson GN. 2007. The role of PGR5 in the redox poising of photosynthetic electron transport. *Biochimica et Biophysica Acta (BBA) - Bioenergetics* **1767**(10): 1252-1259.

Naumburg E, Ellsworth DS, Katul GG. 2001. Modeling dynamic understory photosynthesis of contrasting species in ambient and elevated carbon dioxide. *Oecologia* **126**(4): 487-499.

Navrátil M, Špunda V, Marková I, Janouš D. 2007. Spectral composition of photosynthetically active radiation penetrating into a Norway spruce canopy: The opposite dynamics of the blue/red spectral ratio during clear and overcast days. *Trees - Structure and Function* **21**(3): 311-320.

Nawrocki WJ, Bailleul B, Picot D, Cardol P, Rappaport F, Wollman FA, Joliot P. 2019. The mechanism of cyclic electron flow. *Biochimica et Biophysica Acta (BBA) - Bioenergetics* **1860**(5): 433-438.

Nawrocki WJ, Liu X, Raber B, Hu C, de Vitry C, Bennett DIG, Croce R. 2021. Molecular origins of induction and loss of photoinhibition-related energy dissipation q(I). *Science Advances* **7**(52): eabj0055.

Nedbal L, Březina V. 2002. Complex metabolic oscillations in plants forced by harmonic irradiance. *Biophysical Journal* **83**(4): 2180-2189.

Nedbal L, Brezina V, Adamec F, Stys D, Oja V, Laisk A, Govindjee. 2003. Negative feedback regulation is responsible for the non-linear modulation of photosynthetic activity in plants dynamic light and cyanobacteria exposed to a environment. *Biochimica et Biophysica Acta (BBA) - Bioenergetics* **1607**(1): 5-17.

Nedbal L, Březina V, Červený J, Trtílek M. 2005. Photosynthesis in dynamic light: Systems biology of unconventional chlorophyll fluorescence transients in Synechocystis sp. PCC 6803. *Photosynthesis Research* **84**(1): 99-106.

Nedbal L, Koblížek M 2006. Chlorophyll fluorescence as a reporter on in vivo electron transport and regulation in plants. *Chlorophylls and Bacteriochlorophylls: Biochemistry, Biophysics, Functions and Applications*. Dordrecht: Springer Netherlands, 507-519.

Nedbal L, Lazár D. 2021. Photosynthesis dynamics and regulation sensed in the frequency domain. *Plant Physiology* **187**(2): 646-661.

Nicol L, Nawrocki WJ, Croce R. 2019. Disentangling the sites of non-photochemical quenching in vascular plants. *Nature Plants* **5**(11): 1177-1183.

Niedermaier S, Schneider T, Bahl M-O, Matsubara S, Huesgen PF. 2020. Photoprotective acclimation of the arabidopsis thaliana leaf proteome to fluctuating light. *Frontiers in Genetics* **11**: 154.

Nilkens M, Kress E, Lambrev P, Miloslavina Y, Muller M, Holzwarth AR, Jahns P. 2010. Identification of a slowly inducible zeaxanthin-dependent component of non-photochemical quenching of chlorophyll fluorescence generated under steady-state conditions in Arabidopsis. *Biochimica et Biophysica Acta (BBA) - Bioenergetics* **1797**(4): 466-475.

Nishio JN, Whitmarsh J. 1993. Dissipation of the proton electrochemical potential in intact chloroplasts (II. The pH gradient monitored by cytochrome f reduction kinetics). *Plant Physiology* **101**(1): 89-96.

Niu Y, Lazár D, Holzwarth AR, Kramer DM, Matsubara S, Fiorani F, Poorter H, Schrey SD, Nedbal L. 2023. Plants cope with fluctuating light by frequency-dependent nonphotochemical quenching and cyclic electron transport. *New Phytologist* **239**(5): 1869-1886.

Niyogi KK. 2000. Safety valves for photosynthesis. *Current Opinion in Plant Biology* **3**(6): 455-460.

Niyogi KK, Bjorkman O, Grossman AR. 1997. Chlamydomonas xanthophyll cycle mutants identified by video imaging of chlorophyll fluorescence quenching. *The Plant Cell* **9**(8): 1369-1380.

Niyogi KK, Grossman AR, Björkman O. 1998. Arabidopsis mutants define a central role for the xanthophyll cycle in the regulation of photosynthetic energy conversion. *The Plant Cell* **10**(7): 1121-1134.

Noctor G, Rees D, Young A, Horton P. 1991. The relationship between zeaxanthin, energy-dependent quenching of chlorophyll fluorescence, and trans-thylakoid pH gradient in isolated-chloroplasts. *Biochimica et Biophysica Acta (BBA) - Bioenergetics* **1057**(3): 320-330.

Noctor G, Ruban AV, Horton P. 1993. Modulation of ΔpH-dependent nonphotochemical quenching of chlorophyll fluorescence in spinach chloroplasts. *Biochimica et Biophysica Acta (BBA) - Bioenergetics* **1183**(2): 339-344.

Ogata K. 2010. *Modern control engineering*. Boston: Prentice-Hall.

Ögren E, Evans JR. 1993. Photosynthetic light-response curves. *Planta* **189**(2): 182-190.

Oguchi R, Hikosaka K, Hirose T. 2005. Leaf anatomy as a constraint for photosynthetic acclimation: differential responses in leaf anatomy to increasing growth irradiance among three deciduous trees. *Plant, Cell and Environment* **28**(7): 916-927.

Okegawa Y, Kagawa Y, Kobayashi Y, Shikanai T. 2008. Characterization of factors affecting the activity of photosystem I cyclic electron transport in chloroplasts. *Plant and Cell Physiology* **49**(5): 825-834.

Ort DR, Yocum CF. 1996. *Oxygenic photosynthesis: The light reactions*: Springer Science & Business Media.

Pantazopoulou CK, Bongers FJ, Pierik R. 2021. Reducing shade avoidance can improve Arabidopsis canopy performance against competitors. *Plant, Cell and Environment* **44**(4): 1130-1141.

Pascal AA, Liu Z, Broess K, van Oort B, van Amerongen H, Wang C, Horton P, Robert B, Chang W, Ruban A. 2005. Molecular basis of photoprotection and control of photosynthetic light-harvesting. *Nature* **436**(7047): 134-137.

Peale S. 1976. Orbital resonances in the solar system. *Annual review of astronomy and astrophysics* **14**(1): 215-246.

Pearcy RW. 1990. Sunflecks and photosynthesis in plant canopies. *Annual Review of Plant Physiology and Plant Molecular Biology* **41**(1): 421-453.

Pearcy RW, Krall JP, Sassenrath-Cole GF. 1996. Photosynthesis in Fluctuating Light Environments. *Photosynthesis and the Environment*: 321-346.

Pearcy RW, Sims DA. 1994. Photosynthetic acclimation to changing light environments: scaling from the leaf to the whole plant. *Exploitation of Environmental Heterogeneity by Plants: Ecophysiological Processes Above-and Below Ground*: 145-174.

Peltier G, Aro E-M, Shikanai T. 2016. NDH-1 and NDH-2 plastoquinone reductases in oxygenic photosynthesis. *Annual Review of Plant Biology* **67**(1): 55-80.

Peltier G, Tolleter D, Billon E, Cournac L. 2010. Auxiliary electron transport pathways in chloroplasts of microalgae. *Photosynthesis Research* **106**(1): 19-31.

Peressotti A, Marchiol L, Zerbi G. 2001. Photosynthetic photon flux density and sunfleck regime within canopies of wheat, sunflower and maize in different wind conditions. *Italian Journal of Agronomy* **4**: 87-92.

Pérez-Bueno ML, Johnson MP, Zia A, Ruban AV, Horton P. 2008. The Lhcb protein and xanthophyll composition of the light harvesting antenna controls the ΔpH-dependency of non-photochemical quenching in Arabidopsis thaliana. *FEBS Letters* **582**(10): 1477-1482.

Peri PL, Moot DJ, Jarvis P, McNeil DL, Lucas RJ. 2007. Morphological, anatomical, and physiological changes of orchardgrass leaves grown under fluctuating light regimes. *Agronomy Journal* **99**(6): 1502-1513.

Pesaresi P, Hertle A, Pribil M, Kleine T, Wagner R, Strissel H, Ihnatowicz A, Bonardi V, Scharfenberg M, Schneider A, et al. 2009. Arabidopsis STN7 kinase provides a link between short- and long-term photosynthetic acclimation. *Plant Cell* **21**(8): 2402-2423.

Pesaresi P, Hertle A, Pribil M, Schneider A, Kleine T, Leister D. 2010. Optimizing photosynthesis under fluctuating light. *Plant signaling and behavior* **5**(1): 21-25.

Pfitsch WA, Pearcy RW. 1989. Daily carbon gain by Adenocaulon bicolor (Asteraceae), a redwood forest understory herb, in relation to its light environment. *Oecologia* **80**(4): 465-470.

Pfundel EE, Dilley RA. 1993. The pH dependence of violaxanthin deepoxidation in isolated pea chloroplasts. *Plant Physiology* **101**(1): 65-71.

Pietrzykowska M, Suorsa M, Semchonok DA, Tikkanen M, Boekema EJ, Aro EM, Jansson S. 2014. The light-harvesting chlorophyll a/b binding proteins Lhcb1 and Lhcb2 play complementary roles during state transitions in Arabidopsis. *Plant Cell* **26**(9): 3646-3660.

Pineda M, Soukupova J, Matous K, Nedbal L, Baron M. 2008. Conventional and combinatorial chlorophyll fluorescence imaging of tobamovirus-infected plants. *PHOTOSYNTHETICA* **46**(3): 441-451.

Pinheiro J, Duffull S. 2009. Exposure response – getting the dose right. *Pharmaceutical Statistics* **8**(3): 173-175.

Pintelon R, Schoukens J. 2012. *System identification: A frequency domain approach*: John Wiley & Sons.

Poolman MG, Fell DA, Thomas S. 2000. Modelling photosynthesis and its control. *Journal of Experimental Botany* **51**(suppl_1): 319-328.

Poorter H, Niinemets Ü, Ntagkas N, Siebenkäs A, Mäenpää M, Matsubara S, Pons T. 2019. A meta-analysis of plant responses to light intensity for 70 traits ranging from molecules to whole plant performance. *New Phytologist* **223**(3): 1073-1105.

Pospíšil P. 2009. Production of reactive oxygen species by photosystem II. *Biochimica et Biophysica Acta (BBA) - Bioenergetics* **1787**(10): 1151-1160.

Puthiyaveetil S, Tsabari O, Lowry T, Lenhert S, Lewis RR, Reich Z, Kirchhoff H. 2014. Compartmentalization of the protein repair machinery in photosynthetic membranes. *Proceedings of the National Academy of Sciences of the United States of America* **111**(44): 15839-15844.

Ralph PJ, Gademann R. 2005. Rapid light curves: A powerful tool to assess photosynthetic activity. *Aquatic Botany* **82**(3): 222-237.

Rascher U, Nedbal L. 2006. Dynamics of photosynthesis in fluctuating light. *Current Opinion in Plant Biology* **9**(6): 671-678.

Regan MP, Regan D. 1988. A frequency domain technique for characterizing nonlinearities in biological systems. *Journal of Theoretical Biology* **133**(3): 293-317.

Retkute R, Smith-Unna SE, Smith RW, Burgess AJ, Jensen OE, Johnson GN, Preston SP, Murchie EH. 2015. Exploiting heterogeneous environments: does photosynthetic acclimation optimize carbon gain in fluctuating light? *Journal of Experimental Botany* **66**(9): 2437-2447.

Rittweger J, Taiar R 2020. The physics of vibration. *Manual of Vibration Exercise and Vibration Therapy*. Cham: Springer International Publishing, 3-21.

Roach T, Krieger-Liszkay A. 2012. The role of the PsbS protein in the protection of photosystems I and II against high light in Arabidopsis thaliana. *Biochimica et Biophysica Acta (BBA) - Bioenergetics* **1817**(12): 2158-2165.

Roden JS, Pearcy RW. 1993. Effect of leaf flutter on the light environment of poplars. *Oecologia 1993 93:2* **93**(2): 201-207.

Rojas-González JA, Soto-Súarez M, García-Díaz Á, Romero-Puertas MC, Sandalio LM, Mérida Á, Thormählen I, Geigenberger P, Serrato AJ, Sahrawy M. 2015. Disruption of both chloroplastic and cytosolic FBPase genes results in a dwarf phenotype and important starch and metabolite changes in Arabidopsis thaliana. *Journal of Experimental Botany* **66**(9): 2673-2689.

Rosenthal DM, Locke AM, Khozaei M, Raines CA, Long SP, Ort DR. 2011. Over-expressing the C3 photosynthesis cycle enzyme Sedoheptulose-1-7 Bisphosphatase improves photosynthetic carbon gain and yield under fully open air CO2 fumigation (FACE). *BMC Plant Biology* **11**(1): 1-12.

Rothstein DE, Zak DR. 2001. Photosynthetic adaptation and acclimation to exploit seasonal periods of direct irradiance in three temperate, deciduous-forest herbs. *Functional Ecology* **15**(6): 722-731.

Rozak PR, Seiser RM, Wacholtz WF, Wise RR. 2002. Rapid, reversible alterations in spinach thylakoid appression upon changes in light intensity. *Plant, Cell and Environment* **25**(3): 421-429.

Ruan M, Li H, Zhang Y, Zhao R, Zhang J, Wang Y, Gao J, Wang Z, Wang Y, Sun D, et al. 2023. Cryo-EM structures of LHCII in photo-active and photo-protecting states reveal allosteric regulation of light harvesting and excess energy dissipation. *Nature Plants* **9**(9): 1547-1557.

Ruban AV. 2015. Evolution under the sun: optimizing light harvesting in photosynthesis. *Journal of Experimental Botany* **66**(1): 7-23.

Ruban AV. 2016. Nonphotochemical chlorophyll fluorescence quenching: mechanism and effectiveness in protecting plants from photodamage. *Plant Physiology* **170**(4): 1903-1916.

Ruban AV. 2018. Light harvesting control in plants. *FEBS Letters* **592**(18): 3030-3039.

Ruban AV, Berera R, Ilioaia C, van Stokkum IHM, Kennis JTM, Pascal AA, van Amerongen H, Robert B, Horton P, van Grondelle R. 2007. Identification of a mechanism of photoprotective energy dissipation in higher plants. *Nature* **450**(7169): 575-578.

Ruban AV, Johnson MP. 2015. Visualizing the dynamic structure of the plant photosynthetic membrane. *Nature Plants* **1**(11): 1-9.

Ruban AV, Johnson MP, Duffy CDP. 2012. The photoprotective molecular switch in the photosystem II antenna. *Biochimica et Biophysica Acta (BBA) - Bioenergetics* **1817**(1): 167-181.

Ruban AV, Wentworth M, Horton P. 2001. Kinetic analysis of nonphotochemical quenching of chlorophyll fluorescence. 1. Isolated chloroplasts. *Biochemistry* **40**(33): 9896-9901.

Ruban AV, Wilson S. 2021. The mechanism of non-photochemical quenching in plants: localization and driving forces. *Plant and Cell Physiology* **62**(7): 1063-1072.

Rumberg B, Siggel U. 1969. PH changes in the inner phase of the thylakoids during photosynthesis. *Naturwissenschaften* **56**(3): 130-132.

Sacharz J, Giovagnetti V, Ungerer P, Mastroianni G, Ruban AV. 2017. The xanthophyll cycle affects reversible interactions between PsbS and light-harvesting complex II to control non-photochemical quenching. *Nature Plants* **3**(2): 1-9.

Sagun JV, Badger MR, Chow WS, Ghannoum O. 2019. Cyclic electron flow and light partitioning between the two photosystems in leaves of plants with different functional types. *Photosynnthesis Research* **142**(3): 321-334.

Sakai T, Kagawa T, Kasahara M, Swartz TE, Christie JM, Briggs WR, Wada M, Okada K. 2001. Arabidopsis nph1 and npl1: Blue light receptors that mediate both phototropism and chloroplast relocation. *Proceedings of the National Academy of Sciences of the United States of America* **98**(12): 6969-6974.

Sassenrath-Cole GF, Pearcy RW. 1994. Regulation of photosynthetic induction state by the magnitude and duration of low light exposure. *Plant Physiology* **105**(4): 1115-1123.

Sassenrath-Cole GF, Pearcy RW, Steinmaus S. 1994. The role of enzyme activation state in limiting carbon assimilation under variable light conditions. *Photosynthesis Research* **41**(2): 295-302.

Sazanov LA, Burrows PA, Nixon PJ. 1998. The chloroplast Ndh complex mediates the dark reduction of the plastoquinone pool in response to heat stress in tobacco leaves. *FEBS Letters* **429**(1): 115-118.

Schansker G. 2022. Determining photosynthetic control, a probe for the balance between electron transport and Calvin-Benson cycle activity, with the DUAL-KLAS-NIR. *Photosynthesis Research* **153**: 191–204.

Schansker G, Tóth SZ, Kovács L, Holzwarth AR, Garab G. 2011. Evidence for a fluorescence yield change driven by a light-induced conformational change within photosystem II during the fast chlorophyll a fluorescence rise. *Biochimica et Biophysica Acta (BBA) - Bioenergetics* **1807**(9): 1032-1043.

Scheibe R. 1987. NADP+-malate dehydrogenase in C3-plants: Regulation and role of a light-activated enzyme. *Physiologia Plantarum* **71**(3): 393-400.

Scheibe R, Backhausen JE, Emmerlich V, Holtgrefe S. 2005. Strategies to maintain redox homeostasis during photosynthesis under changing conditions. *Journal of Experimental Botany* **56**(416): 1481-1489.

Schneider T, Bolger A, Zeier J, Preiskowski S, Benes V, Trenkamp S, Usadel B, Farré EM, Matsubara S. 2019. Fluctuating light interacts with time of day and leaf development stage to reprogram gene expression. *Plant Physiology* **179**(4): 1632-1657.

Schöttler MA, Tóth SZ. 2014. Photosynthetic complex stoichiometry dynamics in higher plants: Environmental acclimation and photosynthetic flux control. *Frontiers in Plant Science* **5**: 188.

Schöttler MA, Tóth SZ, Boulouis A, Kahlau S. 2015. Photosynthetic complex stoichiometry dynamics in higher plants: Biogenesis, function, and turnover of ATP synthase and the cytochrome b6f complex. *Journal of Experimental Botany* **66**(9): 2373-2400.

Schreiber U 2004. Pulse-amplitude-modulation (PAM) fluorometry and saturation pulse method: an overview. *Chlorophyll a Fluorescence: A Signature of Photosynthesis*. Dordrecht: Springer Netherlands, 279-319.

Schreiber U, Klughammer C. 2016. Analysis of photosystem I donor and acceptor sides with a new type of online-deconvoluting kinetic LED-array spectrophotometer. *Plant and Cell Physiology* **57**(7): 1454-1467.

Schumann T, Paul S, Melzer M, Dörmann P, Jahns P. 2017. Plant growth under natural light conditions provides highly flexible short-term acclimation properties toward high light stress. *Frontiers in Plant Science* **8**: 681.

Schwartz L. 2008. *Mathematics for the physical sciences*: Courier Dover Publications.

Sello S, Moscatiello R, Mehlmer N, Leonardelli M, Carraretto L, Cortese E, Zanella FG, Baldan B, Szabò I, Vothknecht UC, et al. 2018. Chloroplast Ca(2+) fluxes into and across yhylakoids revealed by thylakoid-targeted aequorin probes. *Plant Physiology* **177**(1): 38-51.

Sétif P, Boussac A, Krieger-Liszkay A. 2019. Near-infrared in vitro measurements of photosystem I cofactors and electron-transfer partners with a recently developed spectrophotometer. *Photosynth Research* **142**(3): 307-319.

Setif PQY, Bottin H. 1995. Laser flash absorption spectroscopy study of ferredoxin reduction by photosystem I: Spectral and kinetic evidence for the existence of several photosystem I-ferredoxin complexes. *Biochemistry* **34**(28): 9059-9070.

Shikanai T. 2007. Regulation of photosynthesis via PSI cyclic electron transport. *Photosynthesis Research* **91**(2-3): 246-246.

Shikanai T. 2014. Central role of cyclic electron transport around photosystem I in the regulation of photosynthesis. *Current Opinion in Biotechnology* **26**: 25-30.

Shimakawa G, Miyake C. 2018. Changing frequency of fluctuating light reveals the molecular mechanism for P700 oxidation in plant leaves. *Plant Direct* **2**(7): e00073.

Sipka G, Magyar M, Mezzetti A, Akhtar P, Zhu Q, Xiao Y, Han G, Santabarbara S, Shen J-R, Lambrev PH, et al. 2021. Light-adapted charge-separated state of photosystem II:

Structural and functional dynamics of the closed reaction center. *The Plant Cell* **33**(4): 1286-1302.

Smith H. 1982. Light quality, photoperception, and plant strategy. *Annual Review of Plant Physiology* **33**(1): 481-518.

Smith SW 1997. The scientist and engineer's guide to digital signal processing: California Technical Pub. San Diego.

Smith WK, Berry ZC. 2013. Sunflecks? *Tree Physiology* **33**(3): 233-237.

Solomon S, Portmann RW, Sanders RW, Daniel JS. 1998. Absorption of solar radiation by water vapor, oxygen, and related collision pairs in the Earth's atmosphere. *Journal of Geophysical Research: Atmospheres* **103**(D4): 3847-3858.

Stael S, Rocha AG, Wimberger T, Anrather D, Vothknecht UC, Teige M. 2012. Cross-talk between calcium signalling and protein phosphorylation at the thylakoid. *Journal of Experimental Botany* **63**(4): 1725-1733.

Steen CJ, Morris JM, Short AH, Niyogi KK, Fleming GR. 2020. Complex roles of PsbS and xanthophylls in the regulation of nonphotochemical quenching in Arabidopsis thaliana under fluctuating light. *The Journal of Physical Chemistry B* **124**(46): 10311-10325.

Stewart JJ, Adams WW, Cohu CM, Polutchko SK, Lombardi EM, Demmig-Adams B. 2015. Differences in light-harvesting, acclimation to growth-light environment, and leaf structural development between Swedish and Italian ecotypes of Arabidopsis thaliana. *Planta* **242**(6): 1277-1290.

Stirbet A. 2013. Excitonic connectivity between photosystem II units: What is it, and how to measure it? *Photosynthesis Research* **116**(2-3): 189-214.

Stitt M, Schreiber U. 1988. Interaction between Sucrose Synthesis and CO2 Fixation III. Response of biphasic induction kinetics and oscillations to manipulation of the relation between electron transport, calvin cycle, and sucrose synthesis. *Journal of Plant Physiology* **133**(3): 263-271.

Strand DD, Fisher N, Kramer DM. 2017. The higher plant plastid NAD(P)H dehydrogenase-like complex (NDH) is a high efficiency proton pump that increases ATP production by cyclic electron flow. *The Journal of biological chemistry* **292**(28): 11850-11860.

Streb P, Aubert S, Gout E, Bligny R. 2003. Reversibility of cold- and light-stress tolerance and accompanying changes of metabolite and antioxidant levels in the two high mountain plant species Soldanella alpina and Ranunculus glacialis. *Journal of Experimental Botany* **54**(381): 405-418.

Sugimoto K, Okegawa Y, Tohri A, Long TA, Covert SF, Hisabori T, Shikanai T. 2013. A single amino acid alteration in PGR5 confers resistance to antimycin A in cyclic electron transport around PSI. *Plant and Cell Physiology* **54**(9): 1525-1534.

Sukenik A, Bennett J, Mortain-Bertrand A, Falkowski PG. 1990. Adaptation of the photosynthetic apparatus to irradiance in Dunaliella tertiolecta 1: A kinetic study. *Plant Physiology* **92**(4): 891-898.

Suorsa M, Grieco M, Järvi S, Gollan PJ, Kangasjärvi S, Tikkanen M, Aro E-M. 2013. PGR5 ensures photosynthetic control to safeguard photosystem I under fluctuating light conditions. *Plant signaling and behavior* **8**(1): e22741.

Suorsa M, Järvi S, Grieco M, Nurmi M, Pietrzykowska M, Rantala M, Kangasjärvi S, Paakkarinen V, Tikkanen M, Jansson S, et al. 2012. PROTON GRADIENT REGULATION5 is essential for proper acclimation of Arabidopsis photosystem I to naturally and artificially fluctuating light conditions. *Plant Cell* **24**(7): 2934-2948.

Suorsa M, Rossi F, Tadini L, Labs M, Colombo M, Jahns P, Kater Martin M, Leister D, Finazzi G, Aro E-M, et al. 2016. PGR5-PGRL1-dependent cyclic electron transport modulates linear electron transport rate in Arabidopsis thaliana. *Molecular Plant* **9**(2): 271-288.

Sylak-Glassman EJ, Malnoë A, De Re E, Brooks MD, Fischer AL, Niyogi KK, Fleming GR. 2014. Distinct roles of the photosystem II protein PsbS and zeaxanthin in the regulation of light harvesting in plants revealed by fluorescence lifetime snapshots. *Proceedings of the National Academy of Sciences of the United States of America* **111**(49): 17498-17503.

Tagawa K, Tsujimoto HY, Arnon DI. 1963. Role of chloroplast ferredoxin in the energy conversion process of photosynthesis. *Proceedings of the National Academy of Sciences of the United States of America* **49**(4): 567-572.

Thormählen I, Zupok A, Rescher J, Leger J, Weissenberger S, Groysman J, Orwat A, Chatel-Innocenti G, Issakidis-Bourguet E, Armbruster U, et al. 2017. Thioredoxins play a crucial role in dynamic acclimation of photosynthesis in fluctuating light. *Molecular Plant* **10**(1): 168-182.

Tikhonov AN. 2013. PH-Dependent regulation of electron transport and ATP synthesis in chloroplasts. *Photosynthesis Research* **116**(2): 511-534.

Tikhonov AN. 2014. The cytochrome b6f complex at the crossroad of photosynthetic electron transport pathways. *Plant Physiology and Biochemistry* **81**: 163-183.

Tikhonov AN. 2023. The cytochrome b(6)f complex: plastoquinol oxidation and regulation of electron transport in chloroplasts. *Photosynth Research*: 1-25.

Tikhonov AN, Khomutov GB, Ruuge EK, Blumenfeld LA. 1981. Electron transport control in chloroplasts. Effects of photosynthetic control monitored by the intrathylakoid pH. *Biochimica et Biophysica Acta (BBA) - Bioenergetics* **637**(2): 321-333.

Trouillard M, Shahbazi M, Moyet L, Rappaport F, Joliot P, Kuntz M, Finazzi G. 2012. Kinetic properties and physiological role of the plastoquinone terminal oxidase (PTOX) in a vascular plant. *Biochimica et Biophysica Acta (BBA) - Bioenergetics* **1817**(12): 2140-2148.

Turnbull MH, Yates DJ. 1993. Seasonal variation in the red/far-red ratio and photon flux density in an Australian sub-tropical rainforest. *Agricultural and Forest Meteorology* **64**(1): 111-127.

Tutkus M, Saccon F, Chmeliov J, Venckus O, Ciplys I, Ruban AV, Valkunas L. 2019. Single-molecule microscopy studies of LHCII enriched in Vio or Zea. *Biochimica et Biophysica Acta (BBA) - Bioenergetics* **1860**(6): 499-507.

Ünnep R, Zsiros O, Hörcsik Z, Markó M, Jajoo A, Kohlbrecher J, Garab G, Nagy G. 2017. Low-pH induced reversible reorganizations of chloroplast thylakoid membranes — As revealed by small-angle neutron scattering. *Biochimica et Biophysica Acta (BBA) - Bioenergetics* **1858**(5): 360-365.

van Bezouw RFHM, Keurentjes JJB, Harbinson J, Aarts MGM. 2019. Converging phenomics and genomics to study natural variation in plant photosynthetic efficiency. *The Plant Journal* **97**(1): 112-133.

van Oort B, Roy LM, Xu P, Lu Y, Karcher D, Bock R, Croce R. 2018. Revisiting the role of xanthophylls in nonphotochemical quenching. *The Journal of Physical Chemistry Letters* **9**(2): 346-352.

Vialet-Chabrand S, Matthews JSA, Simkin AJ, Raines CA, Lawson T. 2017. Importance of fluctuations in light on plant photosynthetic acclimation. *Plant Physiology* **173**(4): 2163-2179.

Vierling LA, Wessman CA. 2000. Photosynthetically active radiation heterogeneity within a monodominant Congolese rain forest canopy. *Agricultural and Forest Meteorology* **103**(3): 265-278.

Vistnes AI 2018. Forced oscillations and resonance. *Physics of Oscillations and Waves: With Use of Matlab and Python*. Cham: Springer International Publishing, 31-57.

von Bismarck T, Korkmaz K, Ruß J, Skurk K, Kaiser E, Galvis VC, Cruz J, Strand D, Köhl K, Eirich J, et al. 2021. Light acclimation interacts with thylakoid ion transport to govern the dynamics of photosynthesis: Research Square.

Wada M. 2013. Chloroplast movement. *Plant Science* **210**: 177-182.

Wada S, Amako K, Miyake C. 2021. Identification of a novel mutation exacerbated the PSI photoinhibition in pgr5/pgrl1 mutants; caution for overestimation of the phenotypes in Arabidopsis pgr5-1 mutant. *Cells* **10**(11).

Walker DA. 1992. Concerning oscillations. *Photosynthesis Research* **34**(3): 387-395.

Walters RG. 2005. Towards an understanding of photosynthetic acclimation. *Journal of Experimental Botany* **56**(411): 435-447.

Walters RG, Horton P. 1995. Acclimation of Arabidopsis thaliana to the light environment: Changes in photosynthetic function. *Planta* **197**(2): 306-312.

Wang CJ, Yamamoto H, Shikanai T. 2015. Role of cyclic electron transport around photosystem I in regulating proton motive force. *Biochimica et Biophysica Acta (BBA) - Bioenergetics* **1847**(9): 931-938.

Ware MA, Belgio E, Ruban AV. 2015. Comparison of the protective effectiveness of NPQ in Arabidopsis plants deficient in PsbS protein and zeaxanthin. *Journal of Experimental Botany* **66**(5): 1259-1270.

Waters JW 1976. 2.3. Absorption and emission by atmospheric gases. *Methods in Experimental Physics*: Academic Press, 142-176.

Way DA, Pearcy RW. 2012. Sunflecks in trees and forests: from photosynthetic physiology to global change biology. *Tree Physiology* **32**(9): 1066-1081.

Wehner A, Grasses T, Jahns P. 2006. De-epoxidation of violaxanthin in the minor antenna proteins of photosystem II, LHCB4, LHCB5, and LHCB6. *Journal of Biological Chemistry* **281**(31): 21924-21933.

Wehner A, Storf S, Jahns P, Schmid VHR. 2004. De-epoxidation of violaxanthin in light-harvesting complex I proteins. *Journal of Biological Chemistry* **279**(26): 26823-26829.

Wei Z, Duan F, Sun X, Song X, Zhou W. 2021. Leaf photosynthetic and anatomical insights into mechanisms of acclimation in rice in response to long-term fluctuating light. *Plant, Cell and Environnment* **44**(3): 747-761.

Wolf BC, Isaacson T, Tiwari V, Dangoor I, Mufkadi S, Danon A. 2020. Redox regulation of PGRL1 at the onset of low light intensity. *Plant Journal* **103**(2): 715-725.

Wolfe J, Garnier M, Smith J. 2009. Vocal tract resonances in speech, singing, and playing musical instruments. *HFSP Journal* **3**(1): 6-23.

Wollman F-A. 2001. State transitions reveal the dynamics and flexibility of the photosynthetic apparatus. *The EMBO Journal* **20**(14): 3623-3630.

Wood WHJ, Barnett SFH, Flannery S, Hunter CN, Johnson MP. 2019. Dynamic thylakoid stacking is regulated by LHCII phosphorylation but not its interaction with PSI. *Plant Physiology* **180**(4): 2152-2166.

Wood WHJ, MacGregor-Chatwin C, Barnett SFH, Mayneord GE, Huang X, Hobbs JK, Hunter CN, Johnson MP. 2018. Dynamic thylakoid stacking regulates the balance between linear and cyclic photosynthetic electron transfer. *Nature Plants* **4**(2): 116-127.

Woodrow IE, Berry JA. 1988. Enzymatic regulation of photosynthetic CO2, fixation in C3 plants. *Annual Review of Plant Physiology and Plant Molecular Biology* **39**(1): 533-594.

Wullschleger SD. 1993. Biochemical limitations to carbon assimilation in C3 plants—a retrospective analysis of the A/Ci curves from 109 species. *Journal of Experimental Botany* **44**(5): 907-920.

Yamamoto H, Peng L, Fukao Y, Shikanai T. 2011. An Src homology 3 domain-like fold protein forms a ferredoxin binding site for the chloroplast NADH dehydrogenase-like complex in Arabidopsis. *Plant Cell* **23**(4): 1480-1493.

Yamamoto H, Shikanai T. 2019. PGR5-dependent cyclic electron flow protects photosystem I under fluctuating light at donor and acceptor sides. *Plant Physiology* **179**(2): 588-600.

Yamori W, Makino A, Shikanai T. 2016. A physiological role of cyclic electron transport around photosystem I in sustaining photosynthesis under fluctuating light in rice. *Scientific Reports* **6**: 20147.

Yamori W, Sakata N, Suzuki Y, Shikanai T, Makino A. 2011. Cyclic electron flow around photosystem I via chloroplast NAD(P)H dehydrogenase (NDH) complex performs a significant physiological role during photosynthesis and plant growth at low temperature in rice. *Plant Journal* **68**(6): 966-976.

Yamori W, Shikanai T. 2016. Physiological functions of cyclic electron transport around photosystem I in sustaining photosynthesis and plant growth. *Annual Review of Plant Biology* **67**: 81-106.

Yamori W, Shikanai T, Makino A. 2015. Photosystem I cyclic electron flow via chloroplast NADH dehydrogenase-like complex performs a physiological role for photosynthesis at low light *Scientific Reports* **5**: 13908.

Yang L, Gao X, Li Z, Jia D. 2022. Quantitative effects of air pollution on regional daily global and diffuse solar radiation under clear sky conditions. *Energy Reports* **8**: 1935-1948.

Zhang H-B, Xu D-Q. 2003. Role of light-harvesting complex 2 dissociation in protecting the photosystem 2 reaction centres against photodamage in soybean leaves and thylakoids. *PHOTOSYNTHETICA* **41**(3): 383-391.

Zhou Q, Yamamoto H, Shikanai T. 2022. Distinct contribution of two cyclic electron transport pathways to P700 oxidation. *Plant Physiology*: 326-341.

Zhu X-G, de Sturler E, Long SP. 2007. Optimizing the distribution of resources between enzymes of carbon metabolism can dramatically increase photosynthetic rate: A numerical simulation using an evolutionary algorithm. *Plant Physiology* **145**(2): 513-526.

Zhu X-G, Long SP, Ort DR. 2008. What is the maximum efficiency with which photosynthesis can convert solar energy into biomass? *Current Opinion in Biotechnology* **19**(2): 153-159.

Zhu X-G, Long SP, Ort DR. 2010. Improving photosynthetic efficiency for greater yield. *Annual Review of Plant Biology* **61**: 235-261.

Acknowledgments

I would like to express my heartfelt gratitude to my supervisors, Ladislav Nedbal, Shizue Matsubara, and Silvia Schrey. Thank you for your critical guidance, insightful feedback, and continuous support throughout the research process of my PhD. Ladi, you always helped me like Superman when I faced difficulties during my research. You always selflessly shared your academic insights and ideas, which greatly inspired me. Your encouragement gives me more confidence to keep going in my academic career. You are not only my mentor but also my family. Shizue, I remember many of our discussions went on late into the evening. Your rigorous approach to scientific research and comprehensive knowledge of biology pointed me in a clear direction for my endeavors. I have learned so much from your monthly group meetings and discussions. Going to an Imagine Dragons concert with a supervisor is something that will always be remembered. Silvia, thank you for giving me so much warmth and support. You always helped me when I was in trouble, whether in research or life. You helped me to analyze my data, revise my writing, and find a place to live. We had a lovely trip to Paris. I also remember that we went up to the mountain together to collect lichens, which made me feel the beauty of this kind of organism that I seldom noticed for the first time. Thank you for always encouraging me and believing in me. I would also like to thank Oliver Ebenhöh for his willingness to be my mentor in HHU, who will also be my thesis and defense examiner. Thank you all for your support along the way as I pursue my Ph.D. Your expertise and support have been very important to me in overcoming challenges and achieving my research goals.

I would like to thank the two groups I had the privilege of working with, the ABB and Shoot groups at IBG-2. I am particularly grateful to Uwe Rascher, Onno Muller, Holger Klose, Philipp Grande, and Juliane Bendig, whose invaluable assistance and insightful feedback have been instrumental in my research. Their willingness to engage in scientific discussions has enriched my understanding and perspective. Thanks to all the researchers, technicians, and peers in both research groups and in the greenhouse, whose friendship and teamwork have made my research process enjoyable and productive.

A big thank you to Dušan Lazar; you are my co-author for three chapters of content; you are not officially my supervisor, but you do all the things a supervisor needs to do! Thank you for always going out of your way to answer my questions, give me comments, revise

my papers, and help me with instrumental protocols and experimental designs. I would also like to extend a special thanks to Hendrick Poorter, Fabio Fiorani, Alfred Holzwarth, and Dave Kramer. Your critical comments, openness to discussion, and willingness to contribute insights and ideas to my work and writing are greatly appreciated.

Many thanks to Ludovic Jullien, who accepted me to do a lab journey in ENS, and Aliénor Lahlou, who helped me with everything during the period I was in Paris. Special thanks to Benjamin Bailleul for giving me a lot of input on interpreting data in Chapter 3. I would not have been able to complete my experiments without the help of Christof Klughammer, Ulrich Schreiber, Gert Schansker, and Erhard Pfündel at Walz, who guided me through the use of the instruments and helped me solve problems.

To my Chinese Pals, Huaiyue (怀月), Xinyu (欣雨), Fang (芳), Congcong (聪聪), Lu (鹭), Genghong (耕泓), Dr. Luo (罗老师), thank you for making me feel at home. When I first came to Germany and experienced the epidemic, you gave me a lot of comfort and help. I will miss all the special meals and festivals we had together. I want to also thank my friends Khadija, Deepthi, Ana, Bow, June, Jimena, David, Daniel, Oliver, Kelvin, Kwabena, Kathrin, Antony, Sofia, Andrea, Erekle, Yasmin for your encouragement and help in keeping optimistic and pleasant during the ups and downs of the researcher life. And Yanrong (彦融), we don't meet in person often, but I'll never forget the days when we wrote our manuscripts together and encouraged each other every day.

To my dearest fiancé Shiyan, when I got this offer for a PhD in Germany, you immediately supported me and decided to come here with me. During these three years, we faced the epidemic and the difficulties in life and working together. Thank you for always supporting me, accommodating me, helping me, and taking care of me with all you have. It is you who make my life journey full of joy and happiness.

Most especially, I would like to thank my mom, my father, and all my family and friends in China; you are the people I miss the most. You have always supported and encouraged me unconditionally.

Finally, I dedicate this thesis to my grandmother, who raised me but left for heaven before I could be by her side.